Polarized plate tectonics and earthquakes

Carlo Doglioni - INGV/Sapienza - in cooperation with Domenico Barberio, Michael Bevis, Christian Bignami, Andrea Billi, Dino Boccaletti, Antonio Carcaterra, Eugenio Carminati, Marco Cuffaro, Mattia Crespi, Giorgio Dal Piaz, Eleonora Ficini, Paolo Harabaglia, Fabrizio Innocenti, Riccardo Lanari, Tolya Levshin, Corrado Mascia, Franco Mongelli, Enzo Nesi, Giuliano Panza, Angelo Peccerillo, Marco Petitta, Patrizio Petricca, Federica Riguzzi, Benedetto Scoppola, Davide Scrocca, Pietro Tizzani, Emanuela Valerio, Francesco Vespe, Davide Zaccagnino, Alik Ismail-Zadeh, Don Anderson

SIF – 15-9-2021

It is the asymmetry that generates the phenomenon
PIERRE CURIE

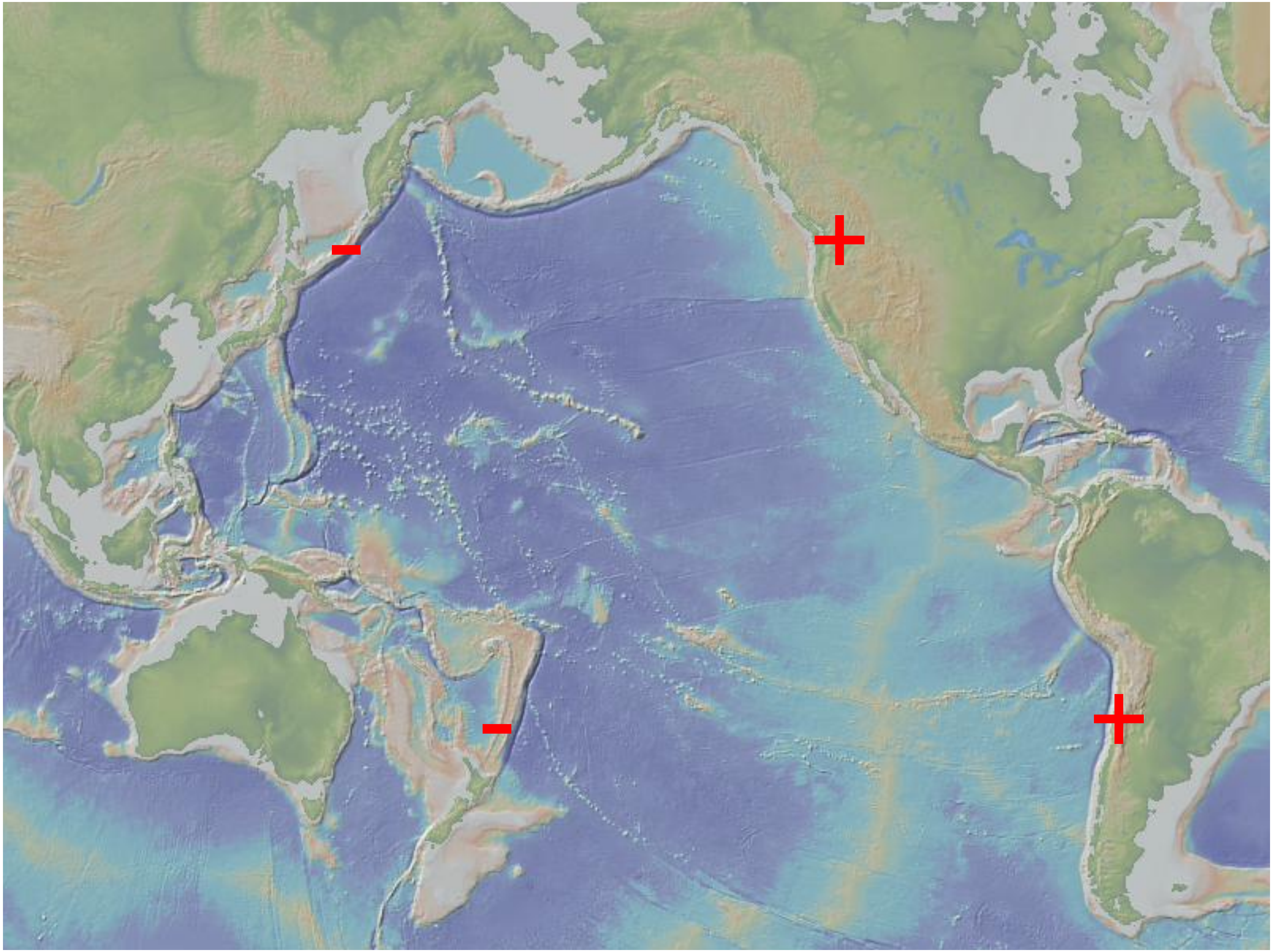

Marianas

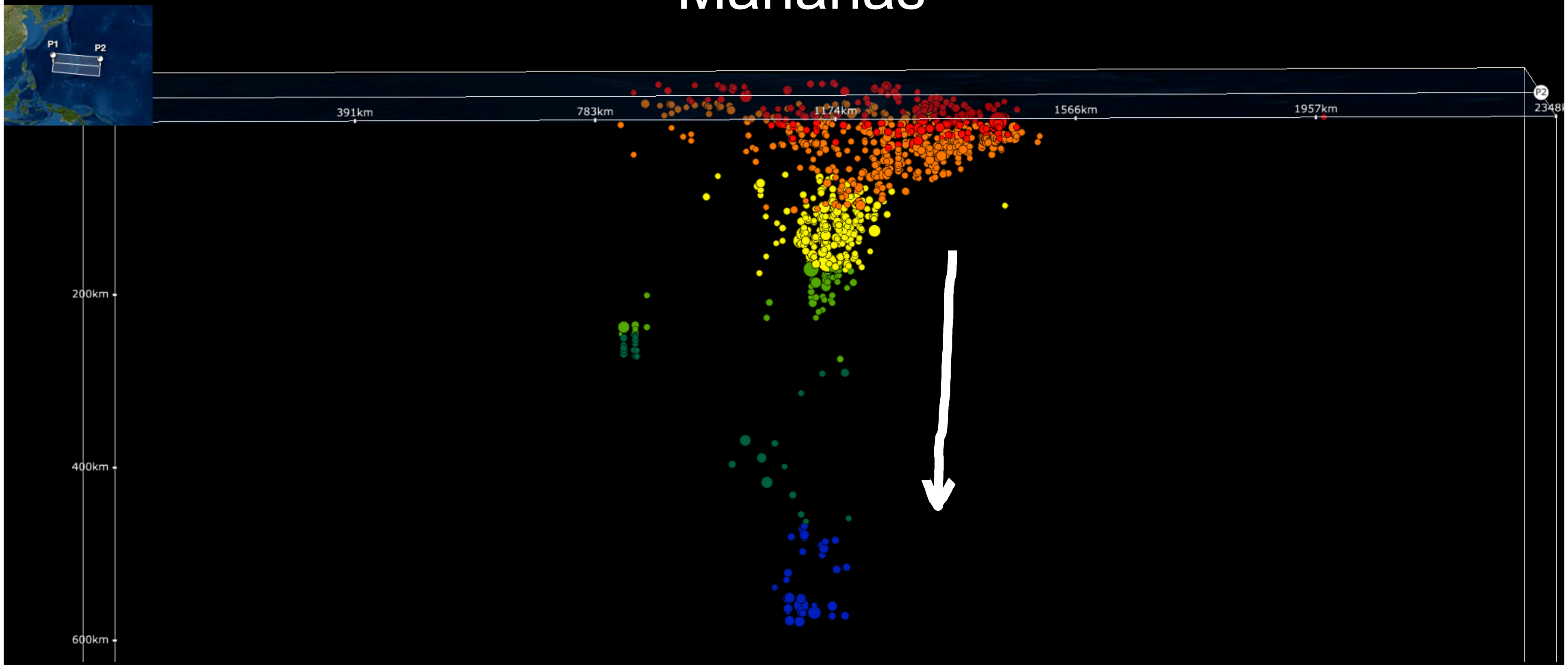

Andes

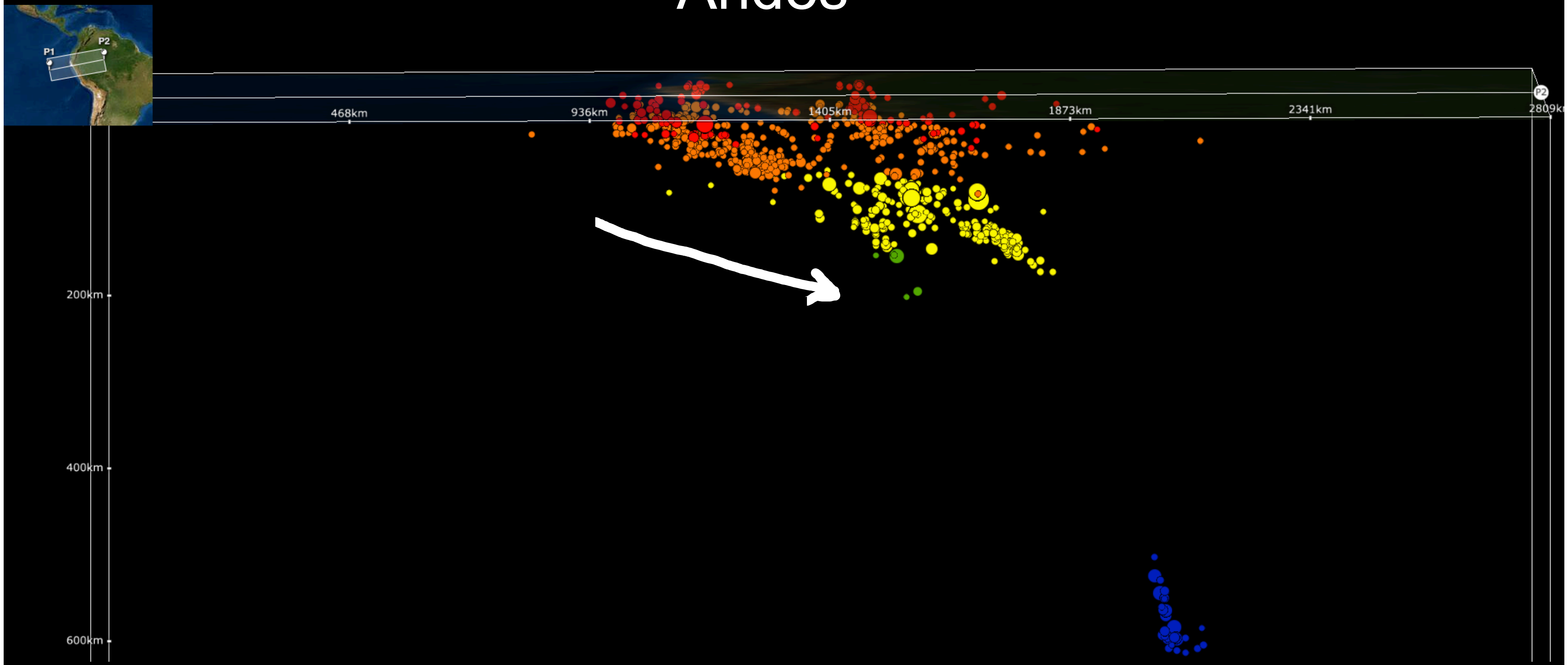
P1
P2
468km
936km
1405km
1873km
2341km
2809km
200km
400km
600km

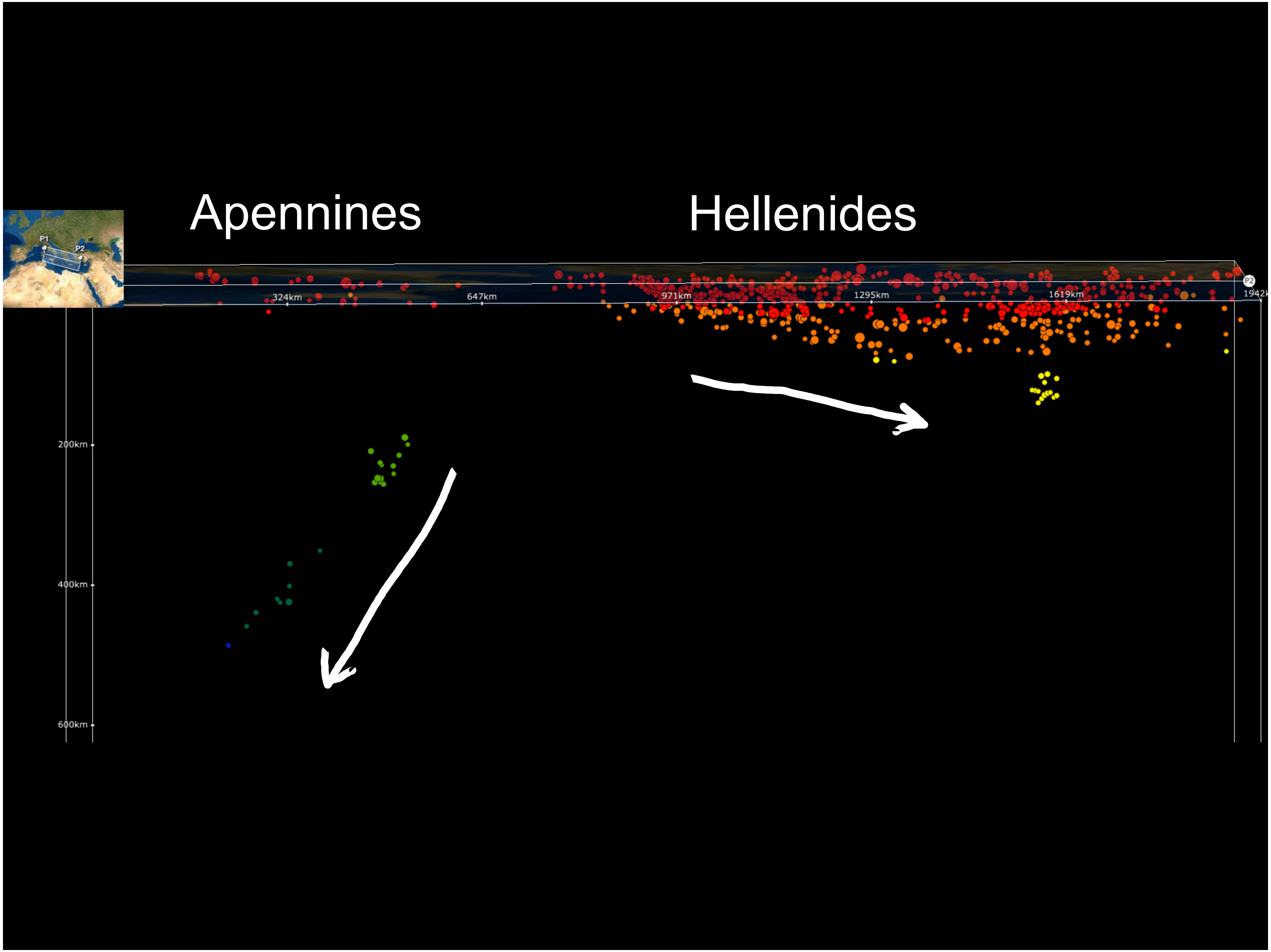

Apennines
Hellenides
P1
P2
324km
647km
971km
1295km
1619km
200km
400km
600km

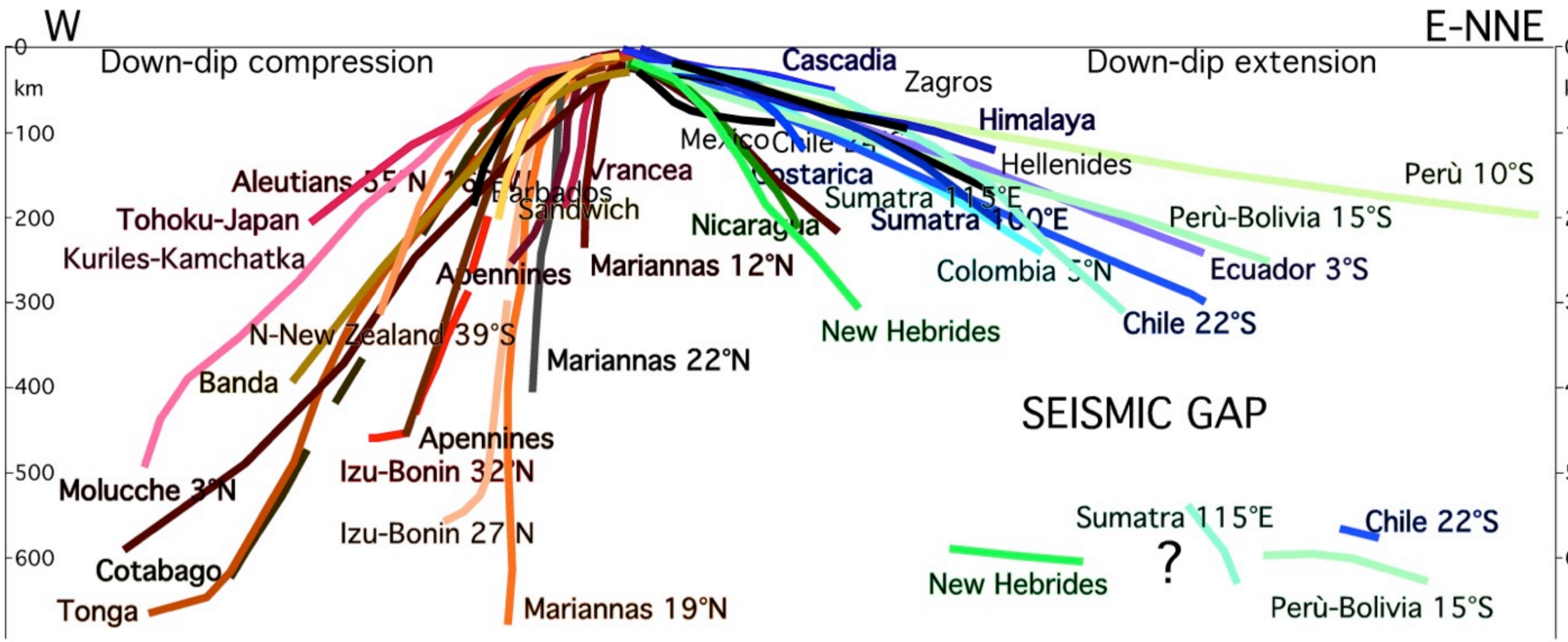

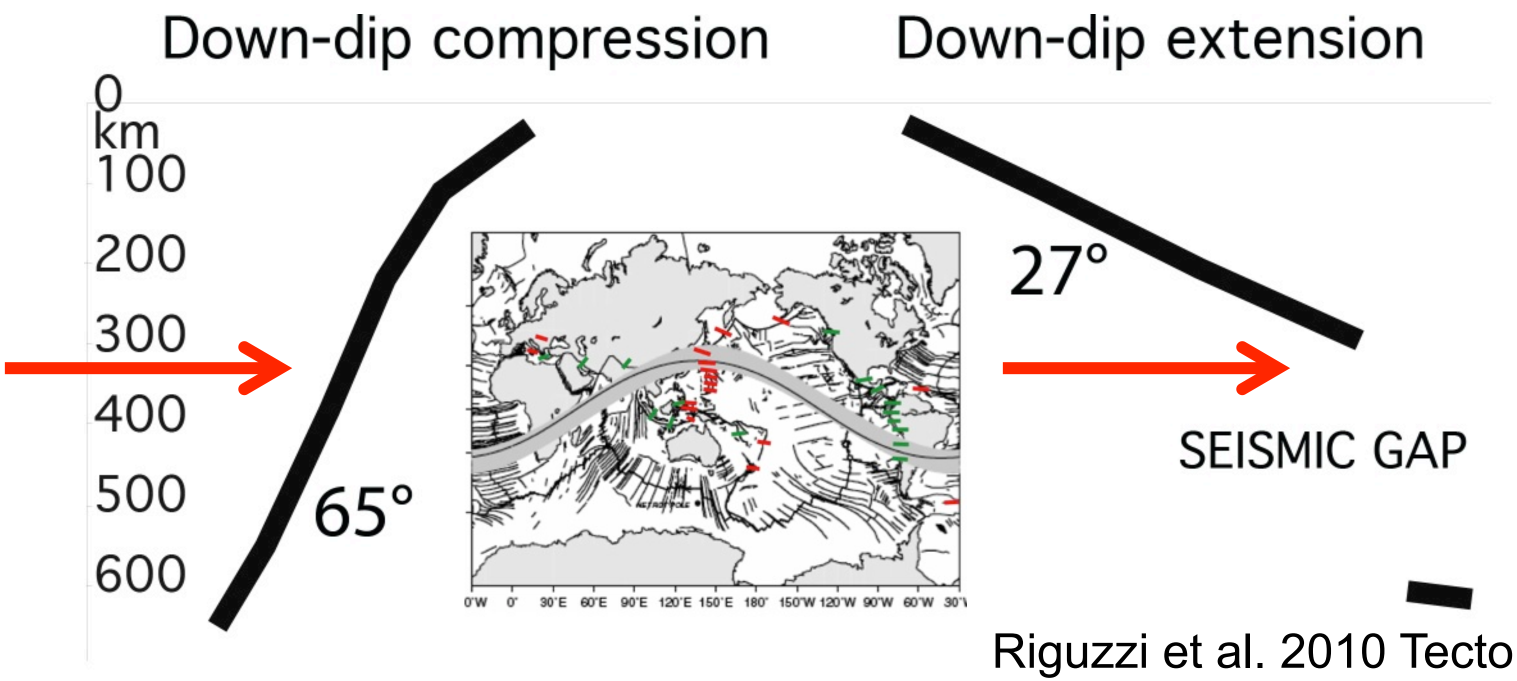

Riguzzi et al. 2010 Tectonophysics

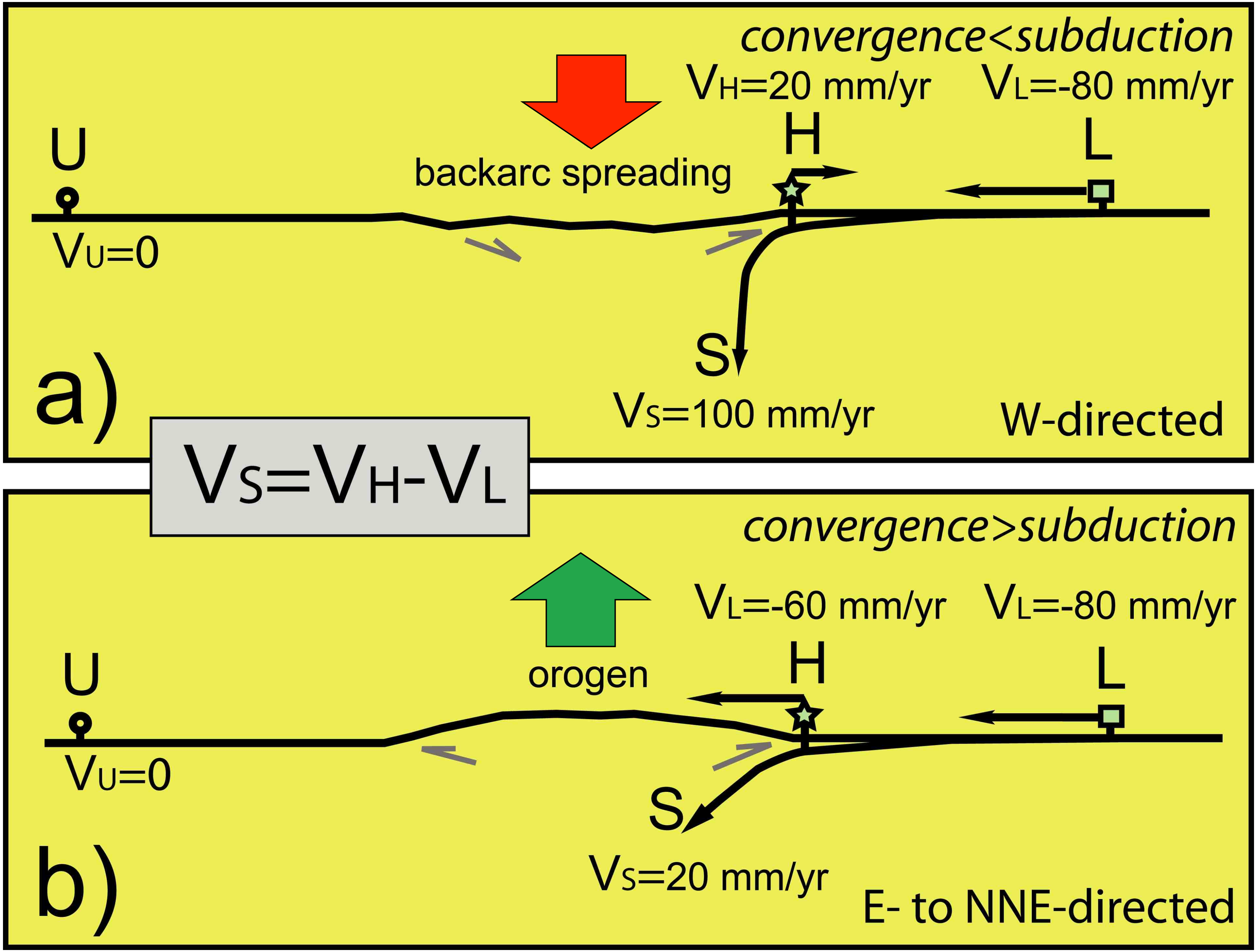
convergence<subduction
VH=20 mm/yr
VL=-80 mm/yr
H
L
U
backarc spreading
VU=0
S
a)
VS=100 mm/yr
W-directed
VS=VH-VL
convergence>subduction
VL=-60 mm/yr
VL=-80 mm/yr
orogen
H
U
L
VU=0
S
b)
VS=20 mm/yr
E- to NNE-directed

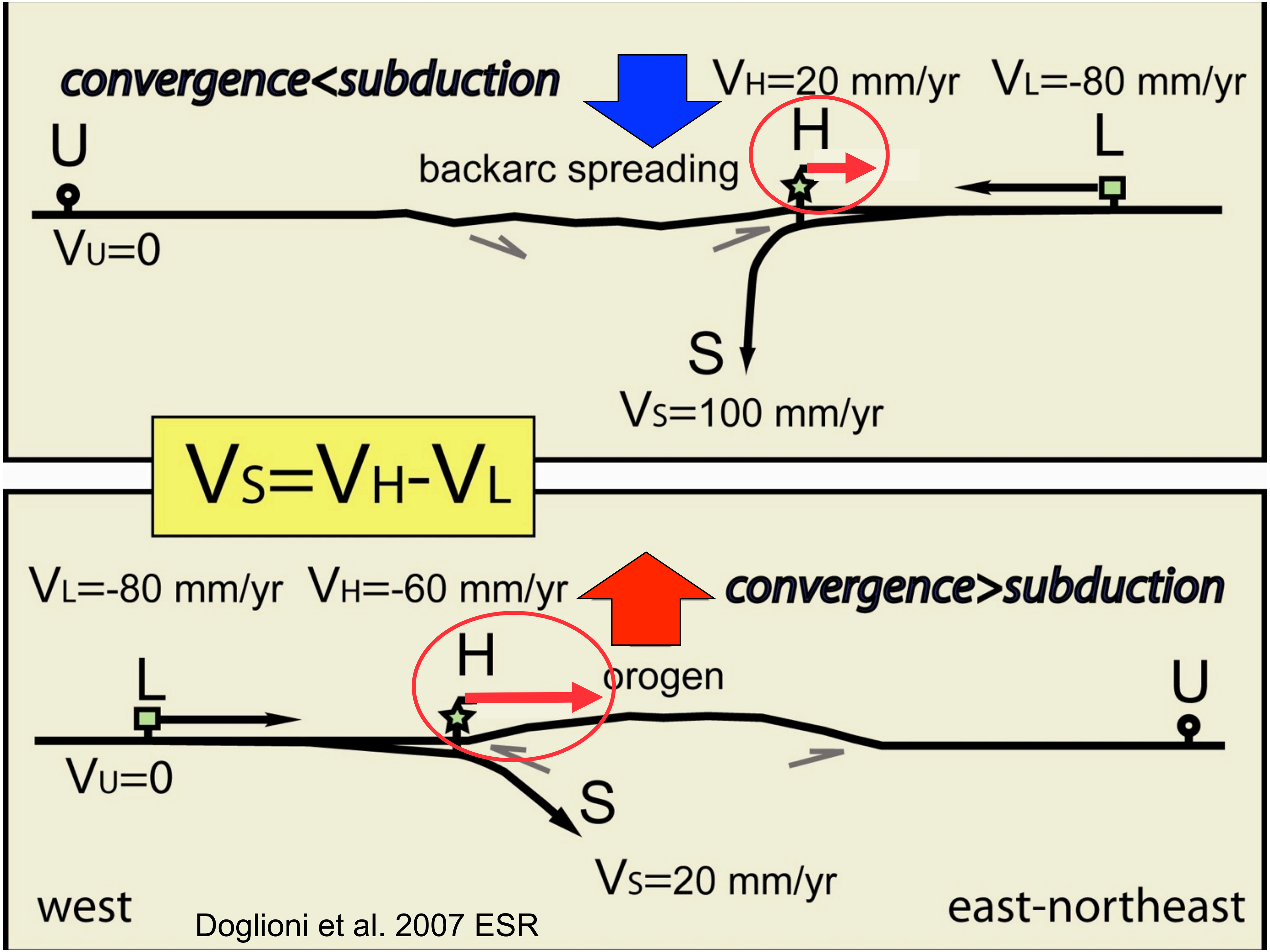

Doglioni et al. 2007 ESR

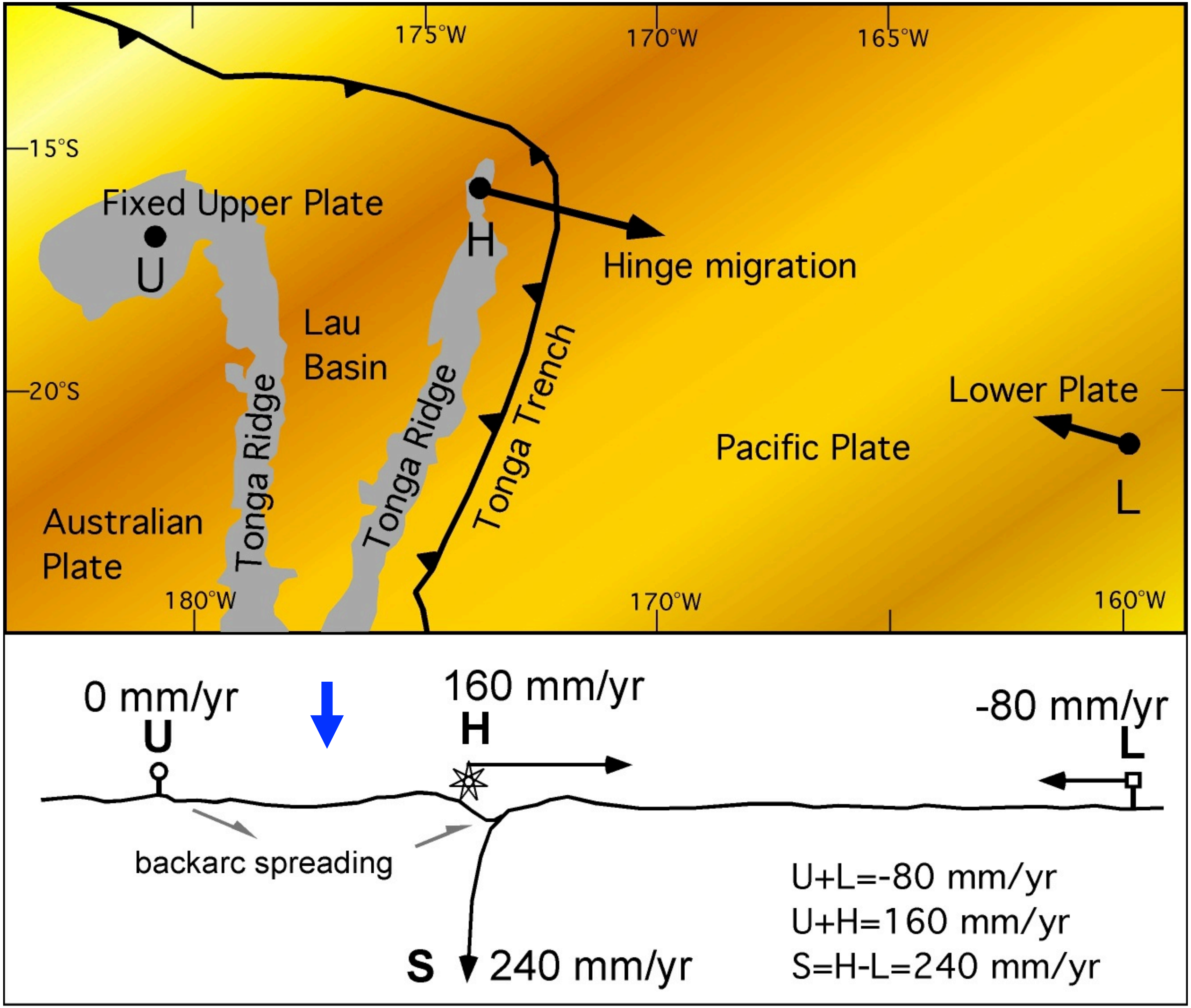
175°W
170°W
165°W
15°S
20°S
Fixed Upper Plate
U
H
Hinge migration
Lau
Basin
Tonga Ridge
Tonga Ridge
Tonga Trench
Lower Plate
Pacific Plate
L
Australian
Plate
180°W
170°W
160°W
0 mm/yr
U
160 mm/yr
H
-80 mm/yr
L
backarc spreading
U+L=-80 mm/yr
U+H=160 mm/yr
S=H-L=240 mm/yr
S
240 mm/yr

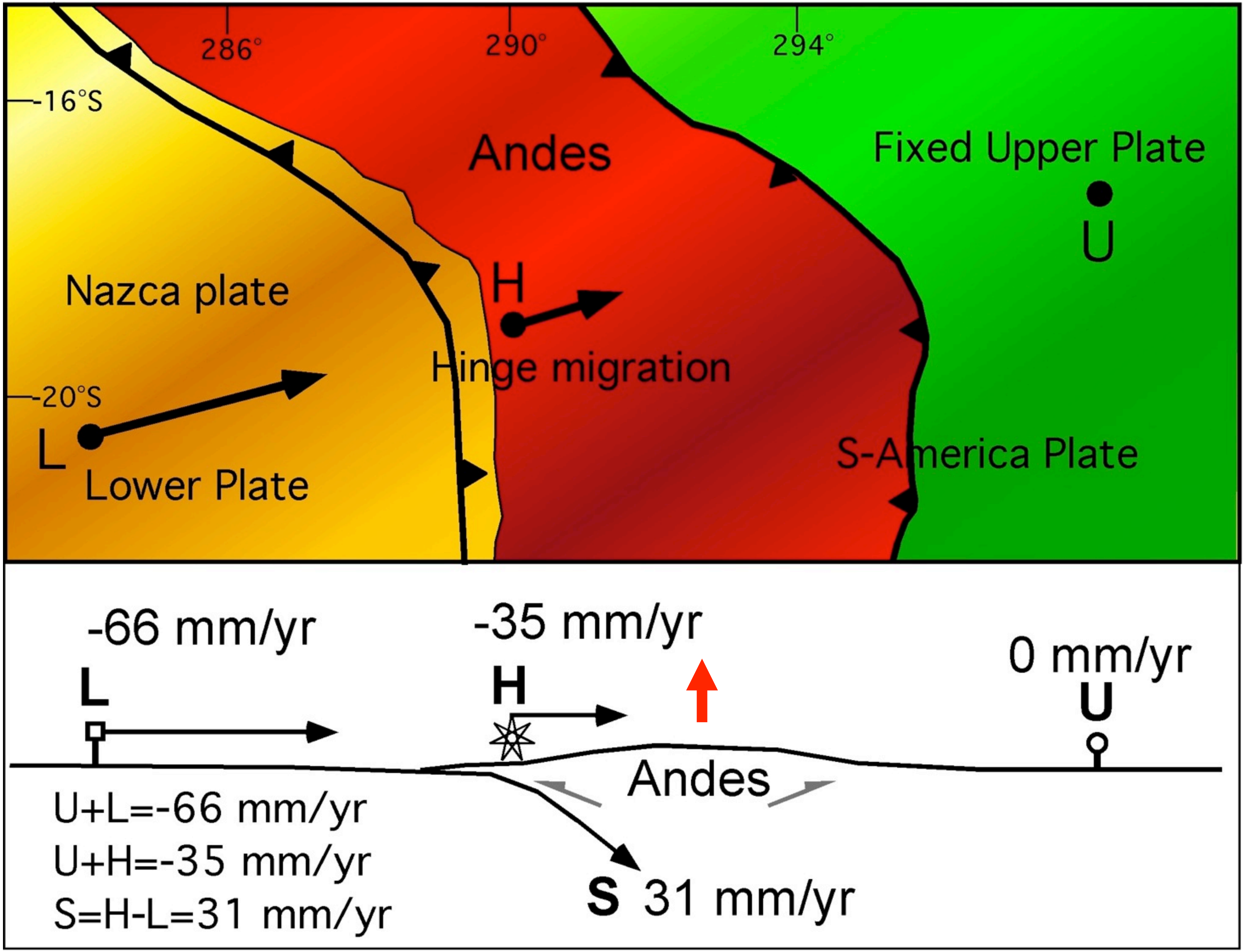
286°
290°
294°
-16°S
-20°S
Andes
Fixed Upper Plate
U
Nazca plate
H
Hinge migration
L
Lower Plate
S-America Plate
-66 mm/yr
-35 mm/yr
0 mm/yr
L
H
U
Andes
U+L=-66 mm/yr
U+H=-35 mm/yr
S=H-L=31 mm/yr
S 31 mm/yr

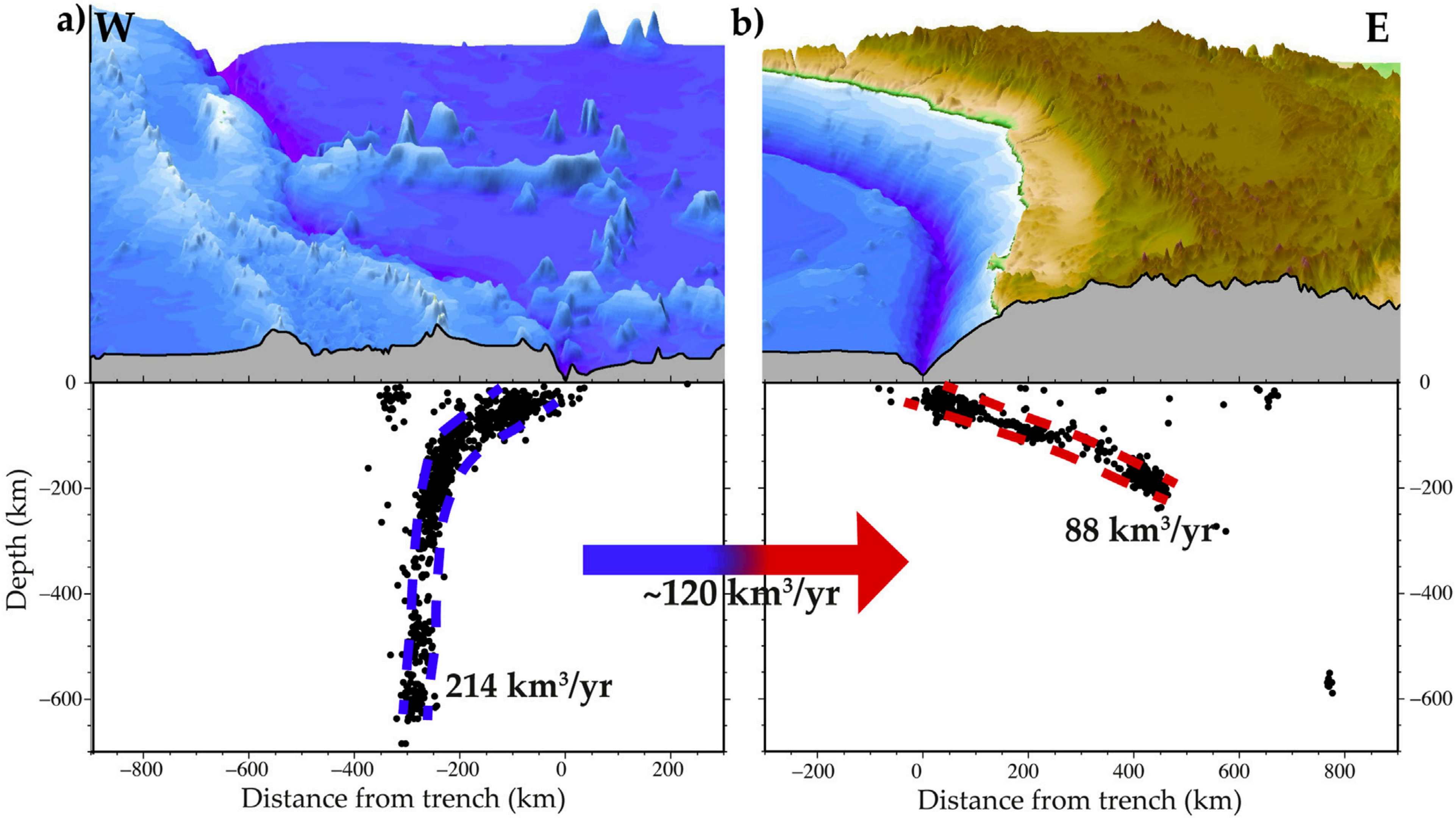

Ficini et al. 2020 Gondwana Res.

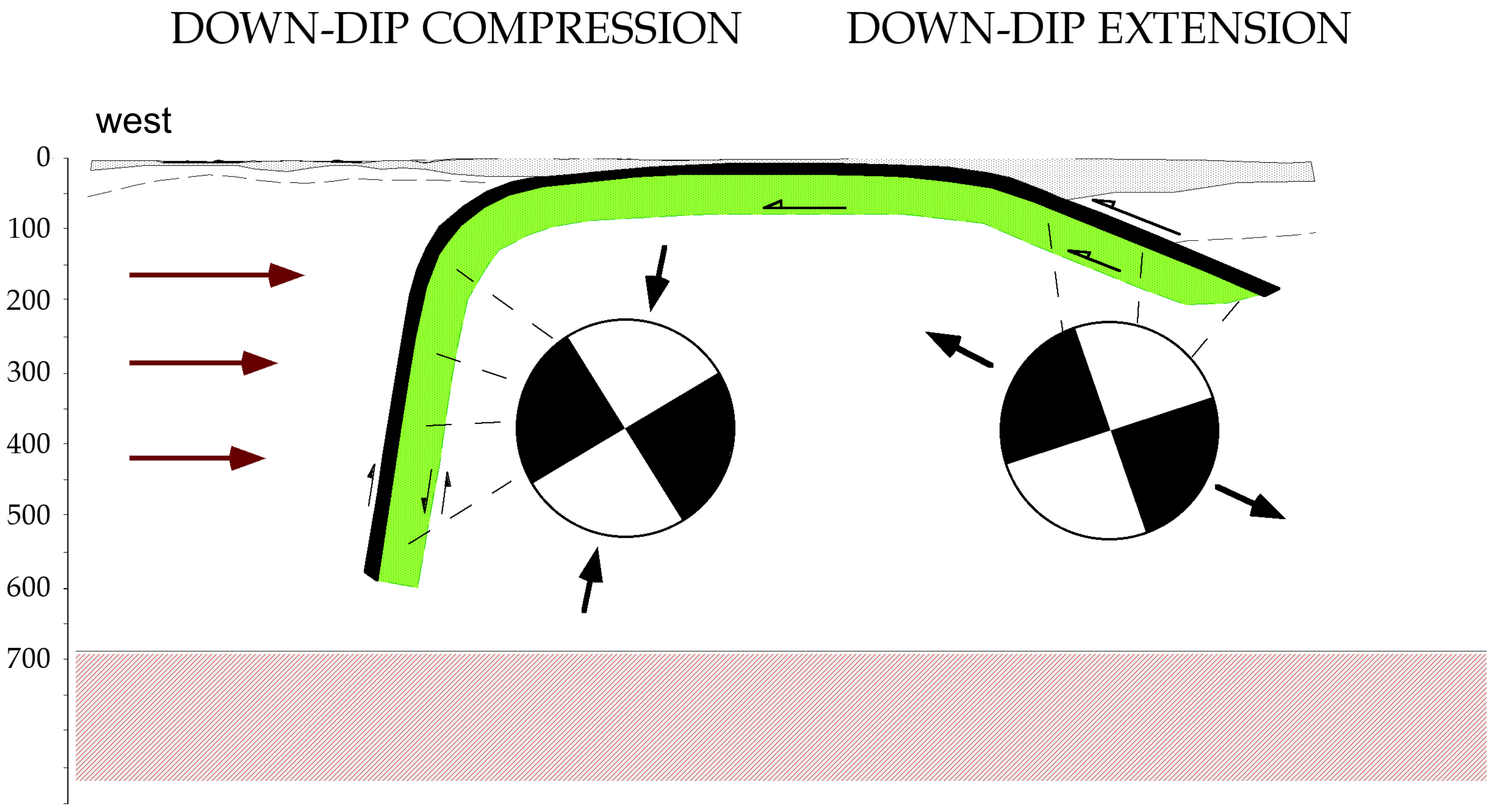
DOWN-DIP COMPRESSION
DOWN-DIP EXTENSION
west
0
100
200
300
400
500
600
700

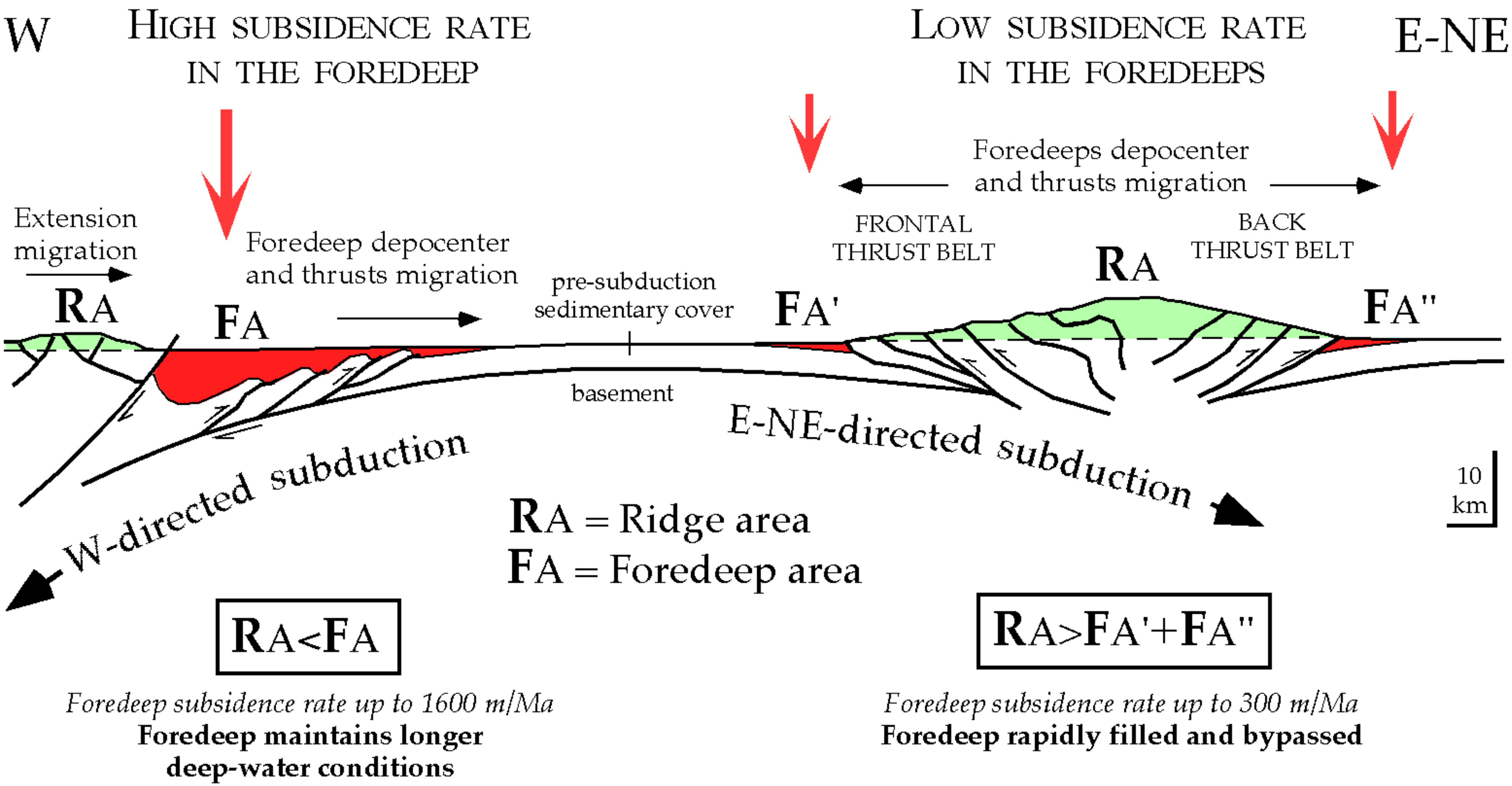

Doglioni 1994 Geology

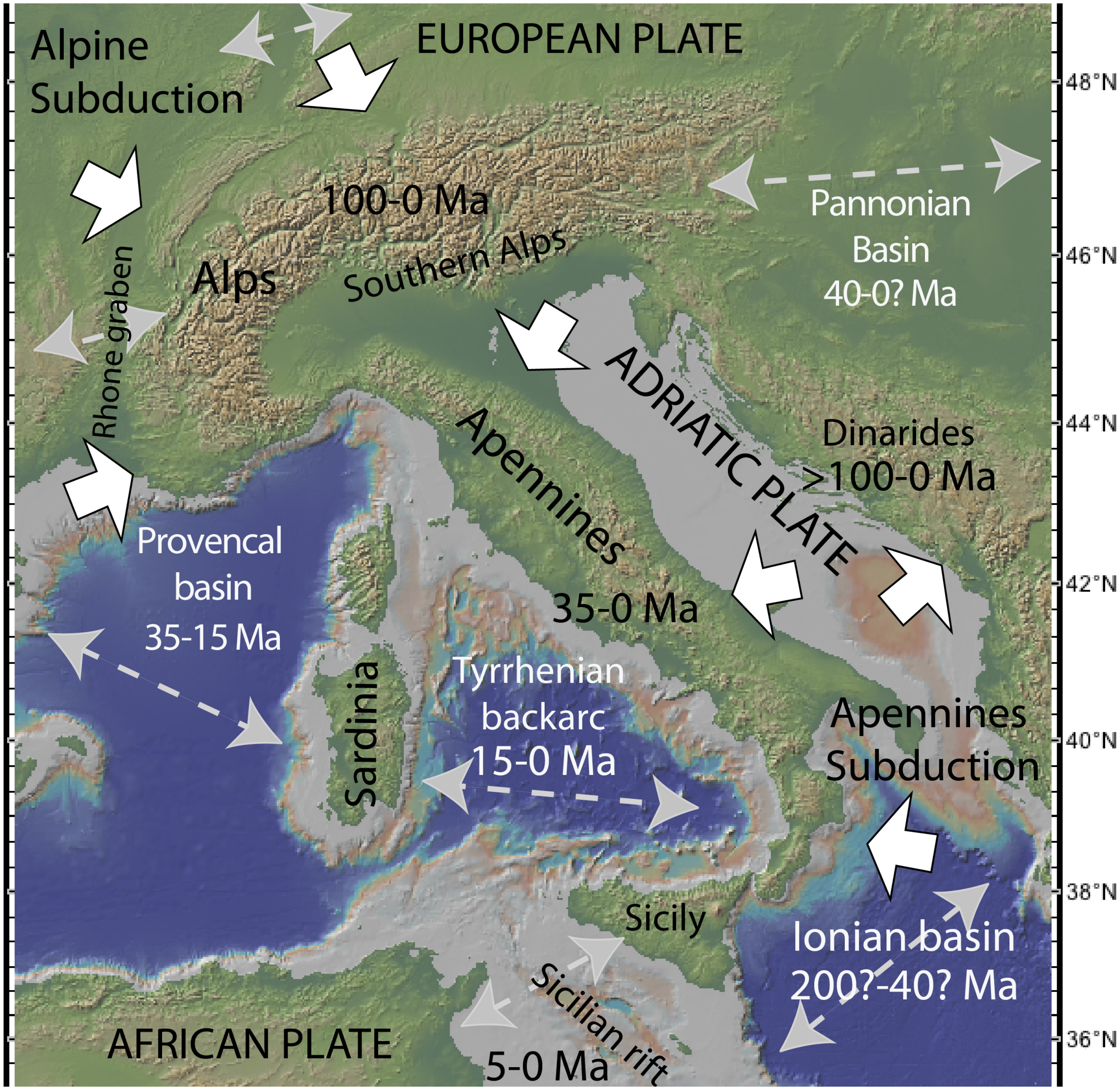

Alpine Subduction
EUROPEAN PLATE
100-0 Ma
Alps
Southern Alps
Rhone graben
Pannonian Basin 40-0? Ma
ADRIATIC PLATE
Apennines
Dinarides >100-0 Ma
Provencal basin 35-15 Ma
35-0 Ma
Tyrrhenian backarc 15-0 Ma
Sardinia
Apennines Subduction
Sicily
Ionian basin 200?-40? Ma
Sicilian rift
5-0 Ma
AFRICAN PLATE
48°N
46°N
44°N
42°N
40°N
38°N
36°N

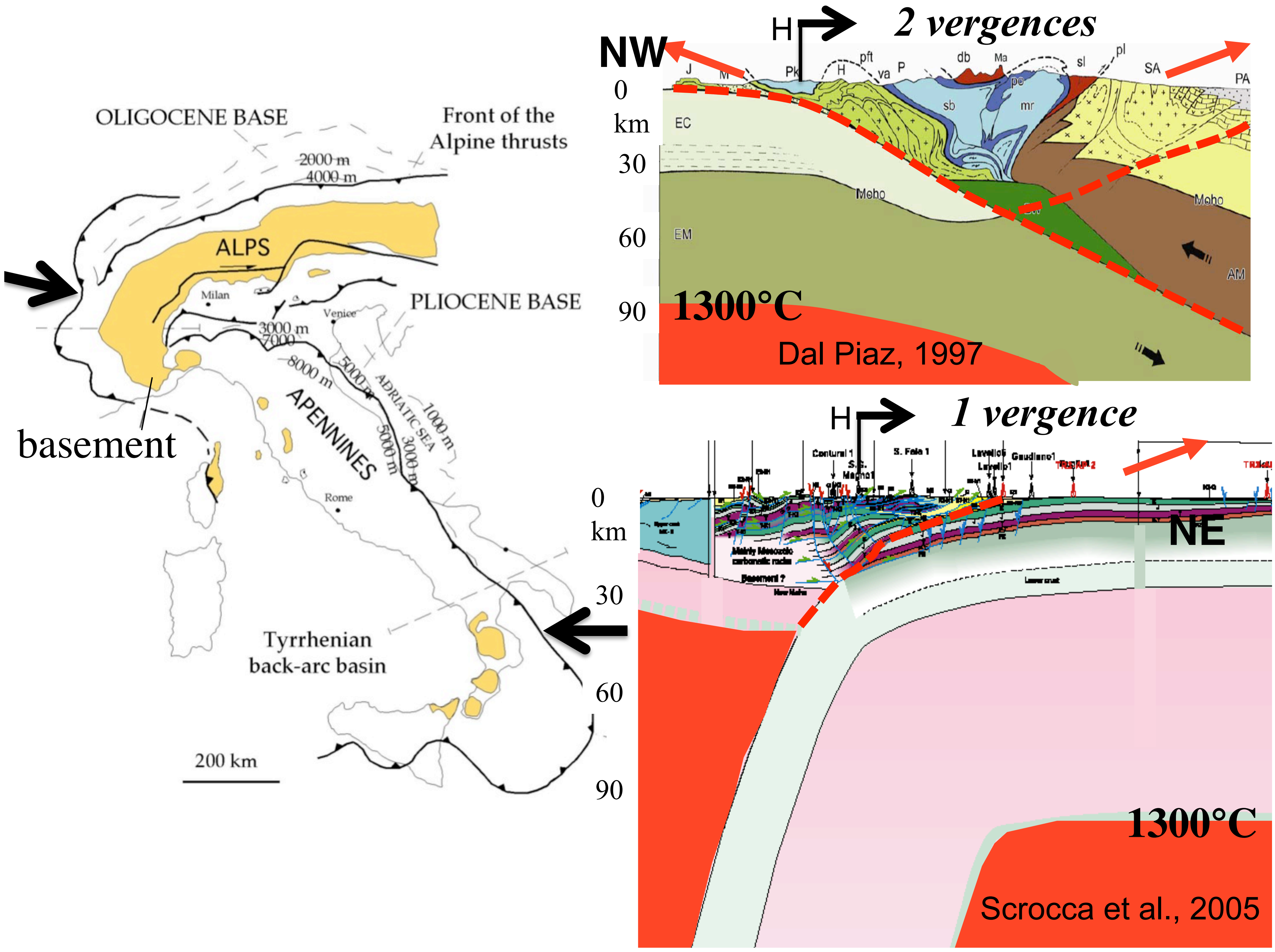

OLIGOCENE BASE
Front of the Alpine thrusts
2000 m
4000 m
ALPS
Milan
Venice
PLIOCENE BASE
3000 m
7000
8000 m
5000 m
ADRIATIC SEA
1000 m
5000 m
3000 m
APENNINES
basement
Rome
Tyrrhenian back-arc basin
200 km
2 vergences
H
NW
0 km
30
60
90
EC
EM
Moho
AM
SA
PA
1300°C
Dal Piaz, 1997
1 vergence
H
NE
0 km
30
60
90
1300°C
Scrocca et al., 2005

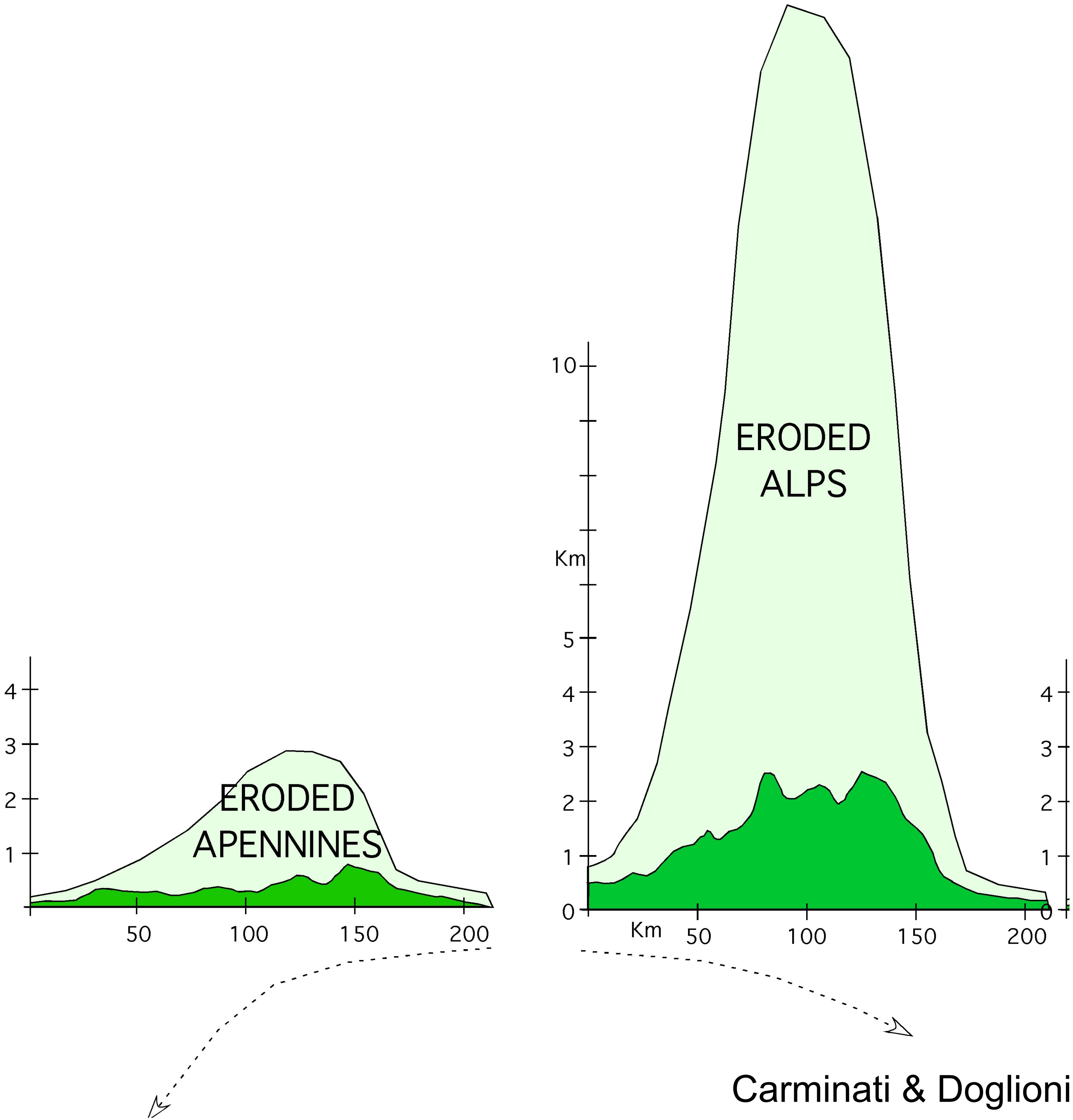

Carminati & Doglioni 2012, ESR

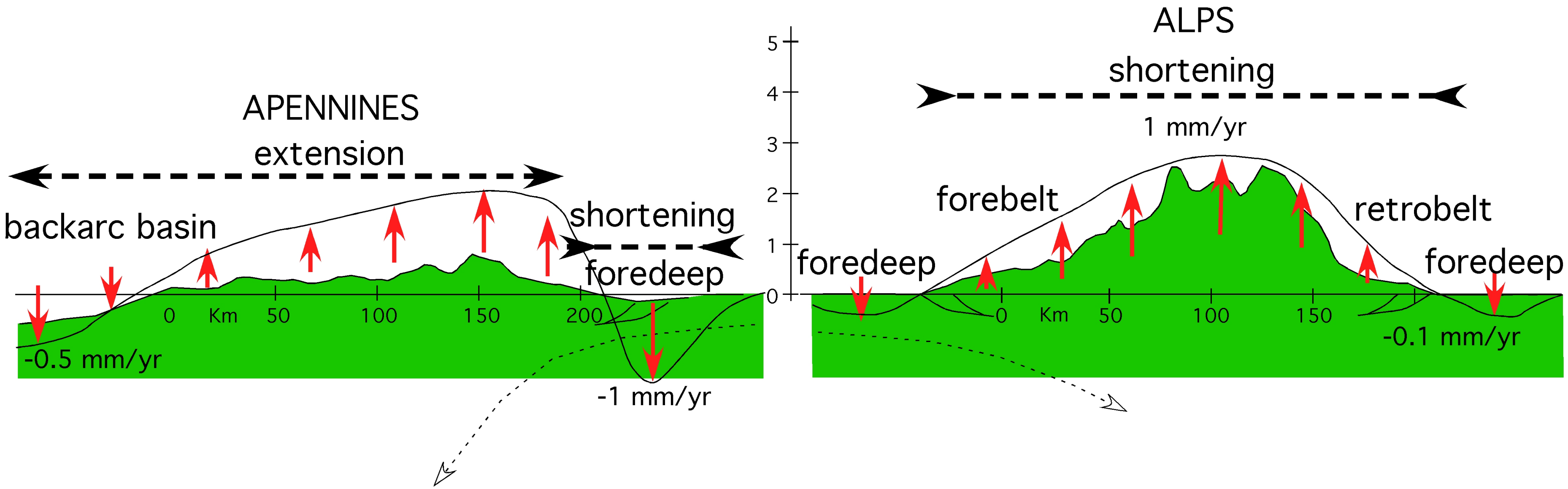

Carminati & Doglioni 2012, ESR

Doglioni et al. 2007 ESR

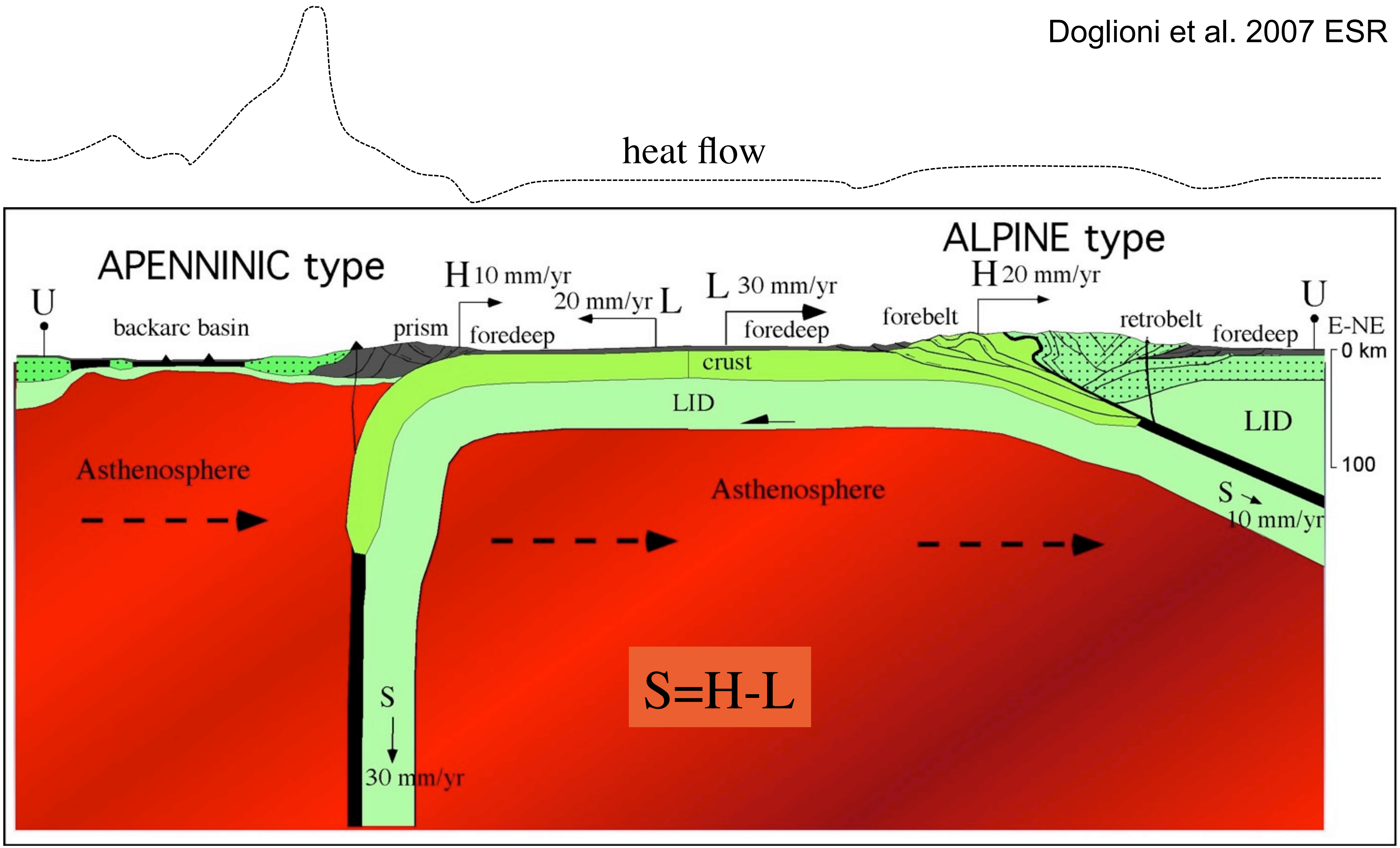

convergence<subduction convergence>subduction

$$< 1 \qquad \frac{\text{CONVERGENCE}}{\text{SHORTENING}} \qquad > 1$$

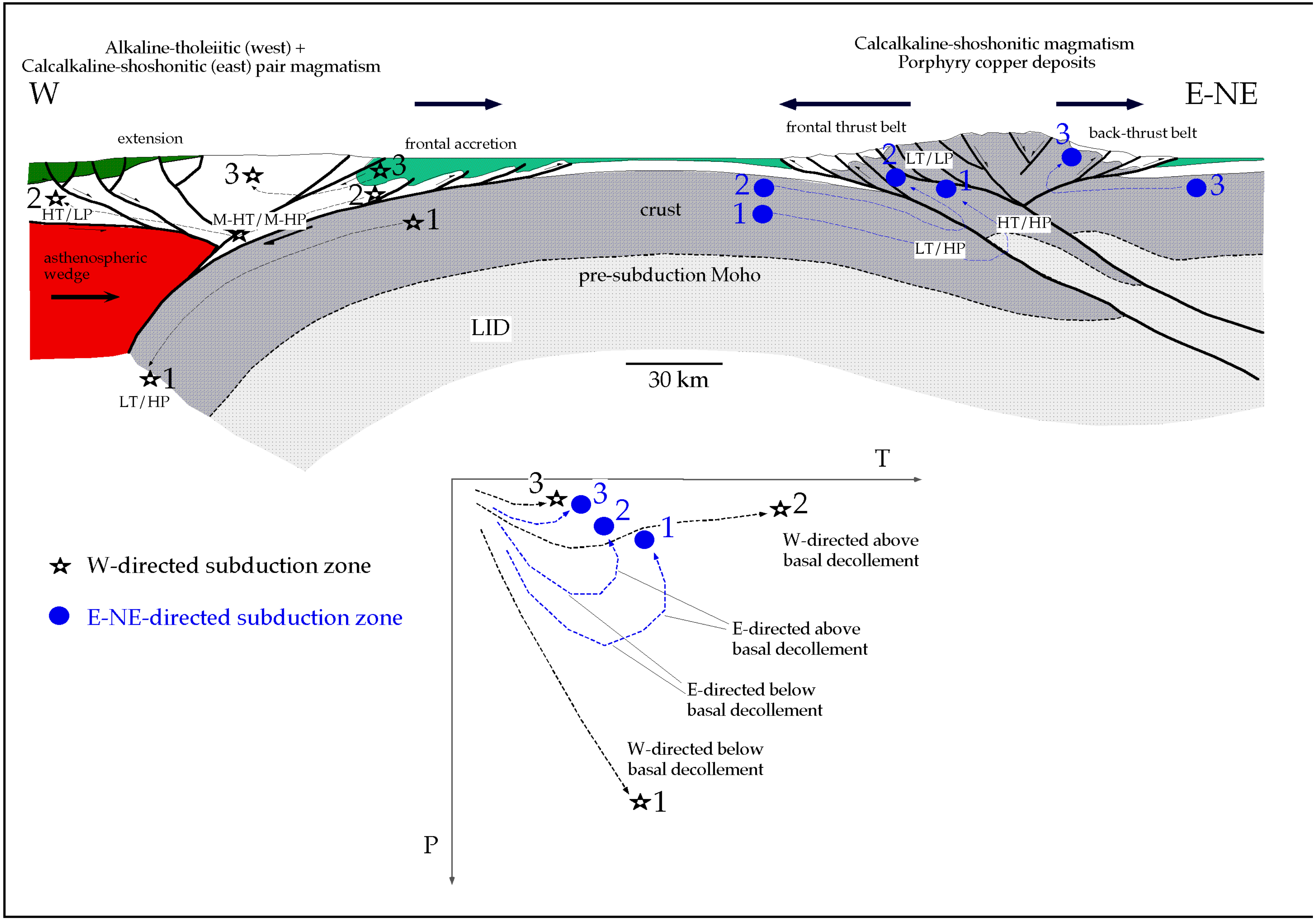

Alkaline-tholeiitic (west) +
Calcalkaline-shoshonitic (east) pair magmatism
Calcalkaline-shoshonitic magmatism
Porphyry copper deposits
W
E-NE
extension
frontal accretion
frontal thrust belt
back-thrust belt
HT/LP
M-HT/M-HP
LT/LP
HT/HP
LT/HP
asthenospheric wedge
crust
pre-subduction Moho
LID
30 km
LT/HP
T
P
W-directed above basal decollement
E-directed above basal decollement
E-directed below basal decollement
W-directed below basal decollement
W-directed subduction zone
E-NE-directed subduction zone

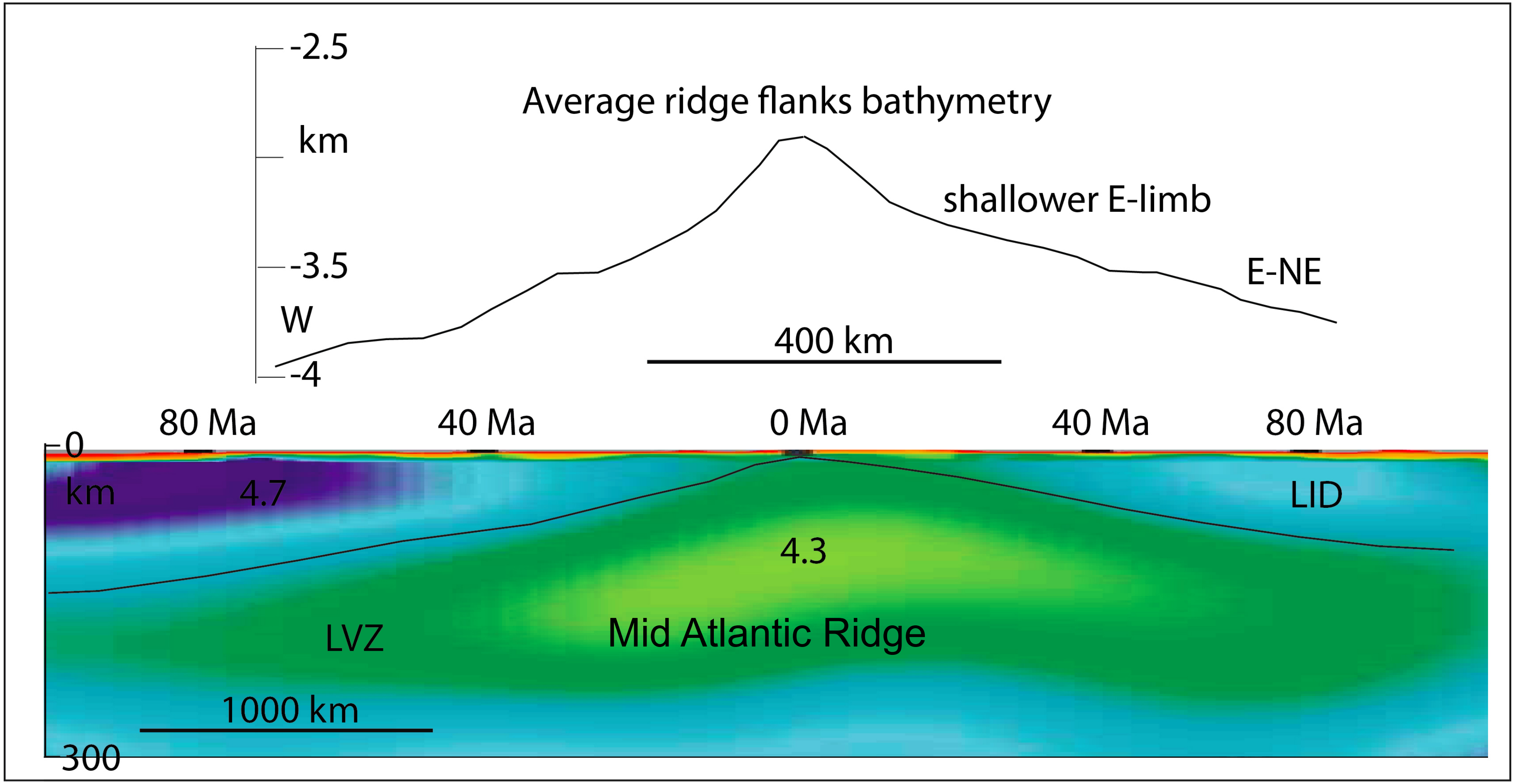

-2.5
km
-3.5
W
-4
Average ridge flanks bathymetry
shallower E-limb
E-NE
400 km
80 Ma
40 Ma
0 Ma
40 Ma
80 Ma
0
km
4.7
LID
4.3
LVZ
Mid Atlantic Ridge
1000 km
300

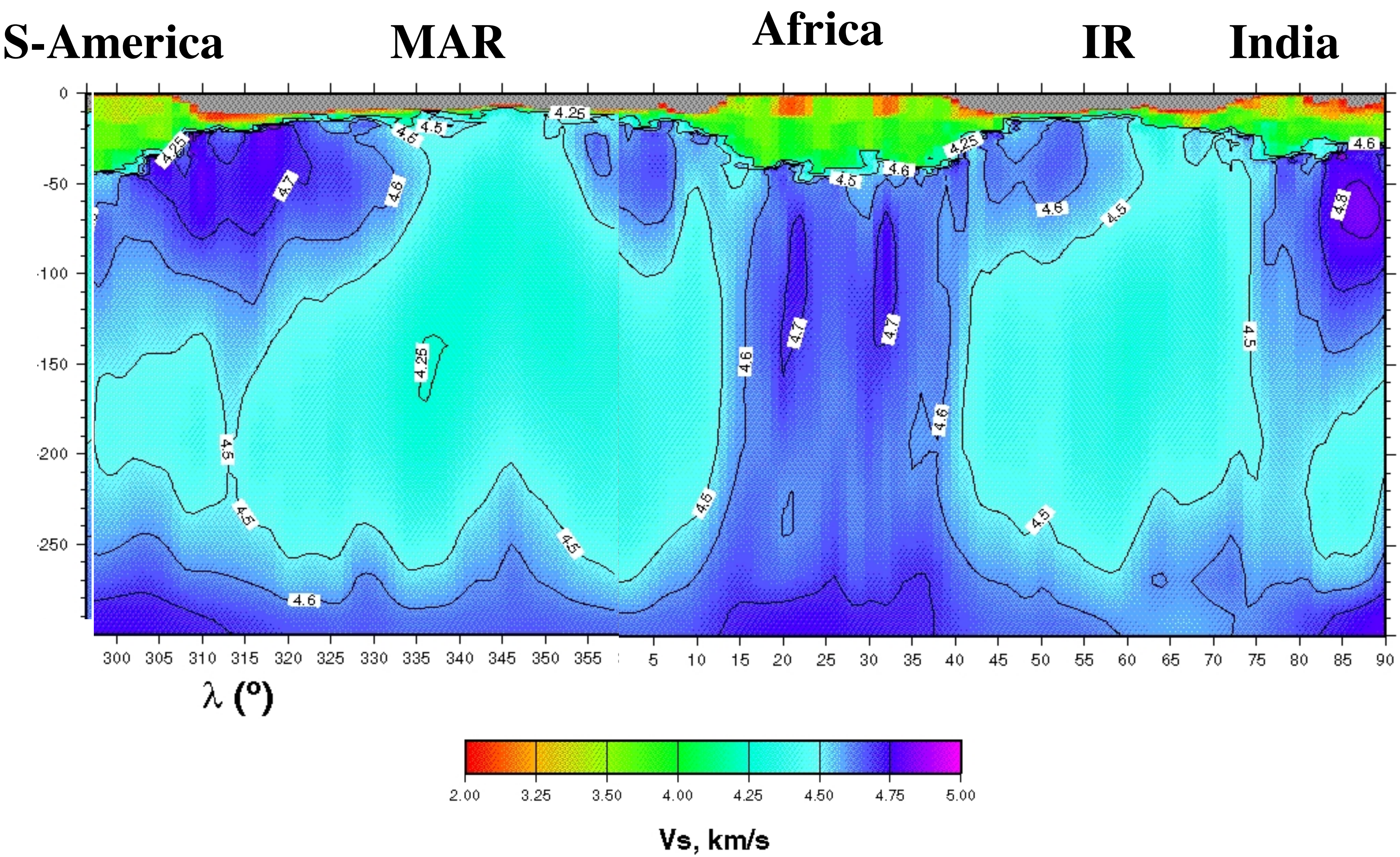

Panza et al. 2010, Geology

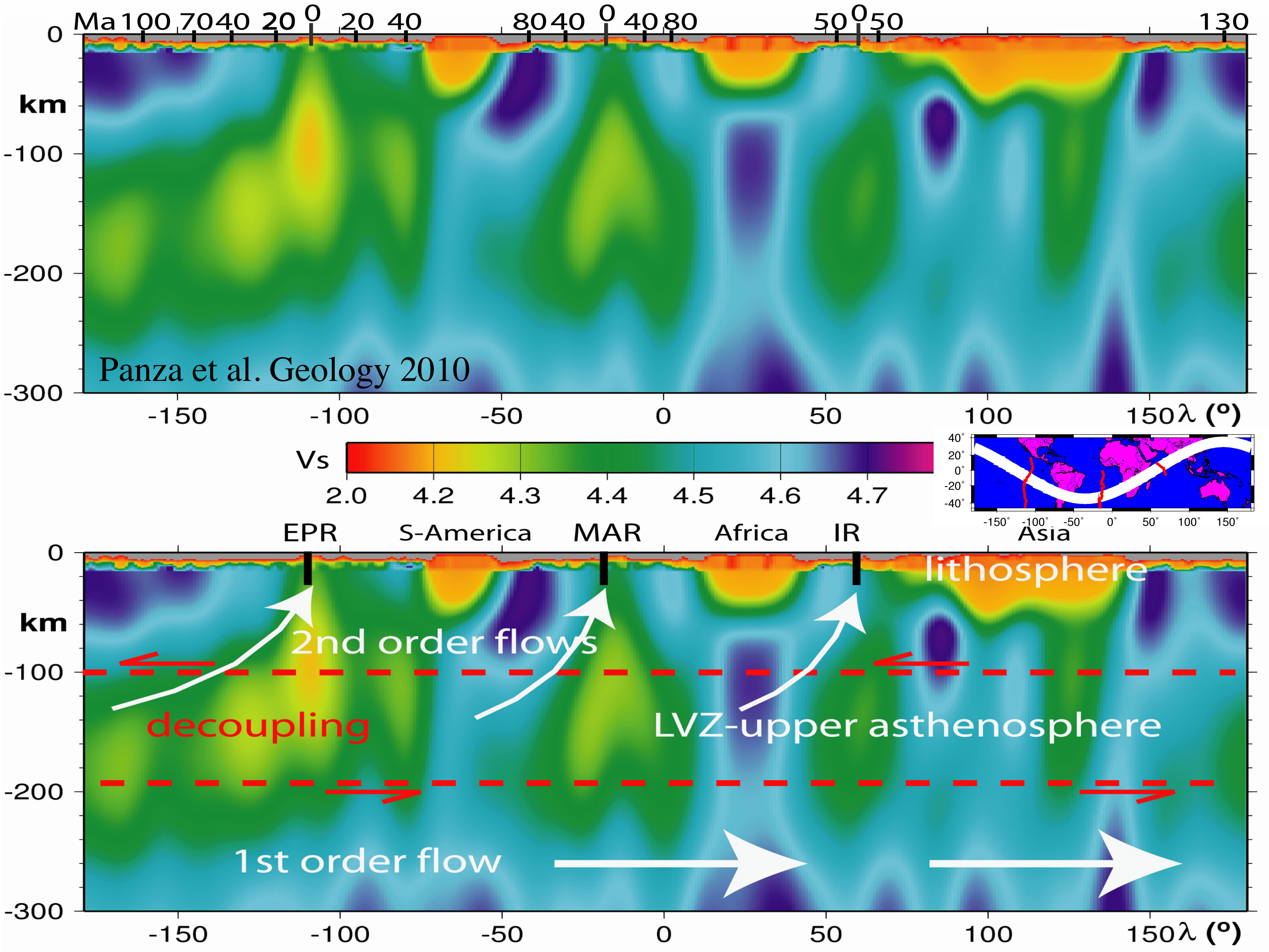

Ma 100 70 40 20 0 20 40 80 40 0 40 80 50 0 50 130
km
Panza et al. Geology 2010
λ (°)
Vs
2.0 4.2 4.3 4.4 4.5 4.6 4.7
EPR
S-America
MAR
Africa
IR
Asia
lithosphere
2nd order flows
decoupling
LVZ-upper asthenosphere
1st order flow

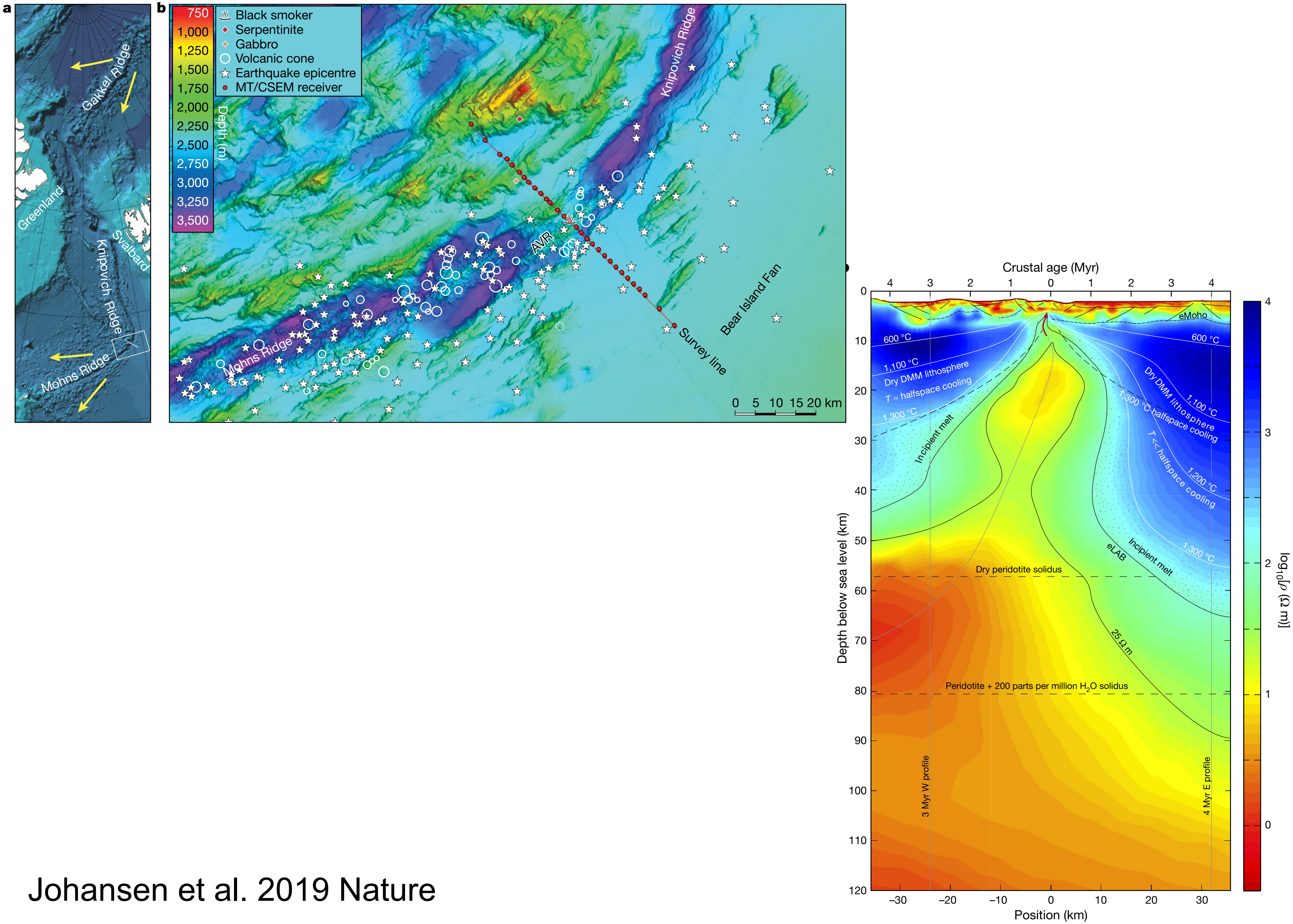

Johansen et al. 2019 Nature

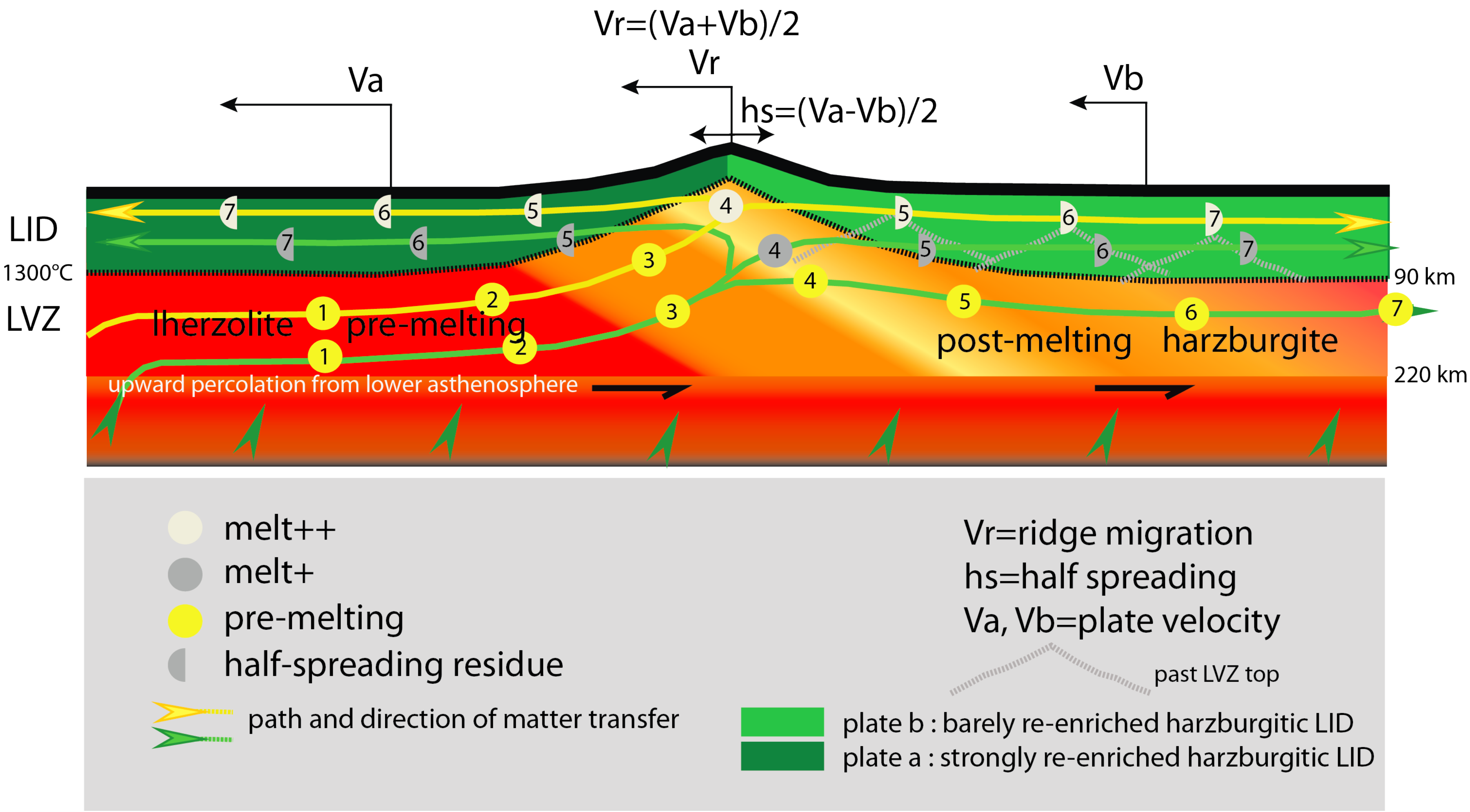

Chalot Prat et al. 2017 Lithos

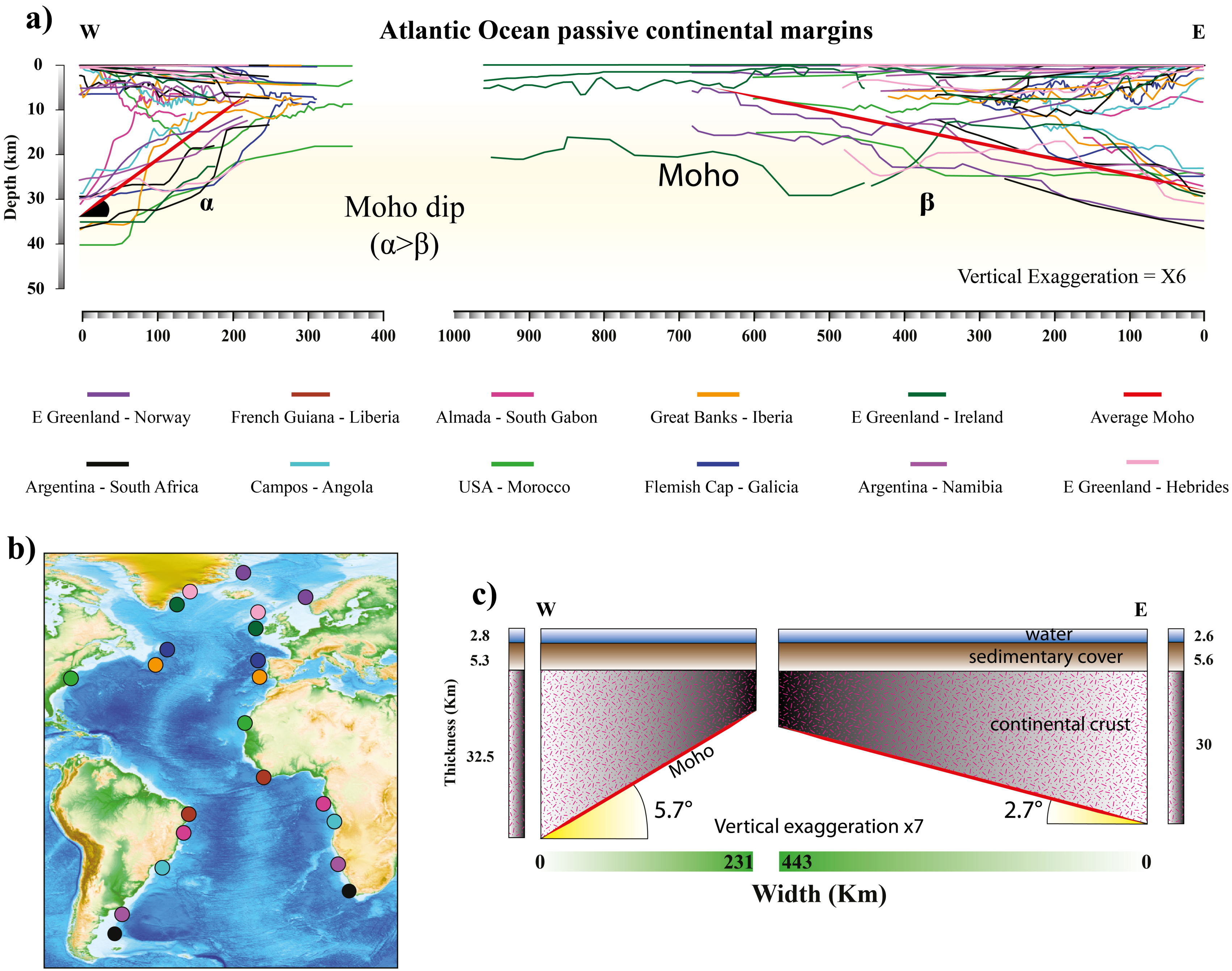

Vangone & Doglioni 2021

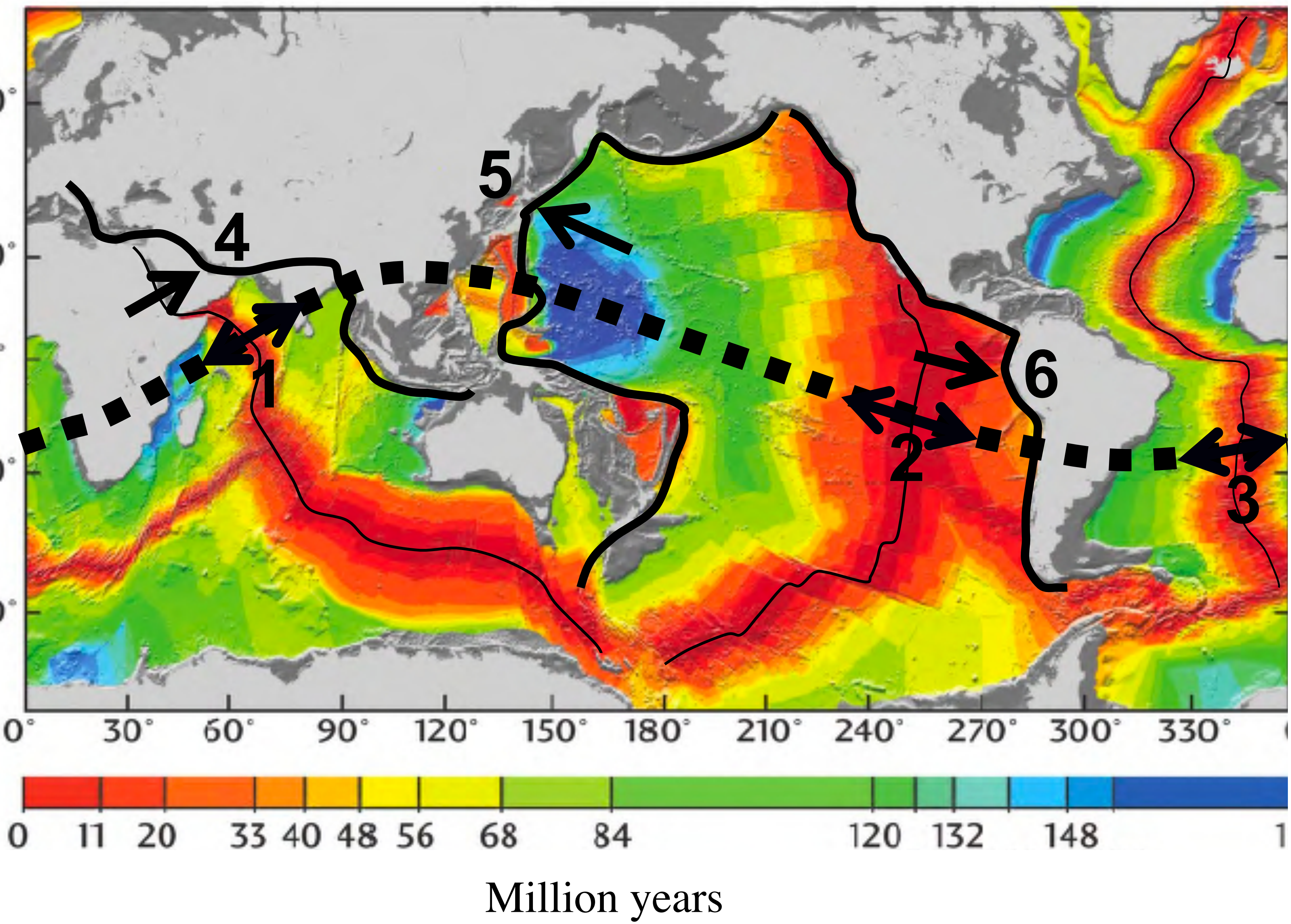

60°
30°
0°
30°
60°
0°
30°
60°
90°
120°
150°
180°
210°
240°
270°
300°
330°
1
2
3
4
5
6
0
11
20
33
40
48
56
68
84
120
132
148
Million years

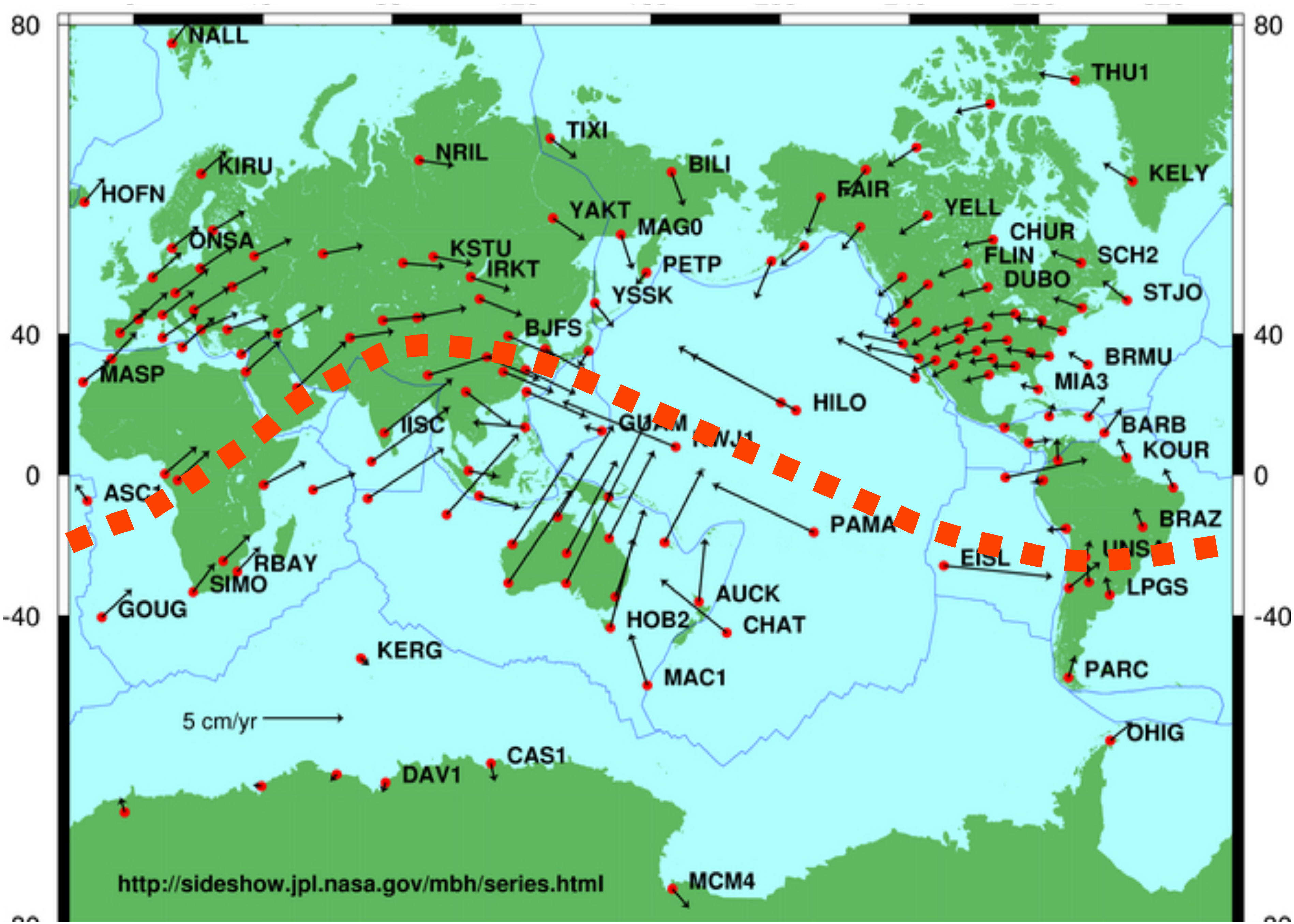
80
40
0
-40
NALL
THU1
TIXI
NRIL
KIRU
BILI
KELY
HOFN
FAIR
YAKT
YELL
MAG0
CHUR
ONSA
SCH2
FLIN
KSTU
PETP
IRKT
DUBO
YSSK
STJO
BJFS
BRMU
MASP
MIA3
HILO
IISC
GUAM
BARB
KWJ1
KOUR
ASC1
BRAZ
PAMA
UNSA
EISL
RBAY
SIMO
AUCK
LPGS
GOUG
CHAT
HOB2
KERG
MAC1
PARC
5 cm/yr
OHIG
CAS1
DAV1
MCM4
http://sideshow.jpl.nasa.gov/mbh/series.html

Past 100 Ma movements

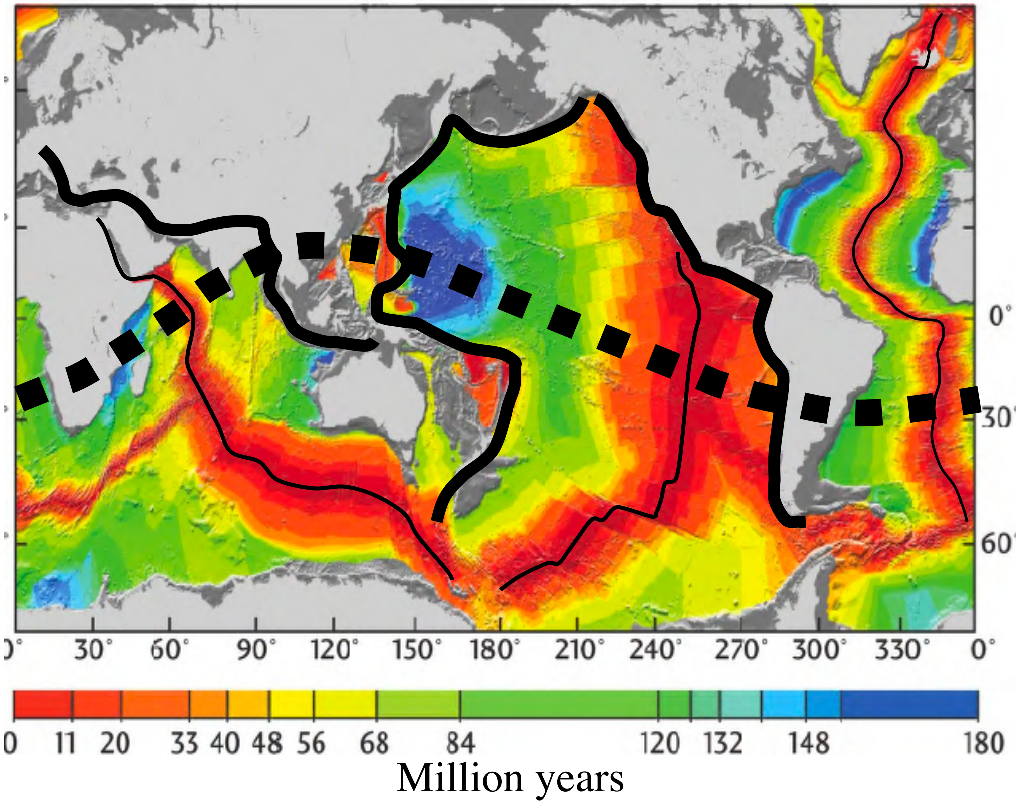

Present movements

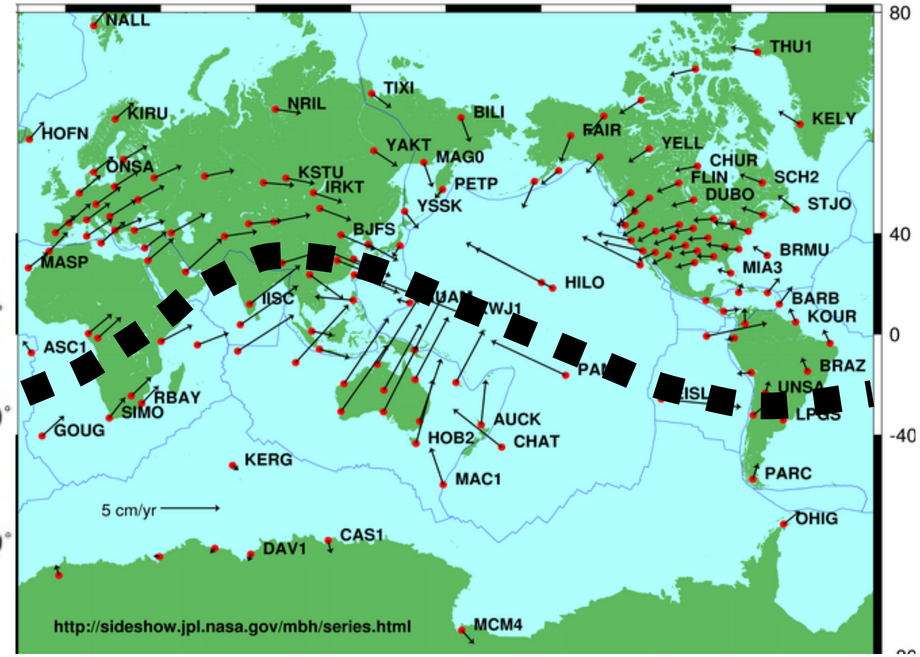

Doglioni & Panza 2015 Advances Geophys.

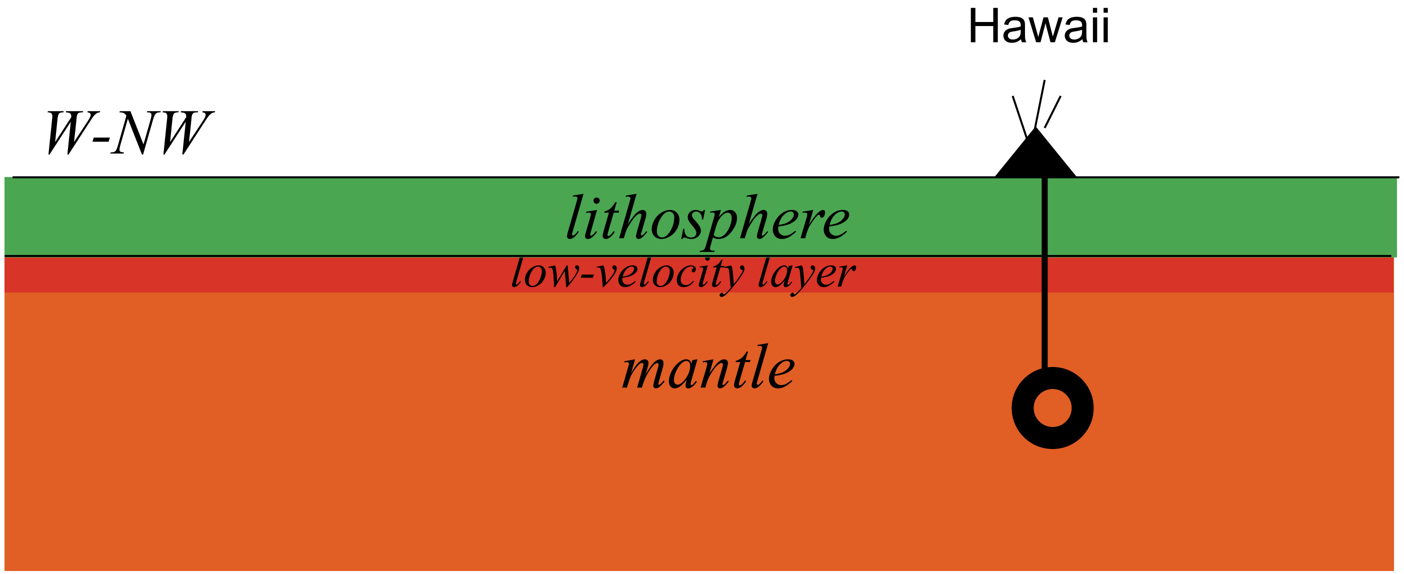
Hawaii
W-NW
lithosphere
low-velocity layer
mantle

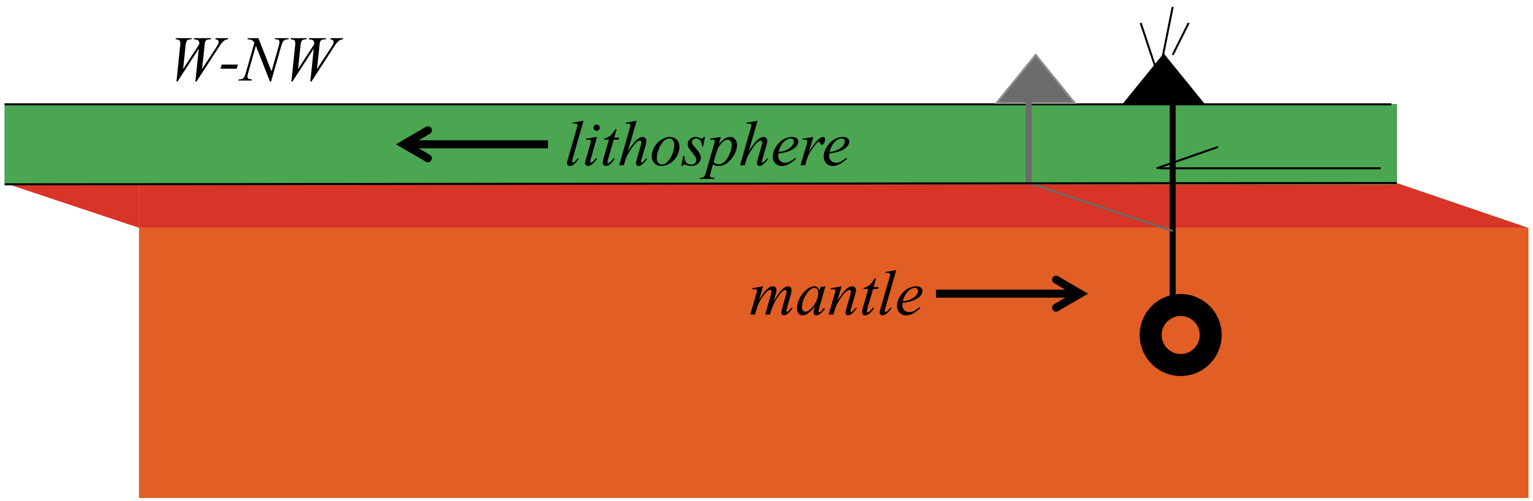

W-NW
lithosphere
mantle

decoupling of the lithosphere

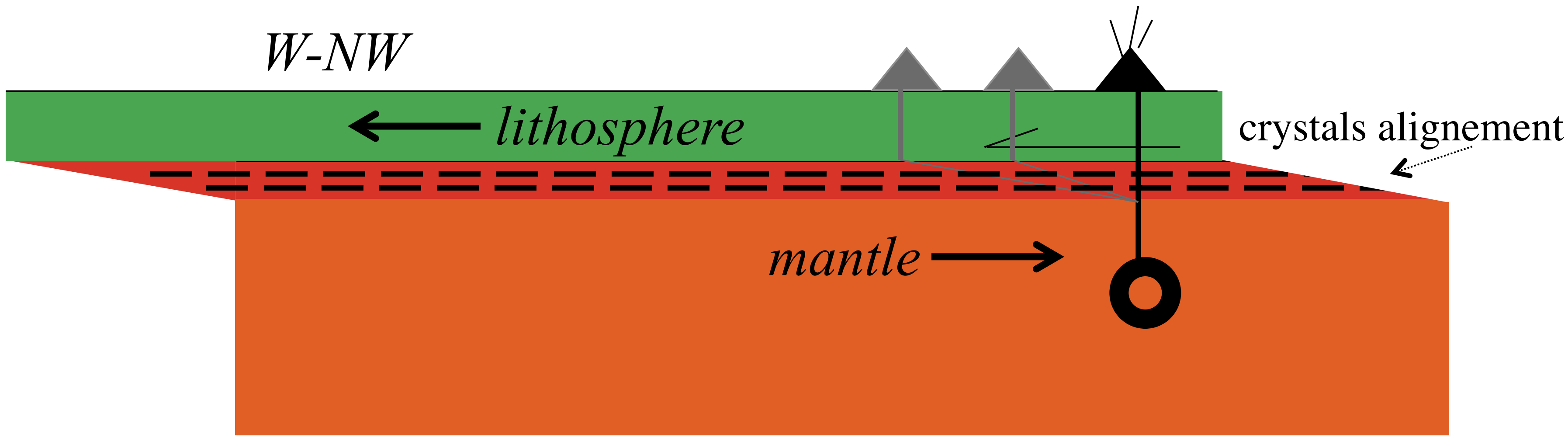

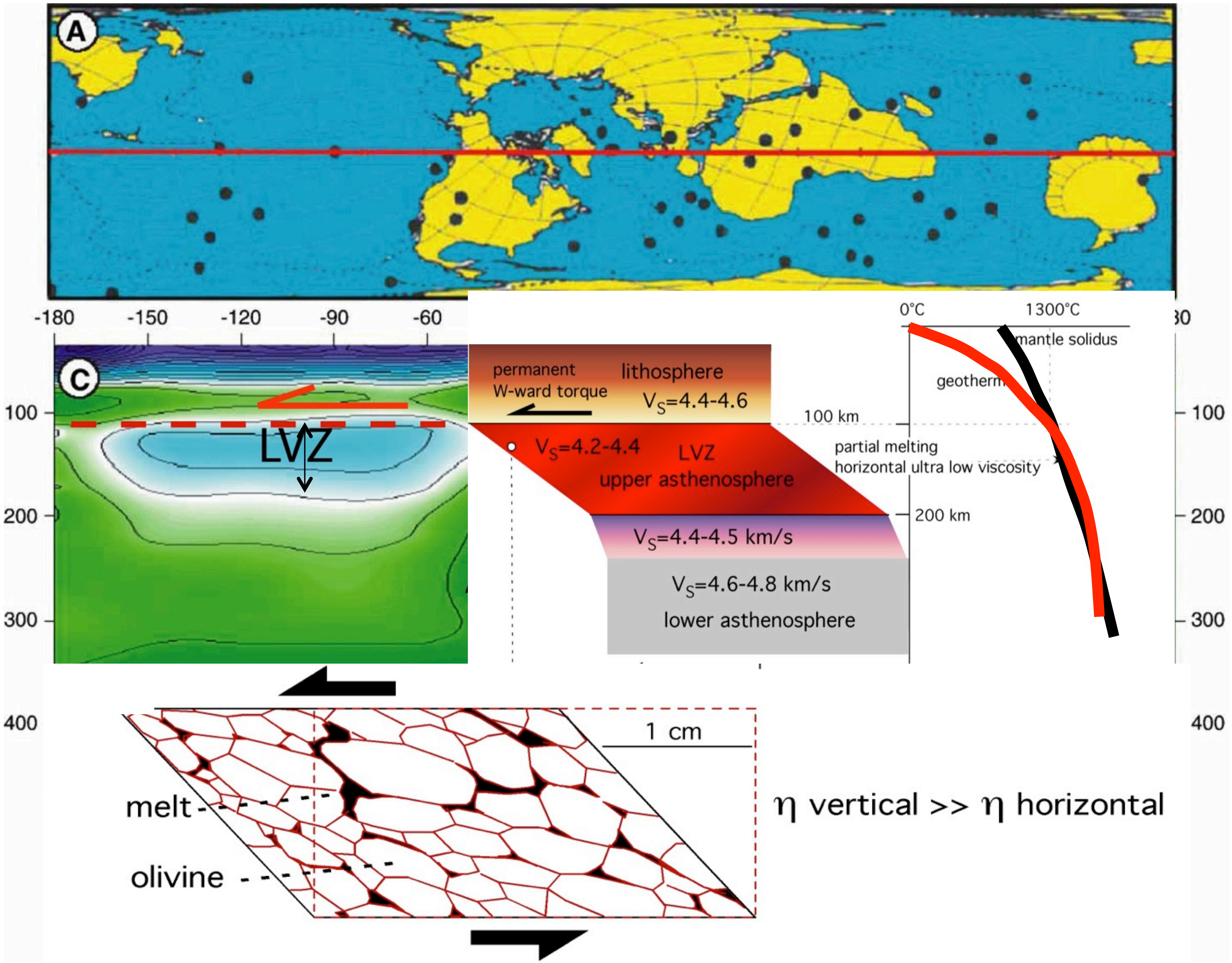

A
-180
-150
-120
-90
-60
C
100
200
300
400
LVZ
permanent
W-ward torque
lithosphere
VS=4.4-4.6
100 km
VS=4.2-4.4
LVZ
upper asthenosphere
VS=4.4-4.5 km/s
VS=4.6-4.8 km/s
lower asthenosphere
200 km
0°C
1300°C
mantle solidus
geotherm
partial melting
horizontal ultra low viscosity
1 cm
melt
olivine
η vertical >> η horizontal

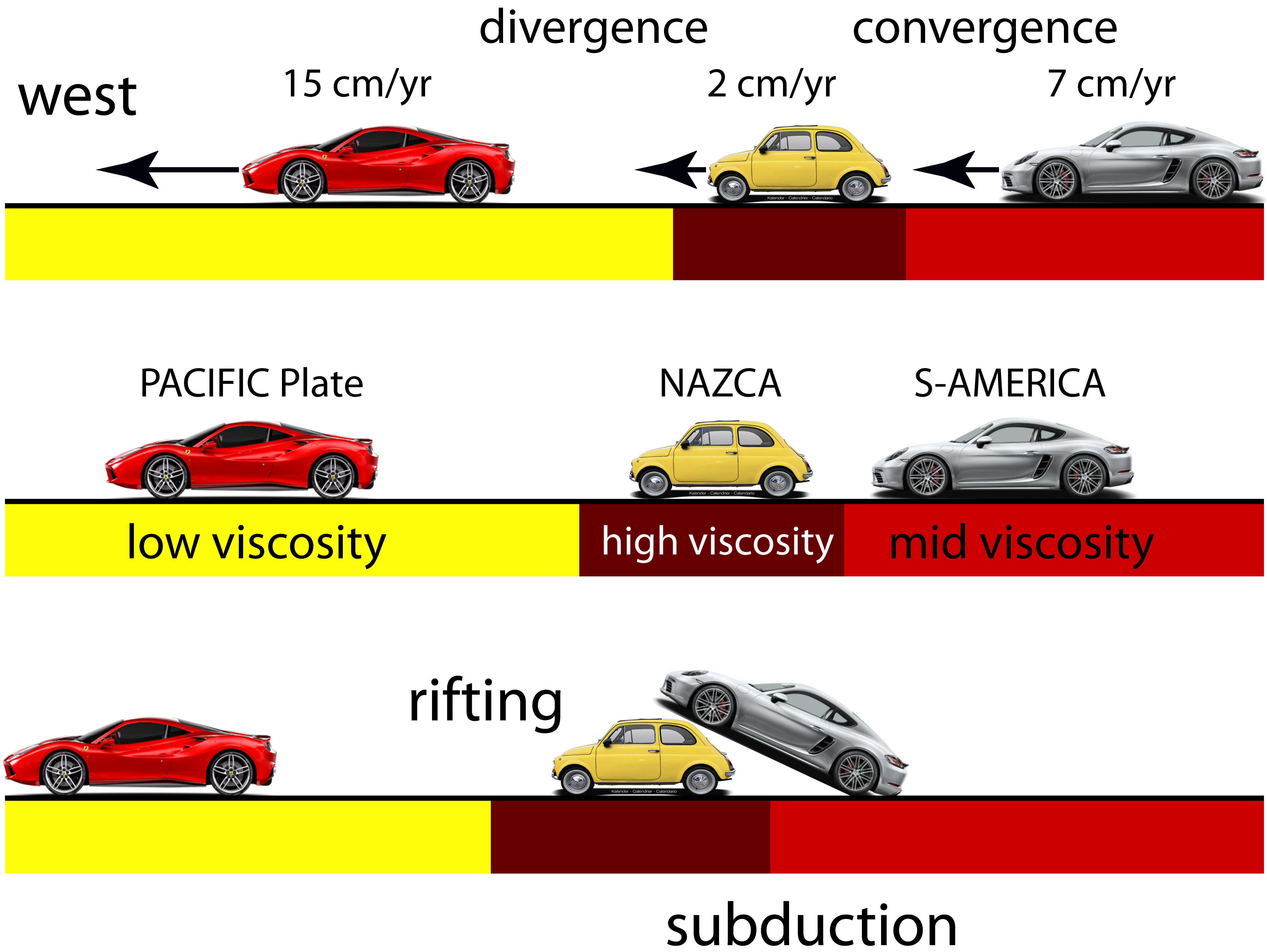

divergence
convergence
west
15 cm/yr
2 cm/yr
7 cm/yr
PACIFIC Plate
NAZCA
S-AMERICA
low viscosity
high viscosity
mid viscosity
rifting
subduction

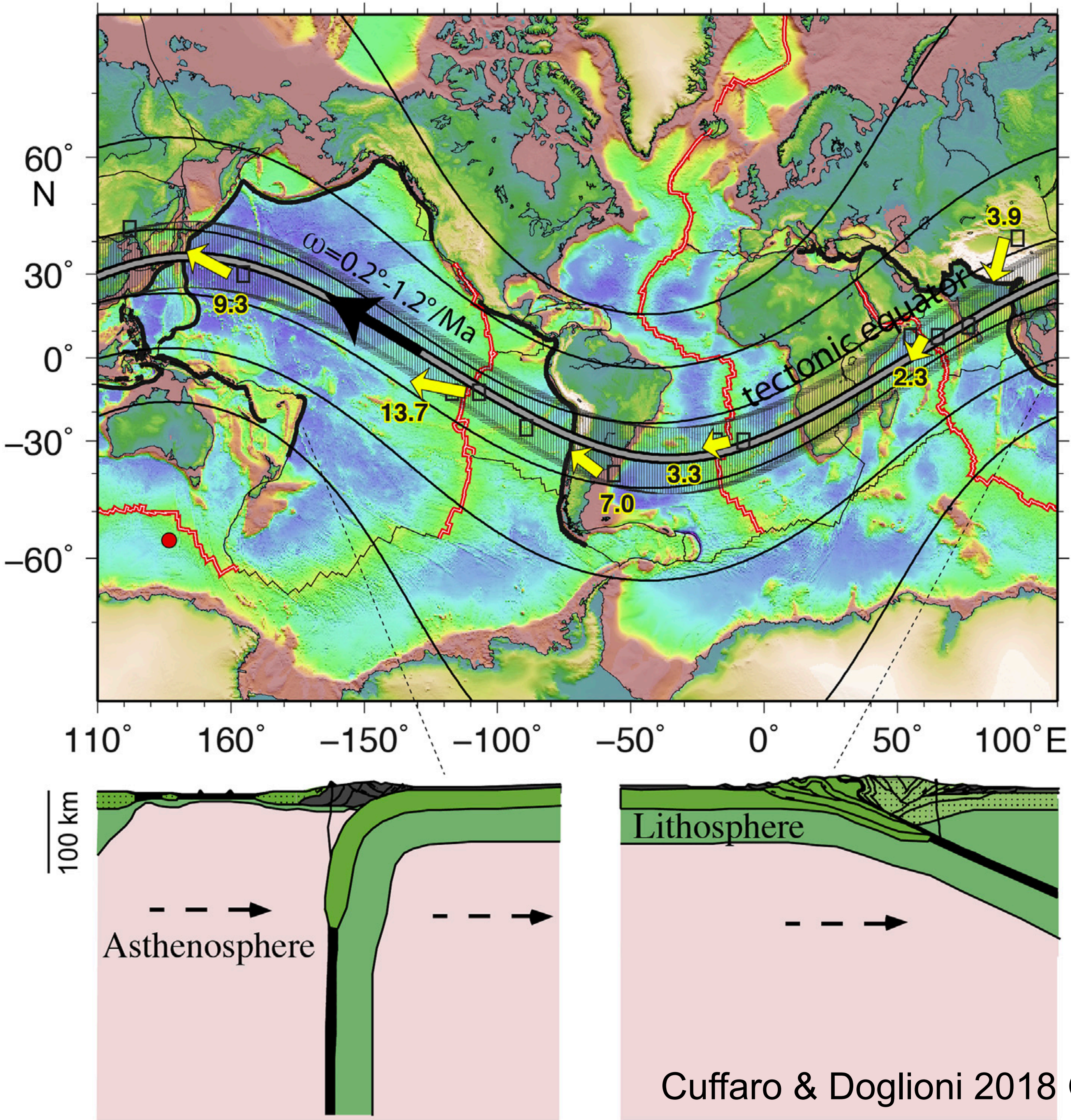

Cuffaro & Doglioni 2018 Gondw. Res.


PLATES MOVE: WHO IS PUSHING THEM??!!

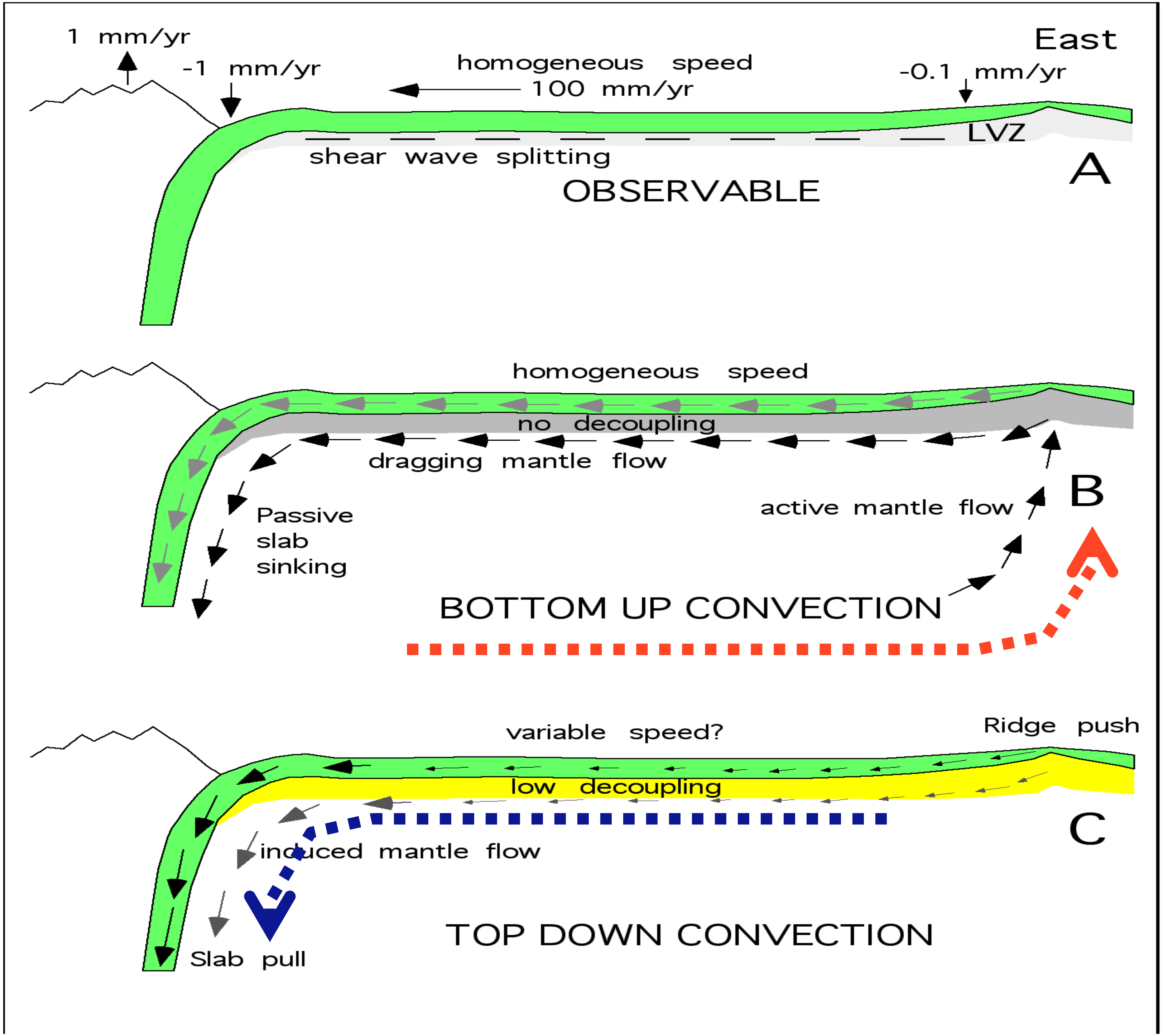

1 mm/yr
-1 mm/yr
homogeneous speed
100 mm/yr
East
-0.1 mm/yr
LVZ
shear wave splitting
OBSERVABLE
A
homogeneous speed
no decoupling
dragging mantle flow
Passive
slab
sinking
active mantle flow
B
BOTTOM UP CONVECTION
variable speed?
Ridge push
low decoupling
C
induced mantle flow
TOP DOWN CONVECTION
Slab pull

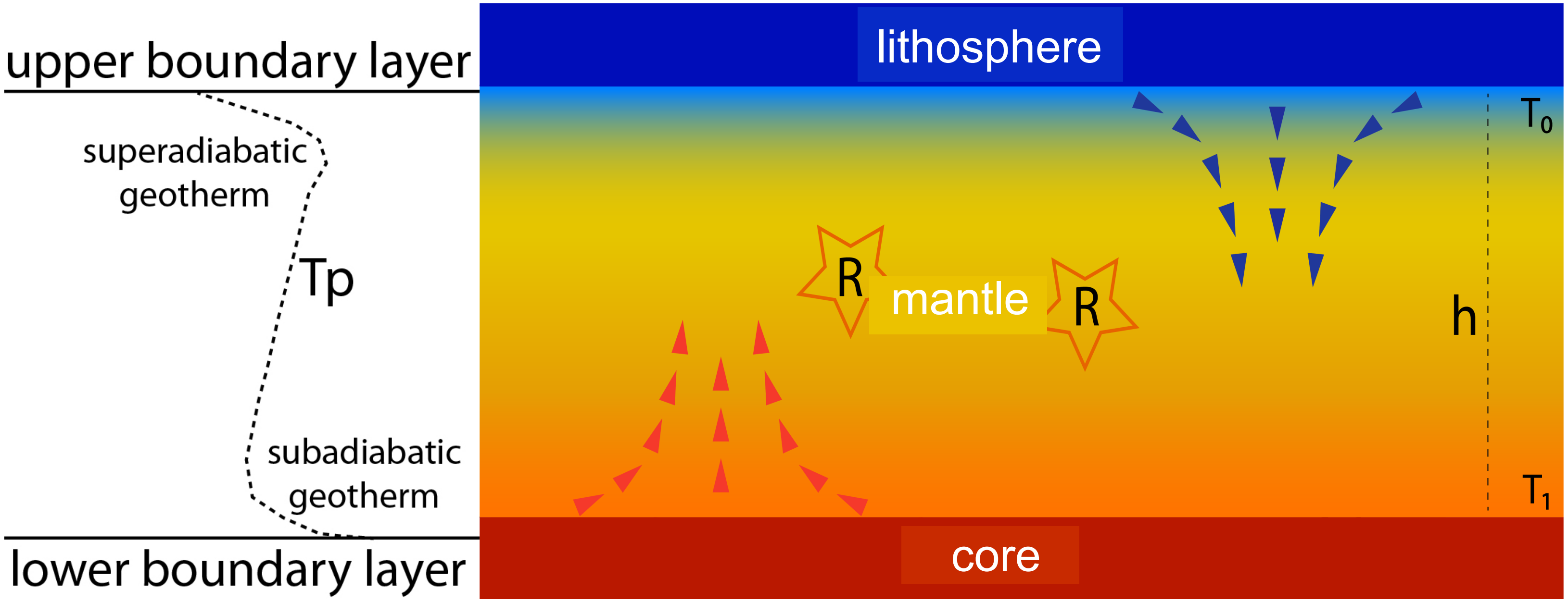

$$Ra = \underbrace{\frac{\rho^2 g\, \alpha\, (T_1 - T_0) h^3}{\eta\, \kappa}}_{\text{basal heat}} \cdot \underbrace{\frac{Q\, h + R\, h^2}{\kappa}}_{\text{internal heat}}$$

Ra Rayleigh number
ρ density
g gravity
α thermal expansion
T temperature
h thickness
η viscosity
κ conductivity
Q heat flow at the base
R internal radiogenic heat

Doglioni & Panza 2015

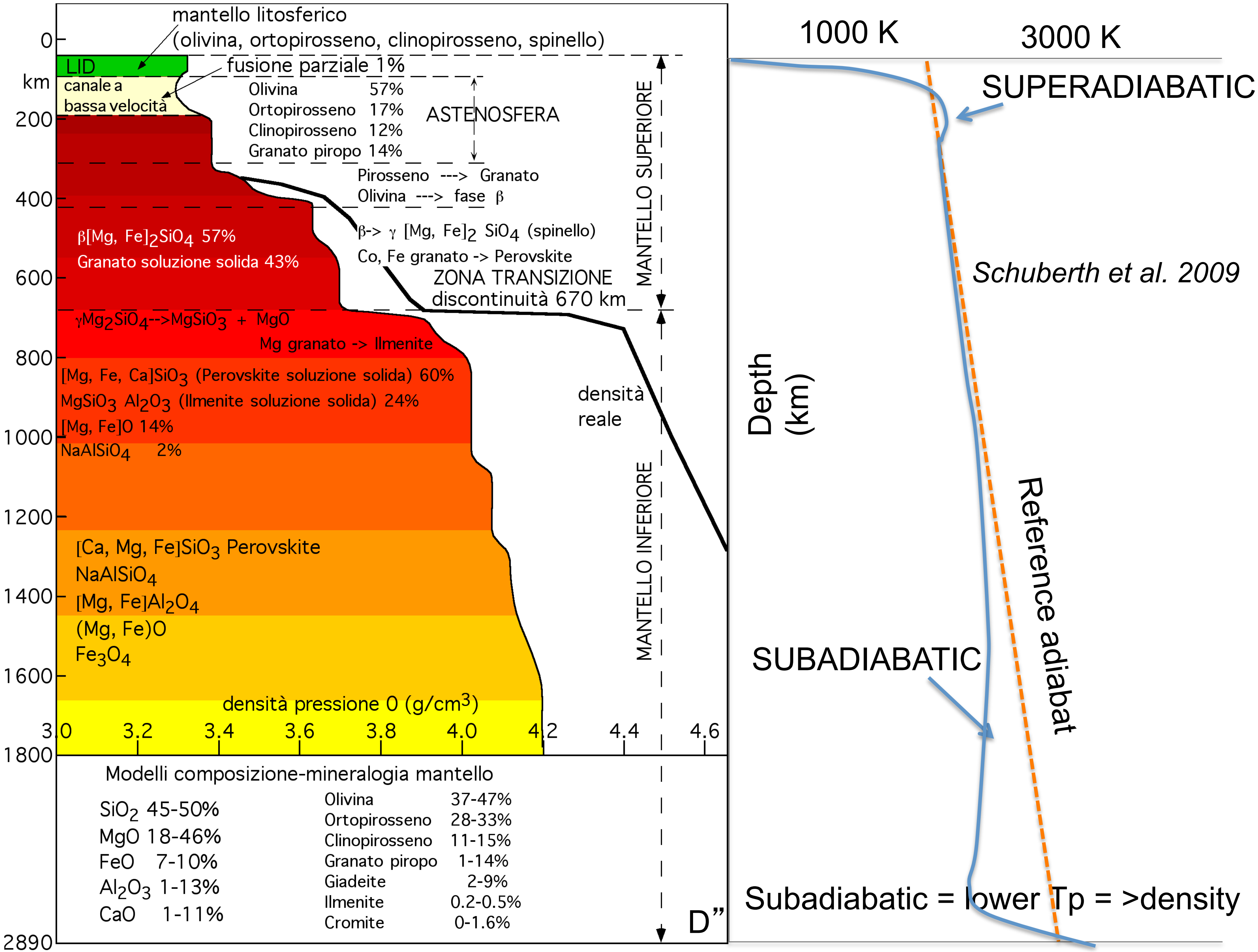

mantello litosferico
(olivina, ortopirosseno, clinopirosseno, spinello)
LID
canale a bassa velocità
fusione parziale 1%
Olivina 57%
Ortopirosseno 17%
Clinopirosseno 12%
Granato piropo 14%
ASTENOSFERA
Pirosseno ---> Granato
Olivina ---> fase β
β[Mg, Fe]2SiO4 57%
Granato soluzione solida 43%
β-> γ [Mg, Fe]2 SiO4 (spinello)
Co, Fe granato -> Perovskite
ZONA TRANSIZIONE
discontinuità 670 km
MANTELLO SUPERIORE
γMg2SiO4-->MgSiO3 + MgO
Mg granato -> Ilmenite
[Mg, Fe, Ca]SiO3 (Perovskite soluzione solida) 60%
MgSiO3 Al2O3 (Ilmenite soluzione solida) 24%
[Mg, Fe]O 14%
NaAlSiO4 2%
densità reale
MANTELLO INFERIORE
[Ca, Mg, Fe]SiO3 Perovskite
NaAlSiO4
[Mg, Fe]Al2O4
(Mg, Fe)O
Fe3O4
densità pressione 0 (g/cm3)
3.0 3.2 3.4 3.6 3.8 4.0 4.2 4.4 4.6
0 km 200 400 600 800 1000 1200 1400 1600 1800 2890
Modelli composizione-mineralogia mantello
SiO2 45-50%
MgO 18-46%
FeO 7-10%
Al2O3 1-13%
CaO 1-11%
Olivina 37-47%
Ortopirosseno 28-33%
Clinopirosseno 11-15%
Granato piropo 1-14%
Giadeite 2-9%
Ilmenite 0.2-0.5%
Cromite 0-1.6%
D”
1000 K
3000 K
SUPERADIABATIC
Schuberth et al. 2009
Depth (km)
Reference adiabat
SUBADIABATIC
Subadiabatic = lower Tp = >density

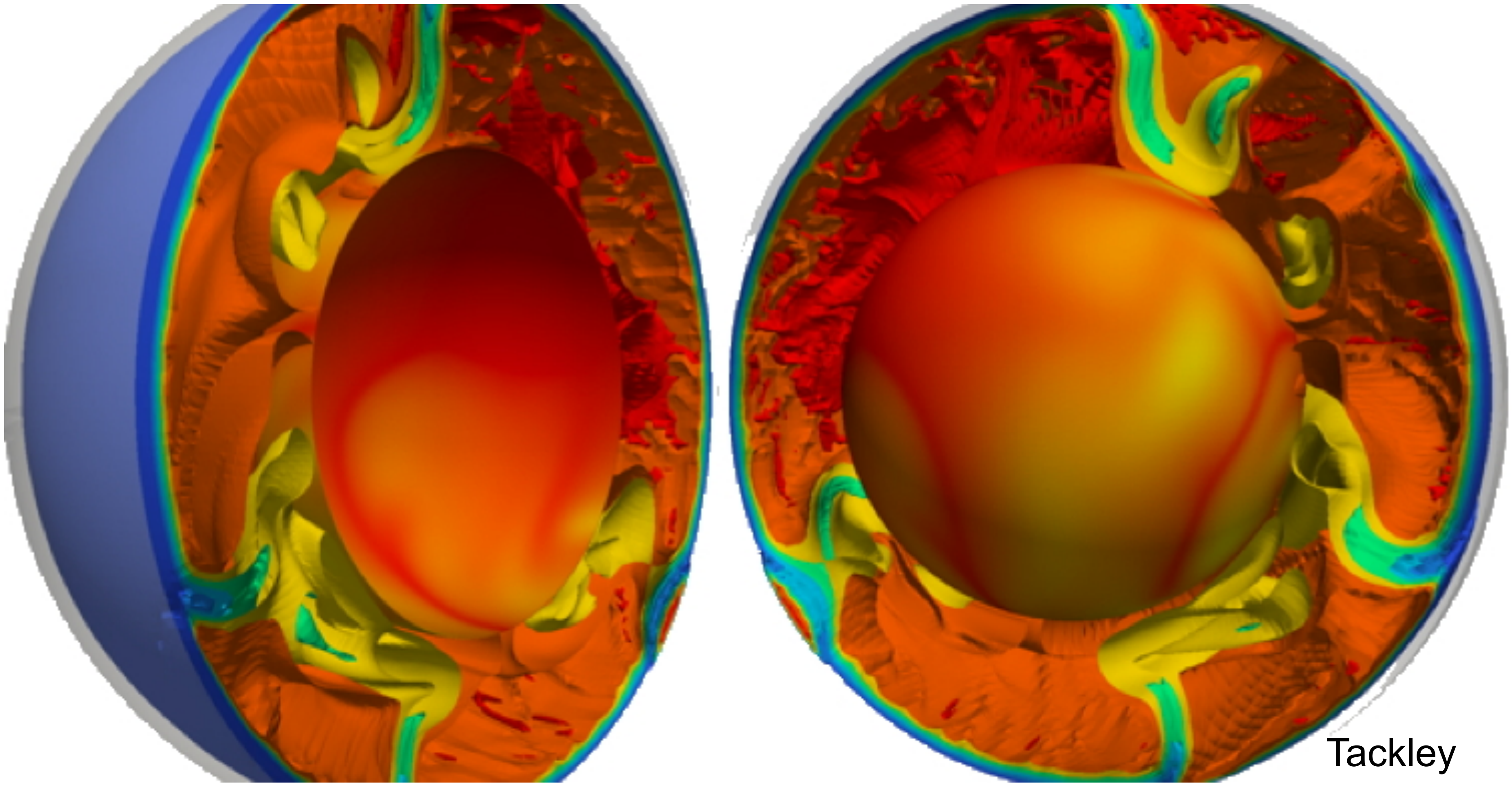

Tackley

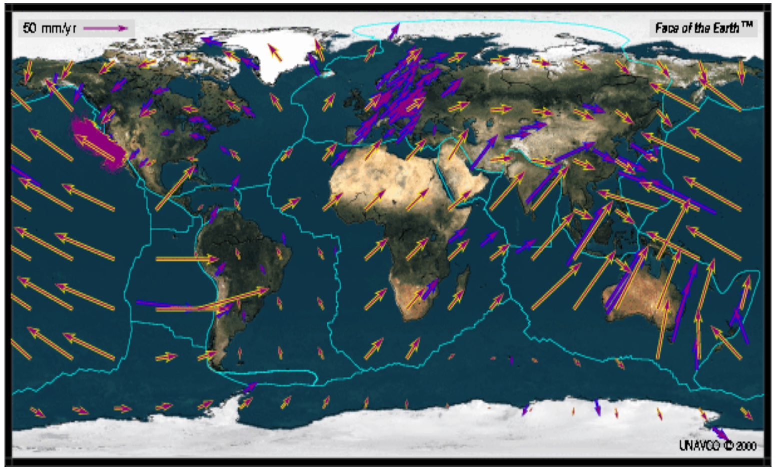

Slab pull = 10^{13} N m^{-1}

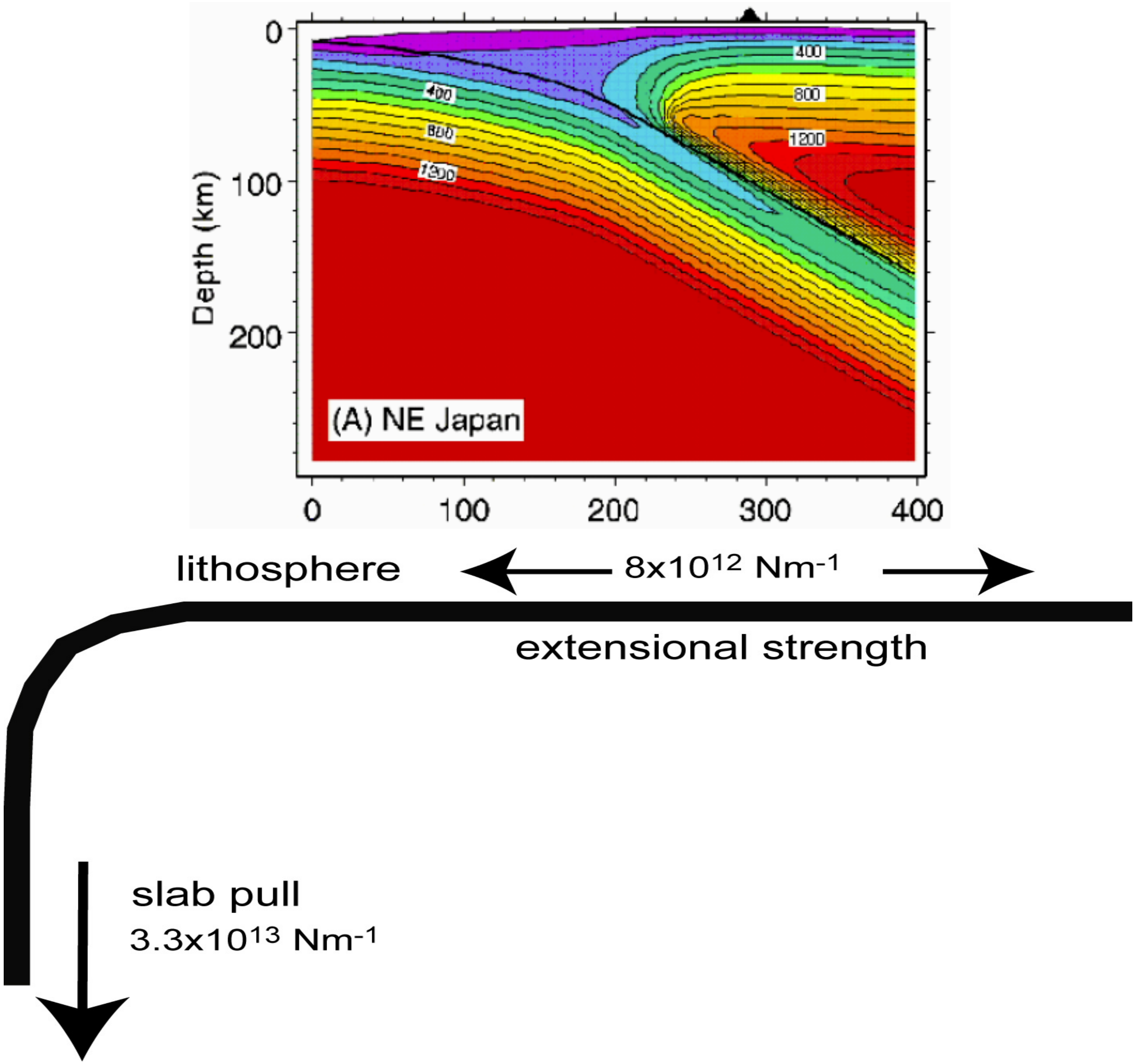

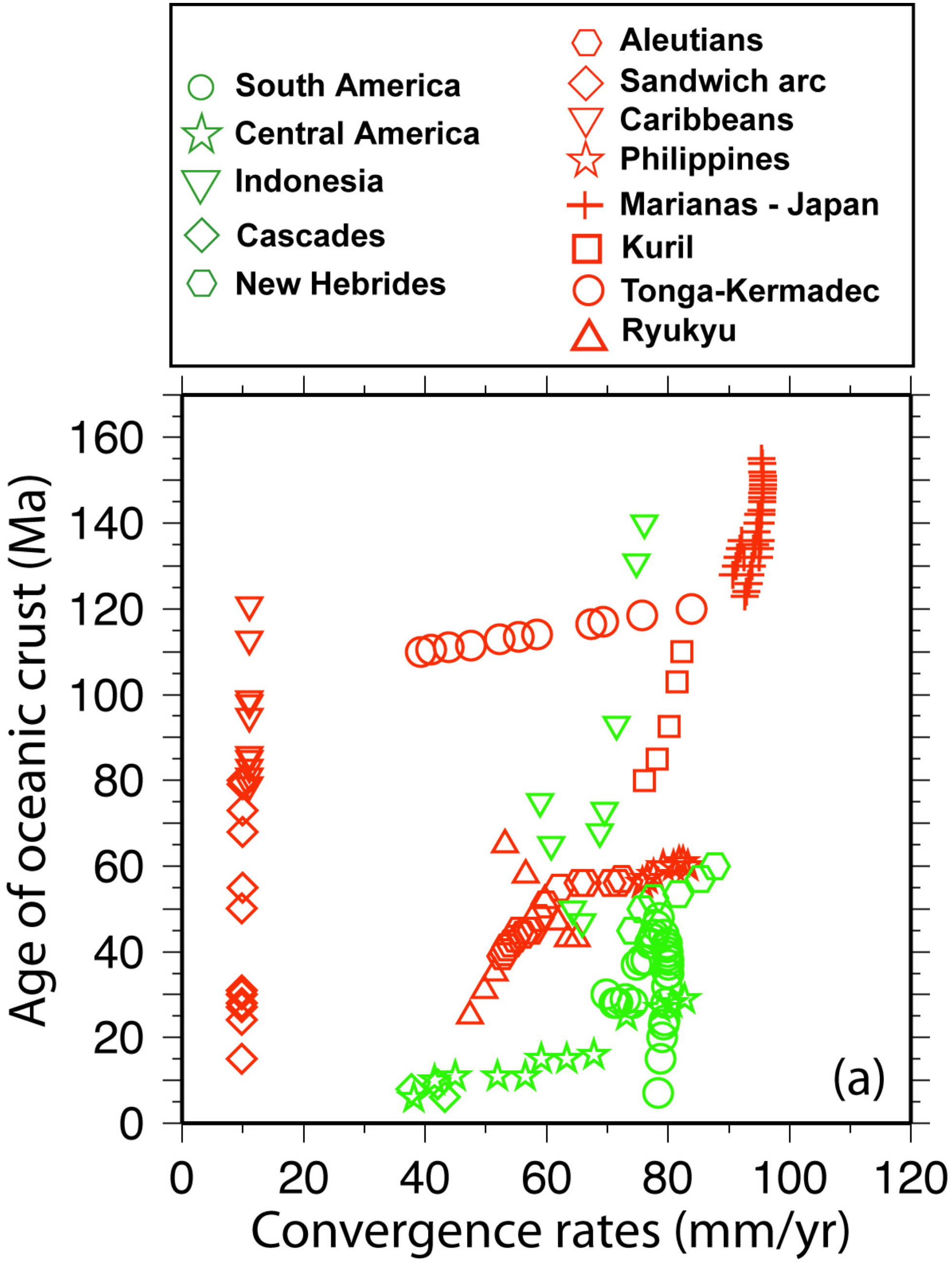

Cruciani et al., 2005 EPSL

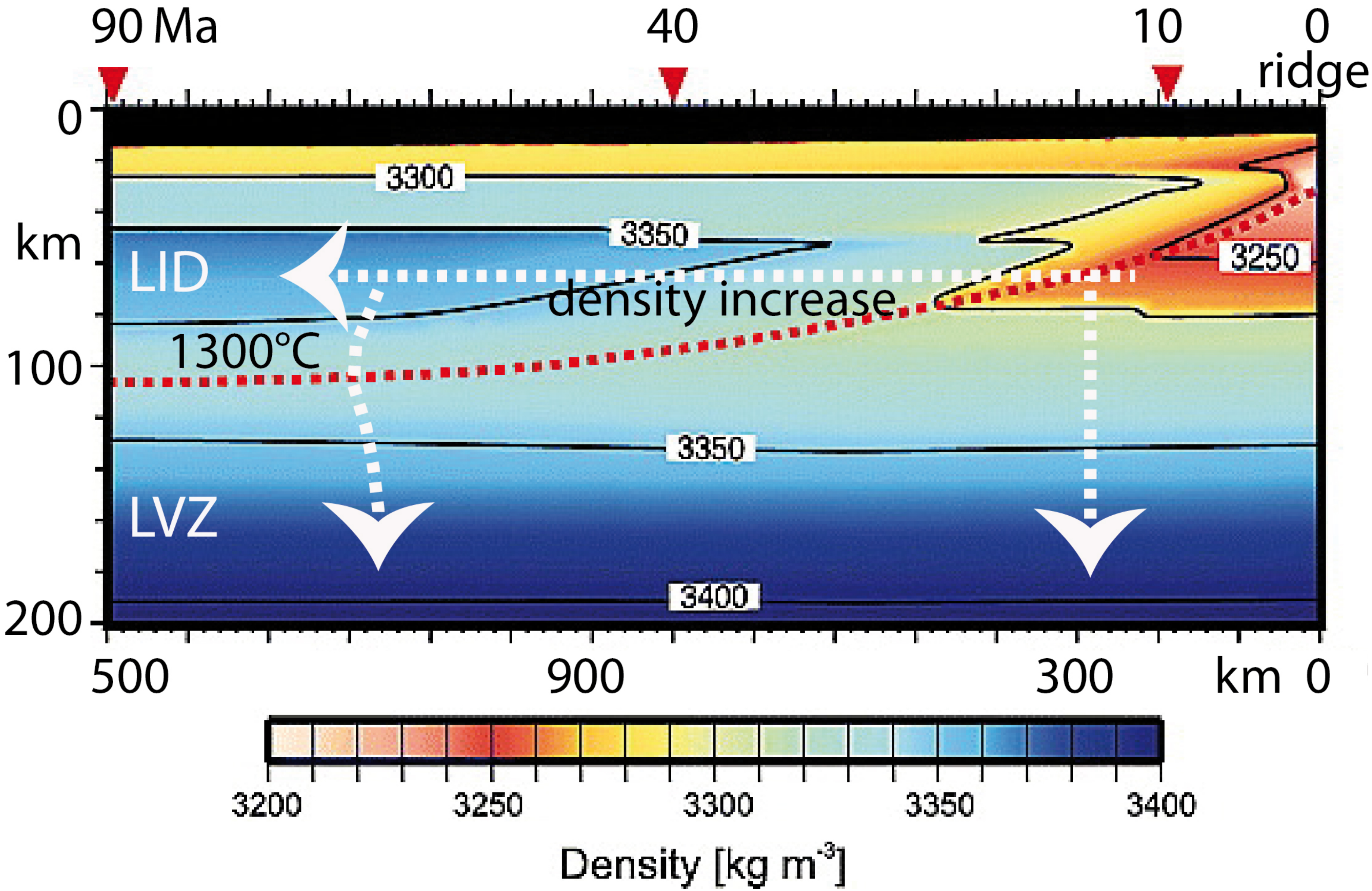

Modified after Afonso et al. 2008 G3

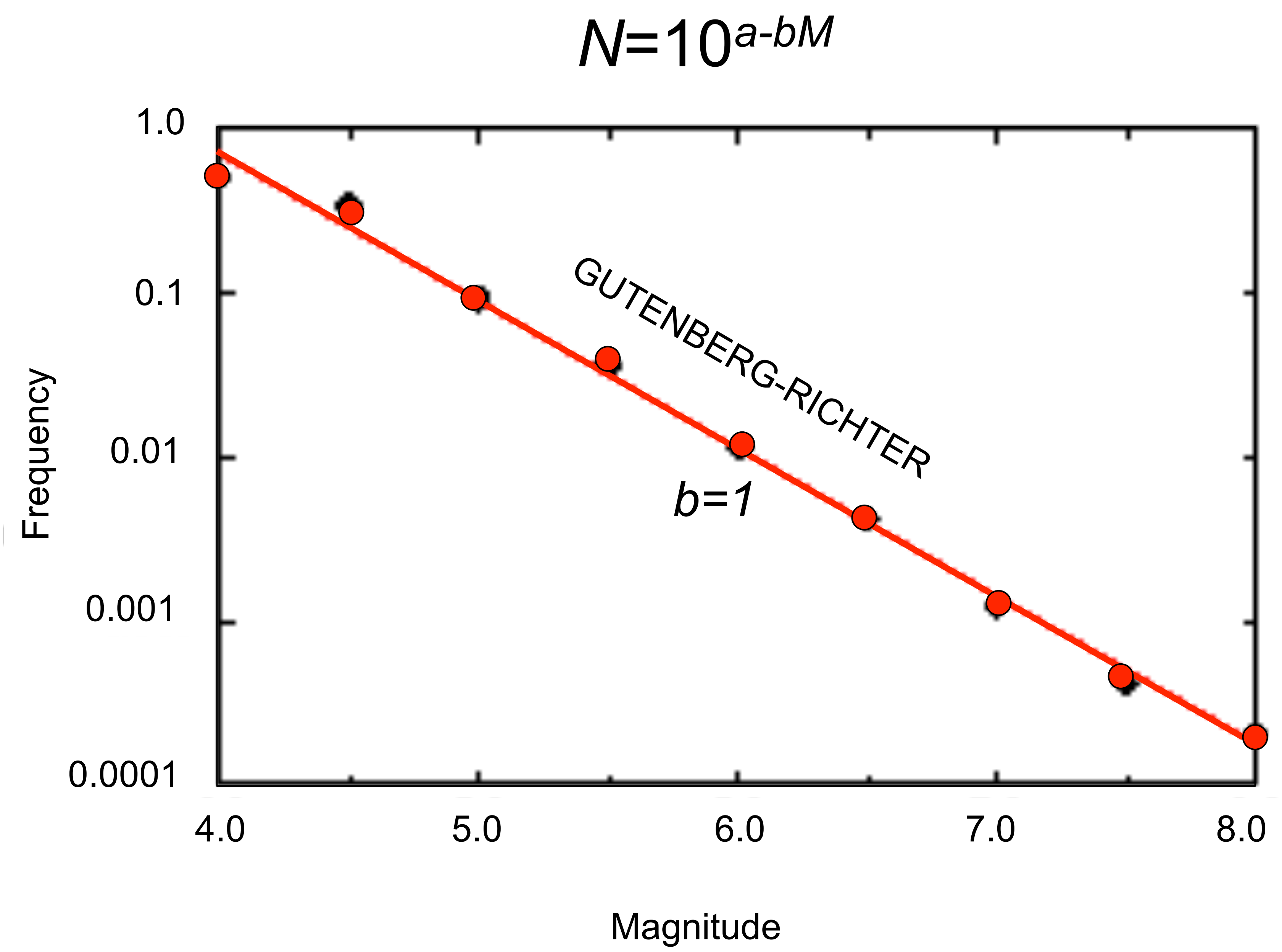

$N=10^{a-bM}$
1.0
0.1
0.01
0.001
0.0001
Frequency
GUTENBERG-RICHTER
$b=1$
4.0
5.0
6.0
7.0
8.0
Magnitude

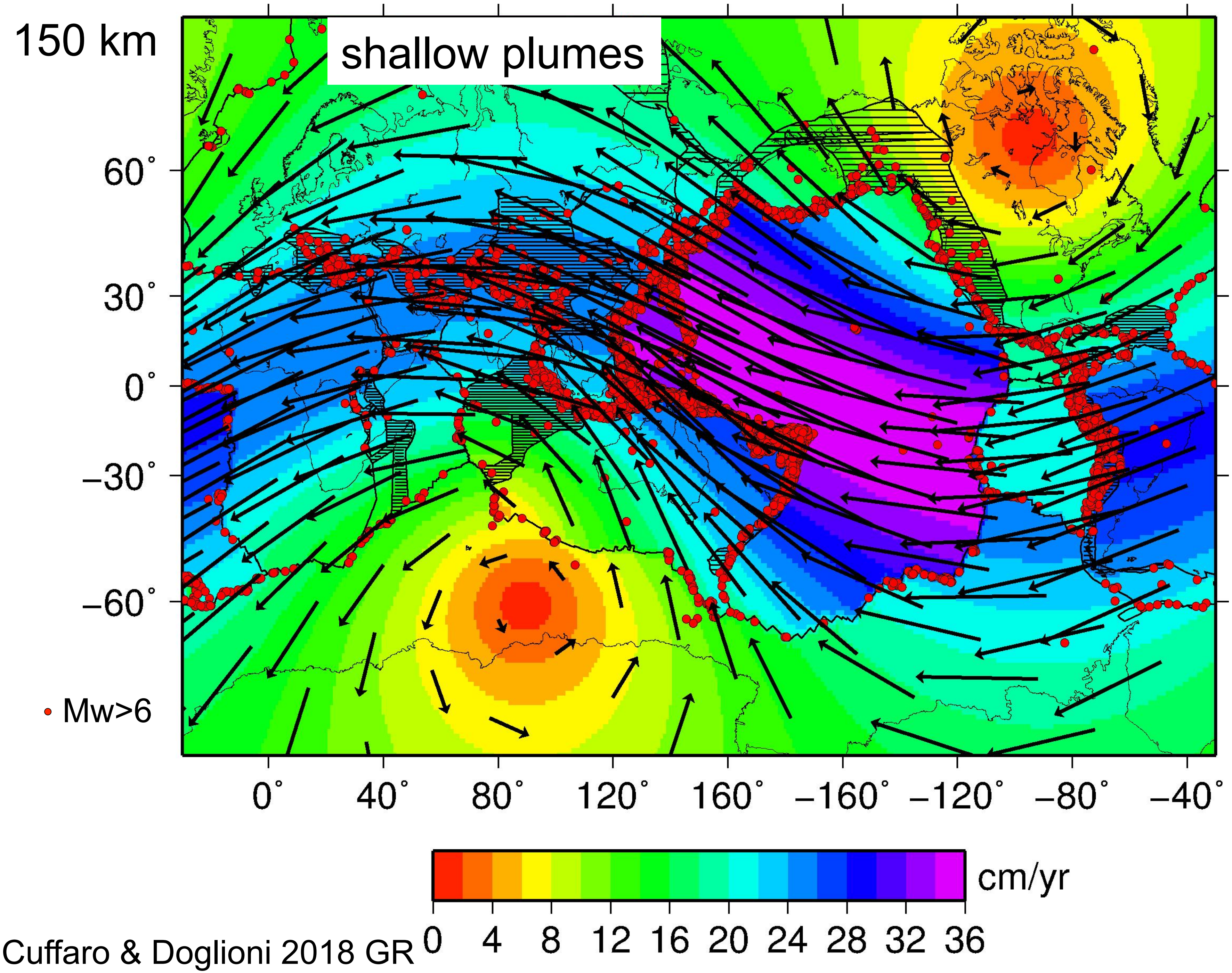
150 km
shallow plumes
60˚
30˚
0˚
−30˚
−60˚
0˚
40˚
80˚
120˚
160˚
−160˚
−120˚
−80˚
−40˚
Mw>6
0
4
8
12
16
20
24
28
32
36
cm/yr
Cuffaro & Doglioni 2018 GR

Global seismicity

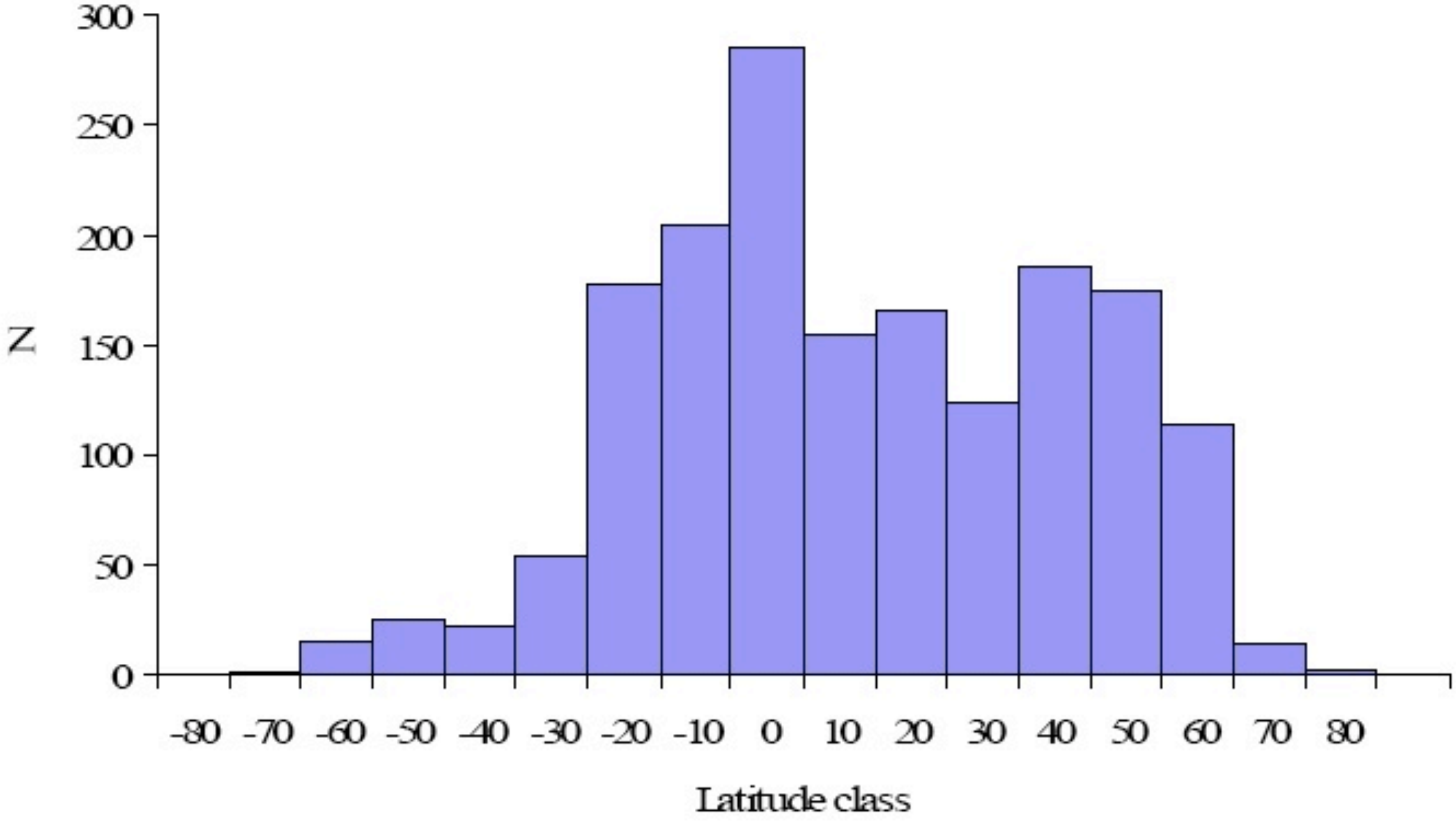

Riguzzi et al., 2010 Tectonophysics

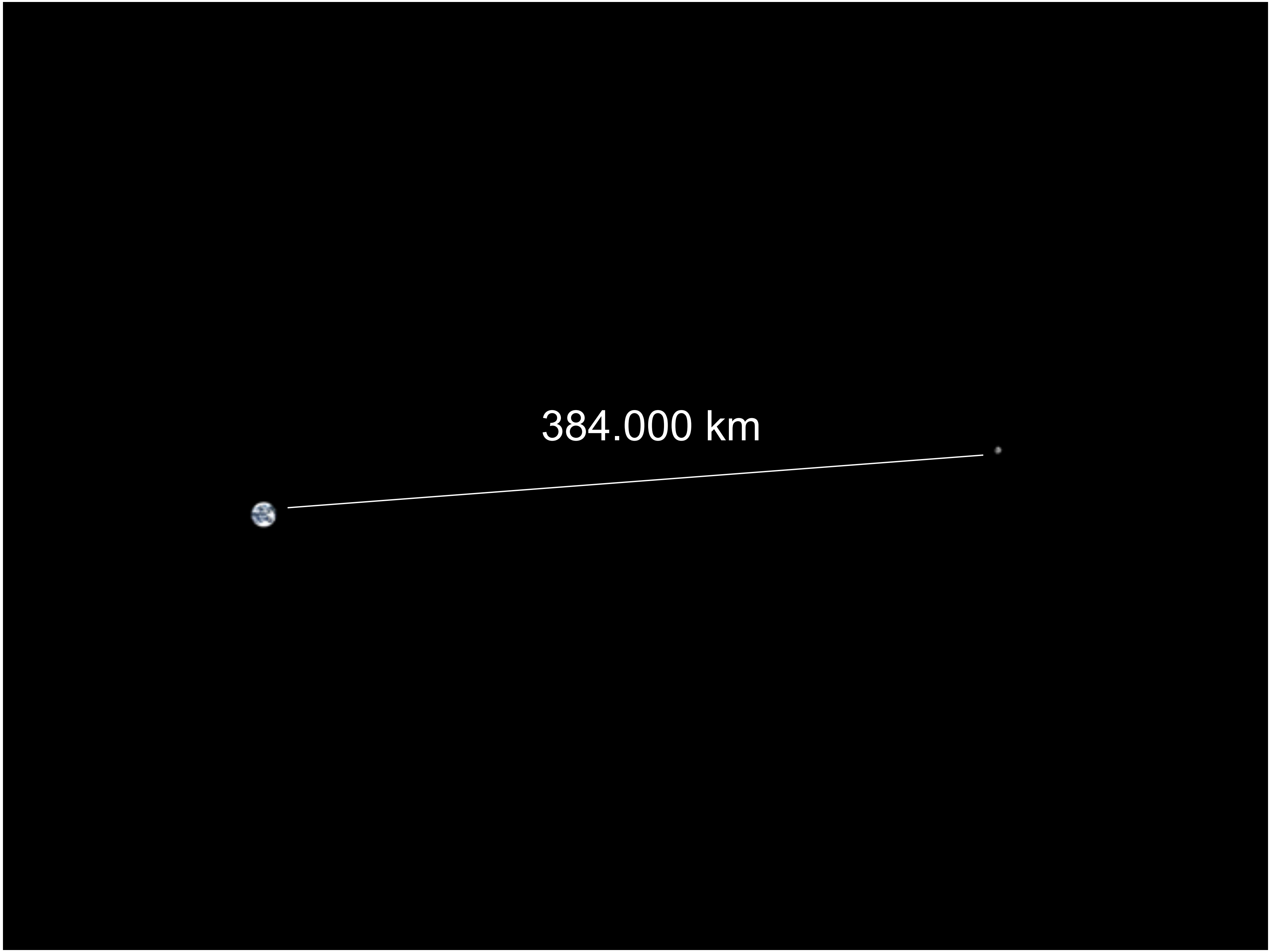
384.000 km

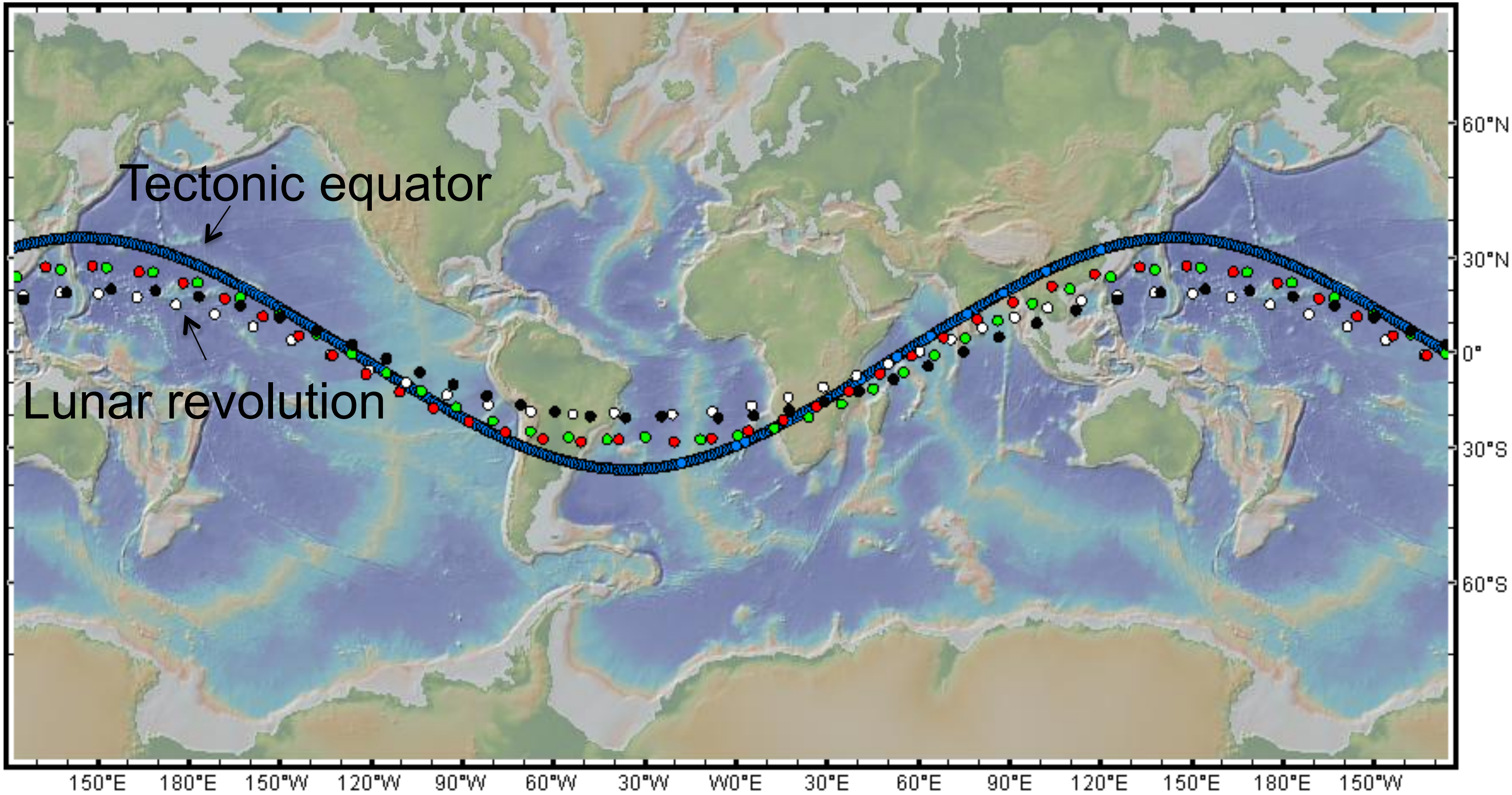

Adinolfi et al. in prep.

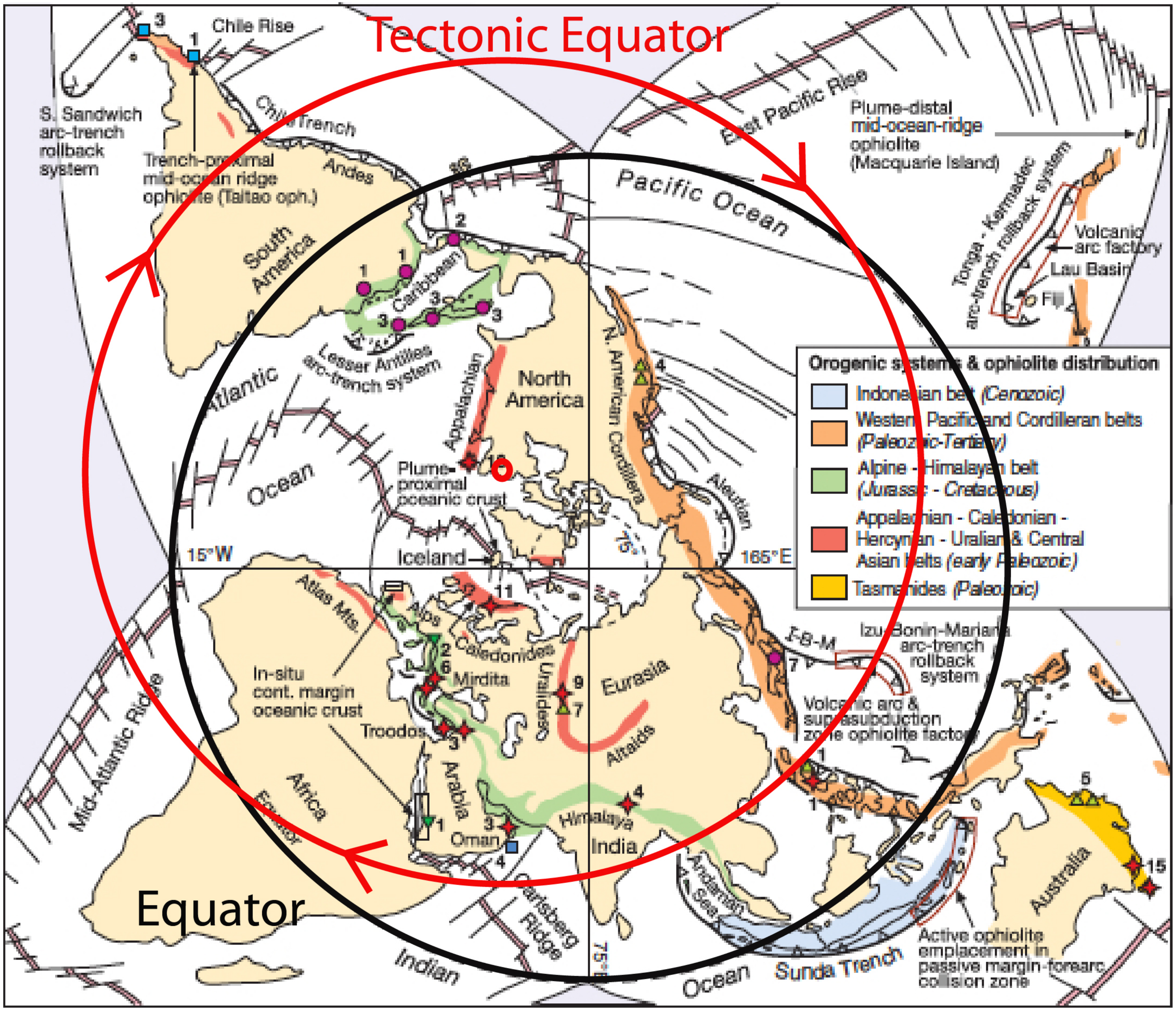

Tectonic Equator
Equator
Chile Rise
S. Sandwich arc-trench rollback system
Trench-proximal mid-ocean ridge ophiolite (Taitao oph.)
Chile Trench
Andes
South America
Caribbean
Lesser Antilles arc-trench system
Atlantic Ocean
Appalachian
North America
Plume-proximal oceanic crust
Iceland
15°W
165°E
East Pacific Rise
Pacific Ocean
Plume-distal mid-ocean-ridge ophiolite (Macquarie Island)
Tonga - Kermadec arc-trench rollback system
Volcanic arc factory
Lau Basin
Fiji
N. American Cordillera
Aleutian
Orogenic systems & ophiolite distribution
Indonesian belt (Cenozoic)
Western Pacific and Cordilleran belts (Paleozoic-Tertiary)
Alpine - Himalayan belt (Jurassic - Cretaceous)
Appalachian - Caledonian - Hercynian - Uralian & Central Asian belts (early Paleozoic)
Tasmanides (Paleozoic)
Atlas Mts.
Alps
Caledonides
Mirdita
Uralides
Eurasia
Altaids
In-situ cont. margin oceanic crust
Troodos
Arabia
Africa
Oman
Himalaya
India
I-B-M
Izu-Bonin-Mariana arc-trench rollback system
Volcanic arc & suprasubduction zone ophiolite factory
Mid-Atlantic Ridge
Carlsberg Ridge
Indian Ocean
Andaman Sea
Sunda Trench
Australia
Active ophiolite emplacement in passive margin-forearc collision zone
75°E

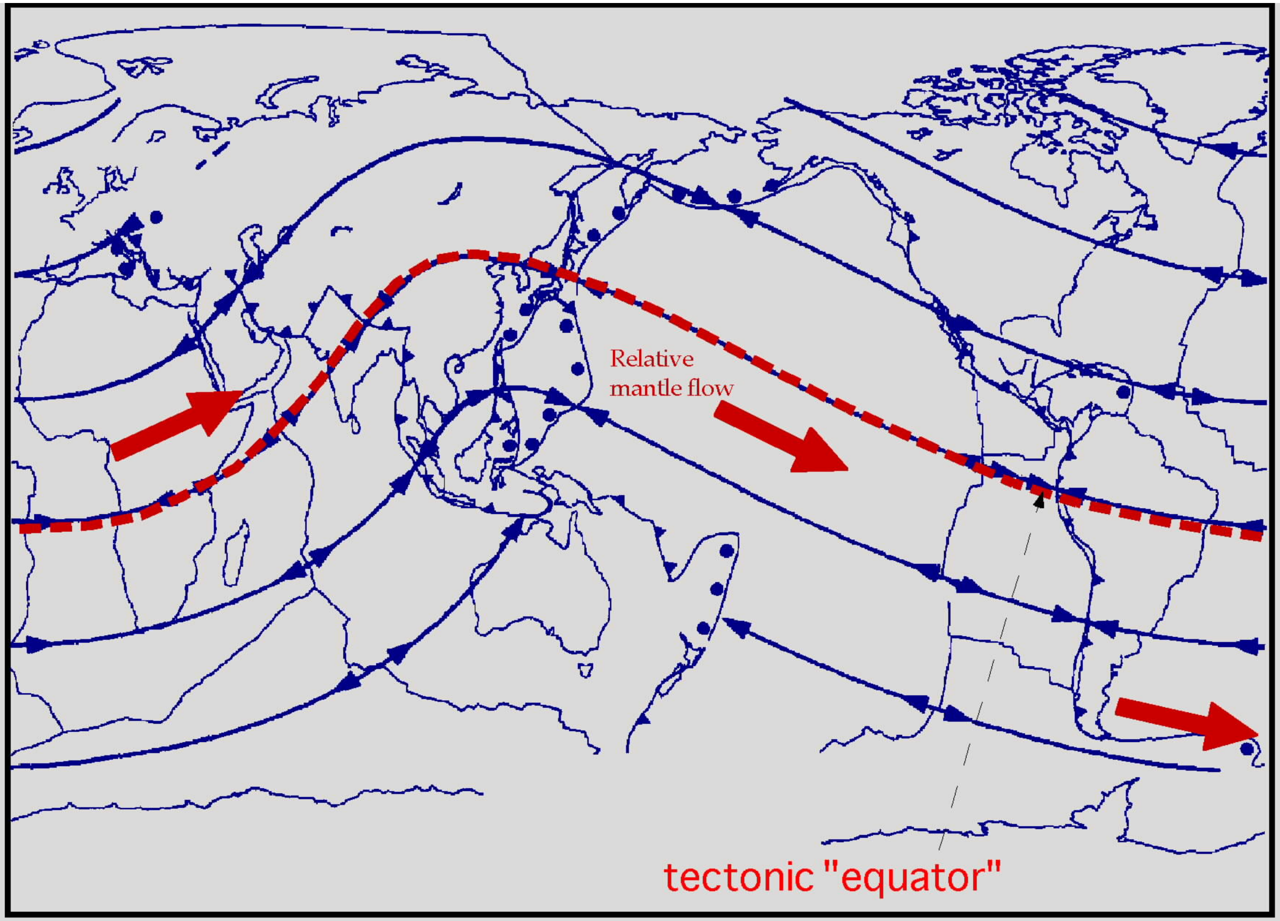
Relative
mantle flow
tectonic "equator"

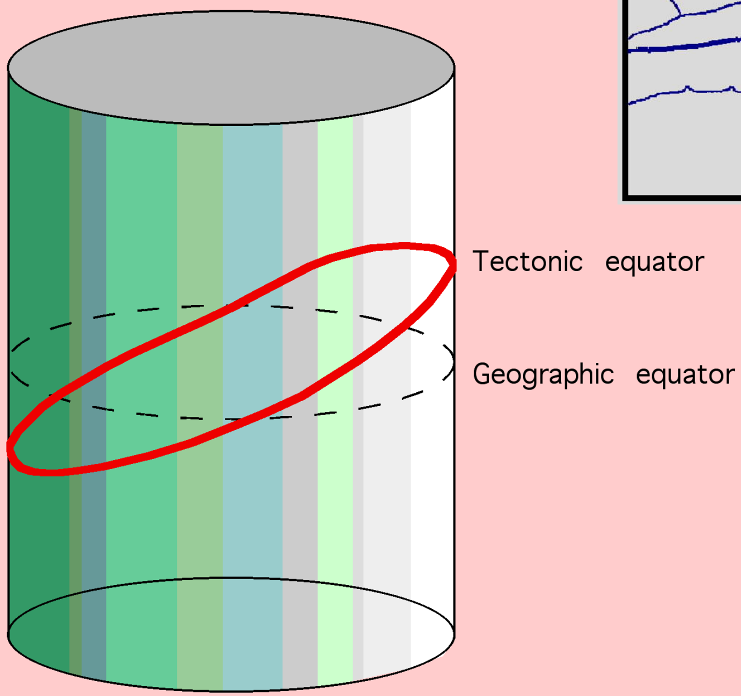
Tectonic equator
Geographic equator

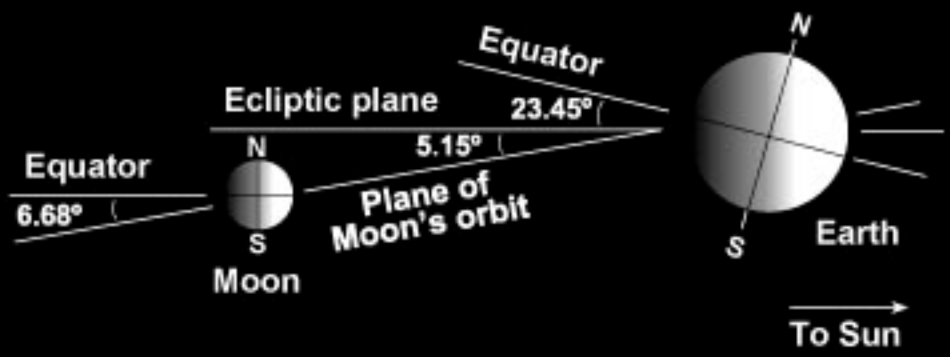
Equator
Ecliptic plane
23.45°
5.15°
Equator
6.68°
N
S
Moon
Plane of
Moon's orbit
N
S
Earth
To Sun

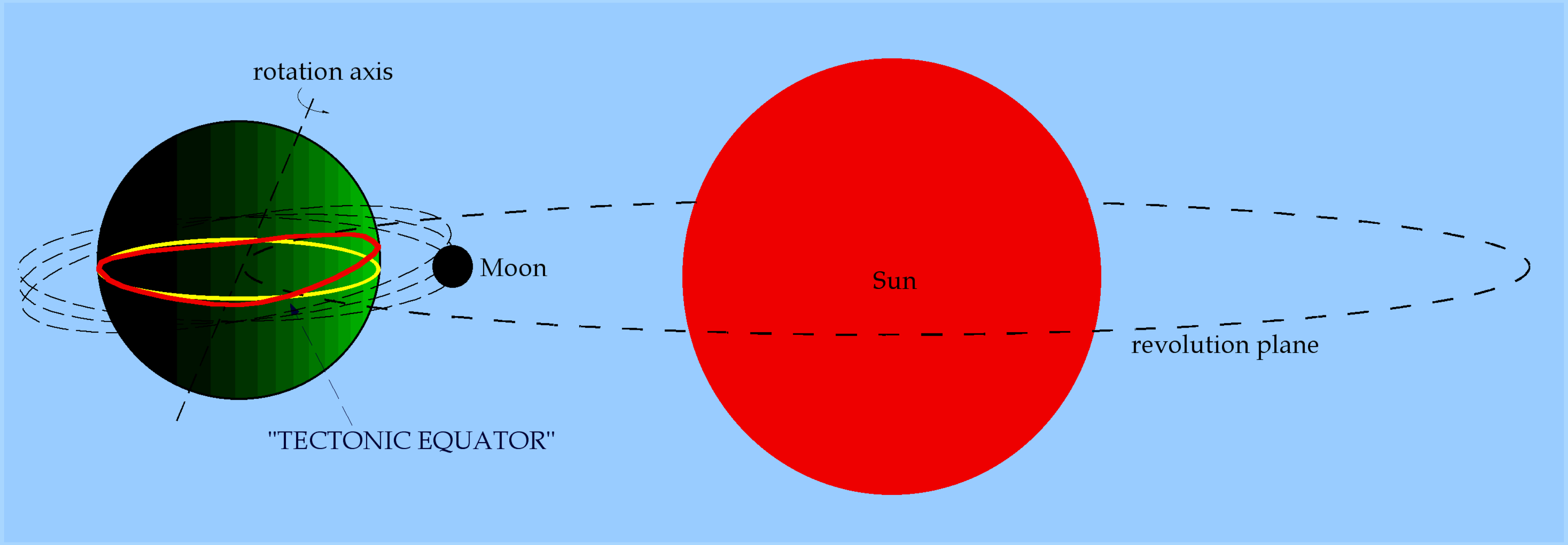

rotation axis
Moon
Sun
revolution plane
"TECTONIC EQUATOR"

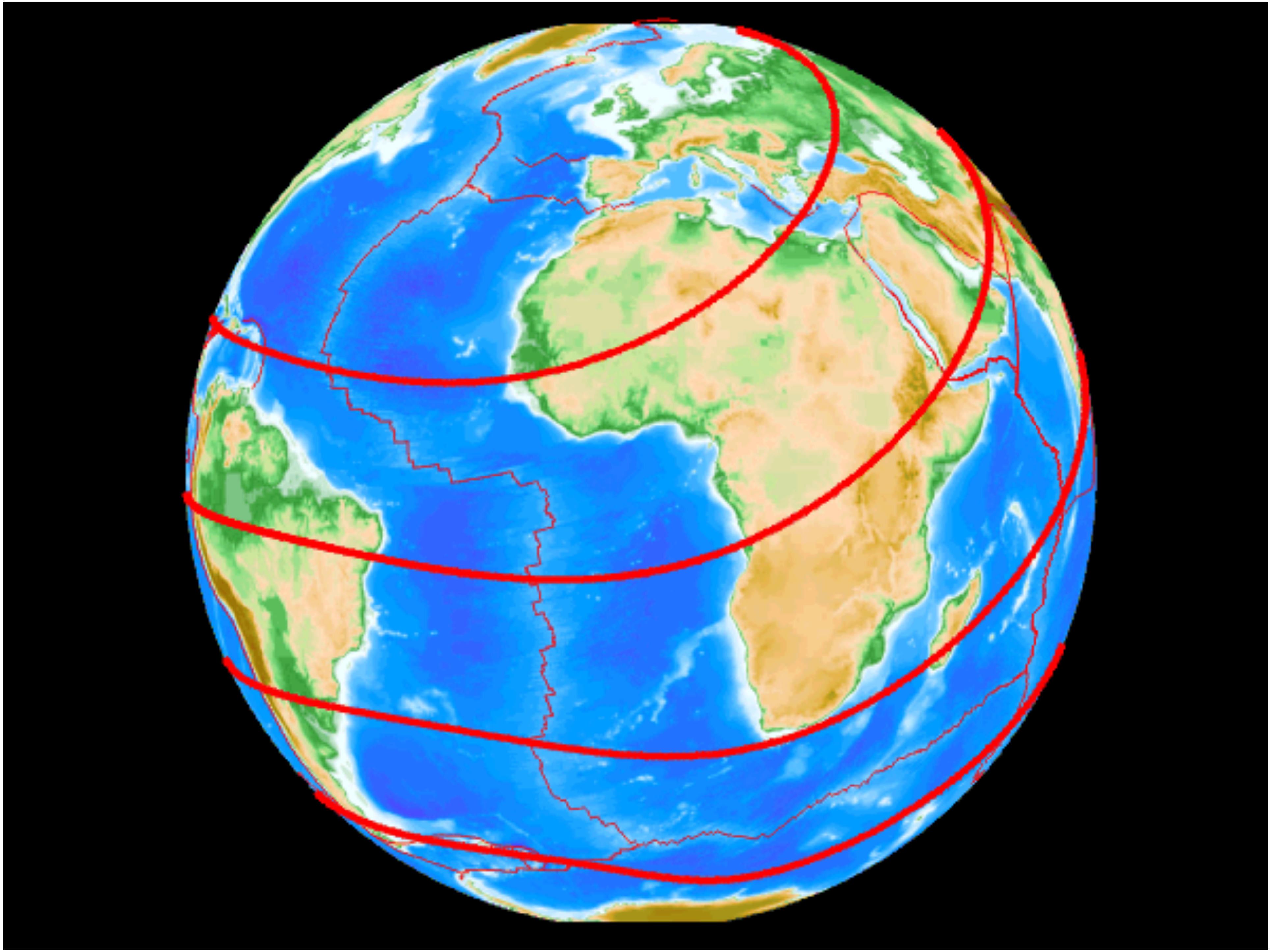

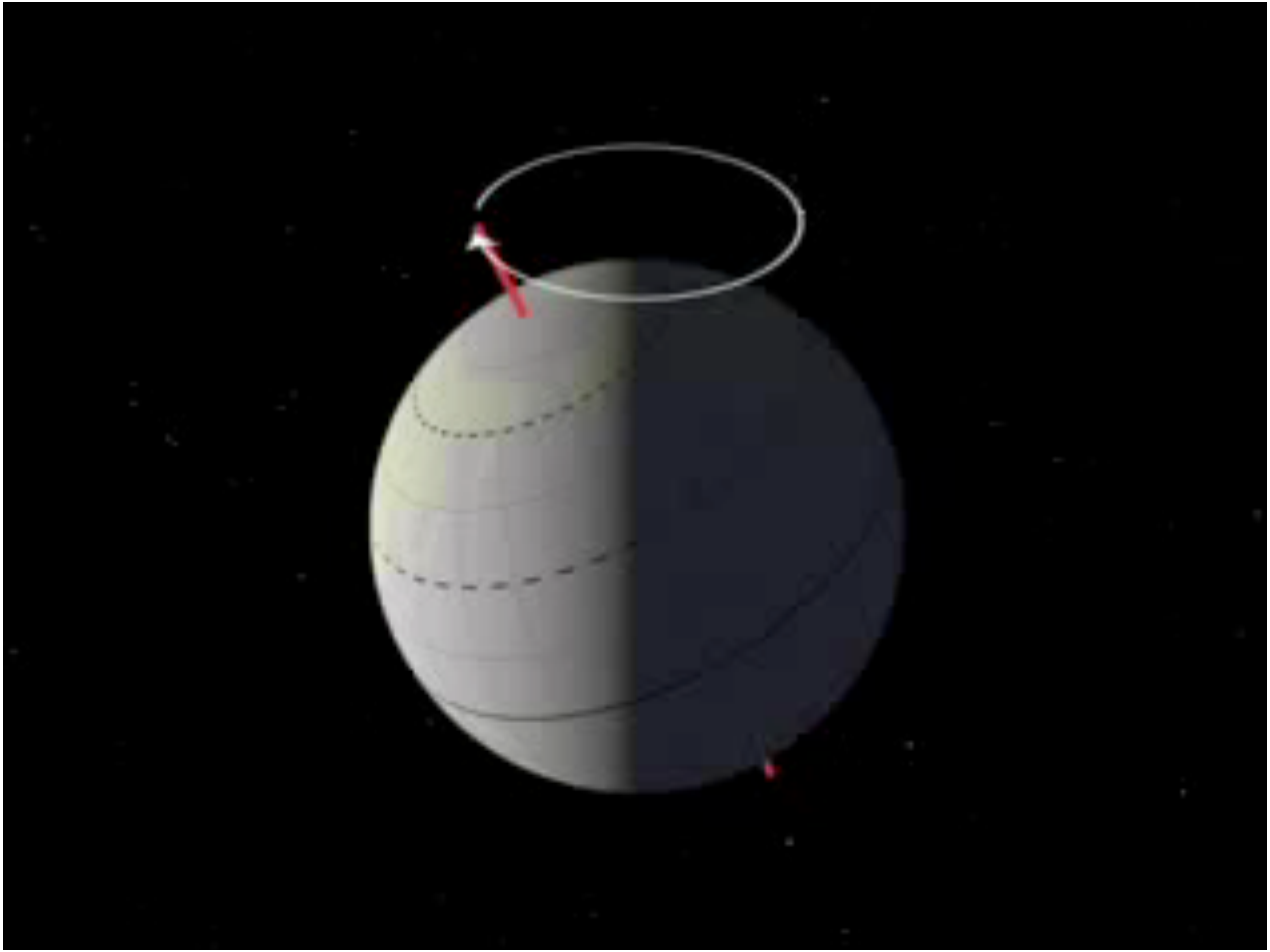

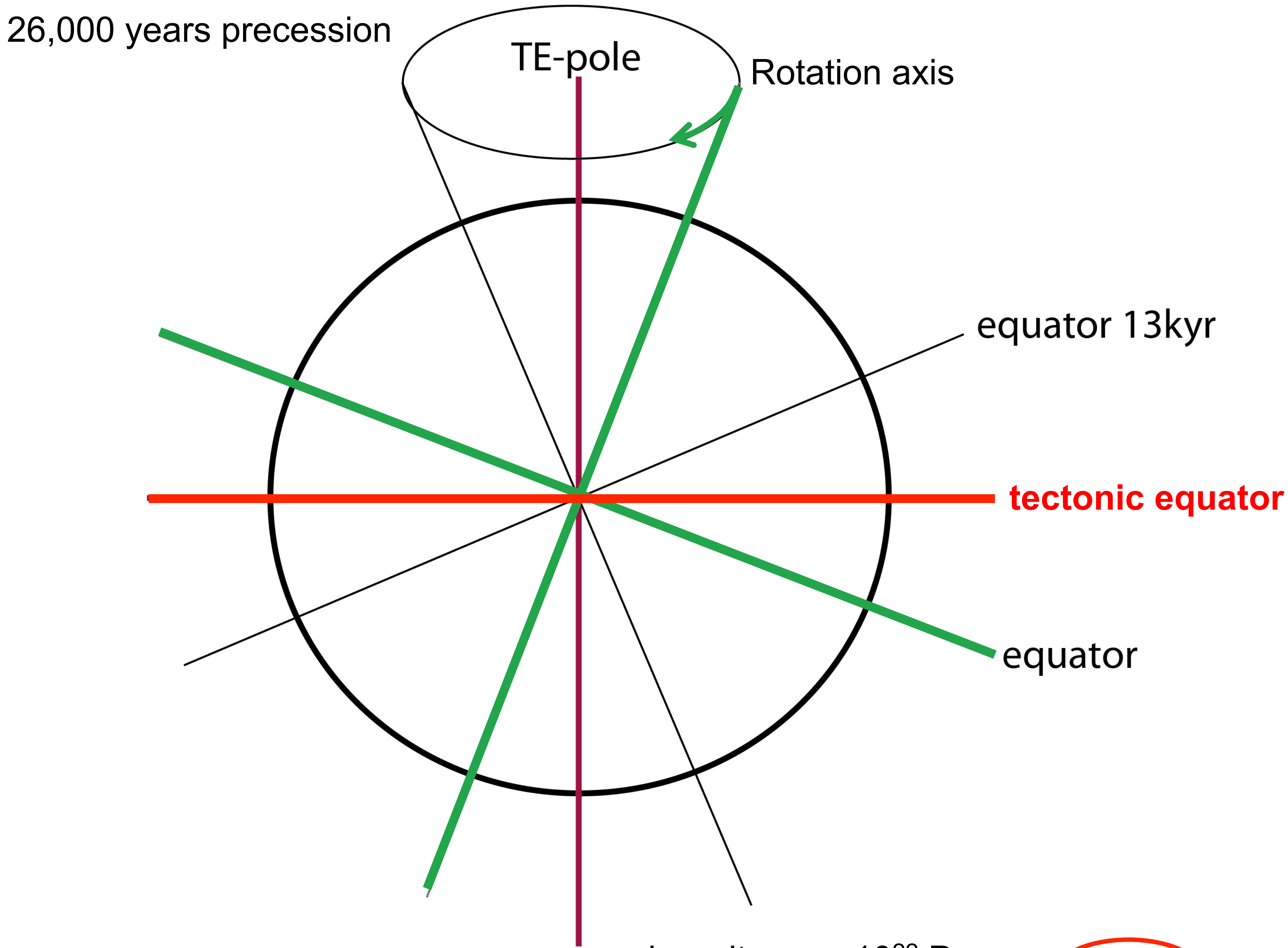

$$\text{Maxwell relaxation time} = \frac{\text{viscosity}}{\text{rigidity}} = \frac{10^{22}\ \text{Pa s}}{10^{11}\ \text{Pa}} = 10^{11}\ \text{s}$$

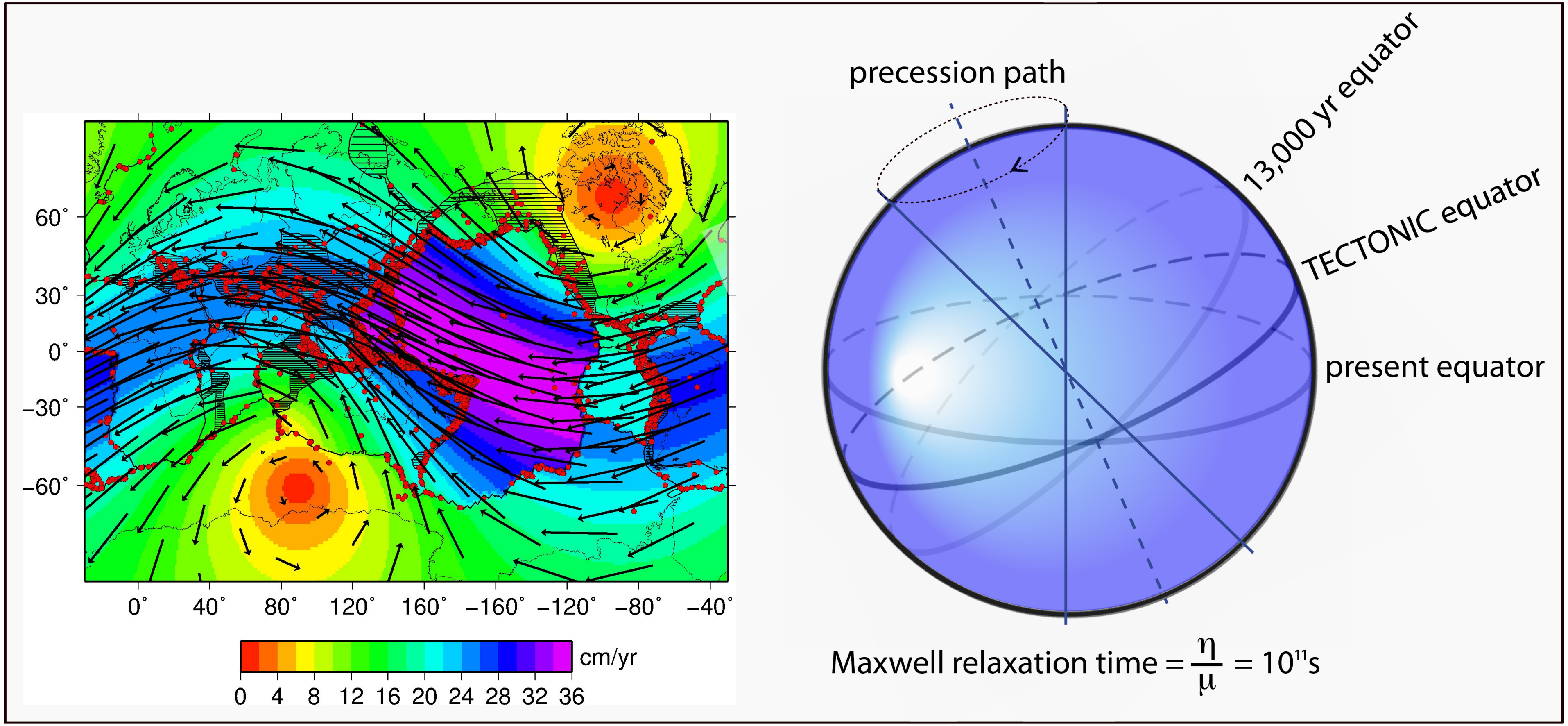

Zaccagnino et al. 2020

TIDAL FRICTION

- Earth's rotation is slowing: with dinosaurs the day was of 22h
- Moon receding at 38 mm/year
- Tidal friction $10^{20\text{-}21}$ J/yr
- Tectonic moment 10^{21} J/yr

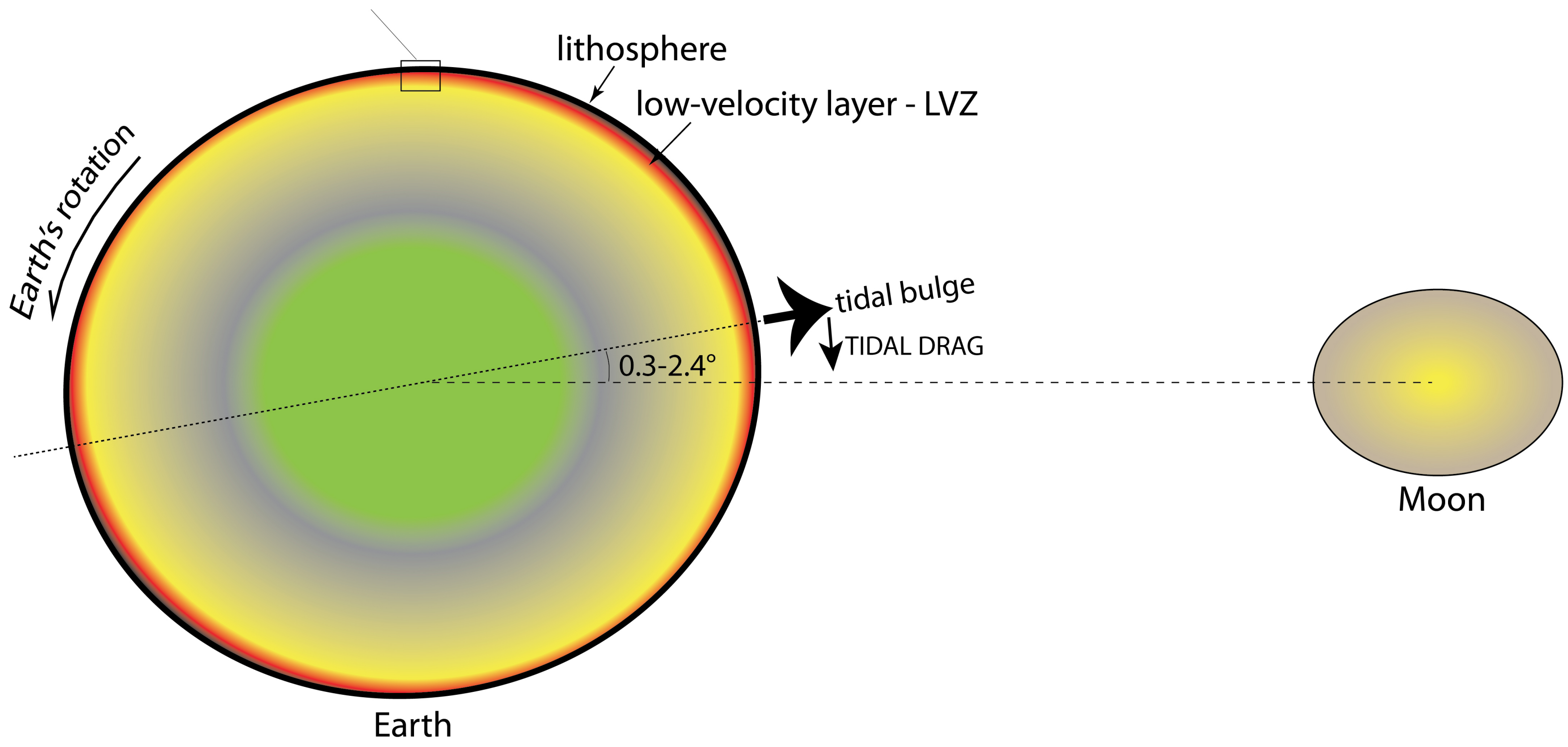

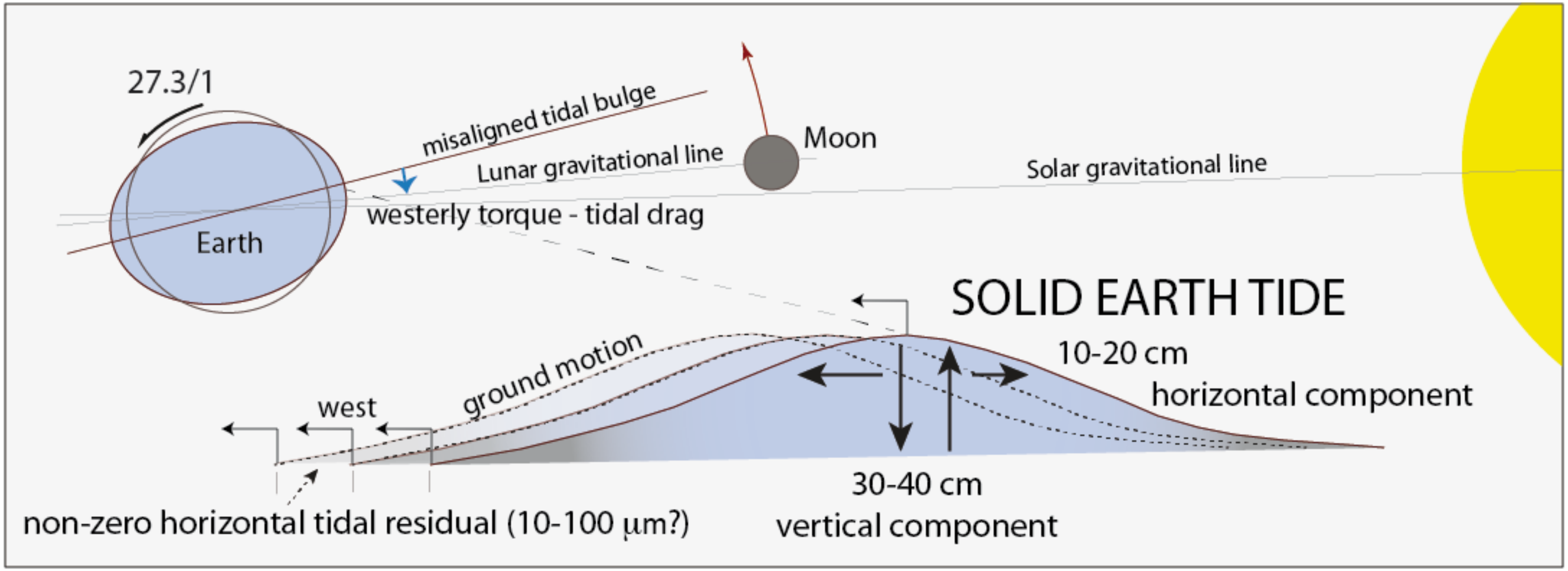

Zaccagnino et al. 2020

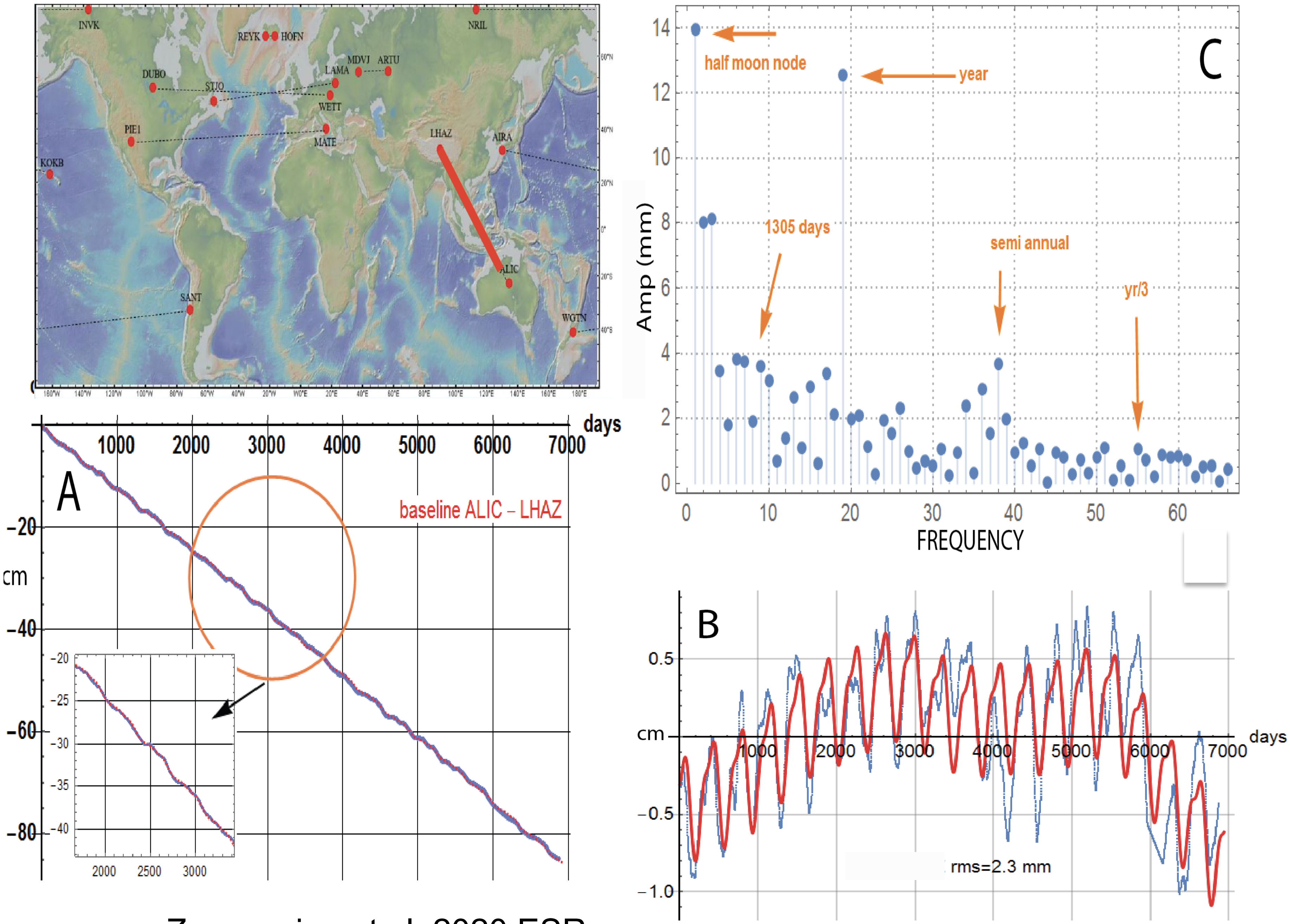

Zaccagnino et al. 2020 ESR

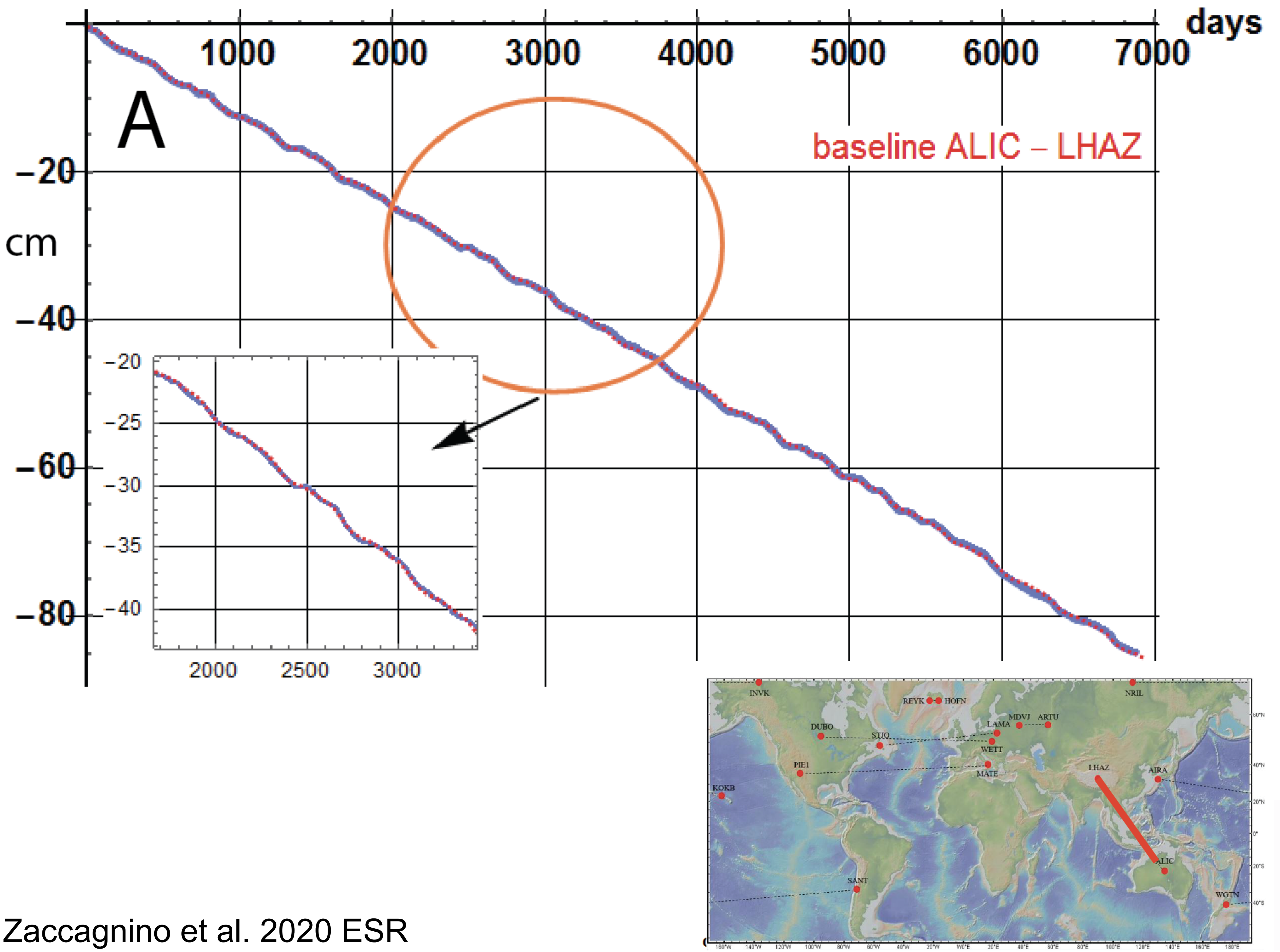

Zaccagnino et al. 2020 ESR

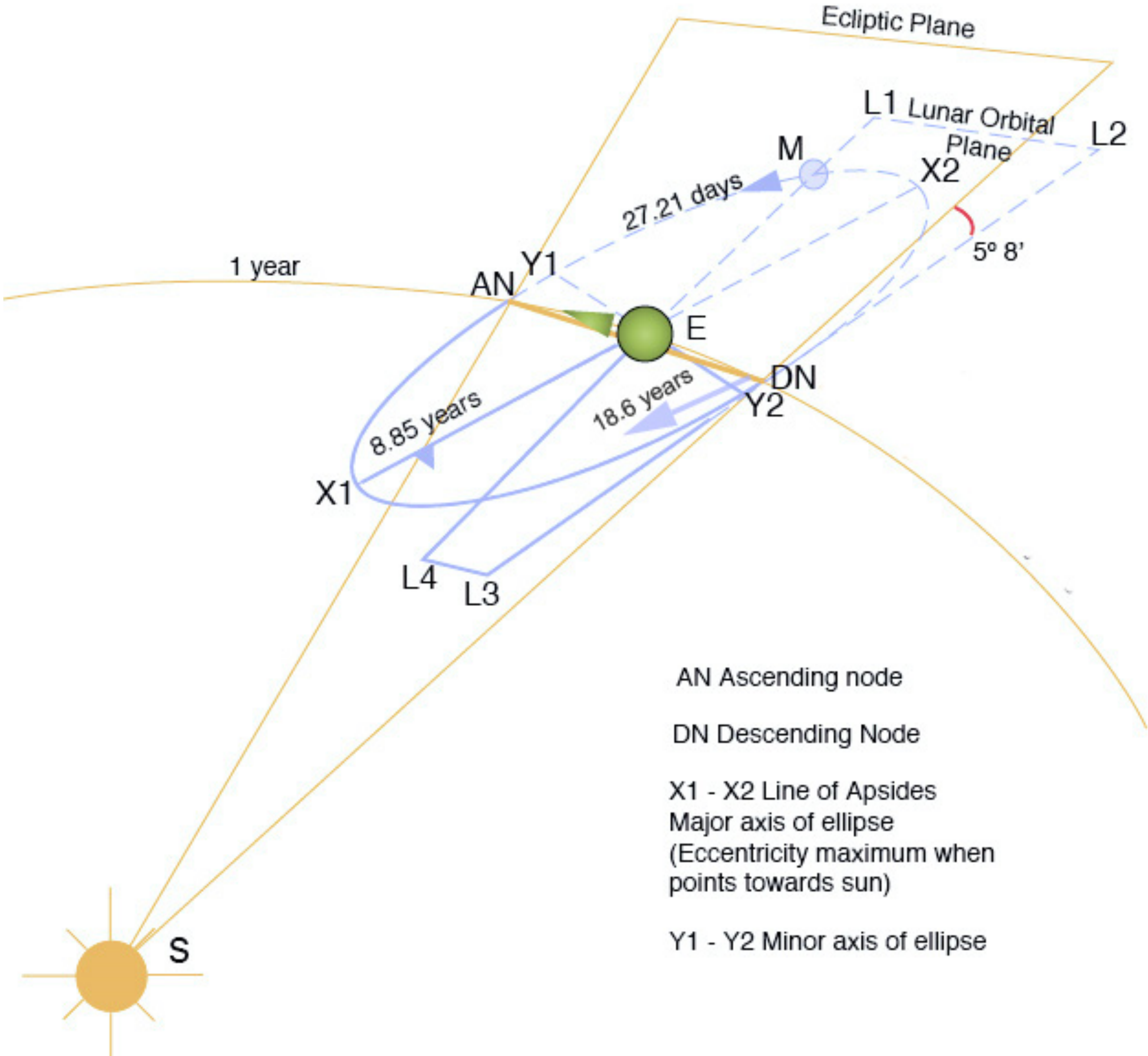

AN Ascending node

DN Descending Node

X1 - X2 Line of Apsides
Major axis of ellipse
(Eccentricity maximum when points towards sun)

Y1 - Y2 Minor axis of ellipse

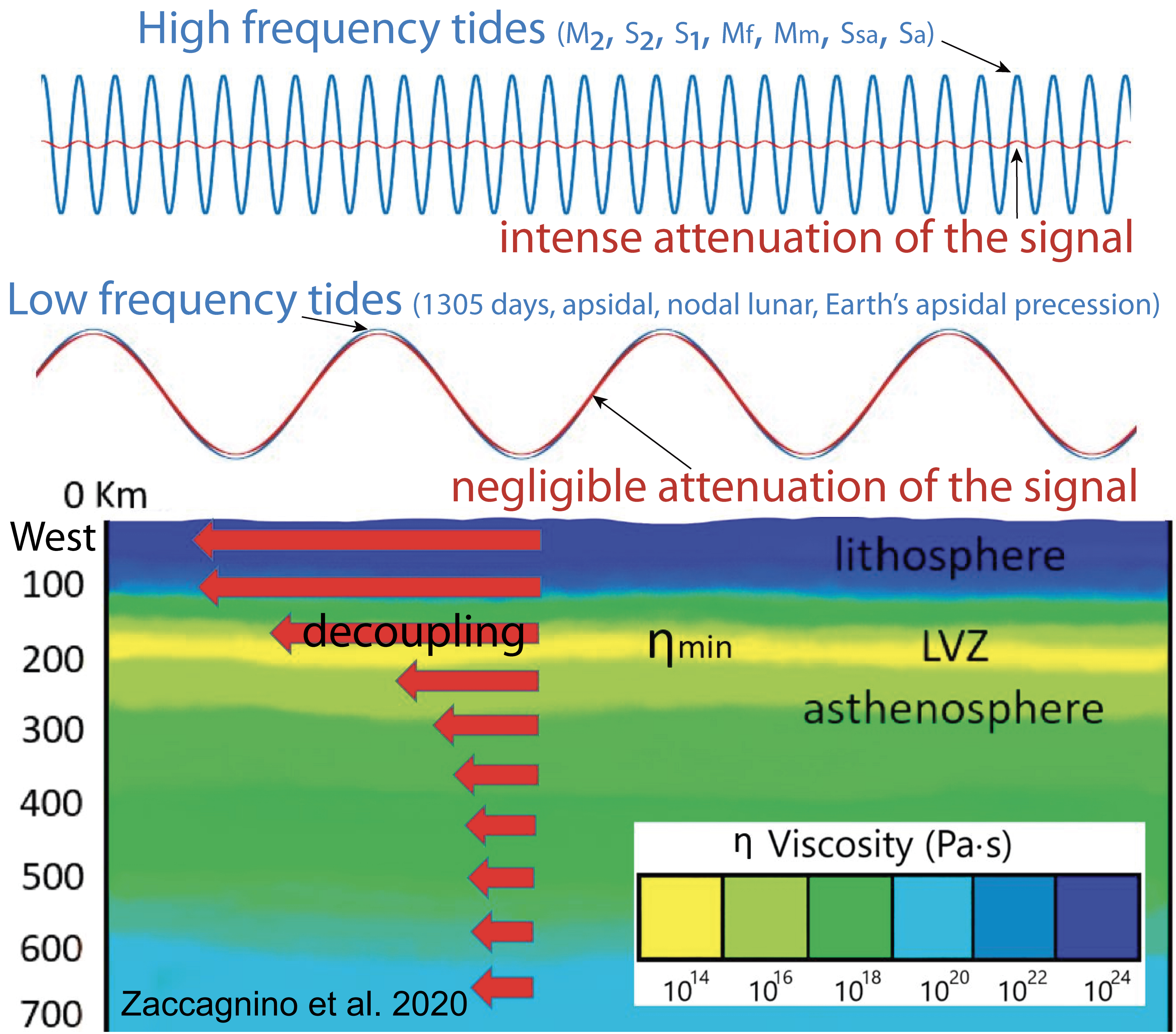

High frequency tides (M2, S2, S1, Mf, Mm, Ssa, Sa)
intense attenuation of the signal
Low frequency tides (1305 days, apsidal, nodal lunar, Earth's apsidal precession)
negligible attenuation of the signal
0 Km
West
100
200
300
400
500
600
700
decoupling
lithosphere
ηmin
LVZ
asthenosphere
η Viscosity (Pa·s)
10^14
10^16
10^18
10^20
10^22
10^24
Zaccagnino et al. 2020

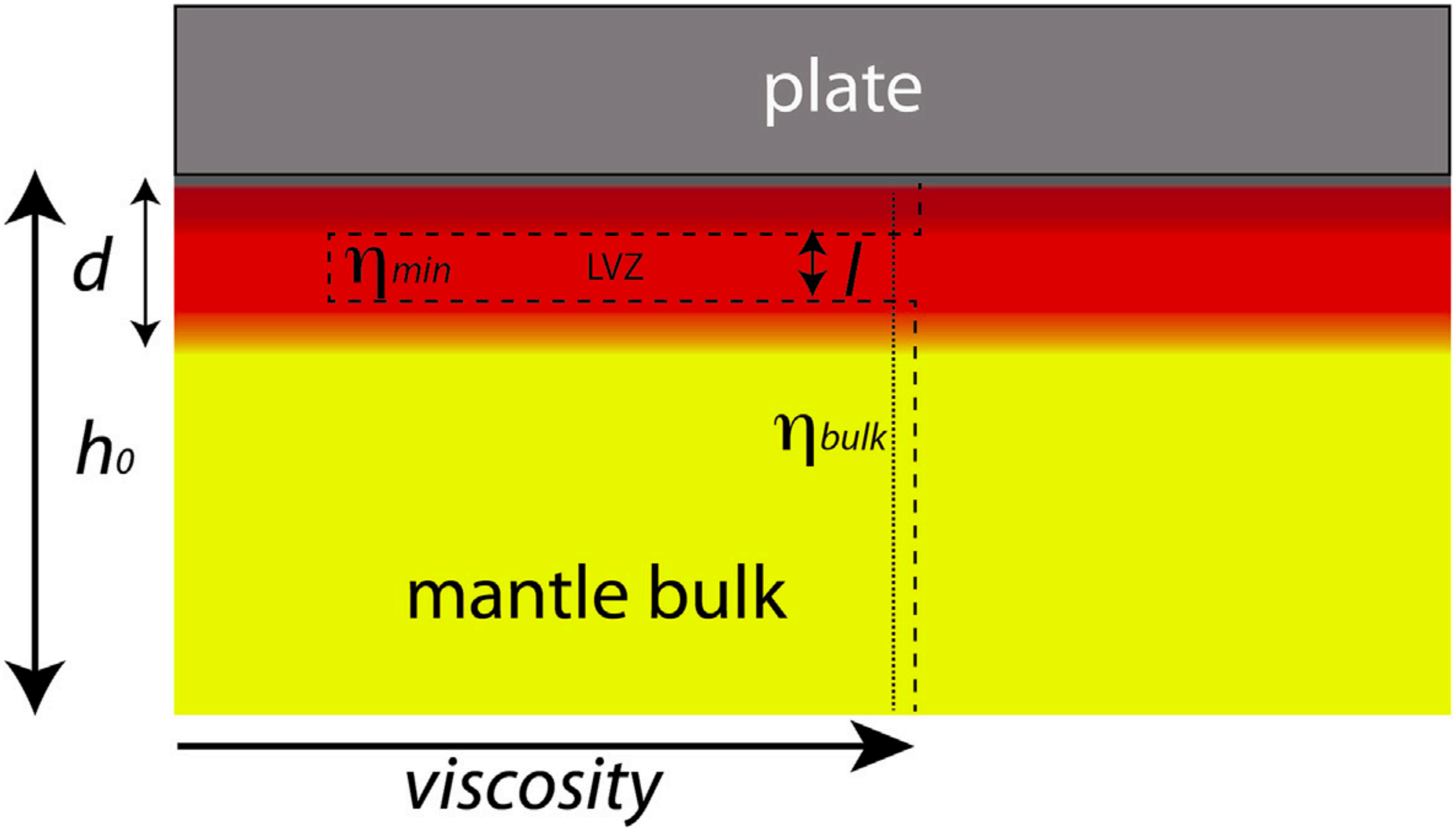

Carcaterra & Doglioni, 2018 Geoscience Front.

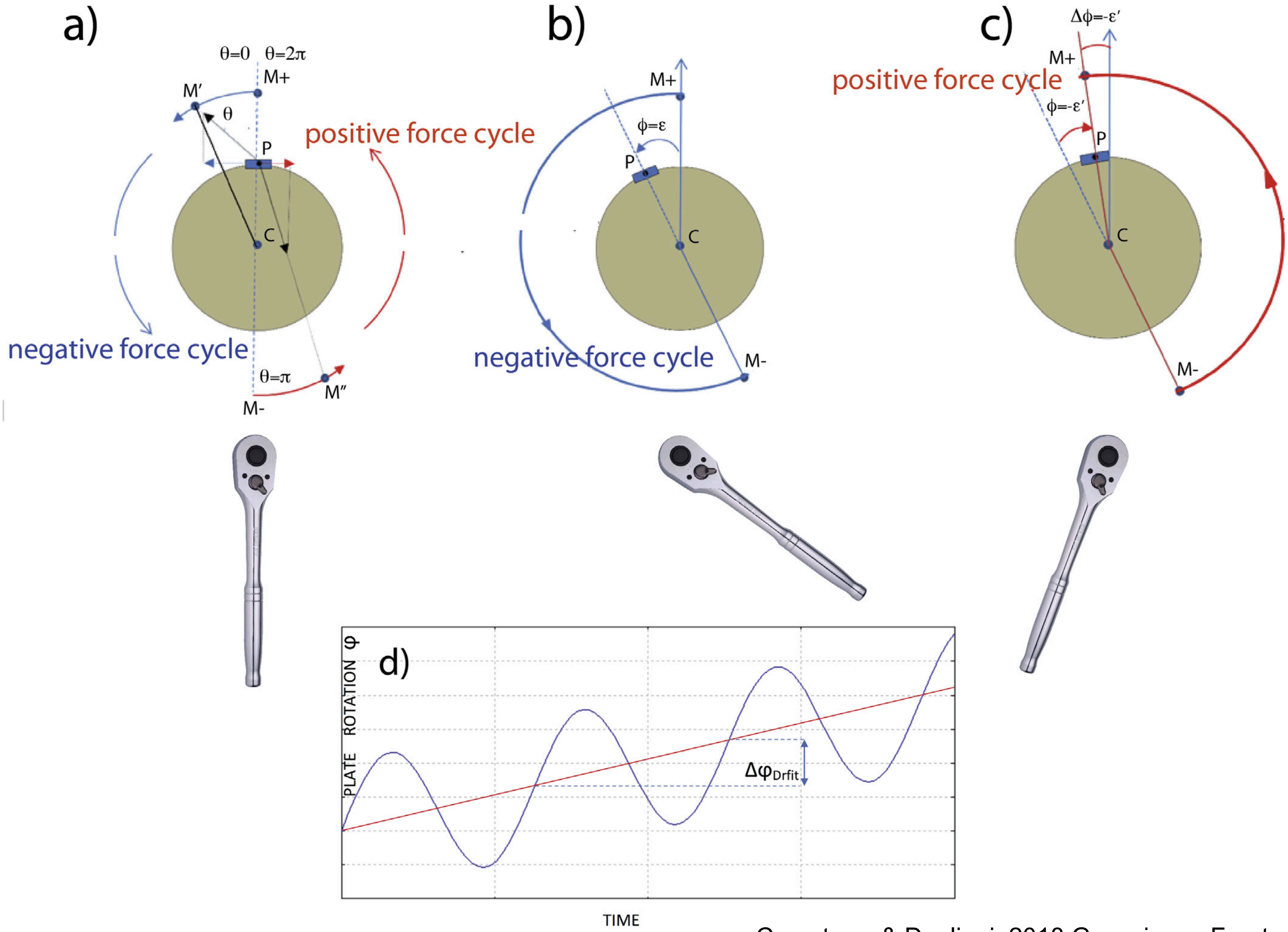

Carcaterra & Doglioni, 2018 Geoscience Front.

ASTRONOMICAL TUNING

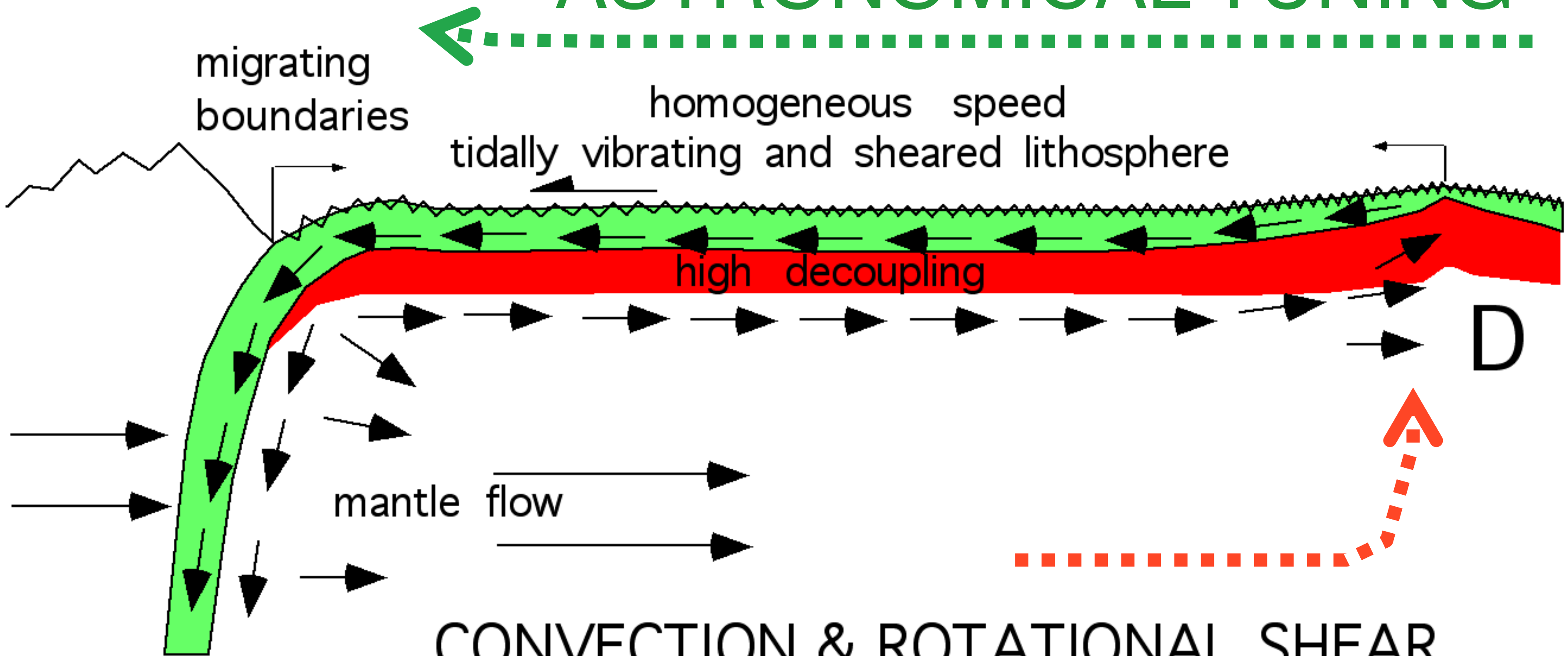

CONVECTION & ROTATIONAL SHEAR

THERMAL COOLING

Self Organized Chaotic System

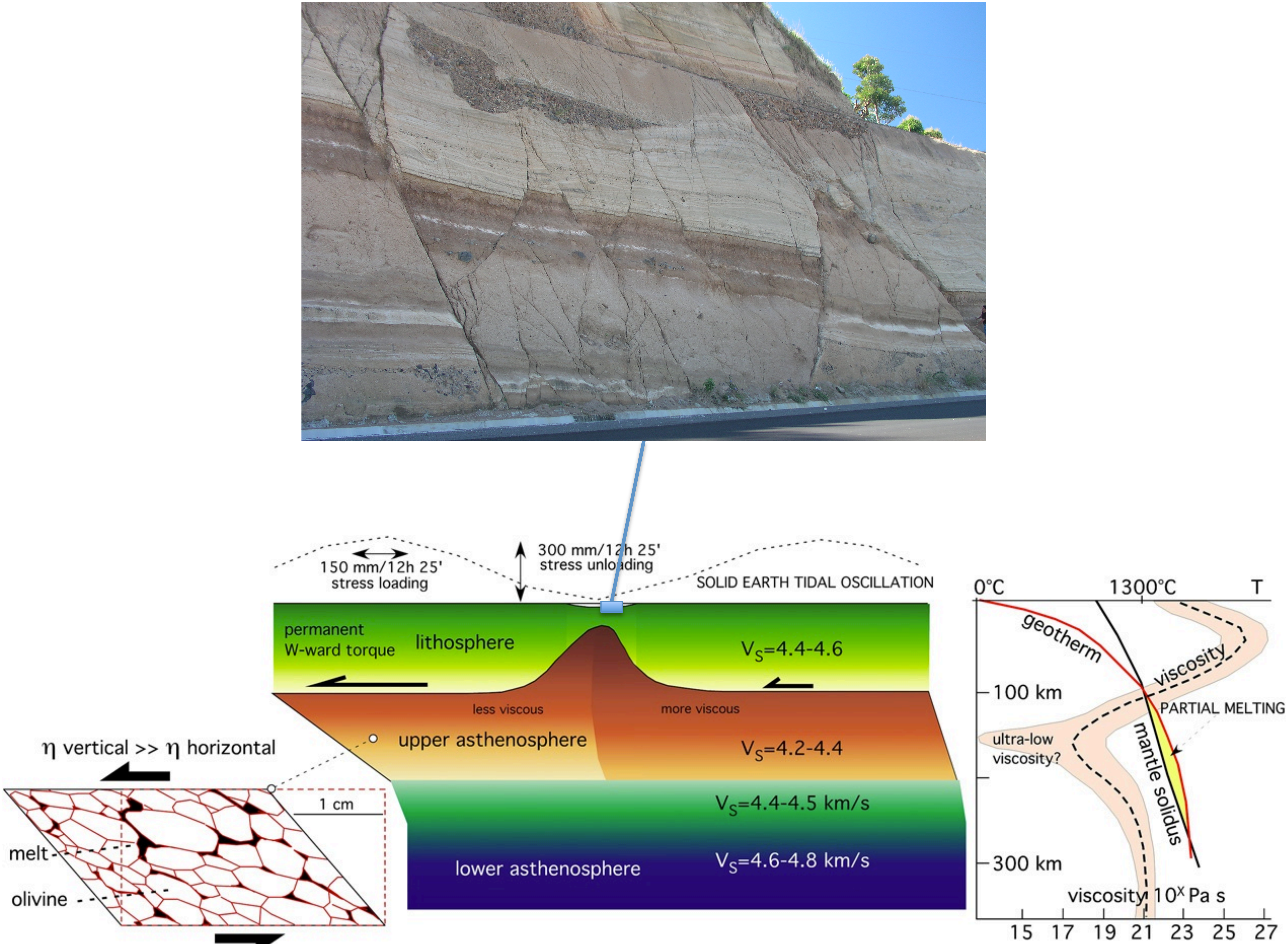
150 mm/12h 25'
stress loading
300 mm/12h 25'
stress unloading
SOLID EARTH TIDAL OSCILLATION
permanent
W-ward torque
lithosphere
V_S=4.4-4.6
less viscous
more viscous
upper asthenosphere
V_S=4.2-4.4
V_S=4.4-4.5 km/s
lower asthenosphere
V_S=4.6-4.8 km/s
η vertical >> η horizontal
1 cm
melt
olivine
0°C
1300°C
T
geotherm
viscosity
100 km
PARTIAL MELTING
ultra-low
viscosity?
mantle solidus
300 km
viscosity 10^x Pa s
15 17 19 21 23 25 27

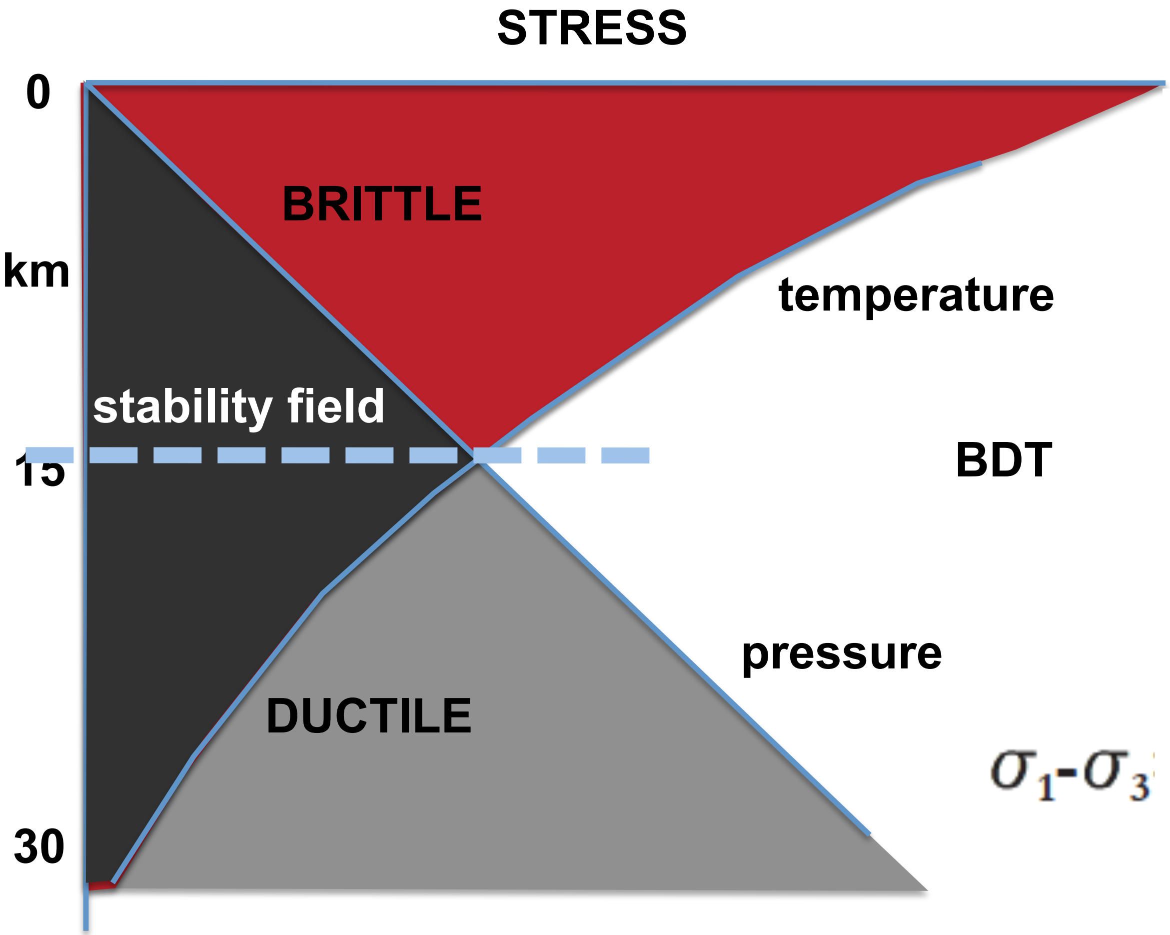

$$\sigma_1\text{-}\sigma_3=\beta\rho g z(1\text{-}\lambda)$$

λ, pore fluids
β, type of fault

$$\sigma_1\text{-}\sigma_3=\left(\frac{\dot{\varepsilon}}{A}\right)^{1/n}\exp\left(\frac{Q}{nRT}\right)$$

Q, activation energy
A, viscosity coefficient
ε, effective strain
n, stress power law

β=3 thrust, 1.2 strike-slip, 0.75 normal fault

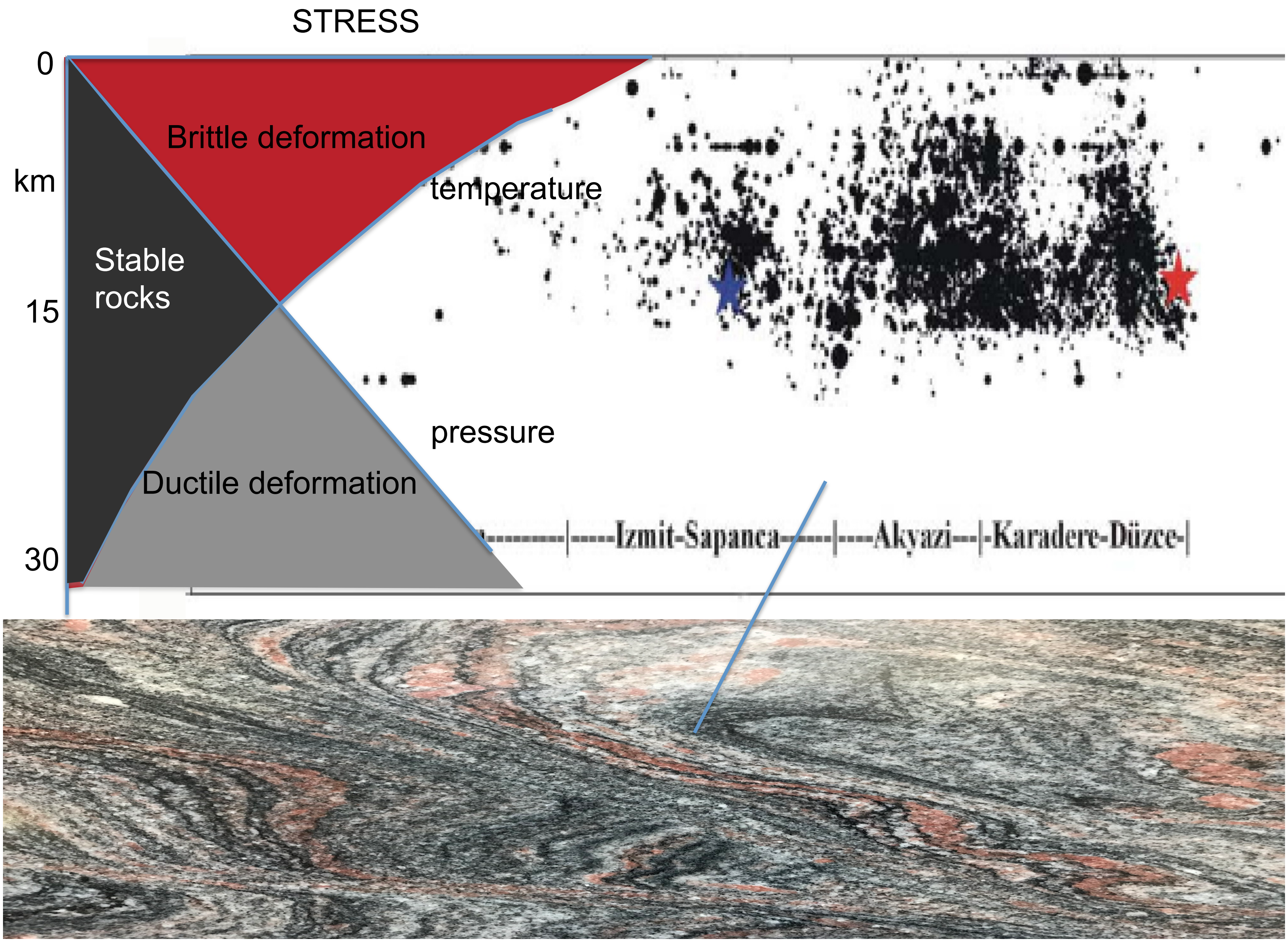

STRESS
0
km
15
30
Brittle deformation
temperature
Stable
rocks
pressure
Ductile deformation
|-----Izmit-Sapanca-----|----Akyazi---|-Karadere-Düzce-|

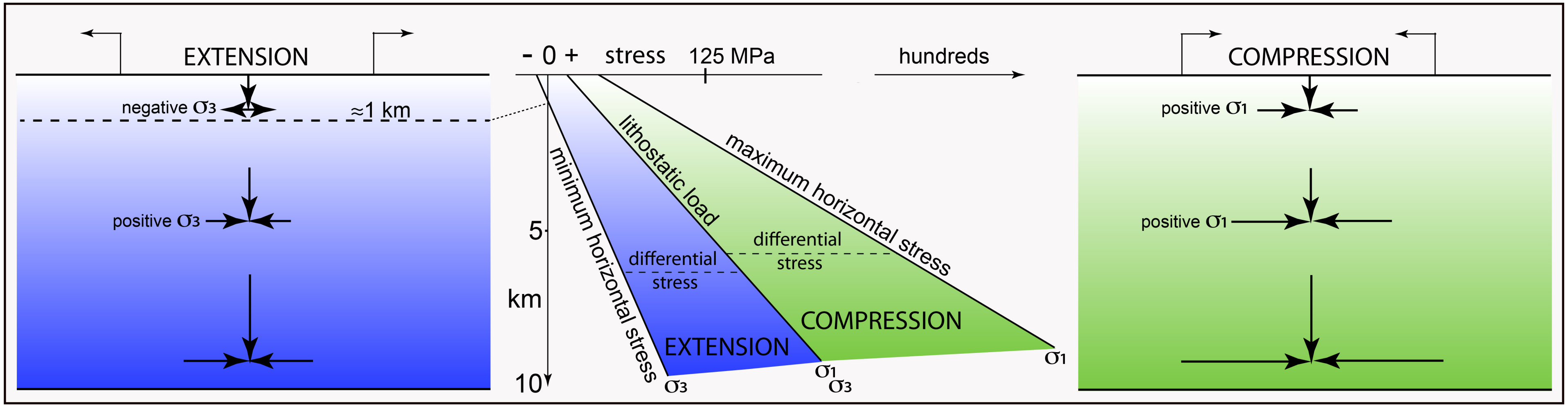
EXTENSION
negative σ3
≈1 km
positive σ3
- 0 + stress 125 MPa
hundreds
5
km
10
minimum horizontal stress
lithostatic load
maximum horizontal stress
differential stress
differential stress
EXTENSION
COMPRESSION
σ3
σ1
σ3
σ1
COMPRESSION
positive σ1
positive σ1

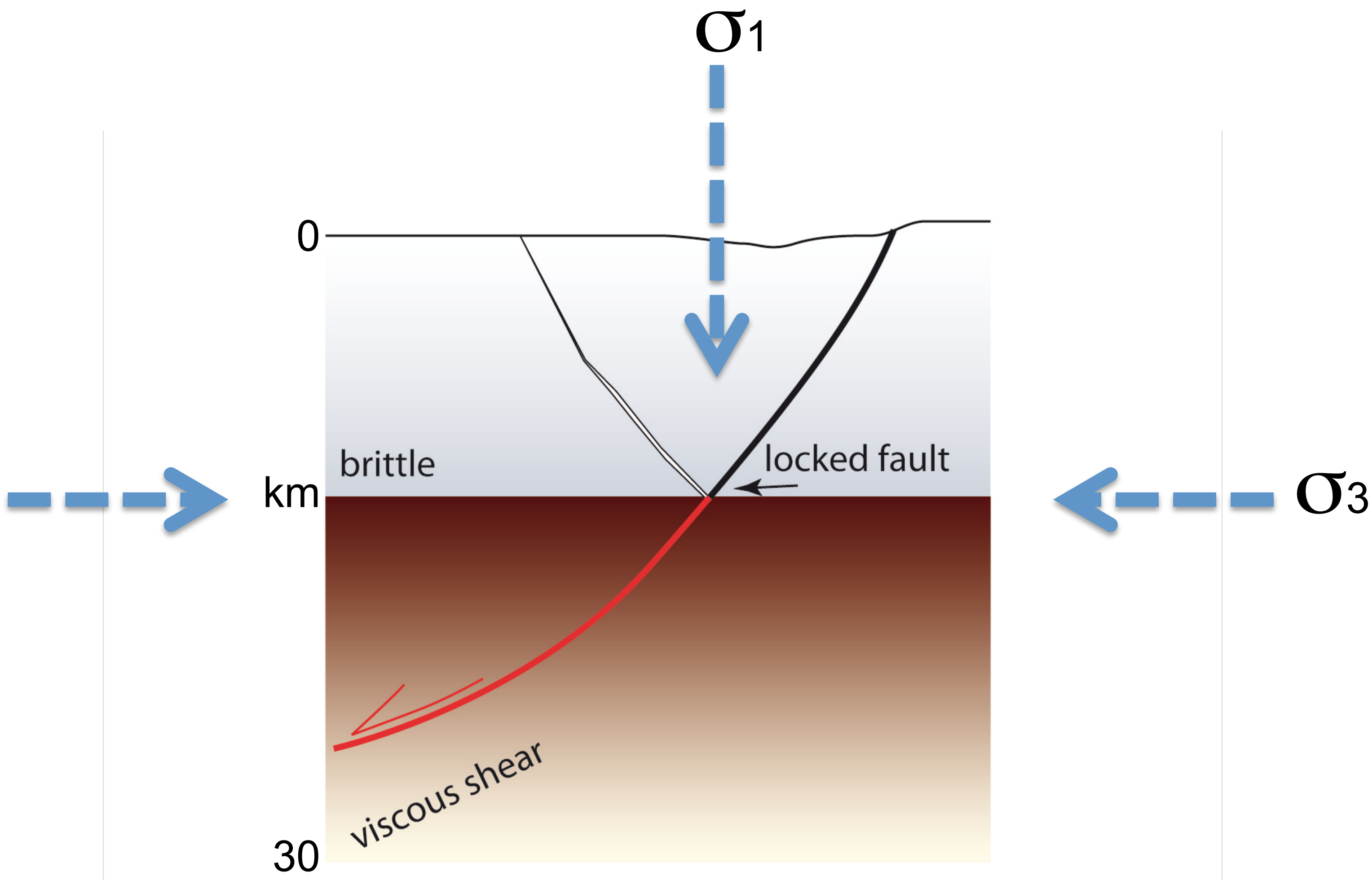

σ_1
0
brittle
locked fault
km
σ_3
viscous shear
30

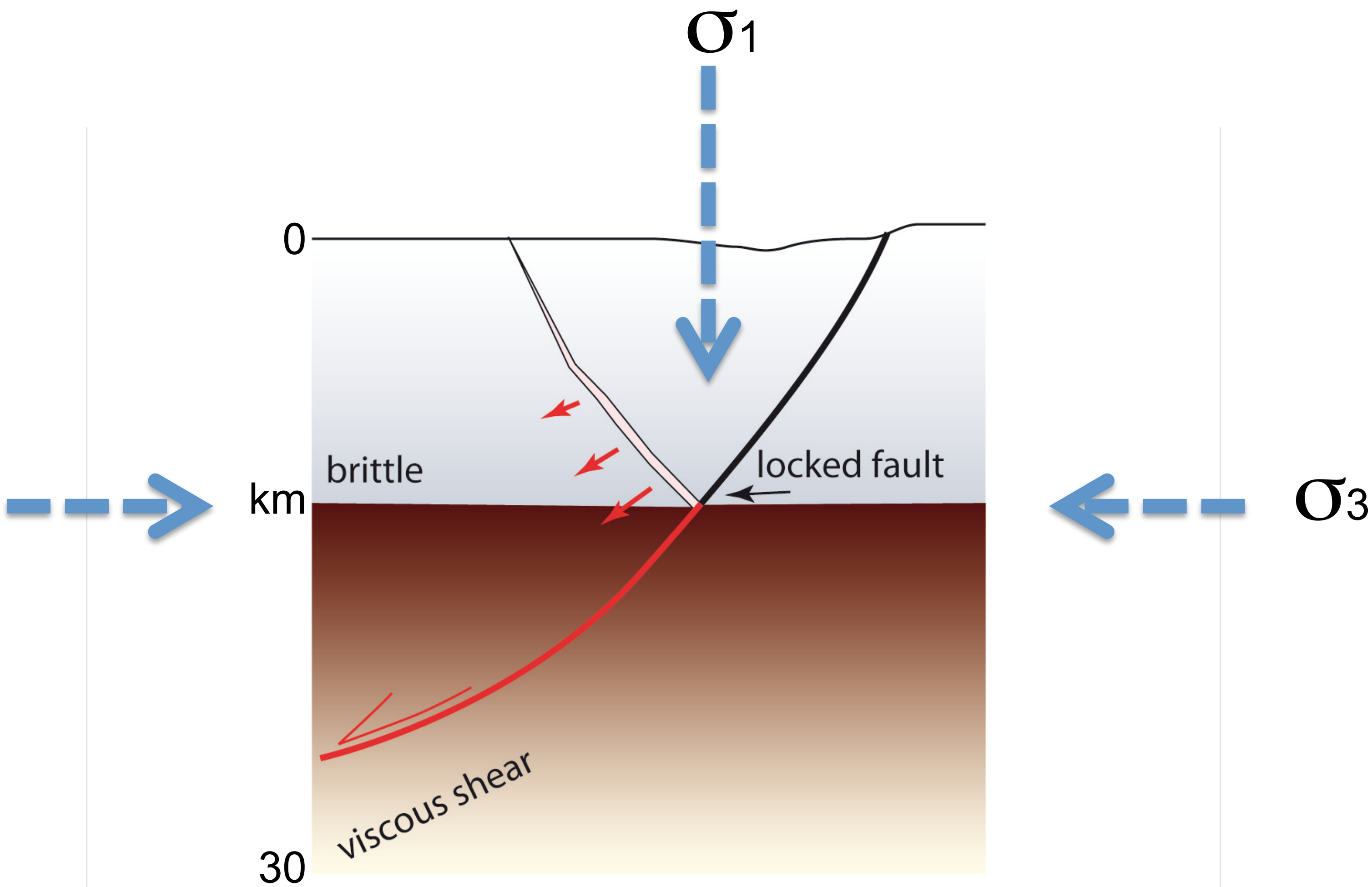

σ1
0
brittle
locked fault
km
σ3
viscous shear
30

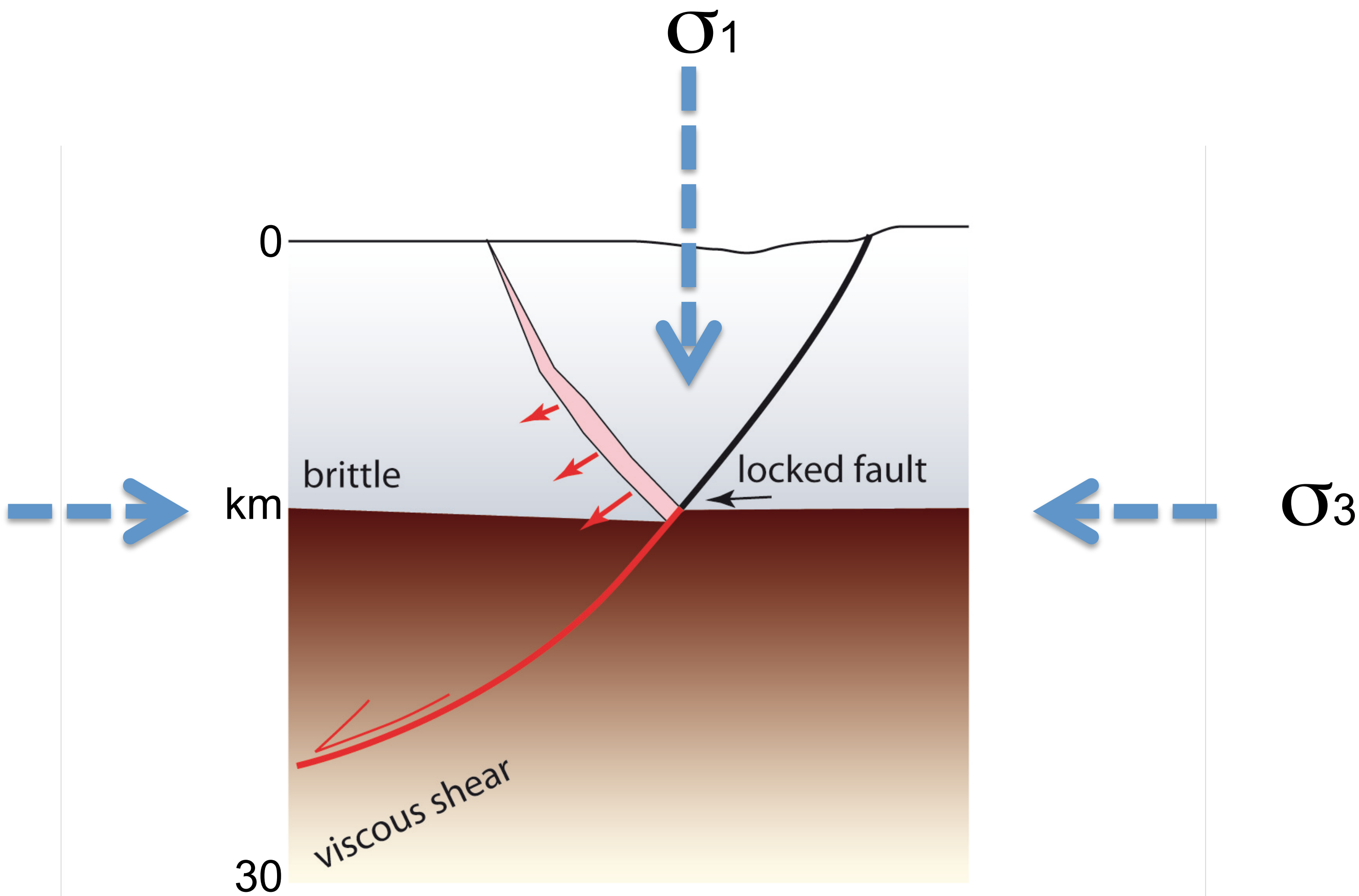

σ1
0
brittle
km
locked fault
σ3
viscous shear
30

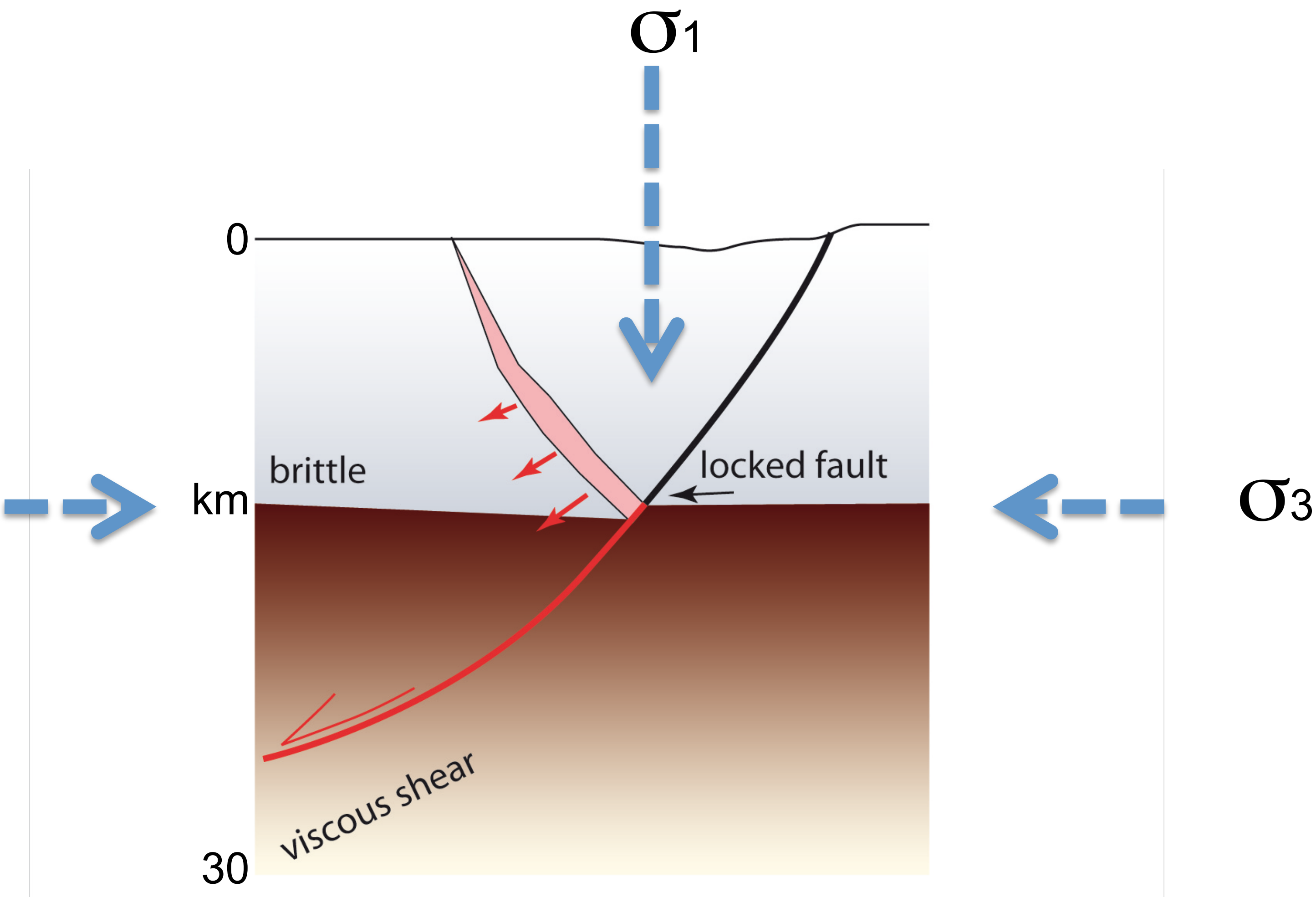
σ1
0
brittle
locked fault
km
σ3
viscous shear
30

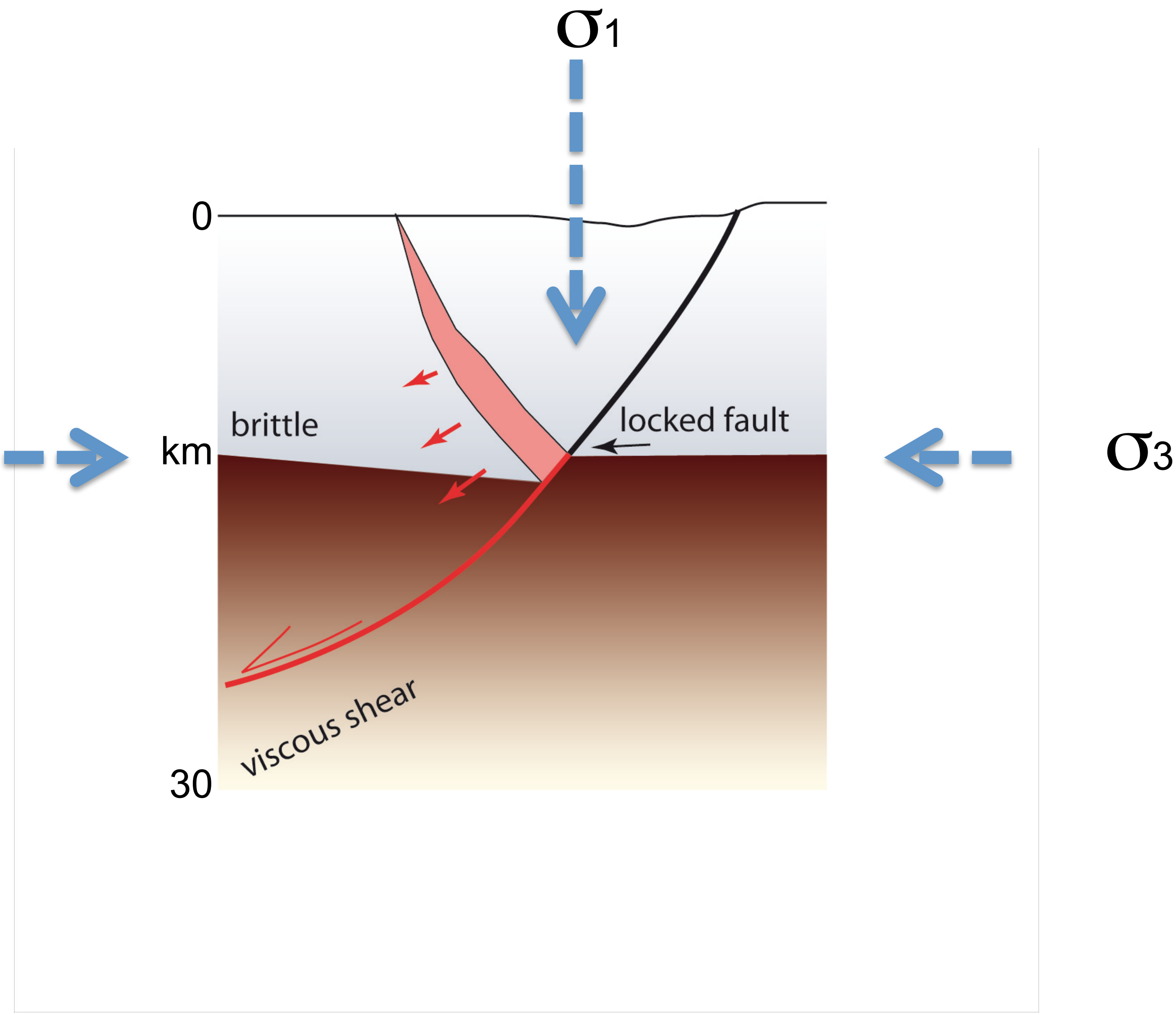

σ1
0
brittle
km
locked fault
σ3
viscous shear
30

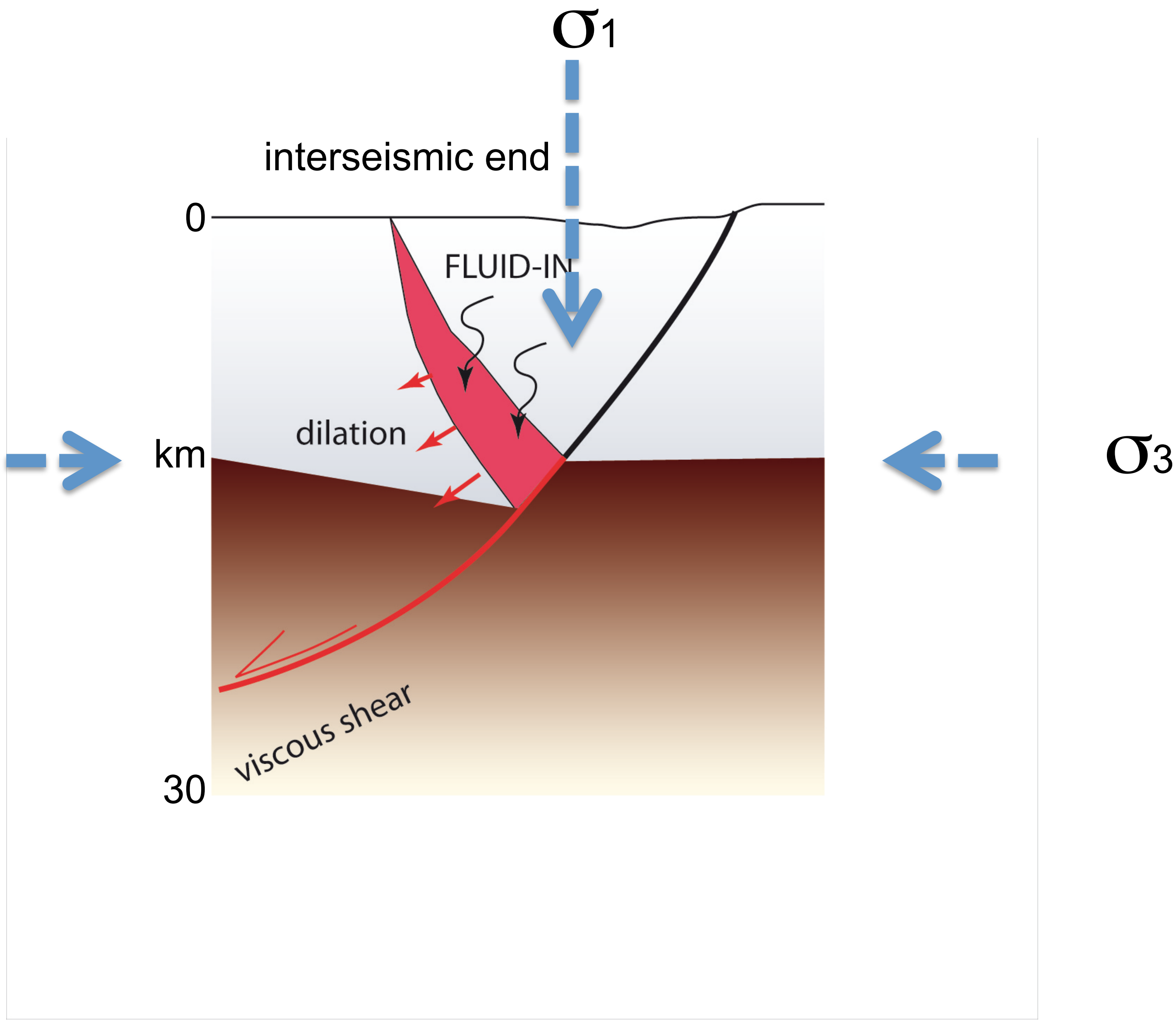
σ1
interseismic end
0
FLUID-IN
dilation
km
σ3
viscous shear
30

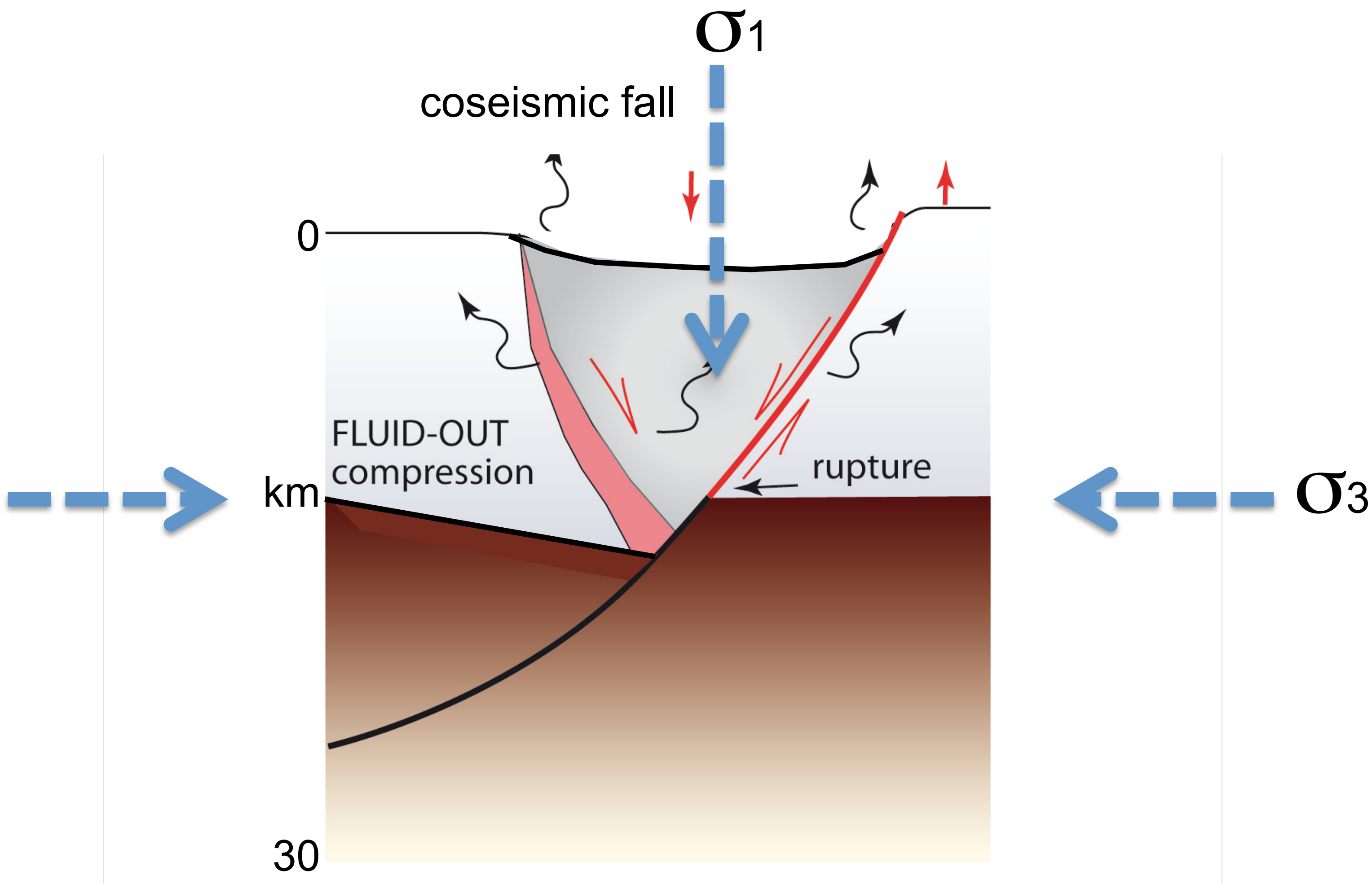
σ1
coseismic fall
0
FLUID-OUT
compression
km
rupture
σ3
30

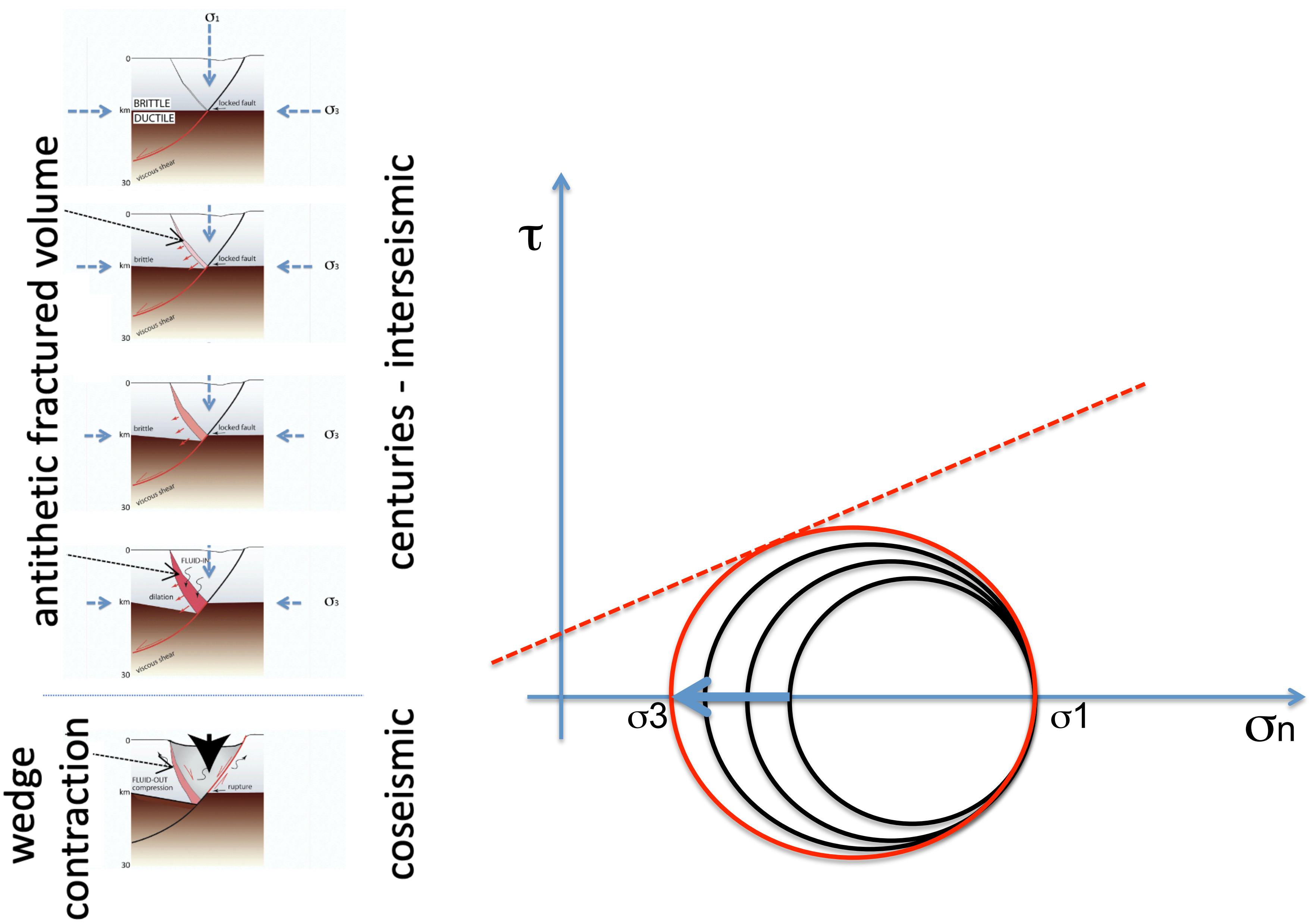

antithetic fractured volume
centuries - interseismic
wedge contraction
coseismic
σ1
σ3
BRITTLE
DUCTILE
locked fault
viscous shear
brittle
dilation
FLUID-IN
FLUID-OUT
compression
rupture
km
0
30
τ
σ3
σ1
σn

normal fault seismic cycle

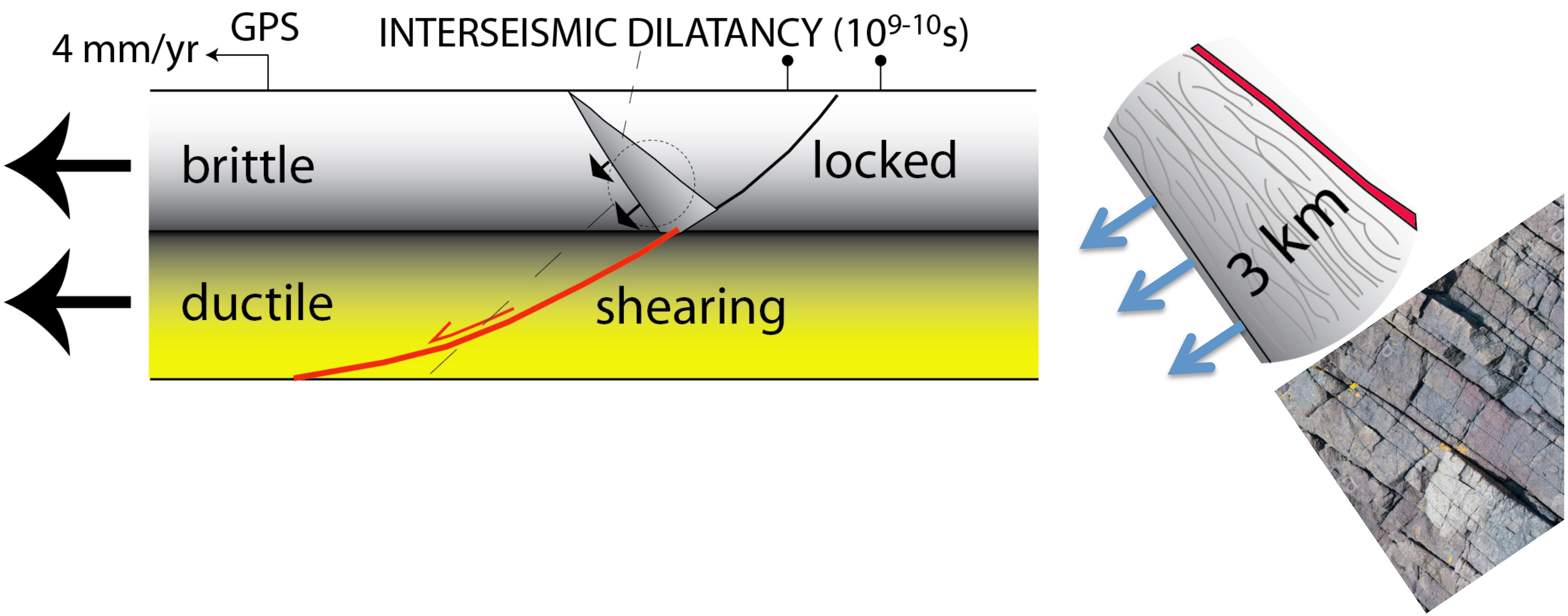


USGS

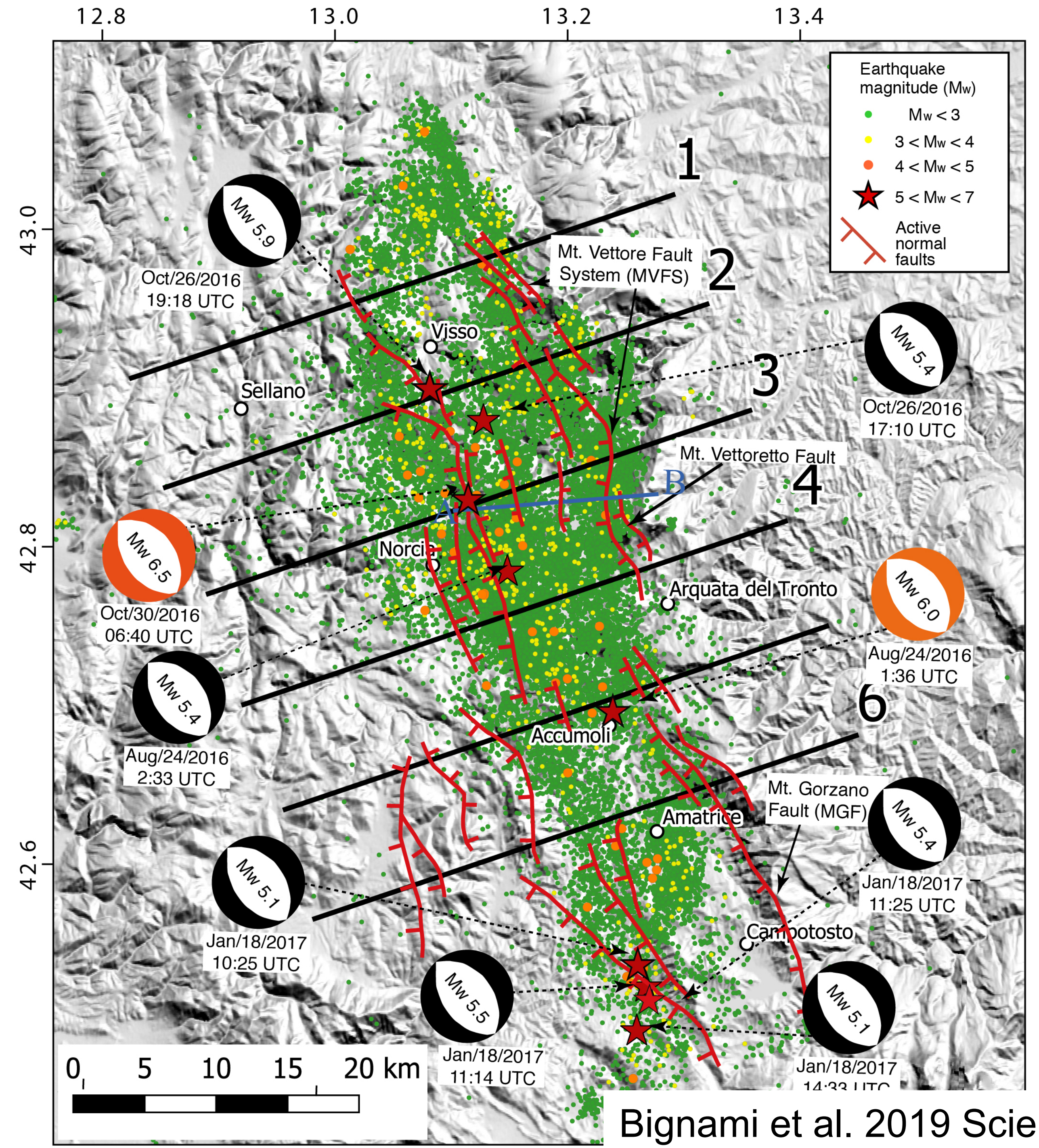

Bignami et al. 2019 Scientific Reports

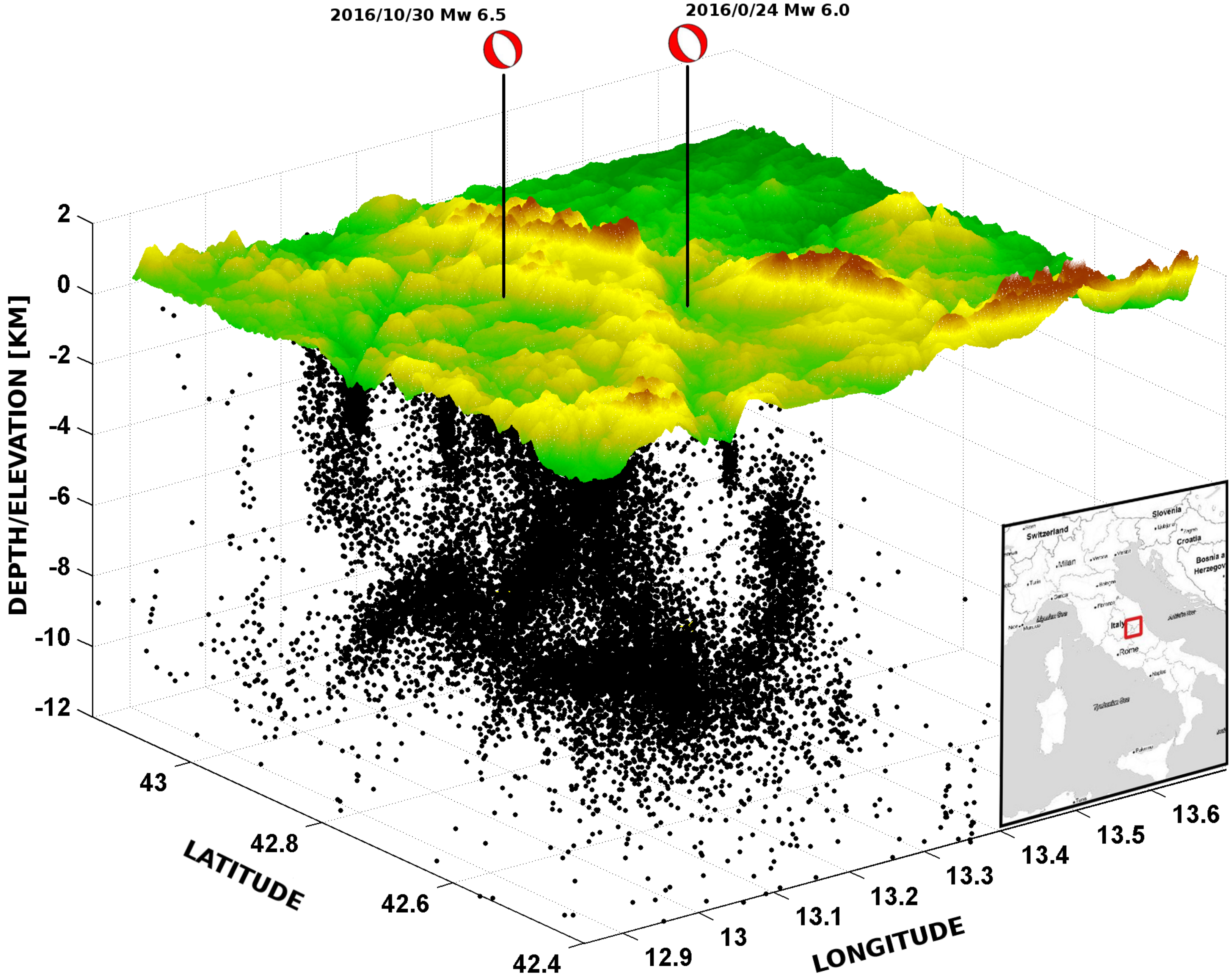

Bignami et al. 2019 Scientific Reports

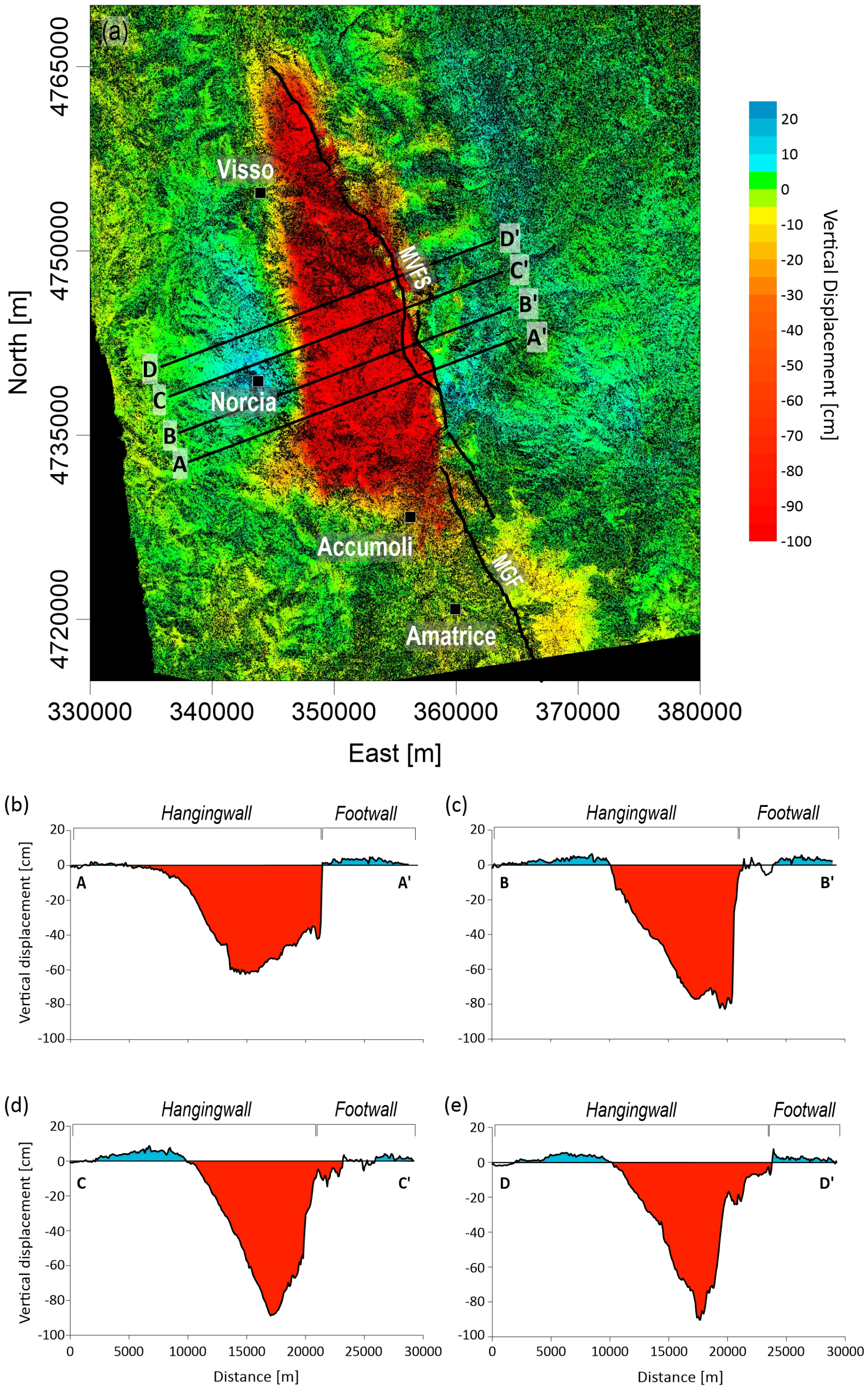

Valerio et al., 2018

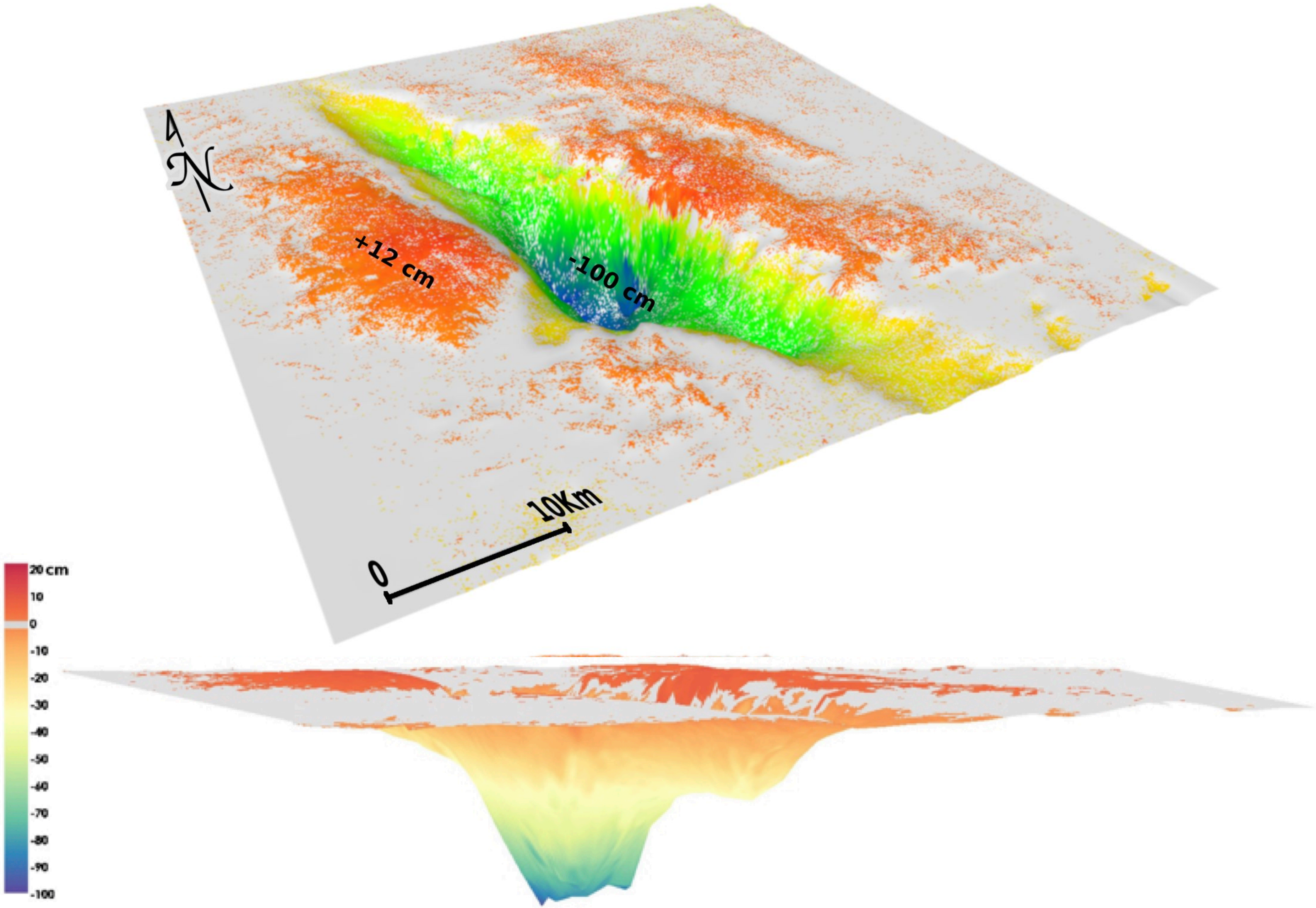

Bignami et al. 2019 Scientific Reports

VERTICAL COSEISMIC MOTION

$\boxed{A \approx 7.5B}$

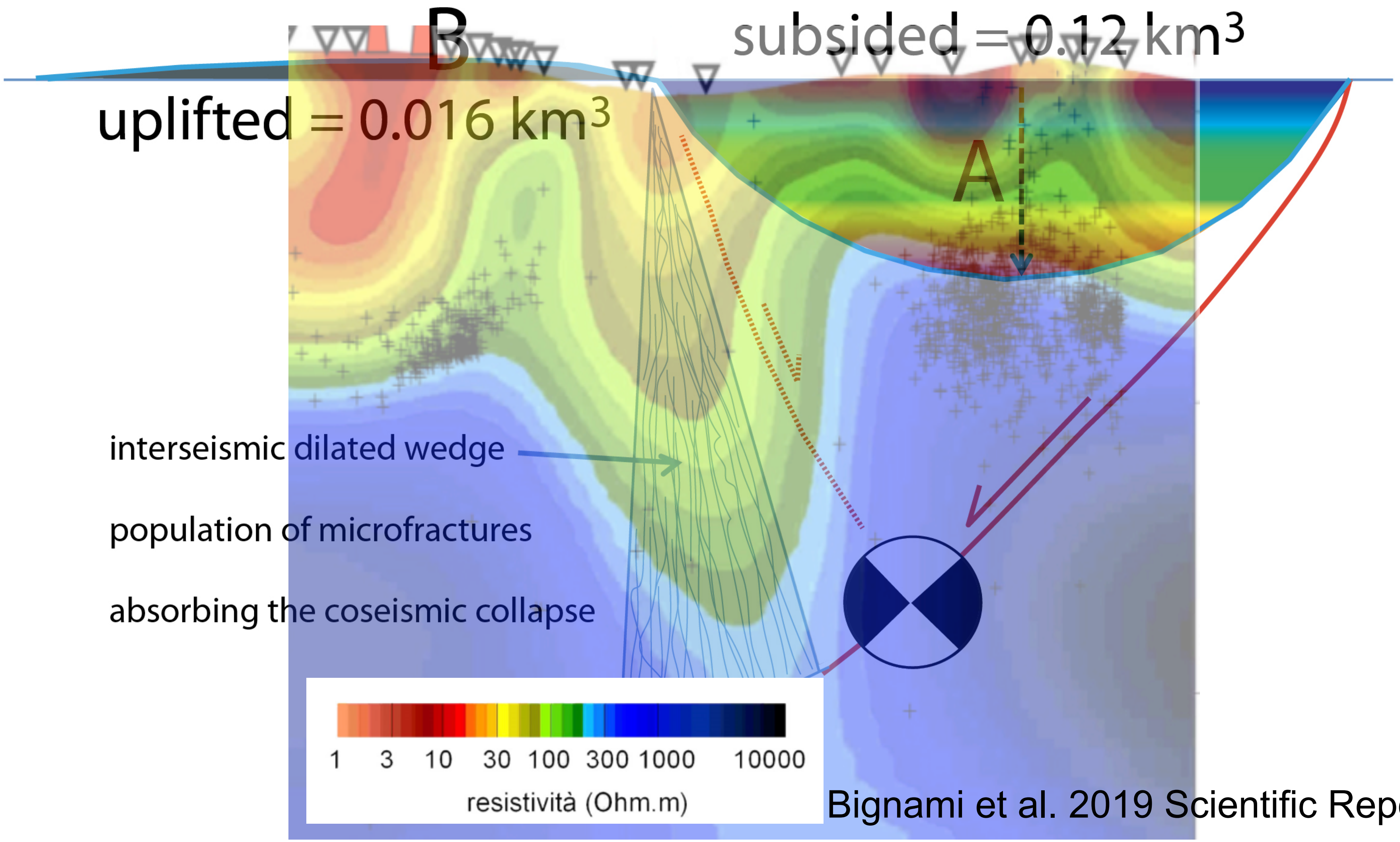

Bignami et al. 2019 Scientific Reports

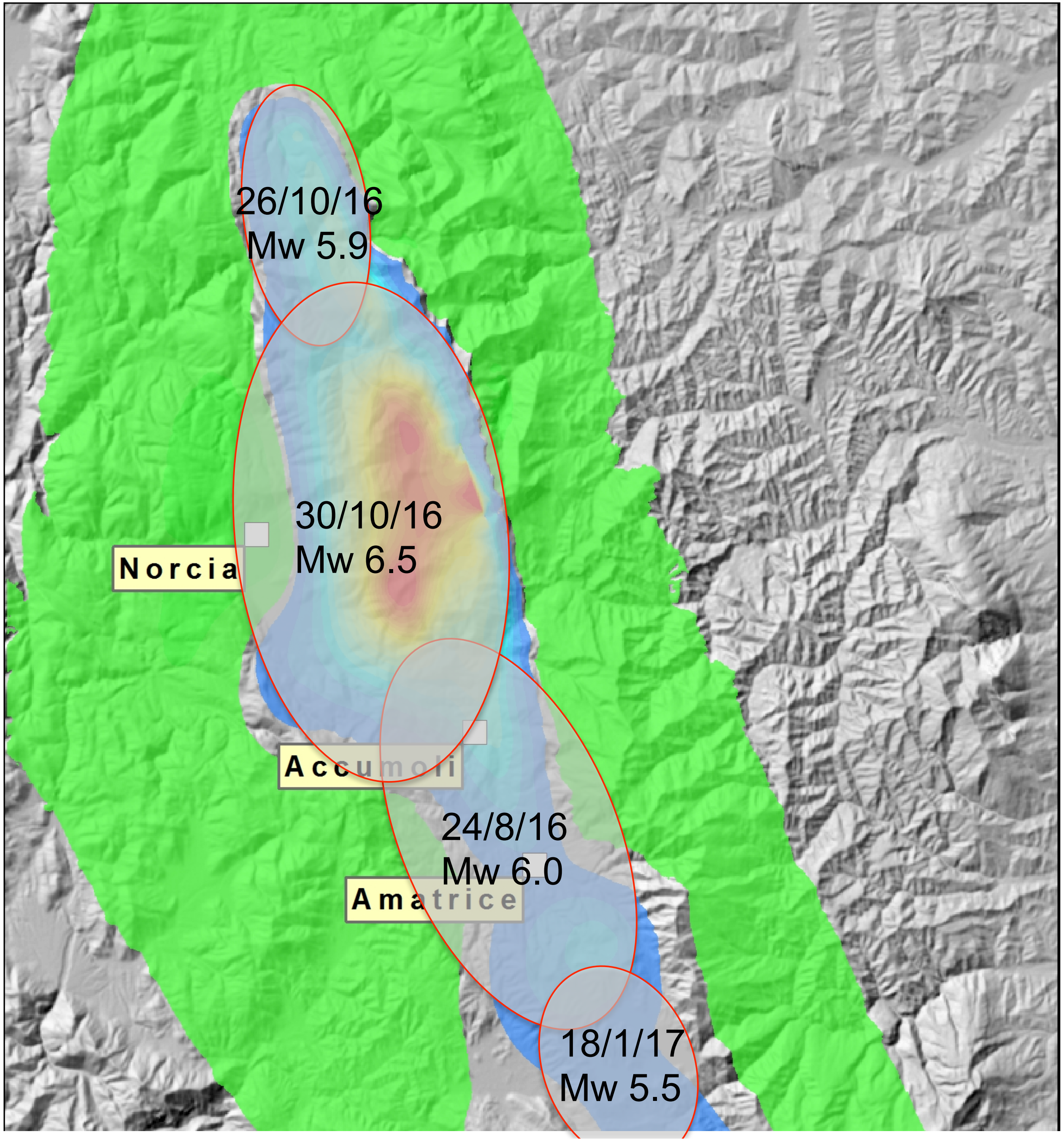

2016-2017
6000 km^3

Vertical displacement m

<VALUE>

-1 - -0.90
-0.89 - -0.85
-0.84 - -0.80
-0.79 - -0.75
-0.74 - -0.70
-0.69 - -0.65
-0.64 - -0.60
-0.59 - -0.55
-0.54 - -0.50
-0.49 - -0.45
-0.44 - -0.40
-0.39 - -0.35


D
C
C
D

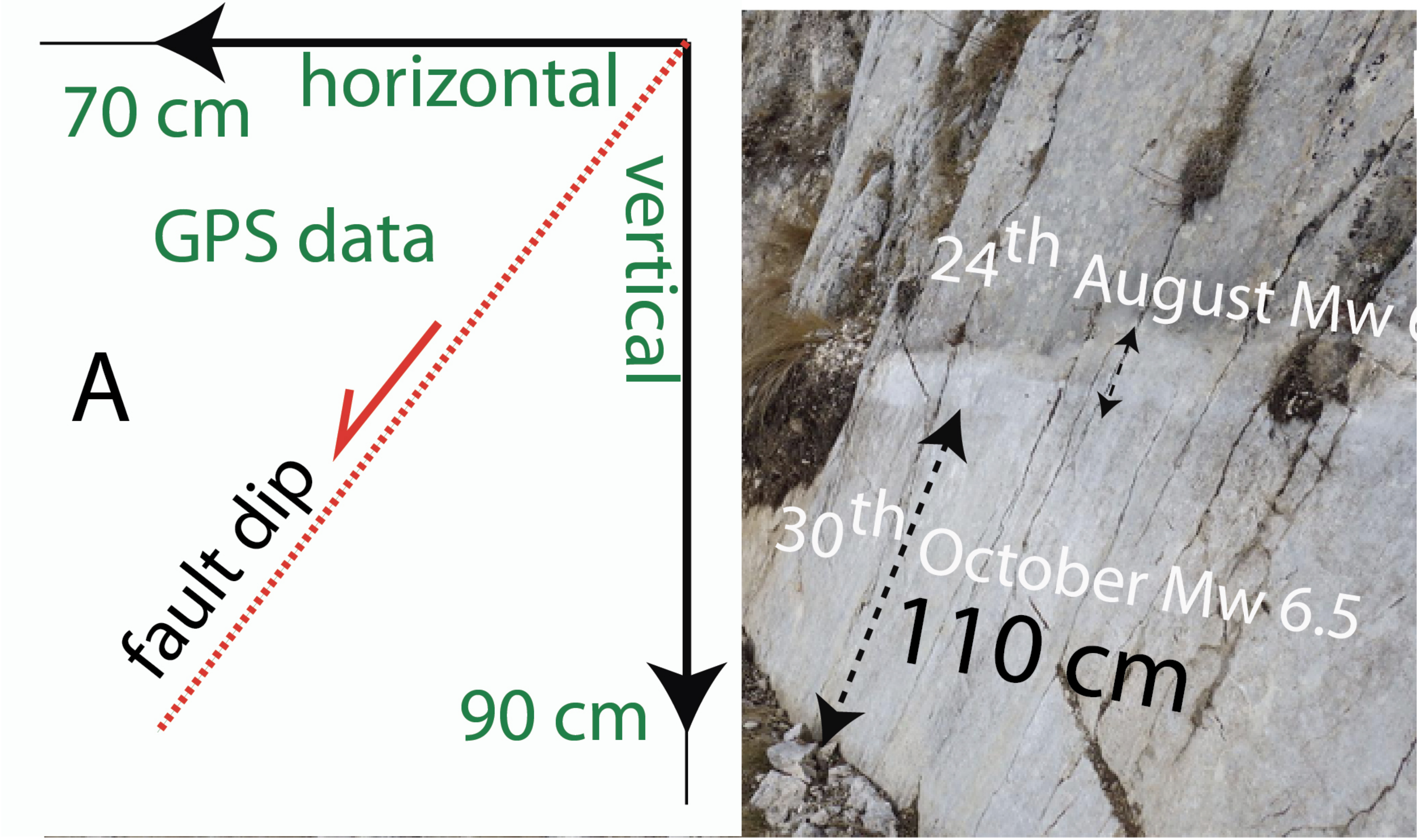

Bignami et al. 2019 Scientific Reports

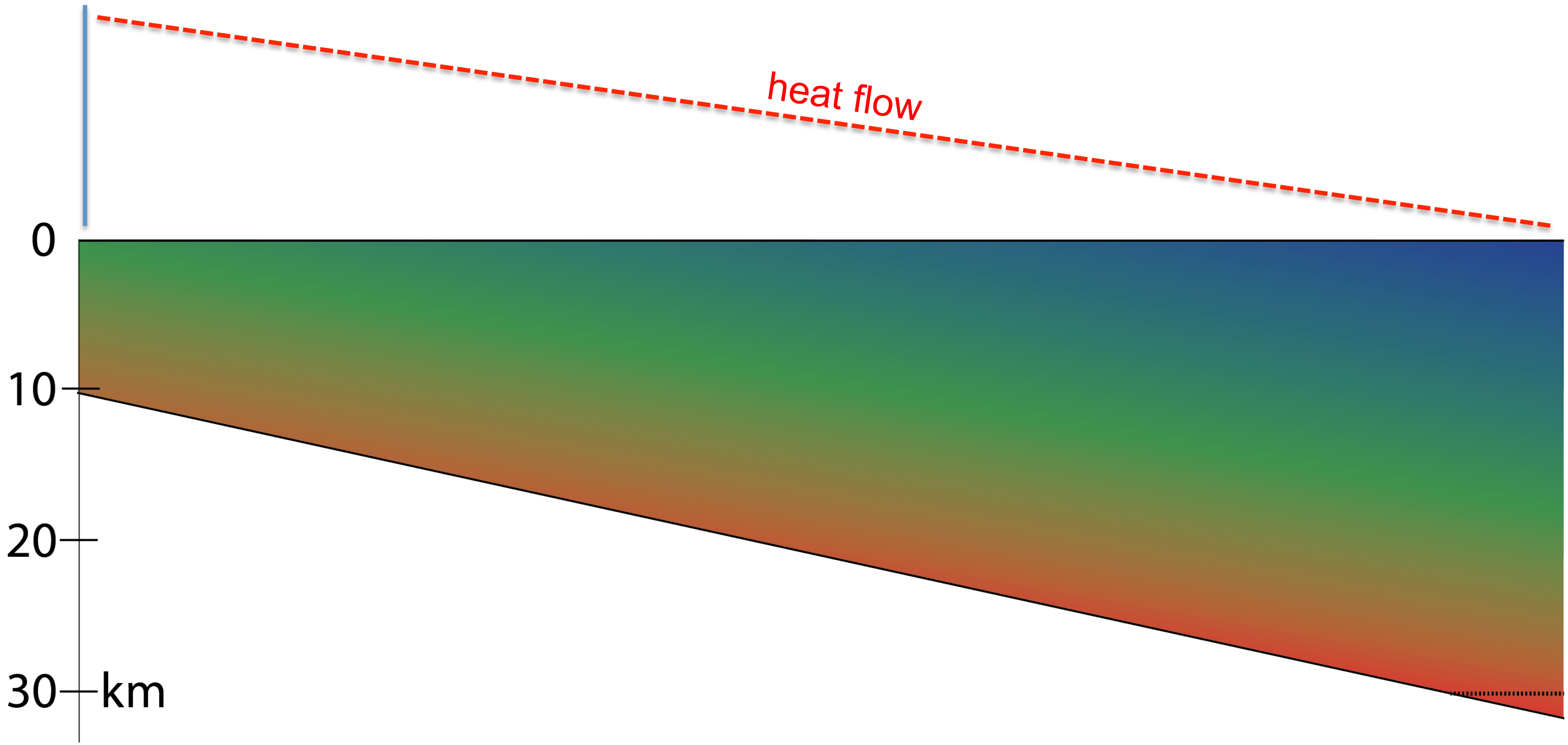

heat flow
0
10
20
30
km

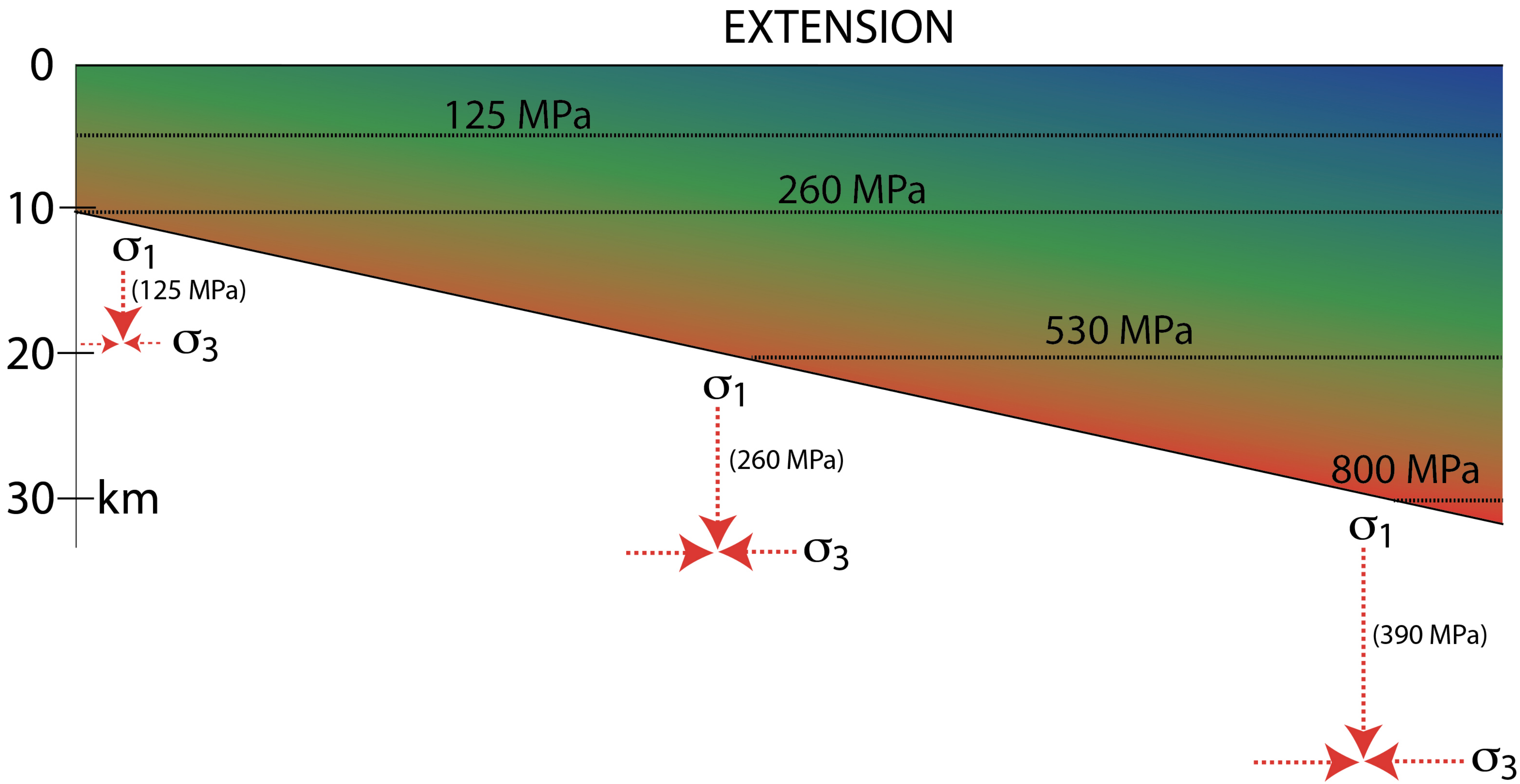

EXTENSION
0
10
20
30
km
125 MPa
260 MPa
530 MPa
800 MPa
σ1
(125 MPa)
σ3
σ1
(260 MPa)
σ3
σ1
(390 MPa)
σ3

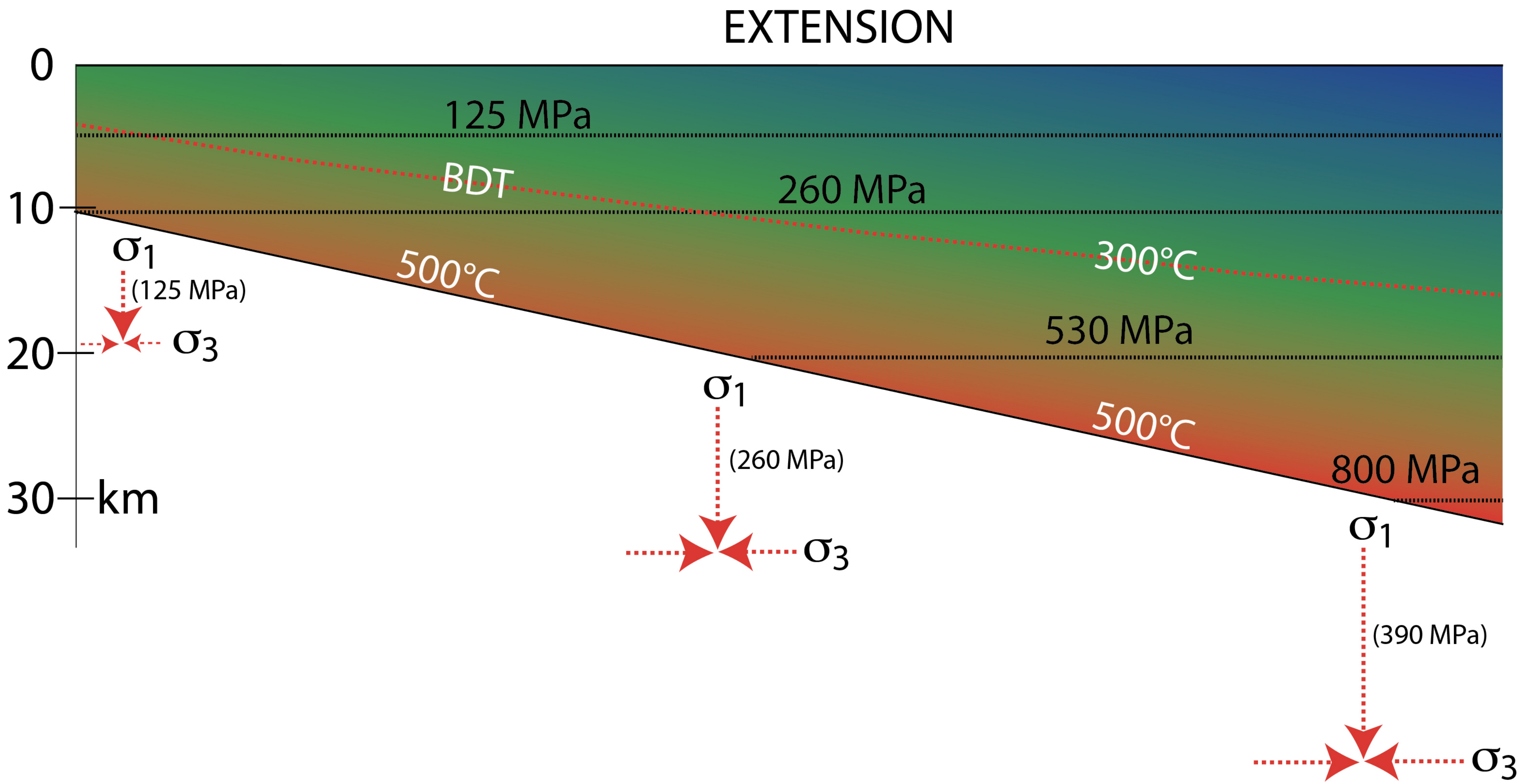

EXTENSION
0
10
20
30
km
125 MPa
BDT
260 MPa
300°C
500°C
530 MPa
500°C
800 MPa
σ1
(125 MPa)
σ3
σ1
(260 MPa)
σ3
σ1
(390 MPa)
σ3

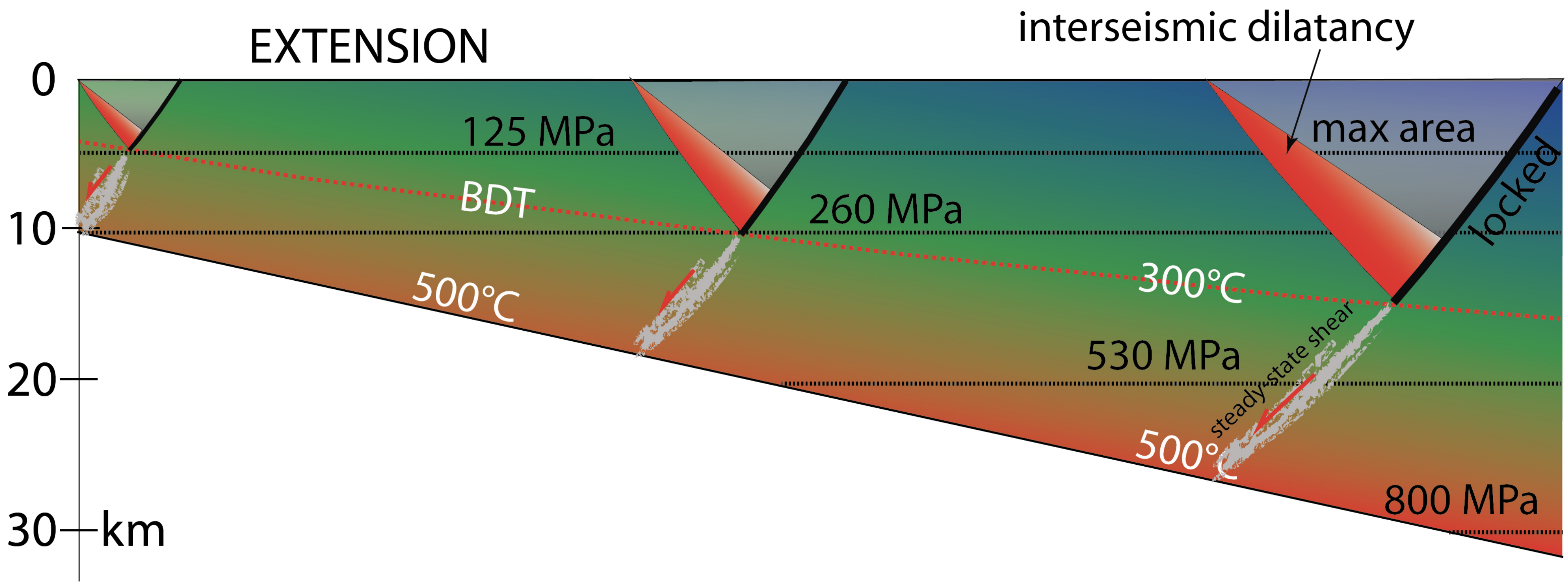
EXTENSION
interseismic dilatancy
0
10
20
30
km
125 MPa
max area
BDT
260 MPa
locked
500°C
300°C
530 MPa
steady-state shear
500°C
800 MPa

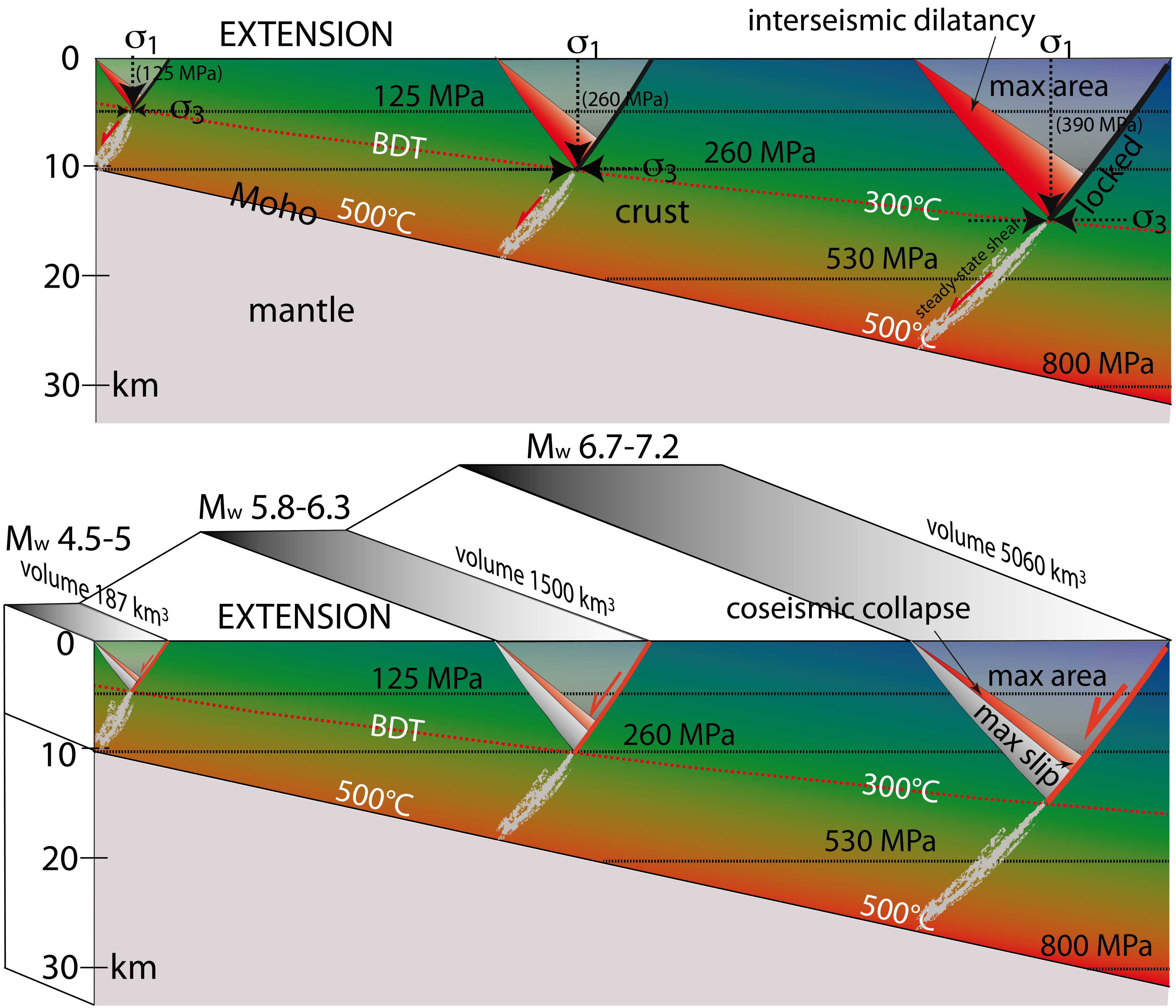

EXTENSION
interseismic dilatancy
σ1
(125 MPa)
σ3
125 MPa
(260 MPa)
max area
(390 MPa)
260 MPa
BDT
locked
Moho
500°C
crust
300°C
530 MPa
steady state shear
mantle
800 MPa
0
10
20
30
km
Mw 6.7-7.2
Mw 5.8-6.3
Mw 4.5-5
volume 187 km3
volume 1500 km3
volume 5060 km3
coseismic collapse
max slip

ESTENSION

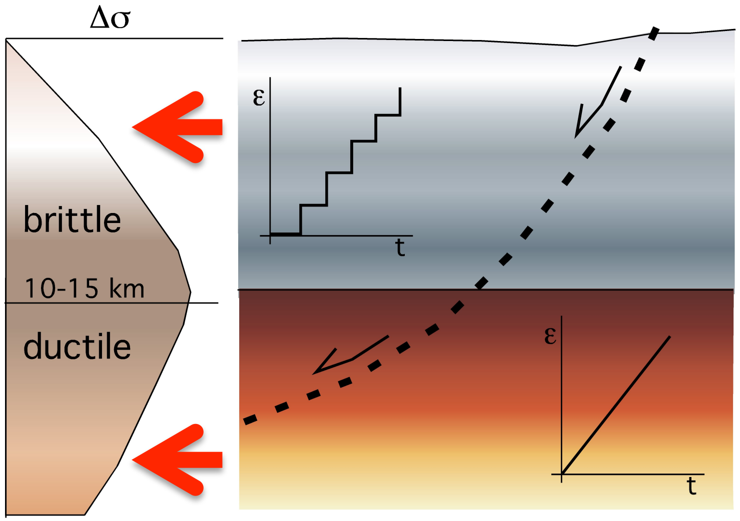

COMPRESSION

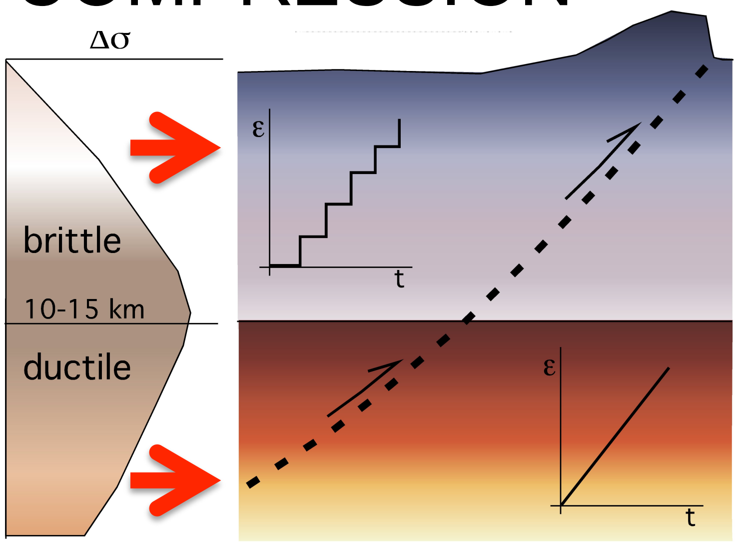

Normal fault

Thrust

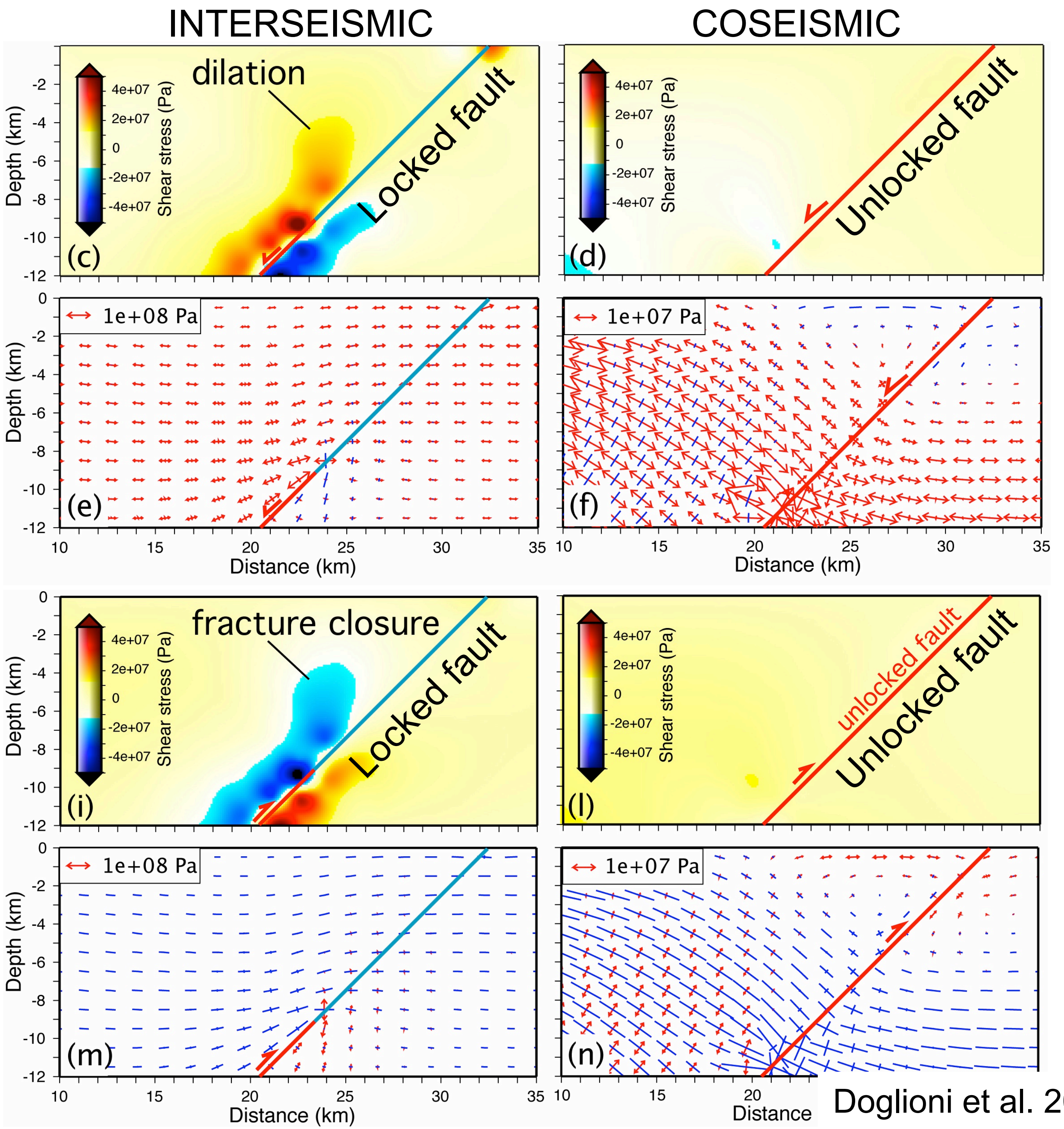

Doglioni et al. 2011 PEPI

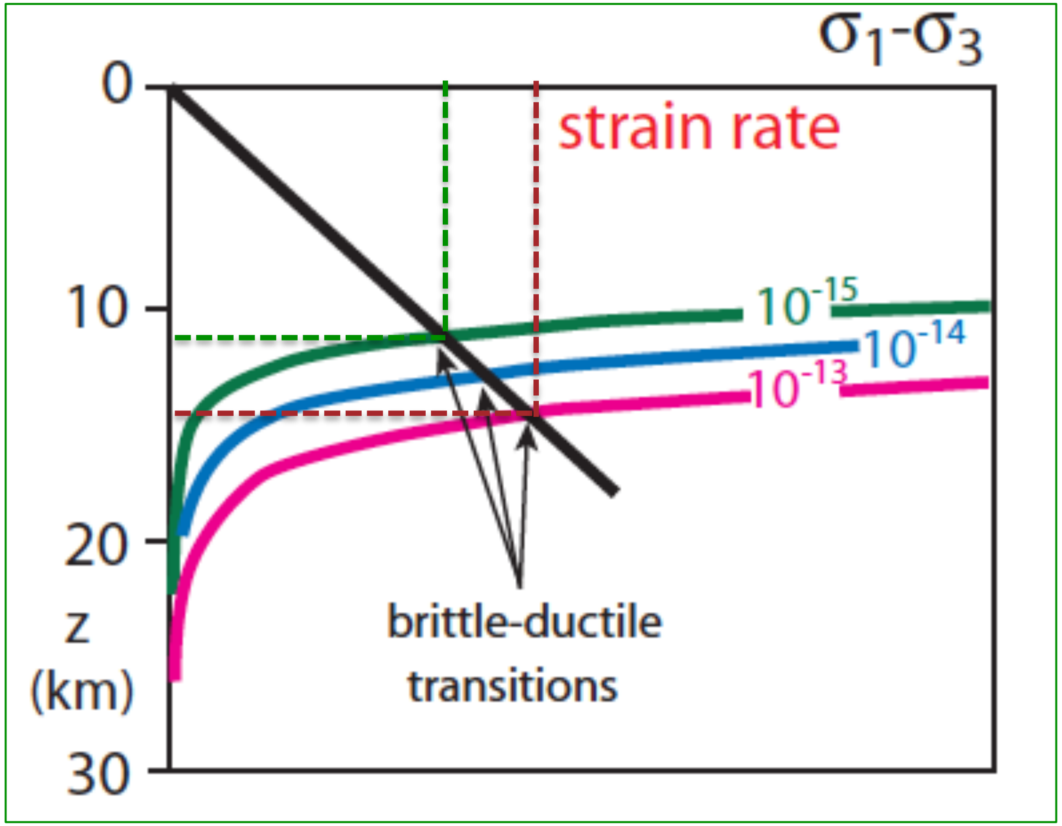

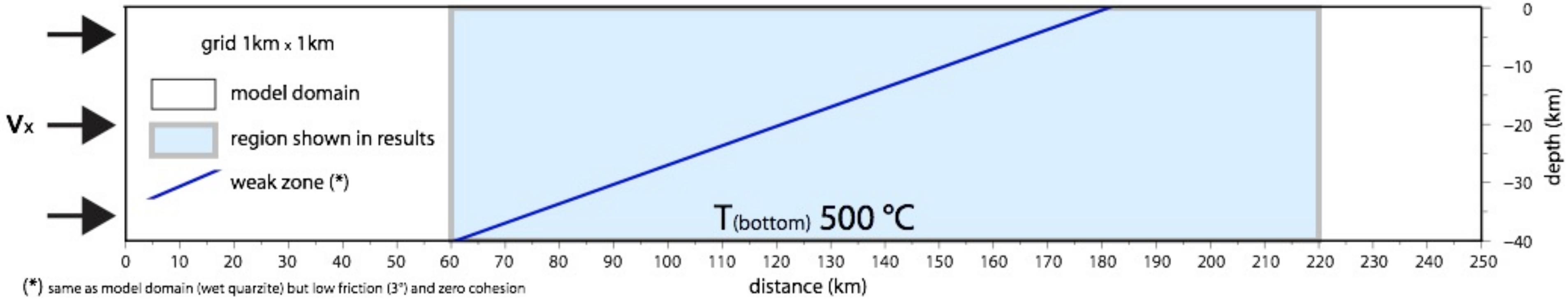

Petricca et al. 2018 PEPI

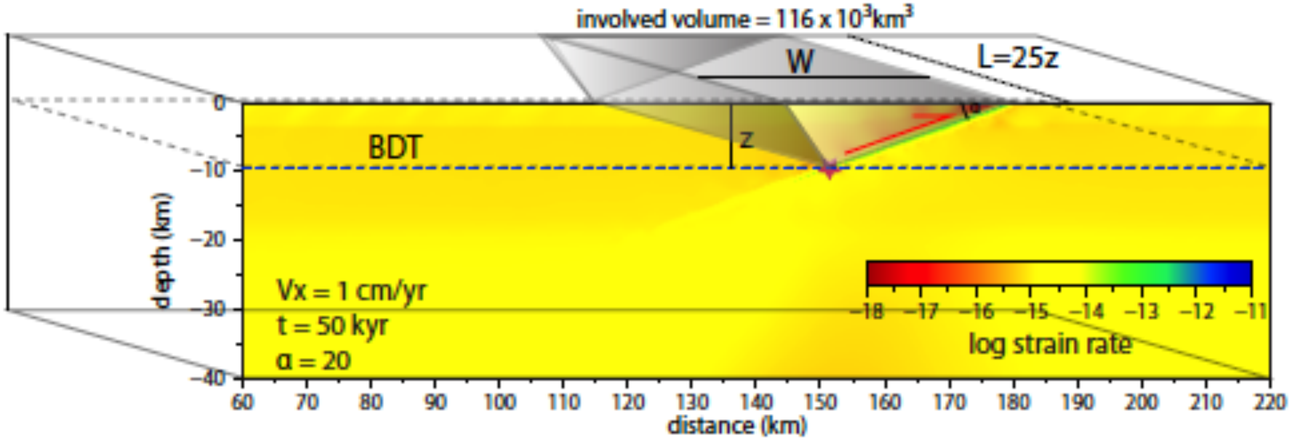

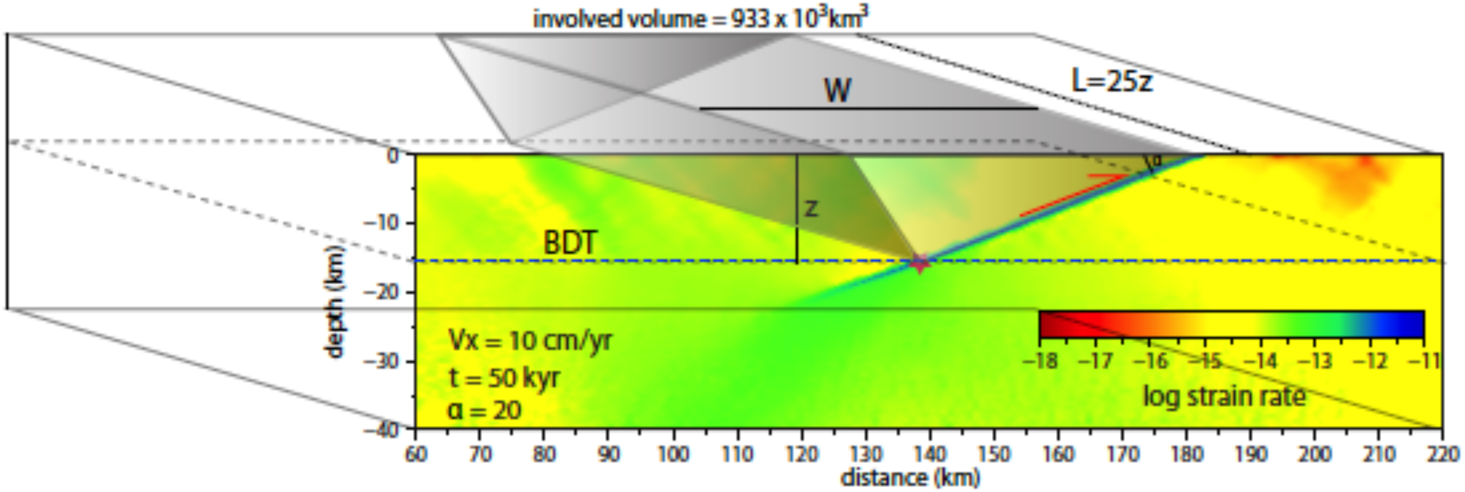

Petricca et al. 2018 PEPI

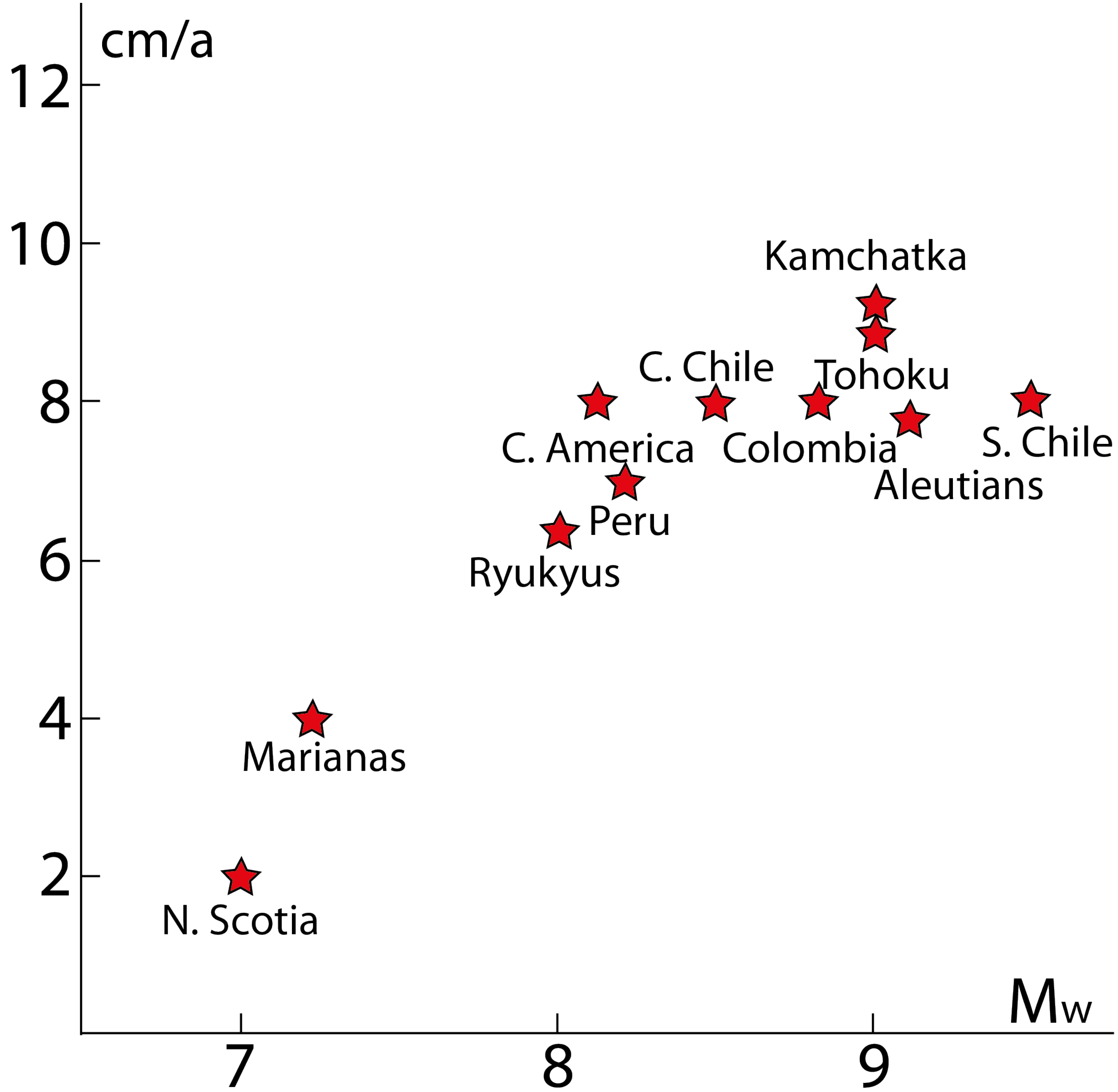
cm/a
12
10
8
6
4
2
Kamchatka
C. Chile
Tohoku
C. America
Colombia
S. Chile
Aleutians
Peru
Ryukyus
Marianas
N. Scotia
Mw
7
8
9

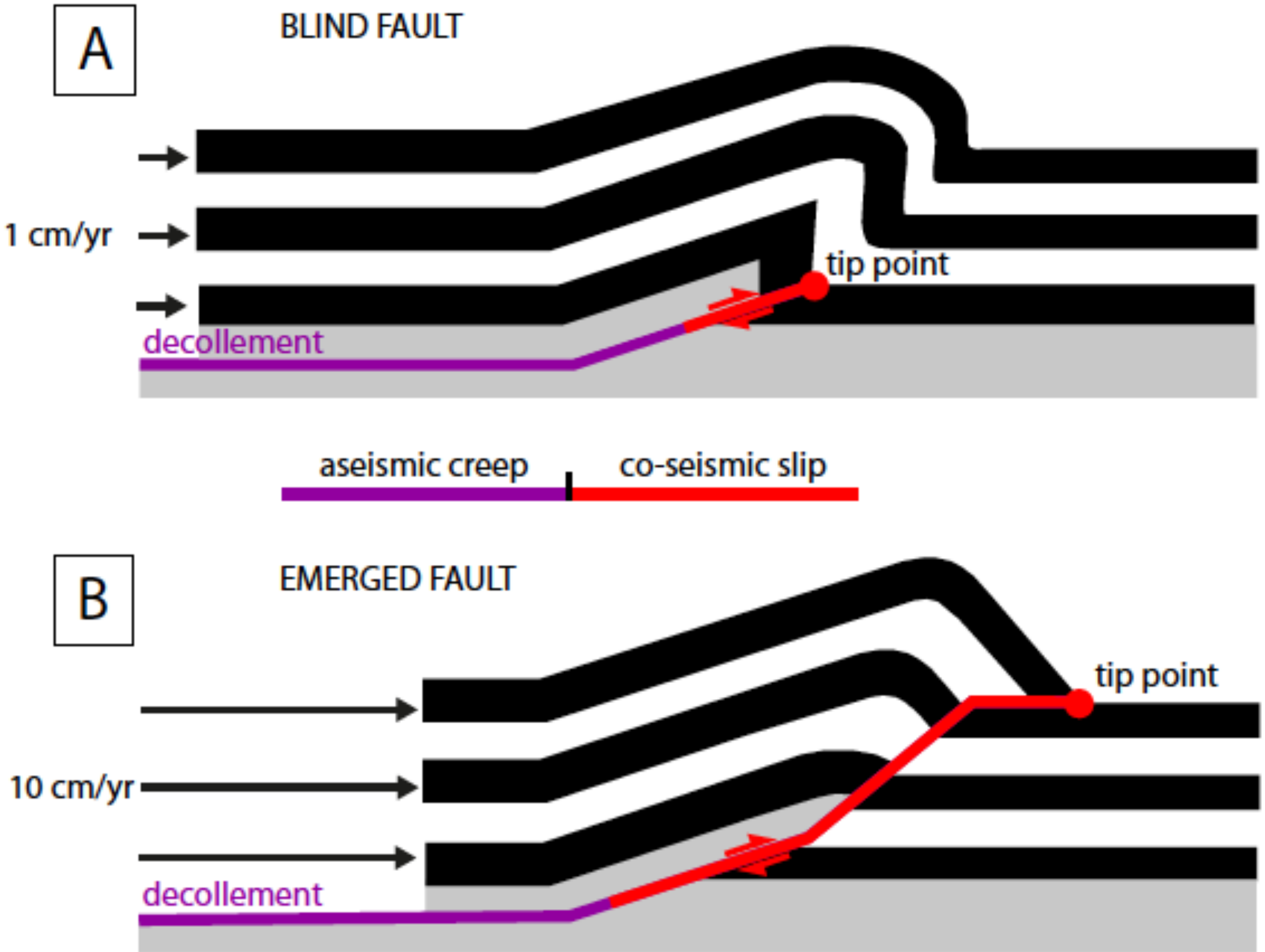

Petricca et al. 2018 PEPI

Doglioni et al. 2015 SREP

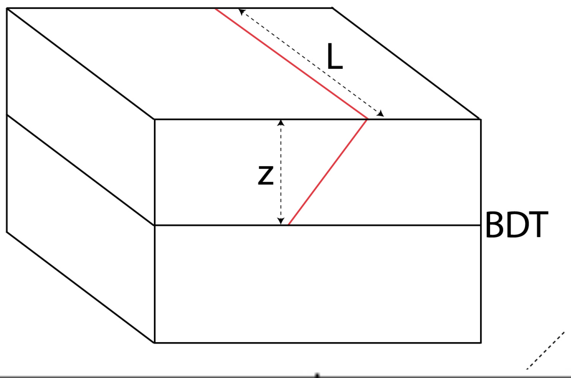

Fault type	Earthquake	M	Z (km)	L (km)	L/z
Normal fault	Pleasant Valley 1915	7.2	15-20	~60	3-4
Normal fault	Irpinia 1980		.5	~45	3
Normal fault	Corinth 1981		.3	~40	3
Normal fault	Edgecumbe 1987		.5	~50	3.3
Normal fault	L'Aquila 2009	6.3	10	~30	3
Strike slip	Macquarie Ridge 1989	8.1	12-15	~140	9.3-11.6
Strike slip	Luzon 1990		.5-20	~150	7.
Strike slip	Landers 1992		.2	~85	7
Strike slip	Izmit 1999		.5	~160	1
Strike slip	Sumatra 2012	8.7	35-40	~400	10-11.4
Thrust	Chile 1960	9.5	30-40	~900	22.5-30
Thrust	Alaska 1964		0-40	~700-800	1
Thrust	Sumatra 2004		5-45	~1200	2
Thrust	Maule 2010		5-30	~500	1
Thrust	Tohoku 2011	9.0	30	~650	21.6

7.5

3

8.7

10

9.5

25

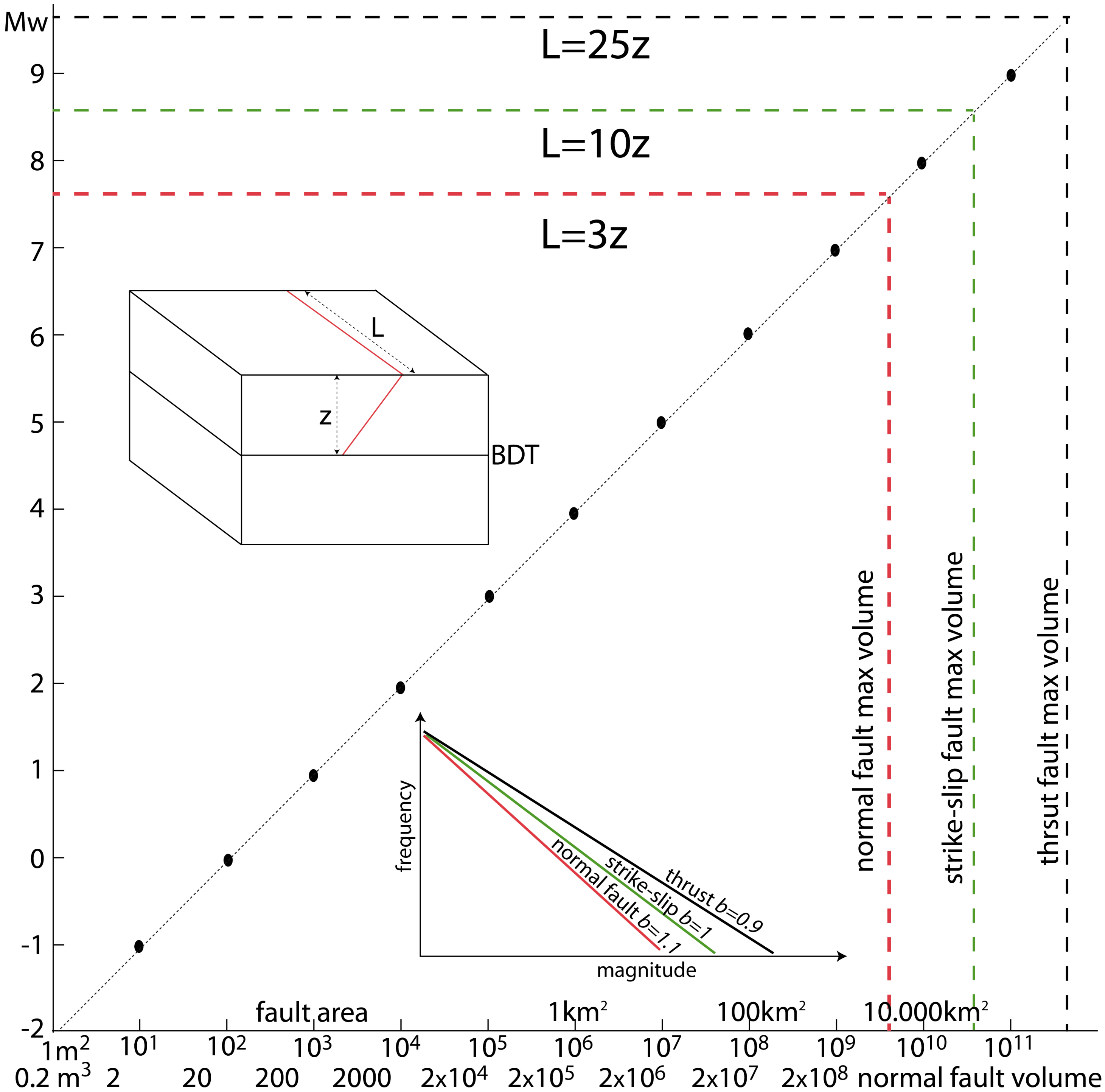

Mw
L=25z
L=10z
L=3z
9
8
7
6
5
4
3
2
1
0
-1
-2
L
z
BDT
frequency
magnitude
thrust b=0.9
strike-slip b=1
normal fault b=1.1
normal fault max volume
strike-slip fault max volume
thrsut fault max volume
fault area
1km²
100km²
10.000km²
1m² 10¹ 10² 10³ 10⁴ 10⁵ 10⁶ 10⁷ 10⁸ 10⁹ 10¹⁰ 10¹¹
0.2 m³ 2 20 200 2000 2x10⁴ 2x10⁵ 2x10⁶ 2x10⁷ 2x10⁸ normal fault volume

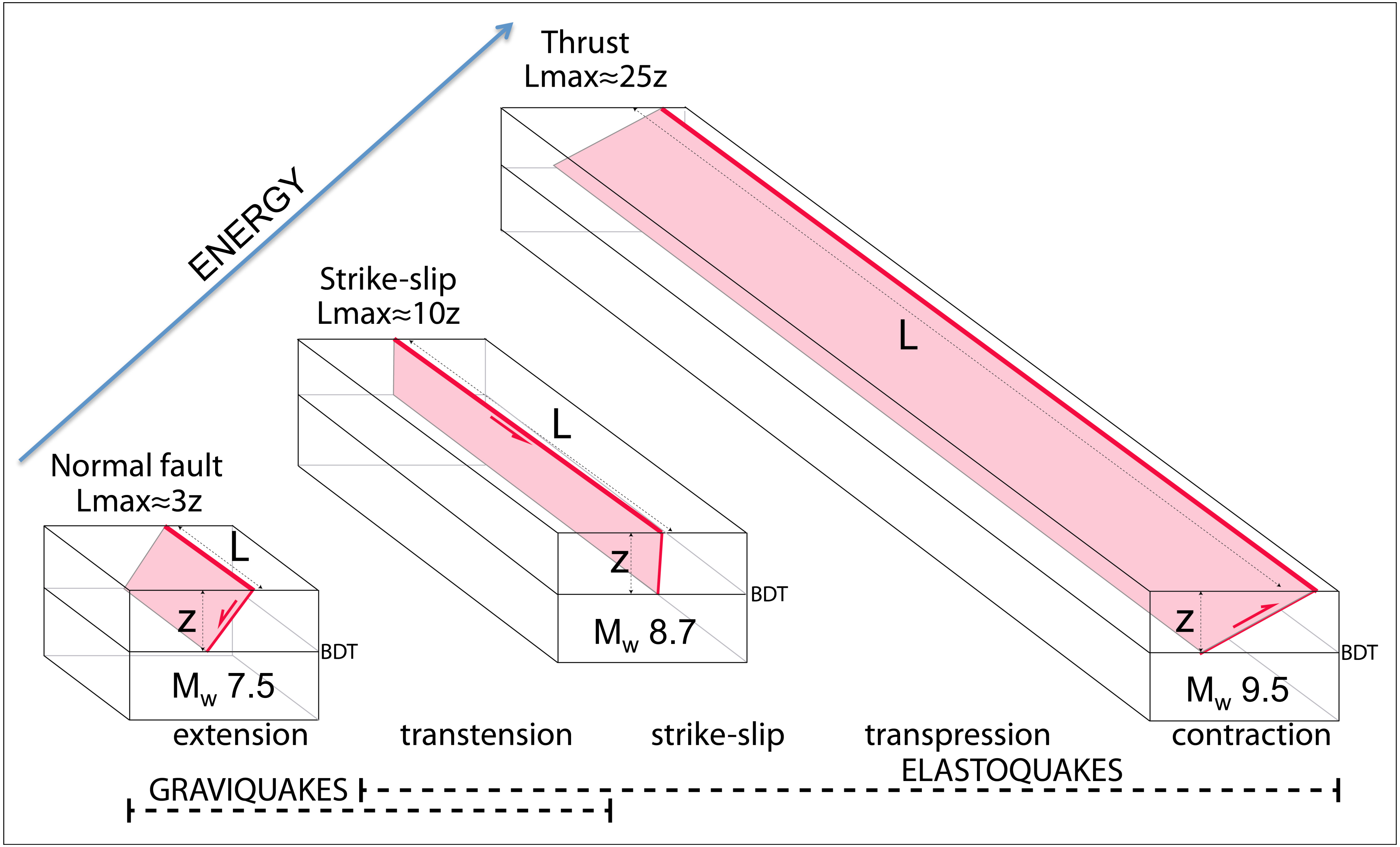

L /z = rupture length / depth activated volume

Doglioni 2016 Lincei

EARTHQUAKE ENERGY

GRAVIQUAKE

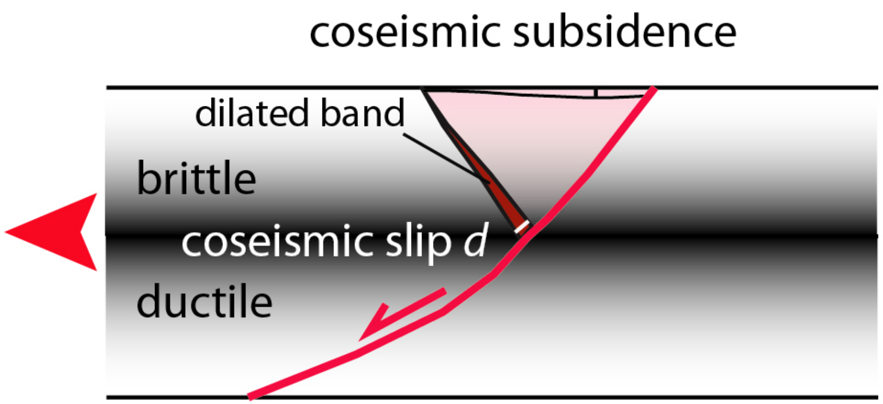

normal faulting

$$E = mgh(\mu_s, \Theta)$$

ELASTOQUAKE

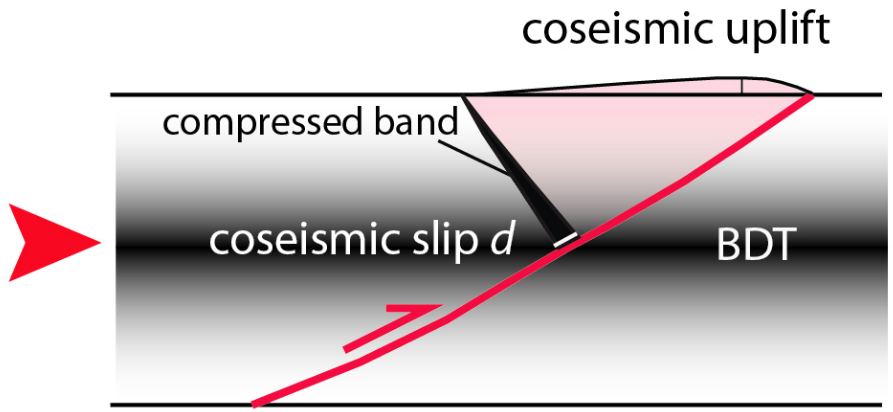

thrust faulting

$$E = \frac{1}{2} K \left(\frac{\Delta V\ (\mu_s, \Theta)}{V} \right)^2 \frac{m}{\rho}$$

pro gravity **against gravity**

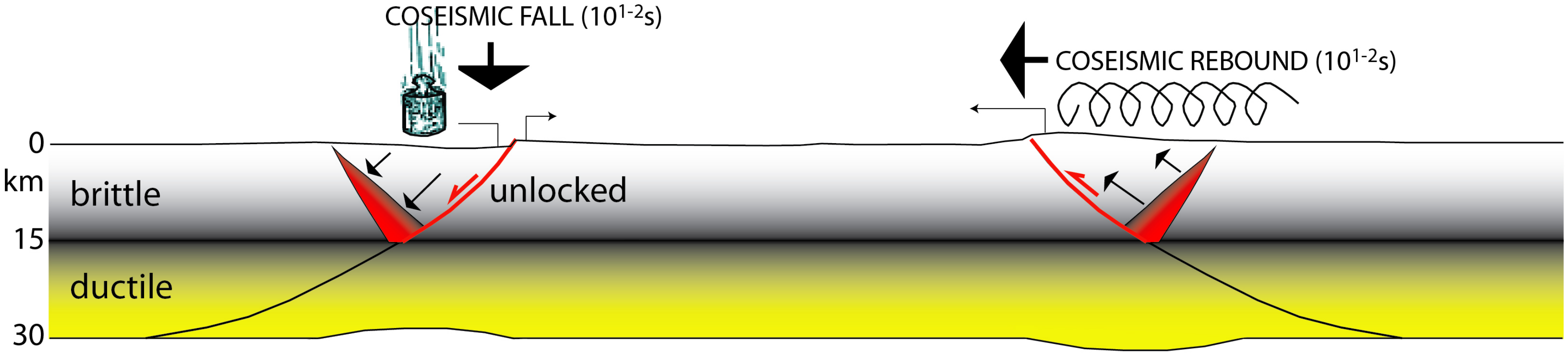

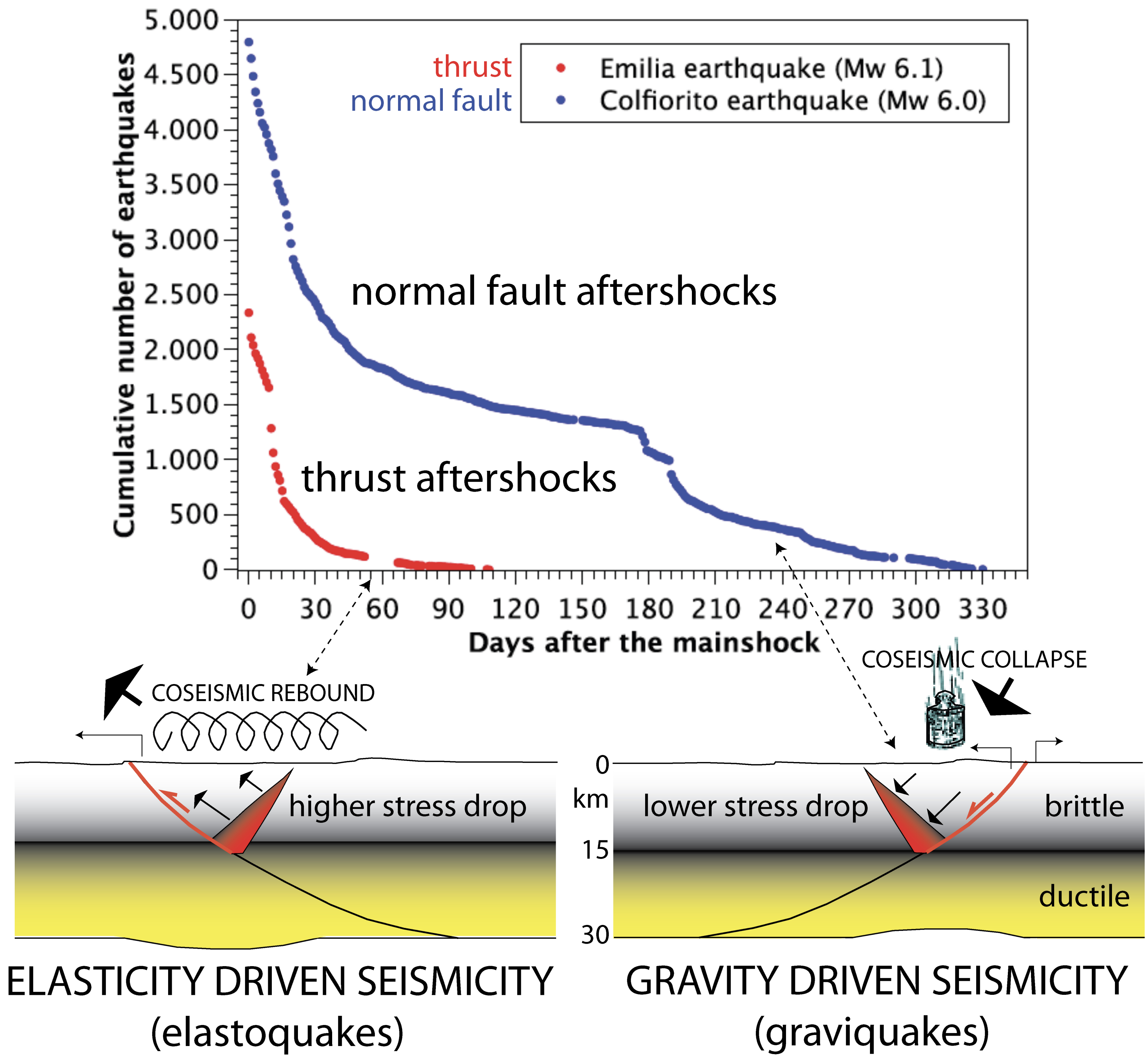

5.000
4.500
4.000
3.500
3.000
2.500
2.000
1.500
1.000
500
0
Cumulative number of earthquakes
thrust
normal fault
Emilia earthquake (Mw 6.1)
Colfiorito earthquake (Mw 6.0)
normal fault aftershocks
thrust aftershocks
0 30 60 90 120 150 180 210 240 270 300 330
Days after the mainshock
COSEISMIC REBOUND
COSEISMIC COLLAPSE
higher stress drop
lower stress drop
0
km
15
30
brittle
ductile
ELASTICITY DRIVEN SEISMICITY
(elastoquakes)
GRAVITY DRIVEN SEISMICITY
(graviquakes)

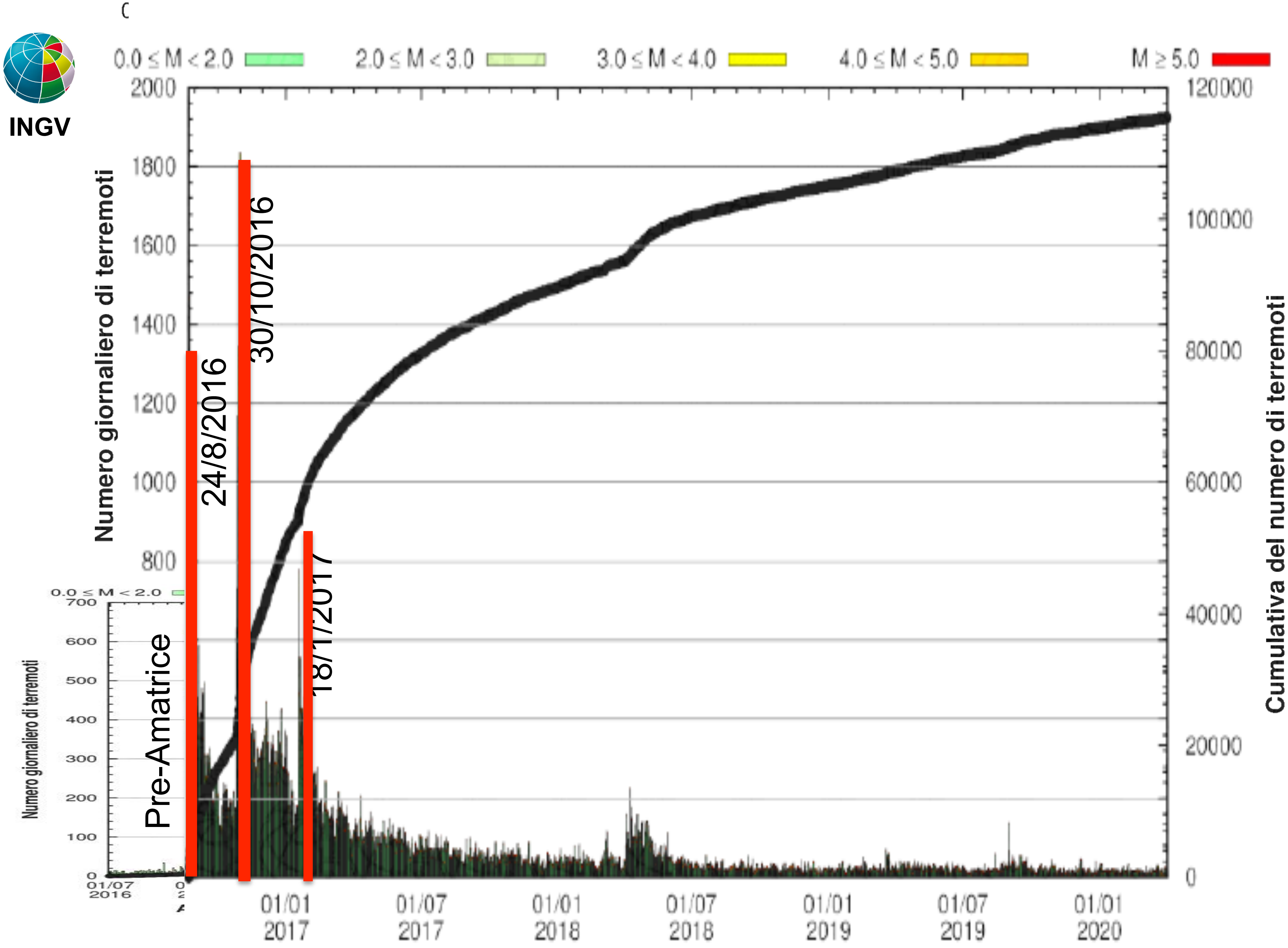
INGV
0.0 ≤ M < 2.0
2.0 ≤ M < 3.0
3.0 ≤ M < 4.0
4.0 ≤ M < 5.0
M ≥ 5.0
Numero giornaliero di terremoti
Cumulativa del numero di terremoti
24/8/2016
30/10/2016
18/1/2017
Pre-Amatrice
01/01 2017
01/07 2017
01/01 2018
01/07 2018
01/01 2019
01/07 2019
01/01 2020
01/07 2016

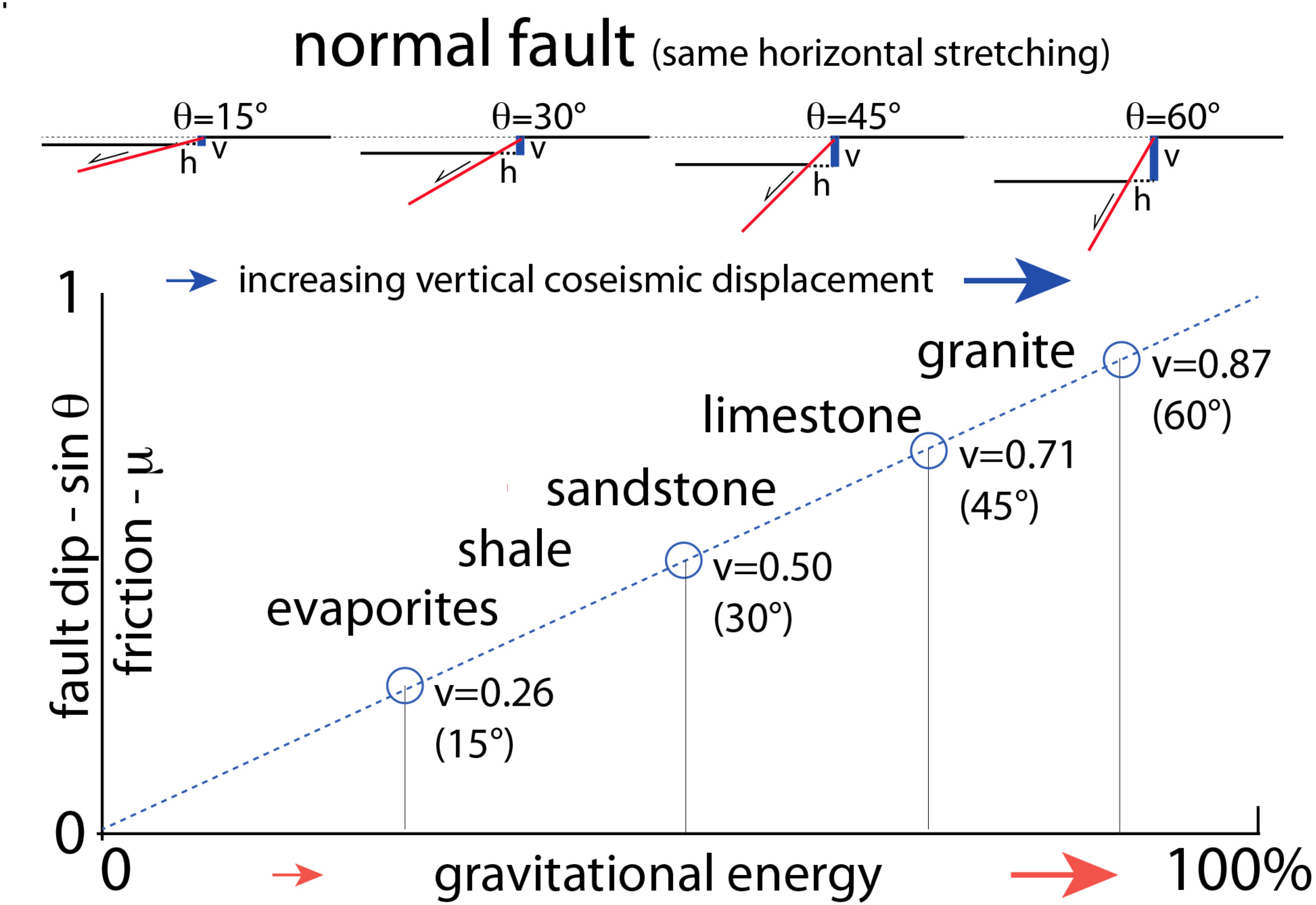

Doglioni et al. 2015 Scientific Reports

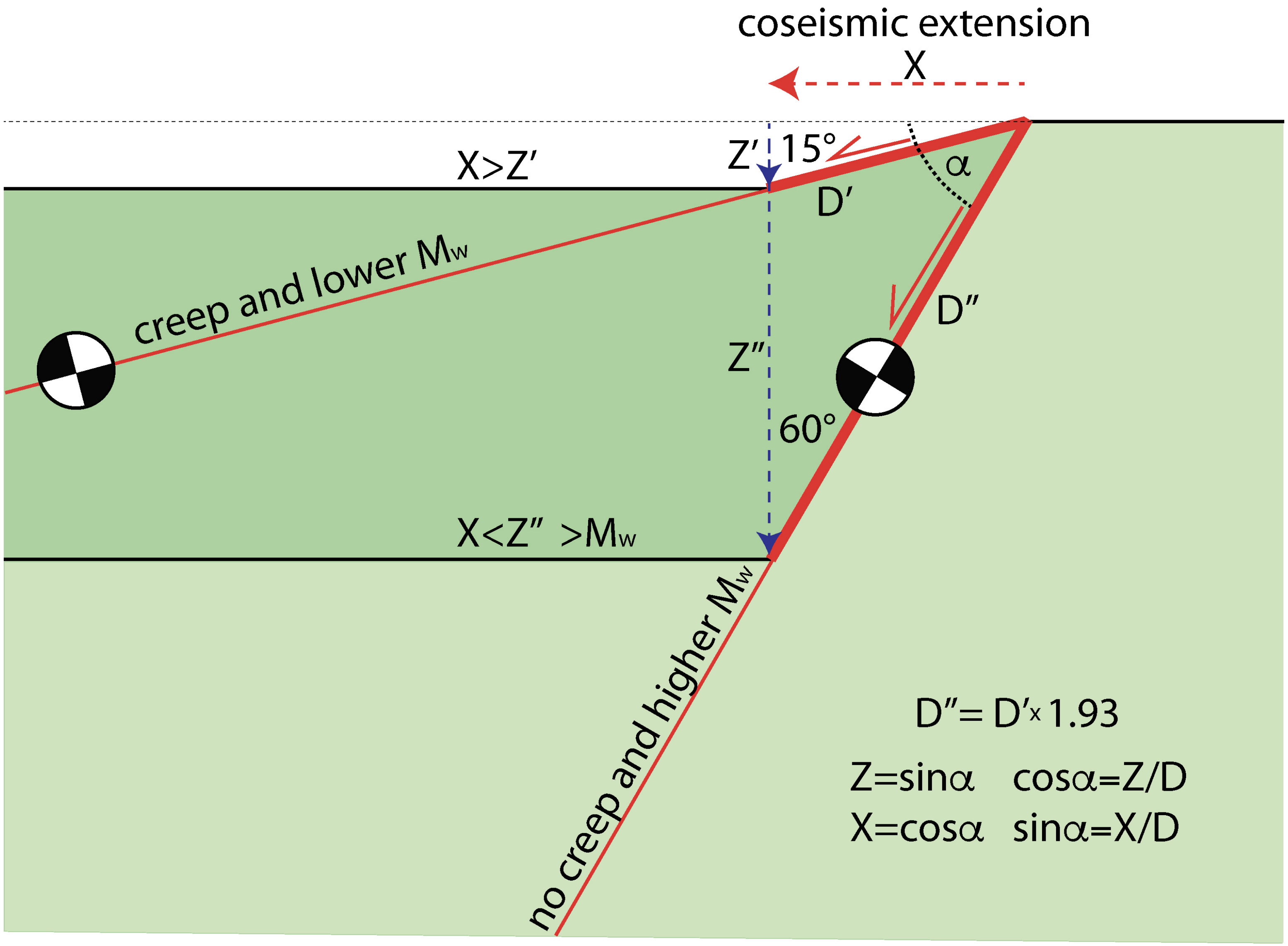
coseismic extension
X
X>Z′
Z′
15°
α
D′
creep and lower Mw
D″
Z″
60°
X<Z″ >Mw
no creep and higher Mw
D″= D′x 1.93
Z=sinα cosα=Z/D
X=cosα sinα=X/D

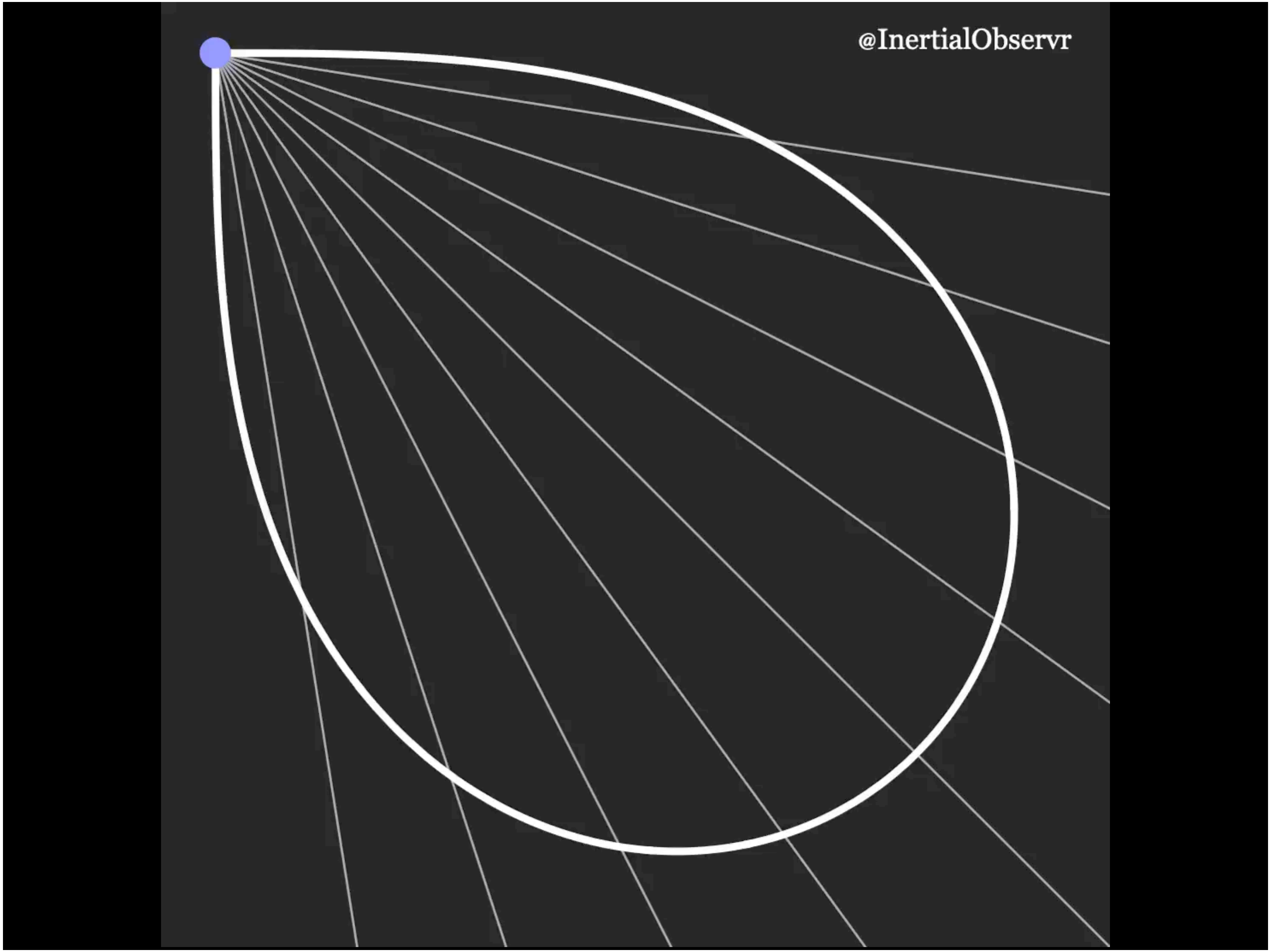
@InertialObservr

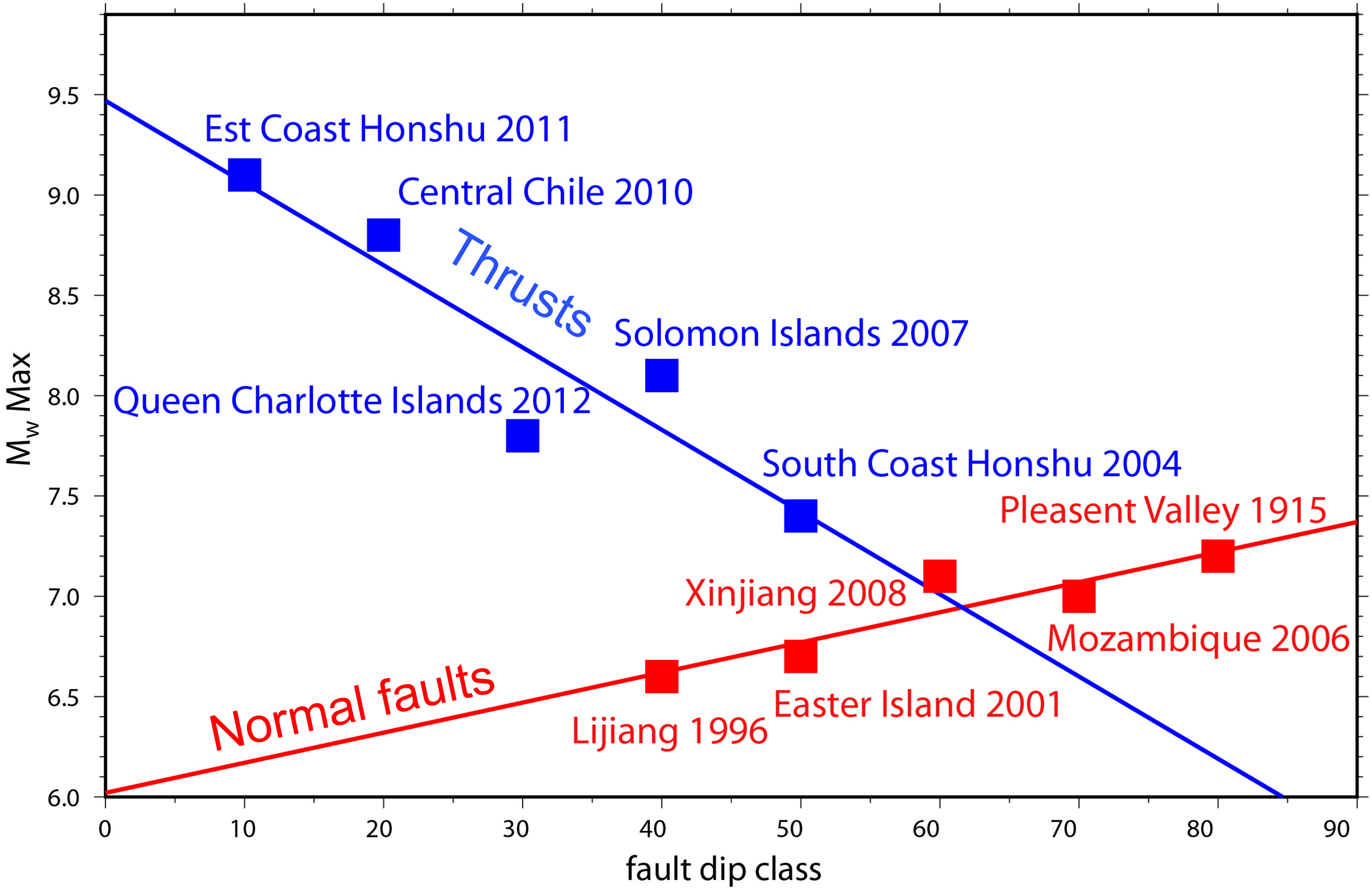

Est Coast Honshu 2011
Central Chile 2010
Thrusts
Solomon Islands 2007
Queen Charlotte Islands 2012
South Coast Honshu 2004
Pleasent Valley 1915
Xinjiang 2008
Mozambique 2006
Normal faults
Easter Island 2001
Lijiang 1996
M_w Max
9.5
9.0
8.5
8.0
7.5
7.0
6.5
6.0
0
10
20
30
40
50
60
70
80
90
fault dip class

INGV

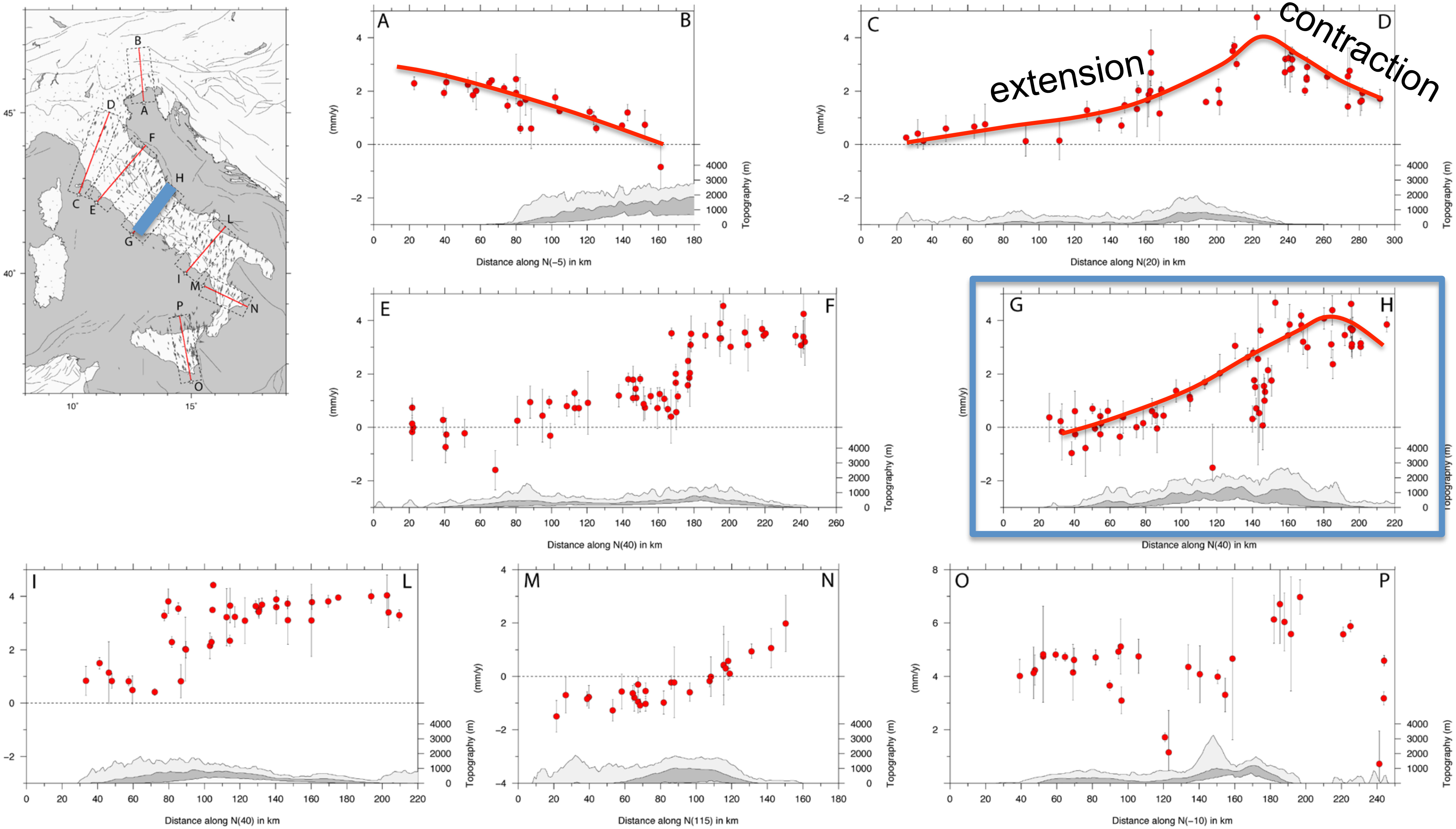

Devoti et al. 2017 Ann. Geophys.

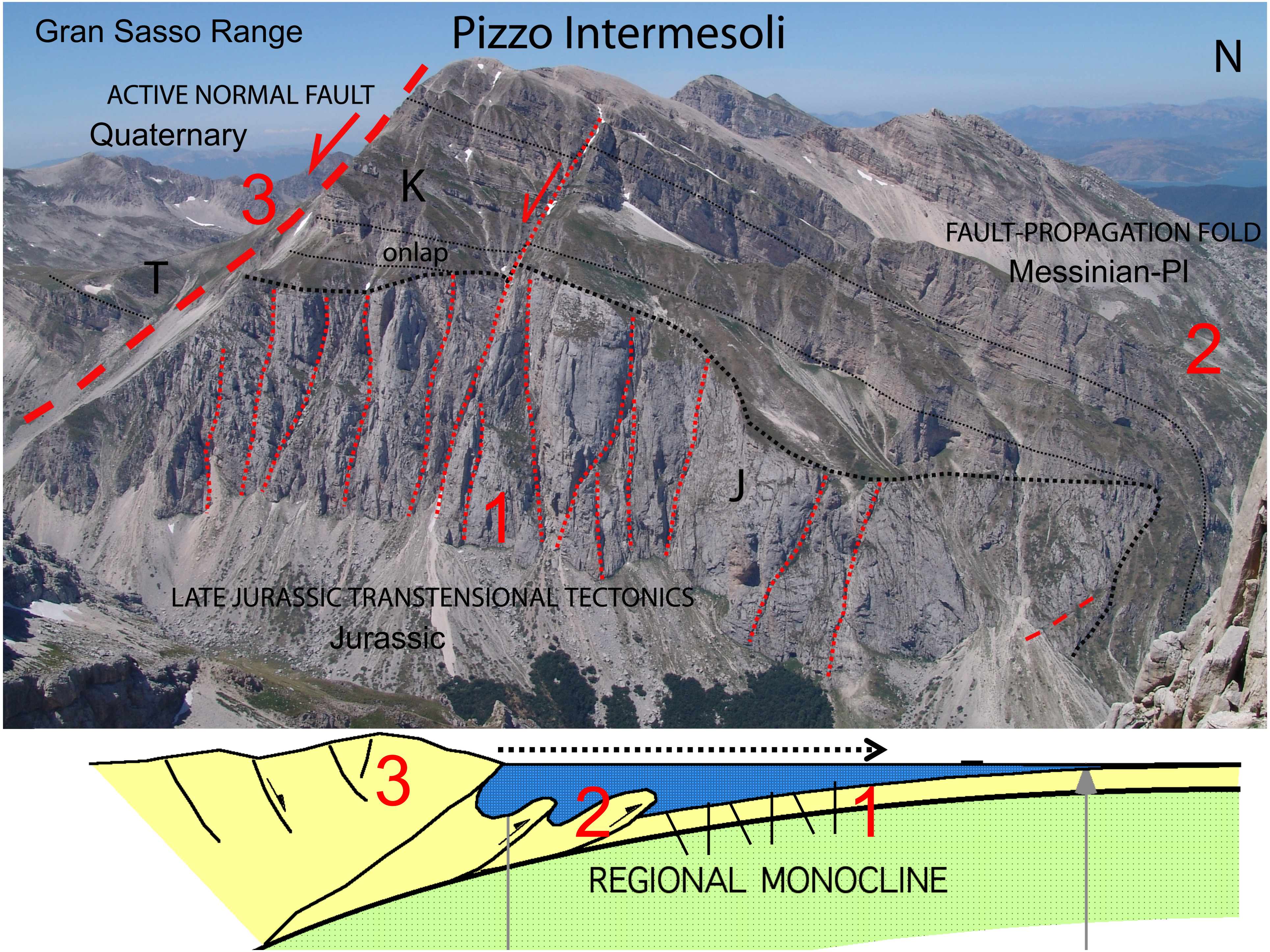

Gran Sasso Range
Pizzo Intermesoli
N
ACTIVE NORMAL FAULT
Quaternary
3
K
T
onlap
FAULT-PROPAGATION FOLD
Messinian-Pl
2
J
1
LATE JURASSIC TRANSTENSIONAL TECTONICS
Jurassic
3
2
1
REGIONAL MONOCLINE

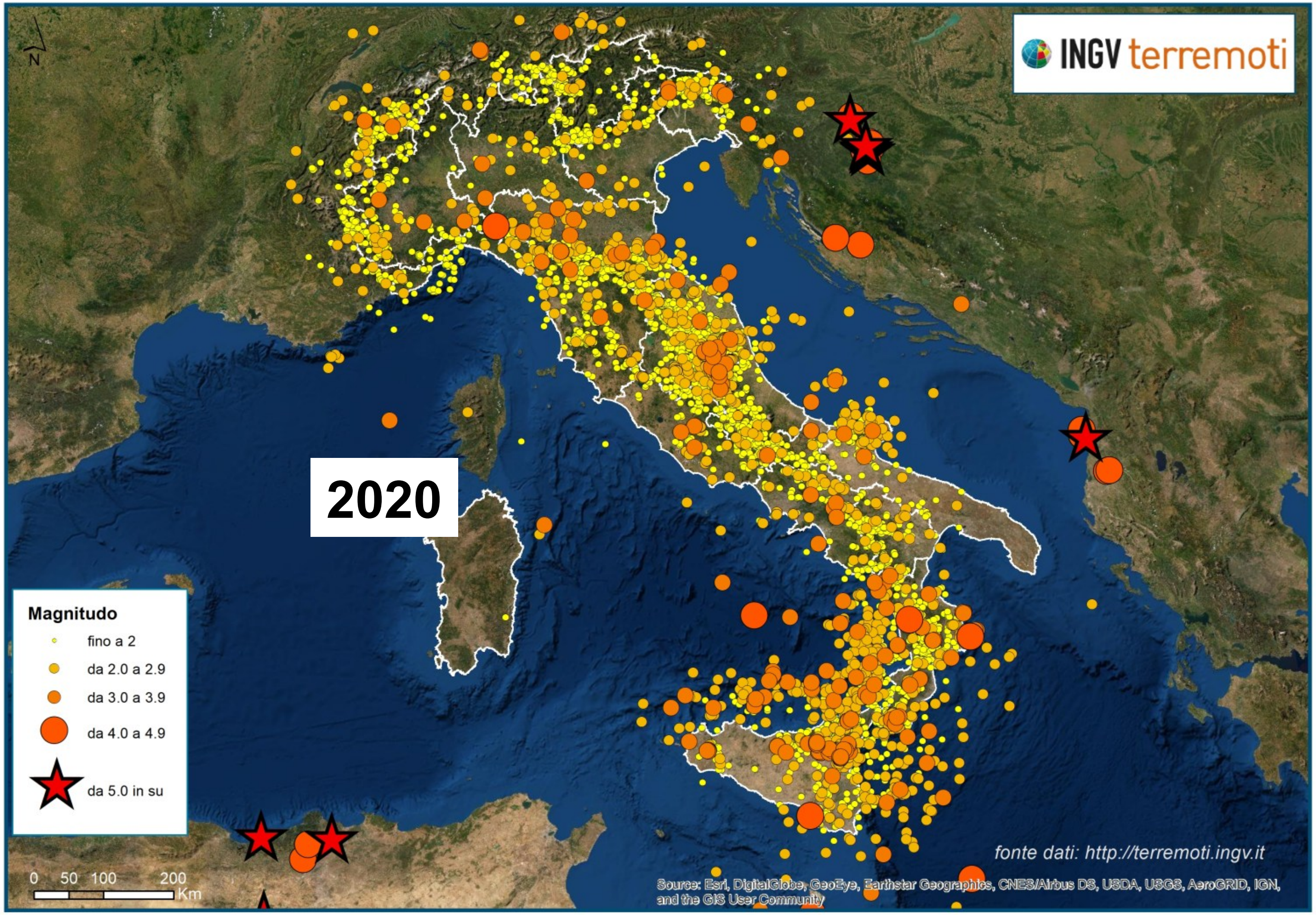
INGV terremoti
2020
Magnitudo
fino a 2
da 2.0 a 2.9
da 3.0 a 3.9
da 4.0 a 4.9
da 5.0 in su
0 50 100 200 Km
fonte dati: http://terremoti.ingv.it
Source: Esri, DigitalGlobe, GeoEye, Earthstar Geographics, CNES/Airbus DS, USDA, USGS, AeroGRID, IGN, and the GIS User Community

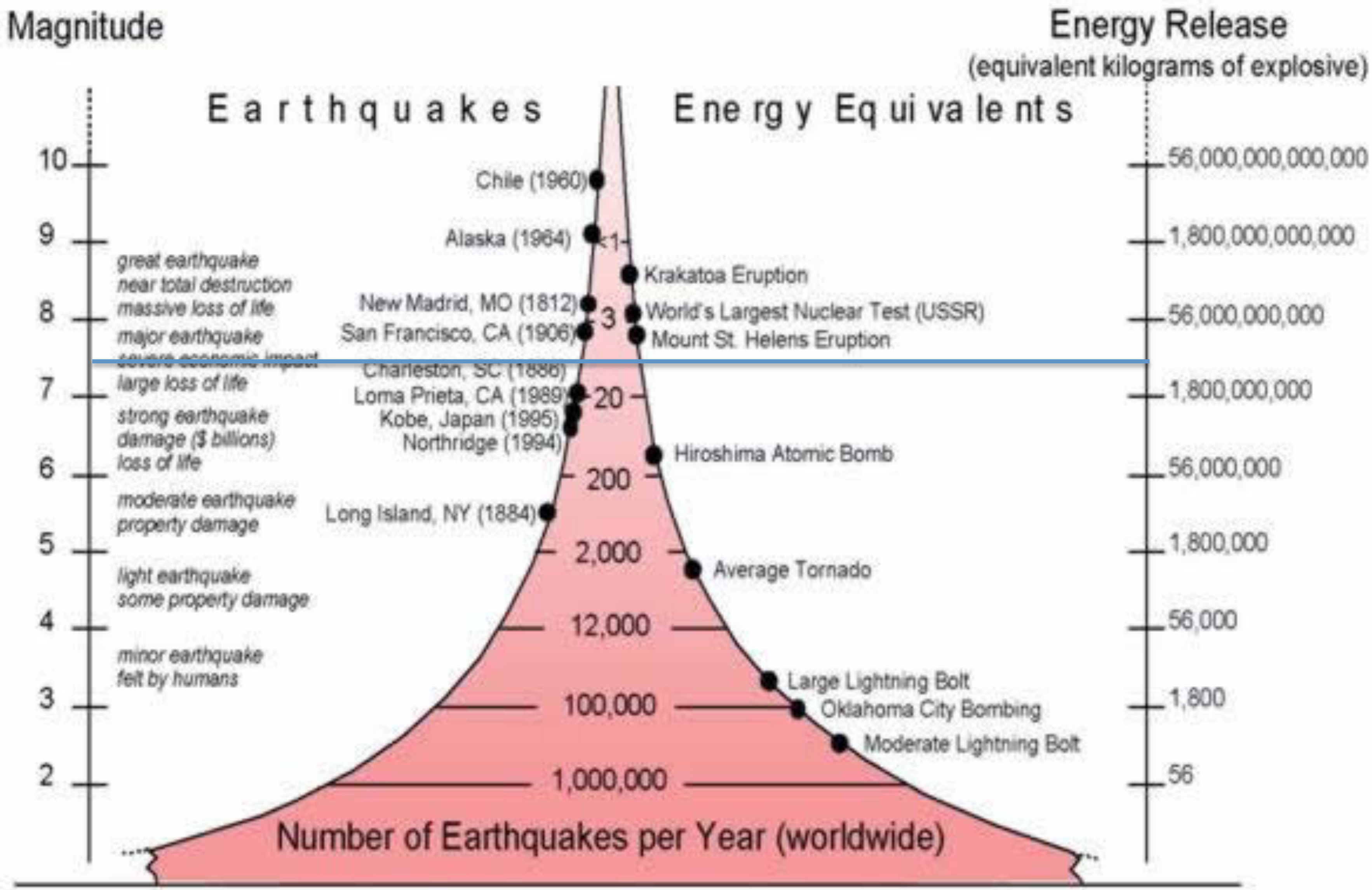

Magnitude
Energy Release
(equivalent kilograms of explosive)
Earthquakes
Energy Equivalents
10
9
8
7
6
5
4
3
2
great earthquake
near total destruction
massive loss of life
major earthquake
severe economic impact
large loss of life
strong earthquake
damage ($ billions)
loss of life
moderate earthquake
property damage
light earthquake
some property damage
minor earthquake
felt by humans
Chile (1960)
Alaska (1964)
New Madrid, MO (1812)
San Francisco, CA (1906)
Charleston, SC (1886)
Loma Prieta, CA (1989)
Kobe, Japan (1995)
Northridge (1994)
Long Island, NY (1884)
<1
3
20
200
2,000
12,000
100,000
1,000,000
Krakatoa Eruption
World's Largest Nuclear Test (USSR)
Mount St. Helens Eruption
Hiroshima Atomic Bomb
Average Tornado
Large Lightning Bolt
Oklahoma City Bombing
Moderate Lightning Bolt
56,000,000,000,000
1,800,000,000,000
56,000,000,000
1,800,000,000
56,000,000
1,800,000
56,000
1,800
56
Number of Earthquakes per Year (worldwide)

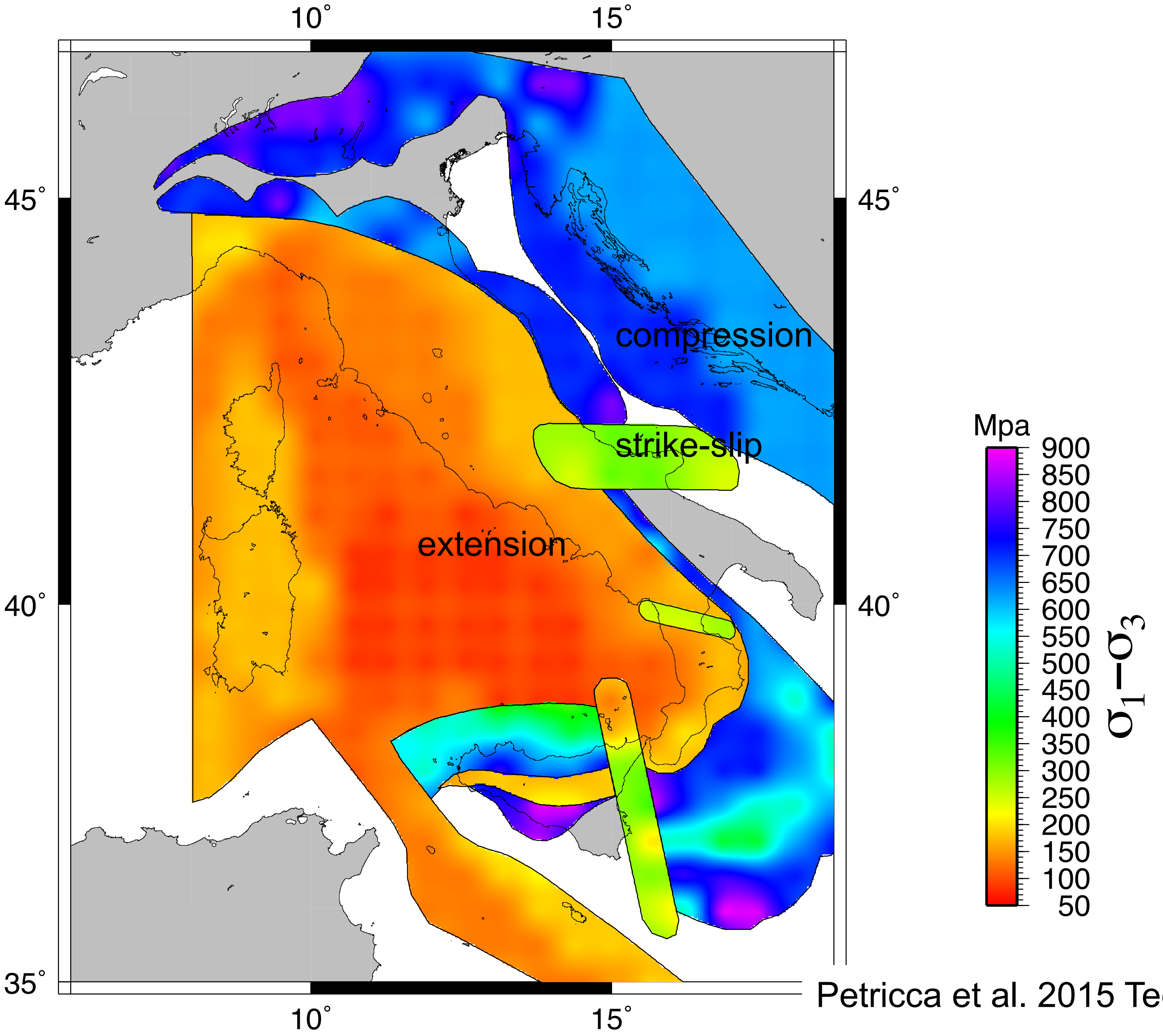

Petricca et al. 2015 Tectonophysics

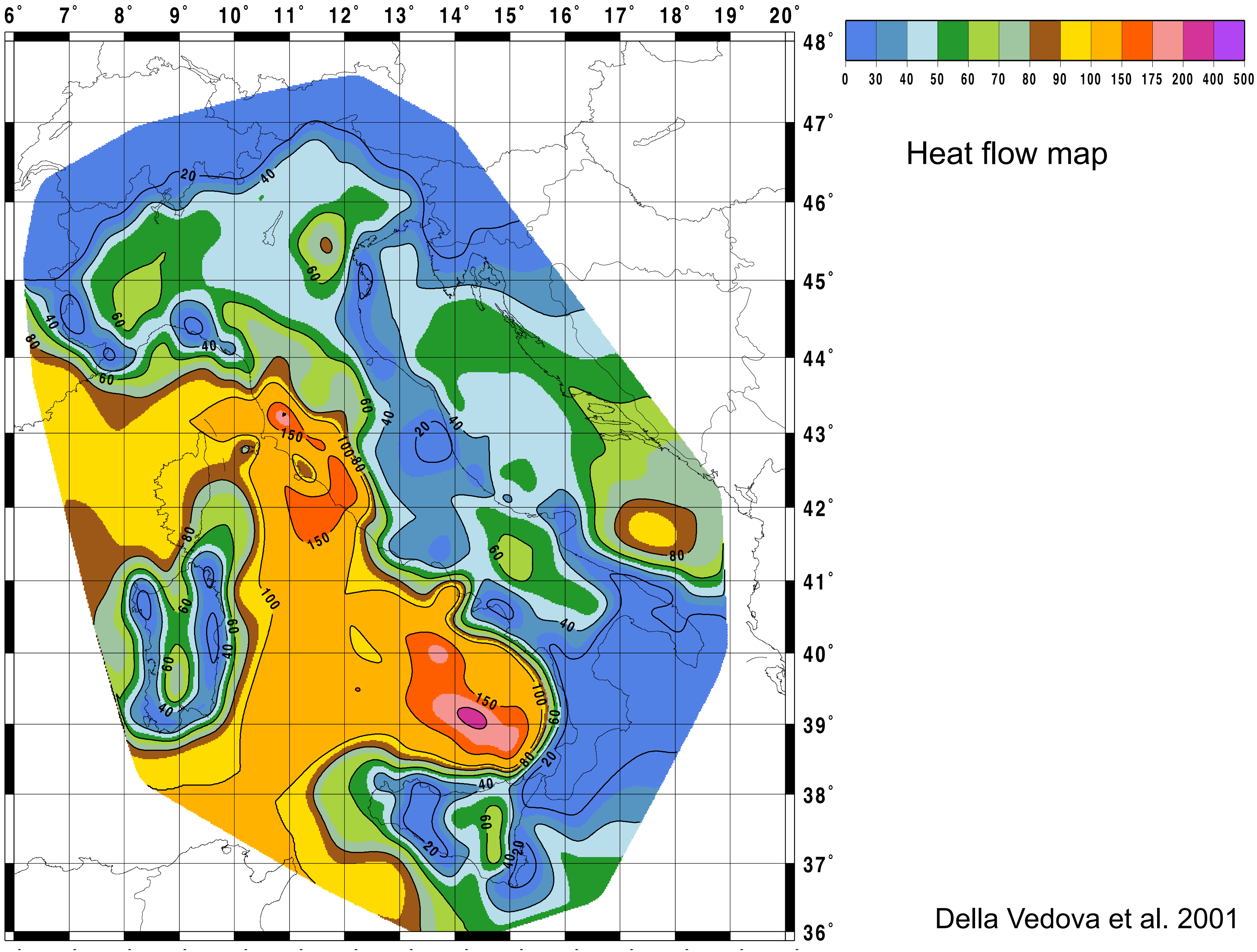

Heat flow map

Della Vedova et al. 2001

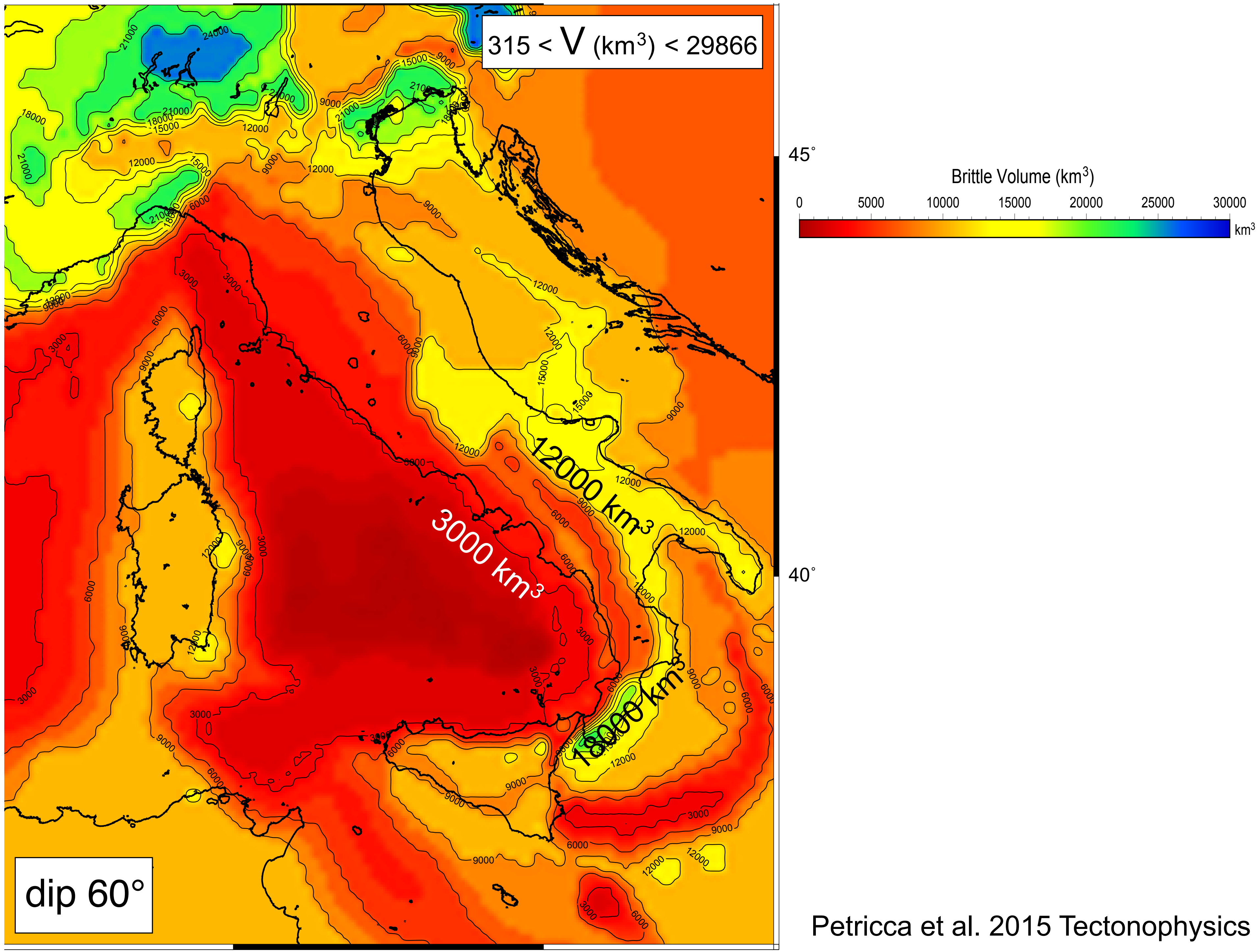

Petricca et al. 2015 Tectonophysics

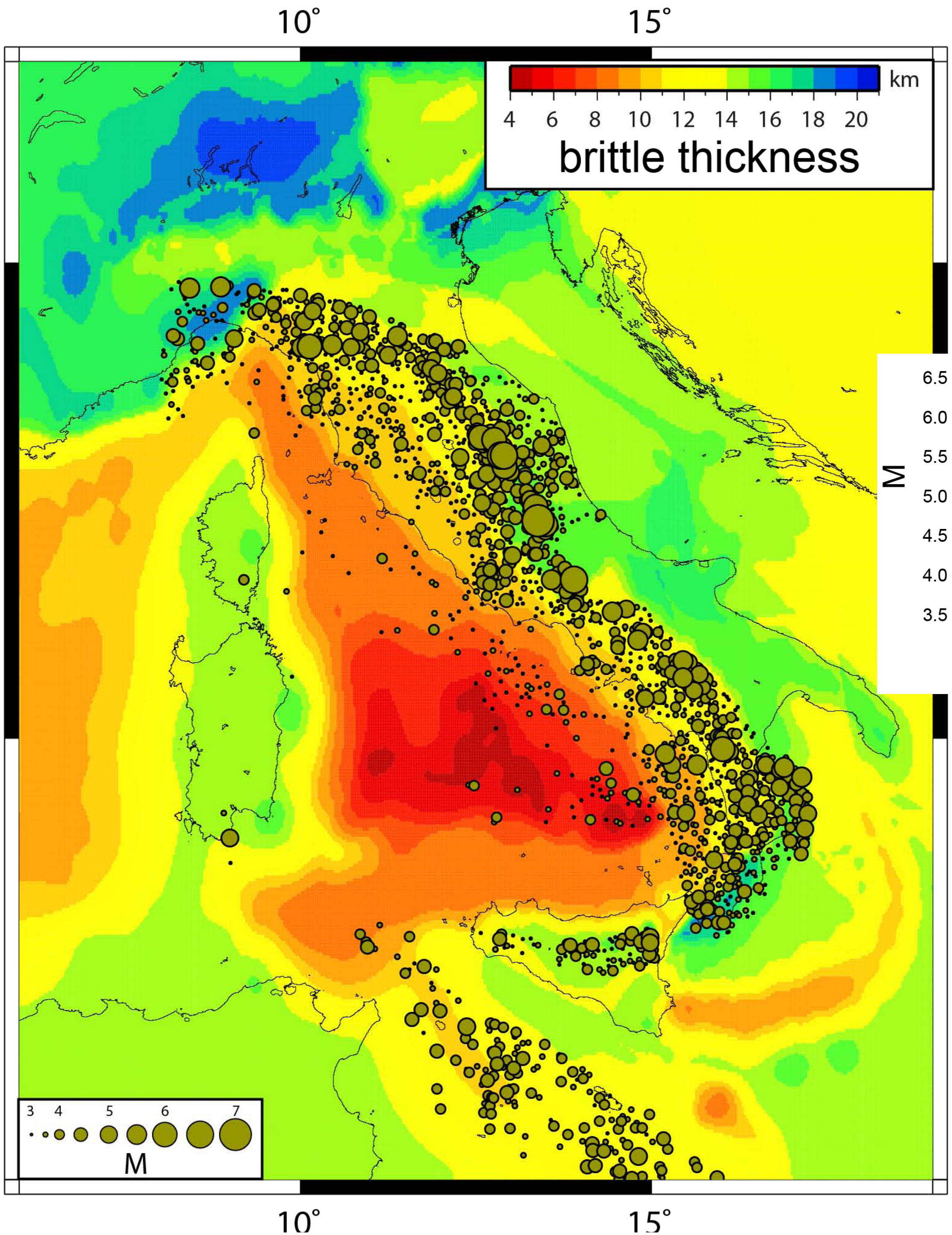

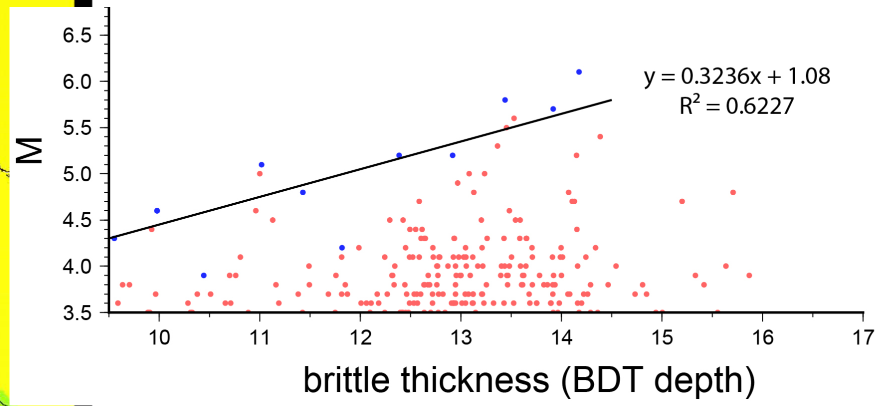

Petricca et al. 2015 Tectonophysics

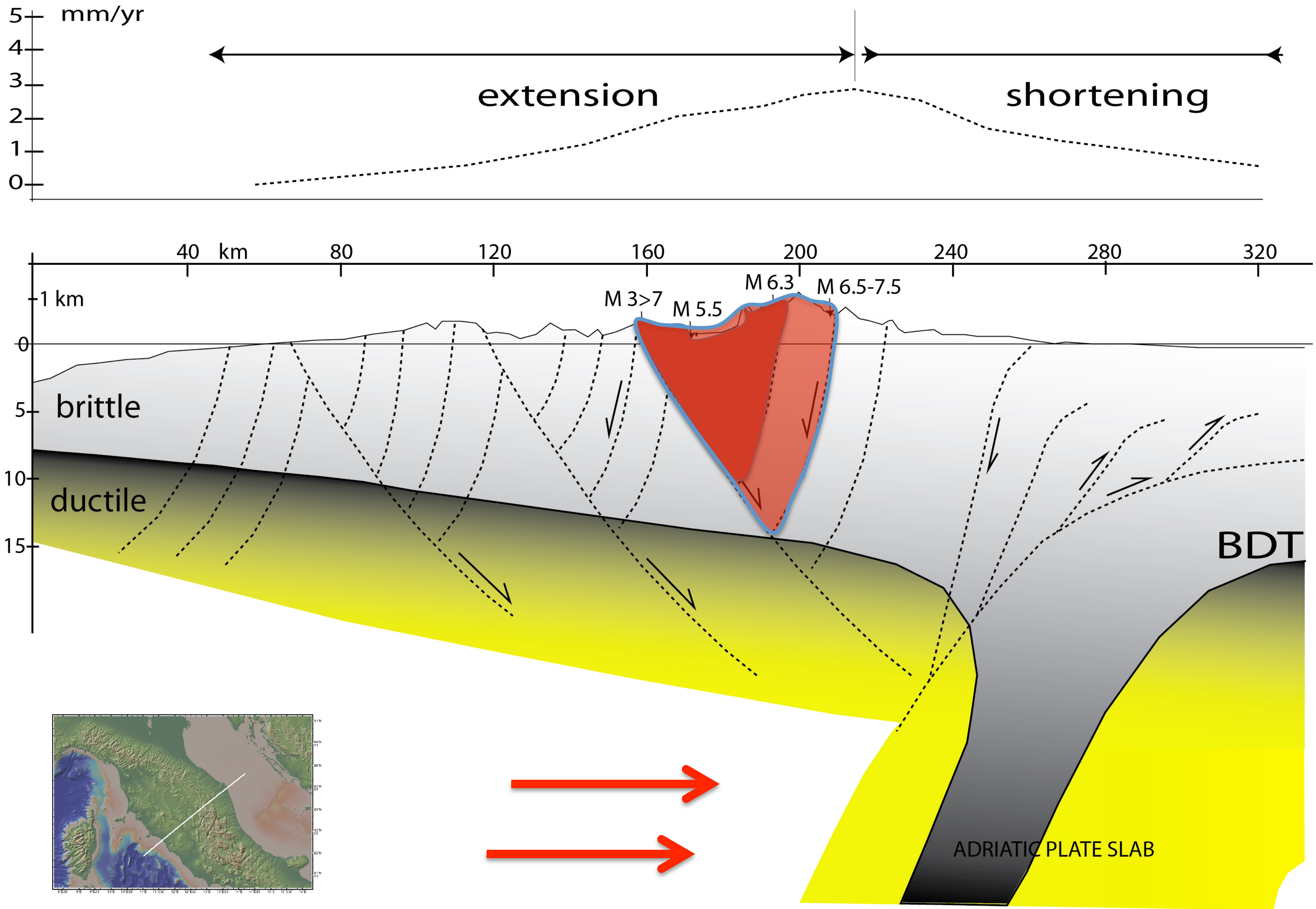

Petricca et al. 2015 Tectonophysics

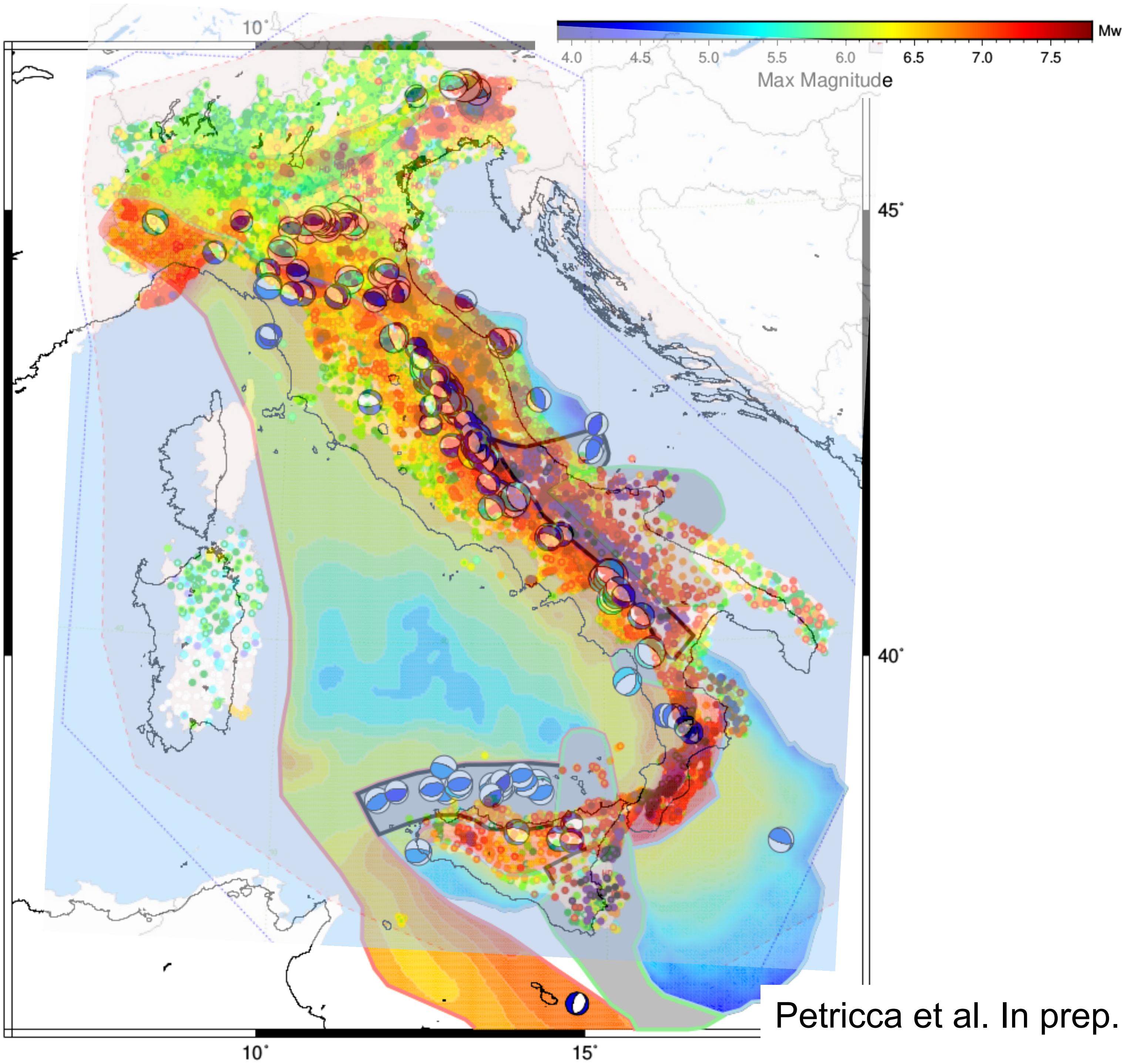

Petricca et al. In prep.

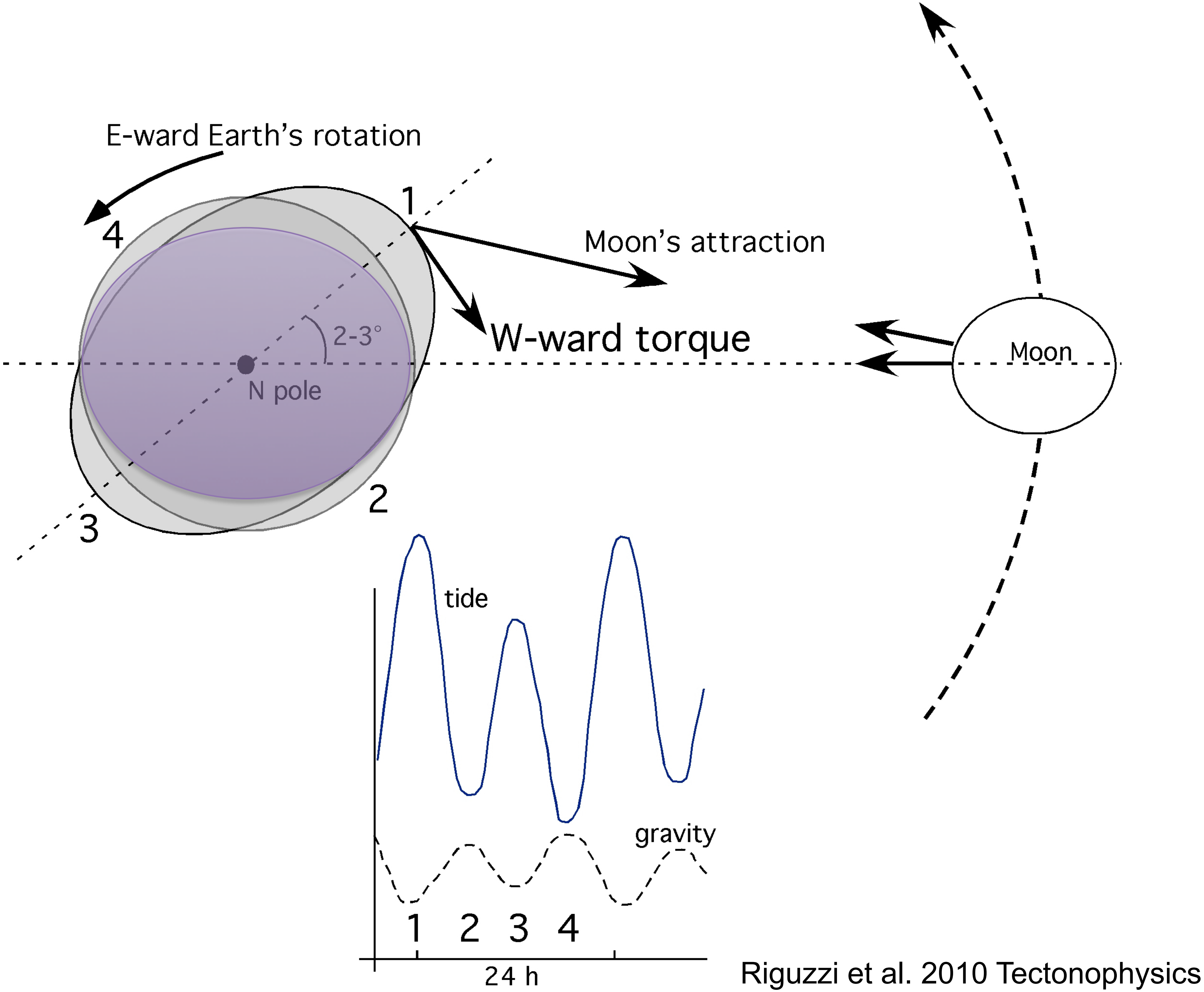
E-ward Earth's rotation
1
4
Moon's attraction
W-ward torque
2-3°
N pole
Moon
2
3
tide
gravity
1 2 3 4
24 h
Riguzzi et al. 2010 Tectonophysics

Cochran et al. 2004 Science

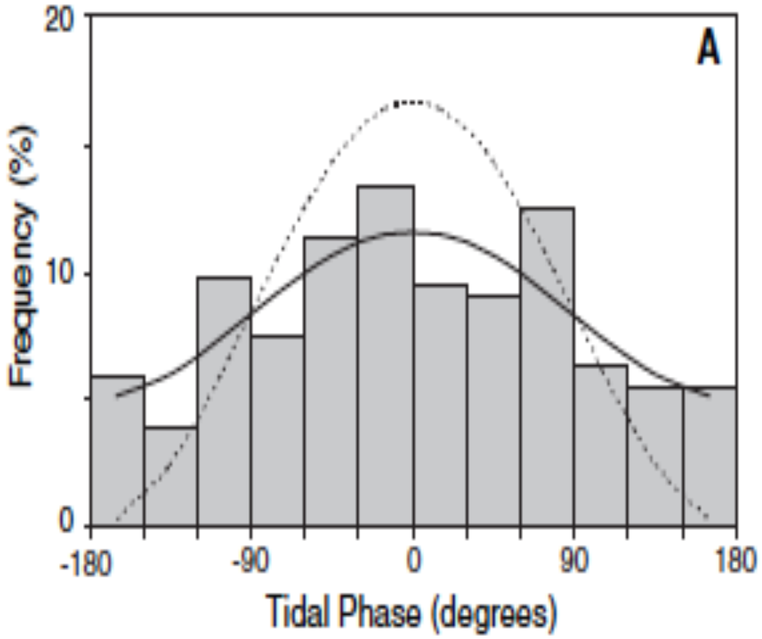

Earthquakes >40 km

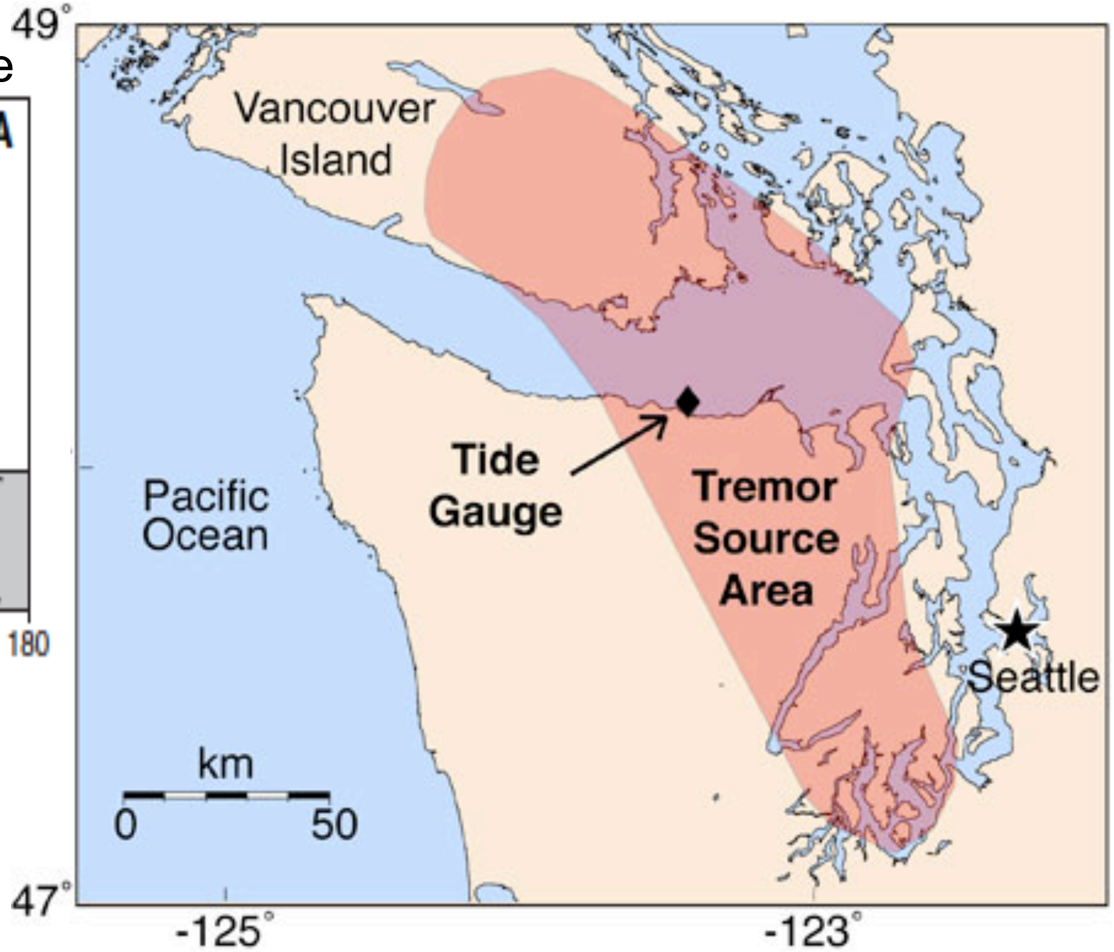

Rubinstein et al. 2009 Science

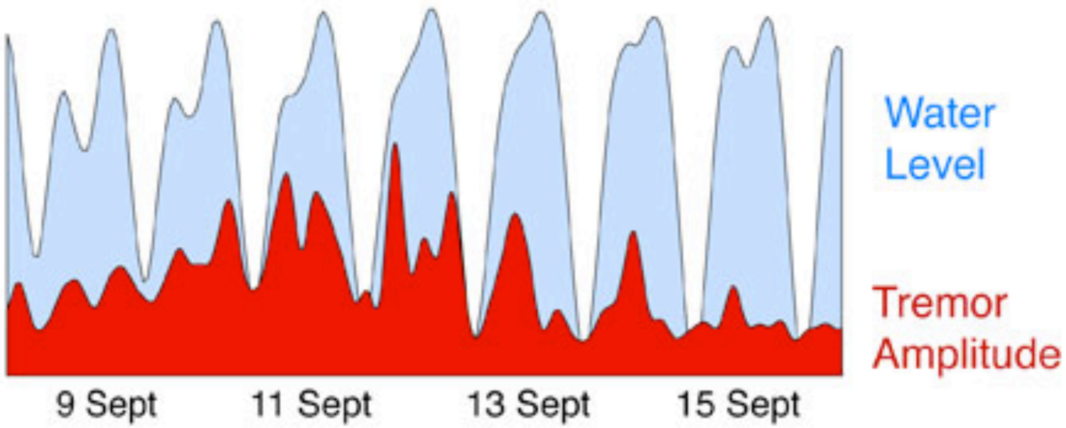

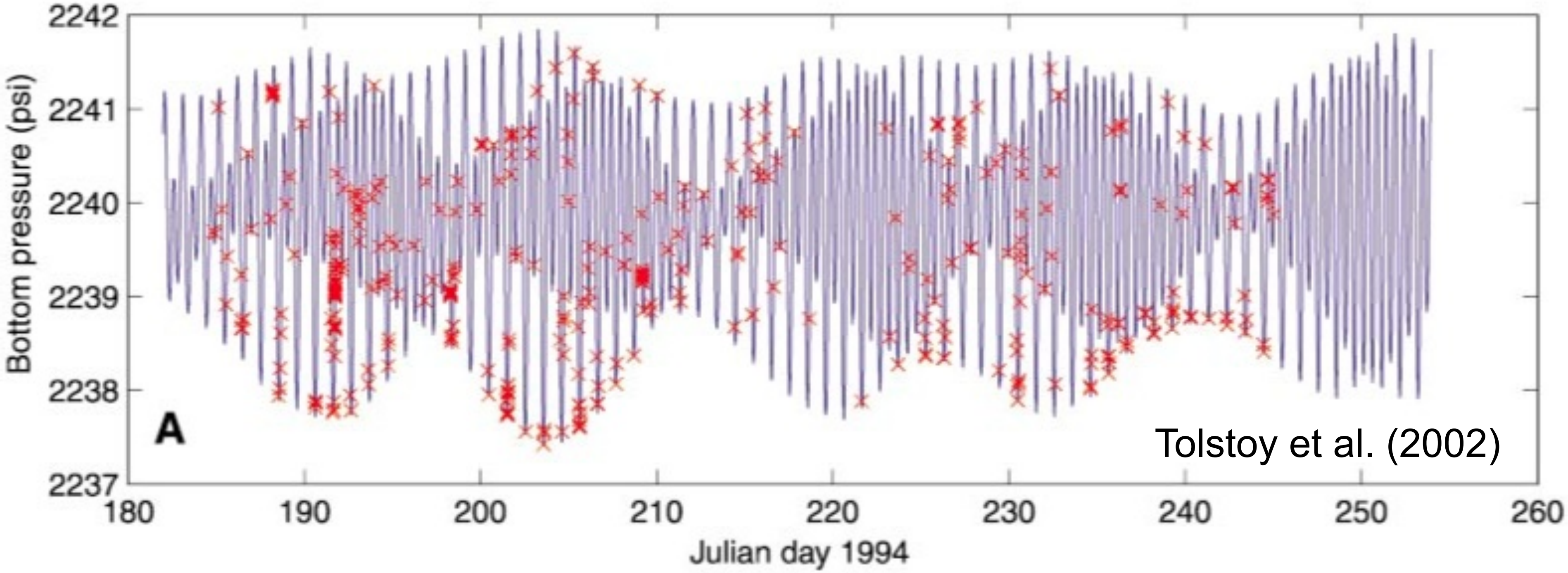

Normal fault earthquakes more frequent during low tide

Thrust fault earthquakes more frequent during high tide

vertical stress = lithostatic load = density x gravity x depth

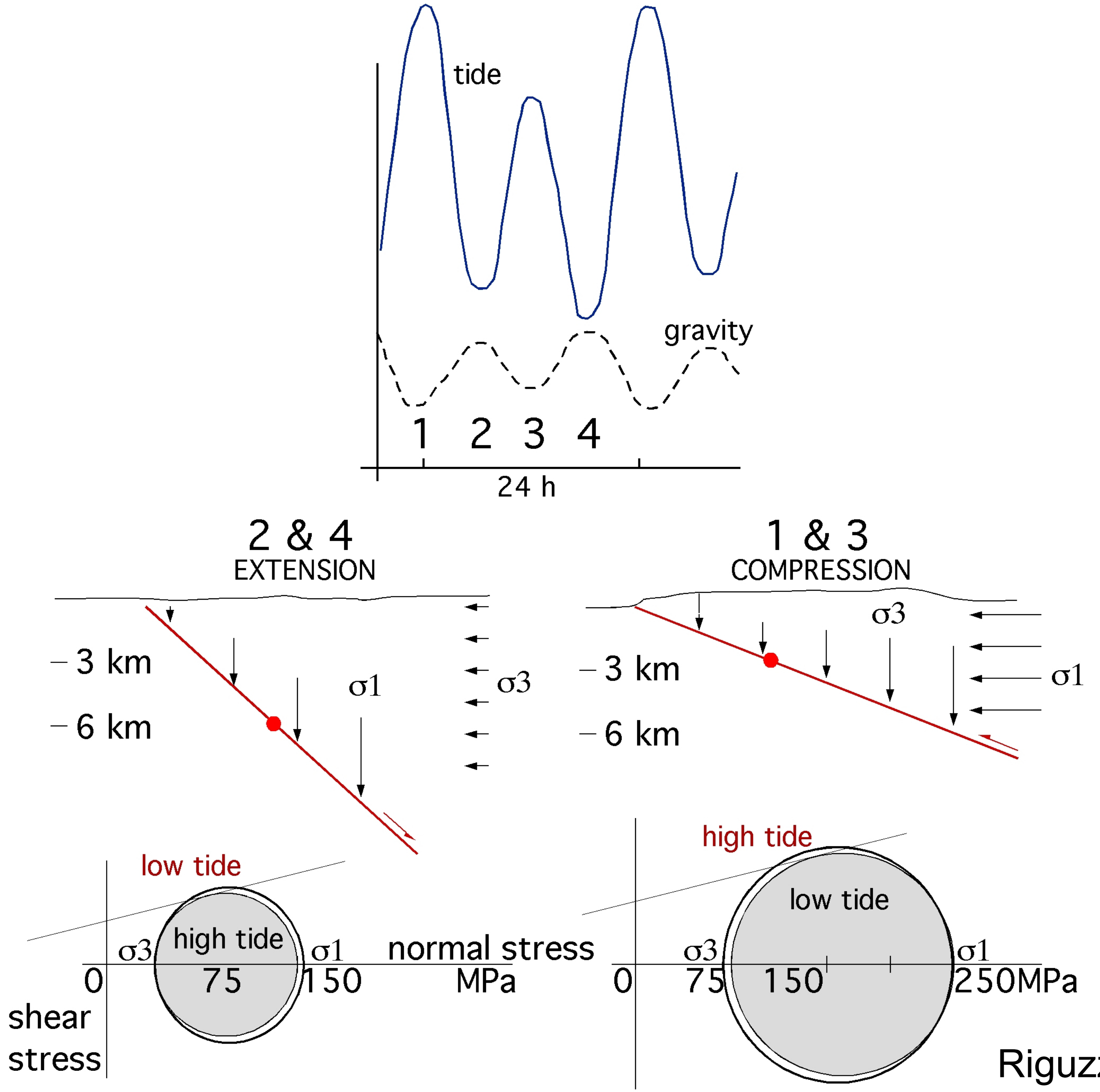

Riguzzi et al. 2010

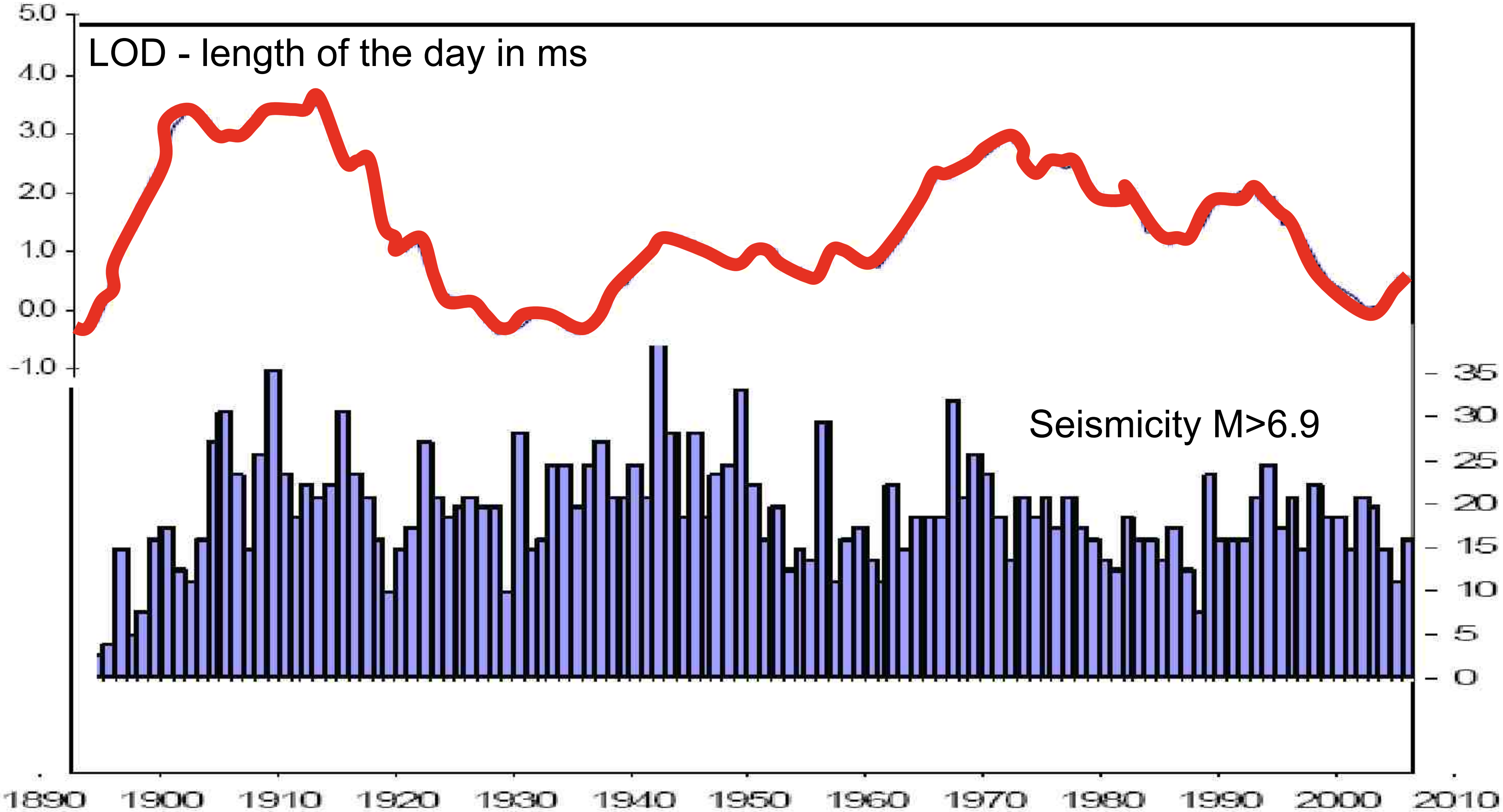

Riguzzi et al., 2010 Tectonophysics

RETE ACCELEROMETRICA NAZIONALE - RAN DOWNLOAD

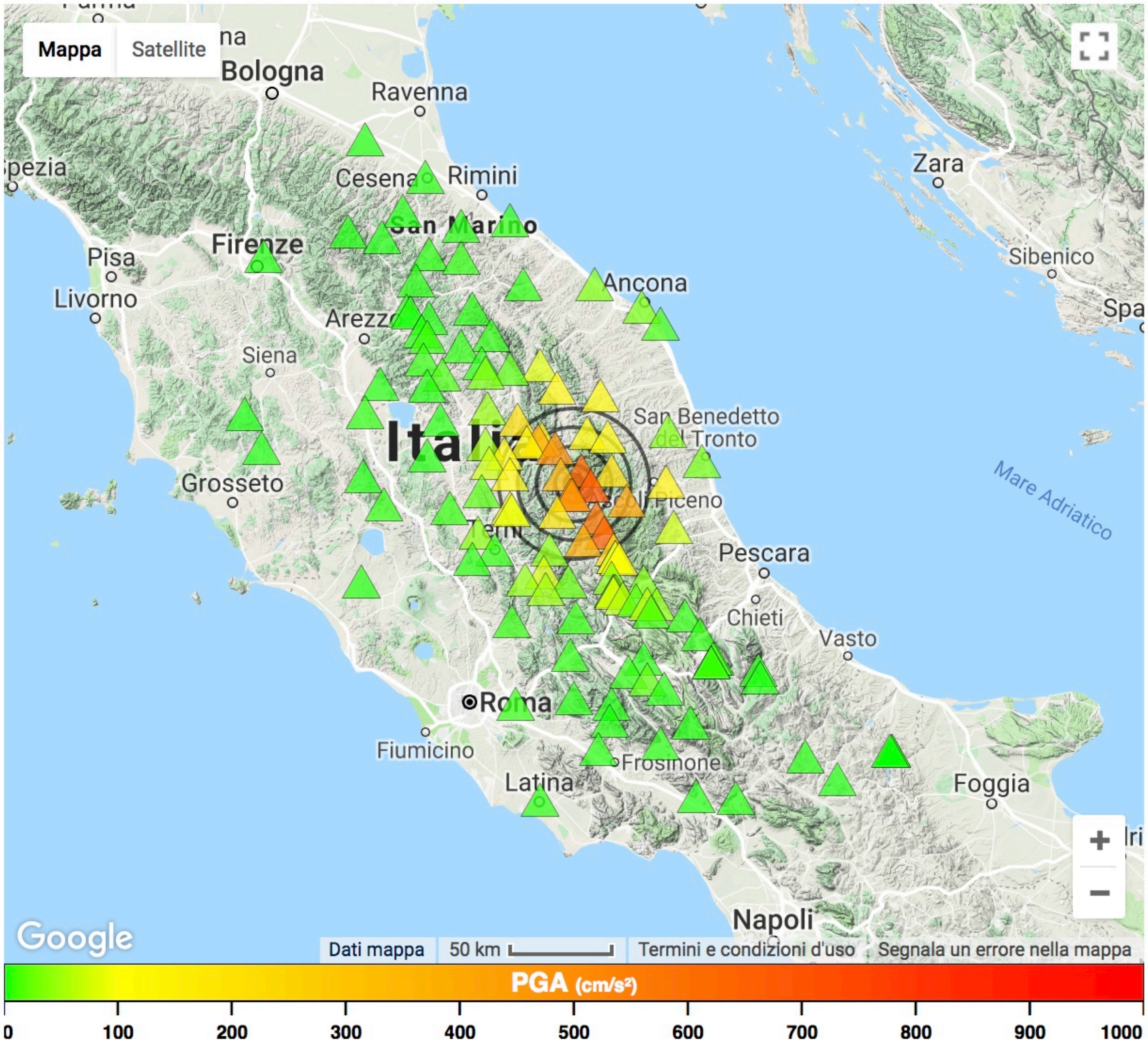

Rete Accelerometrica Nazionale - RAN Download

30/10/2016

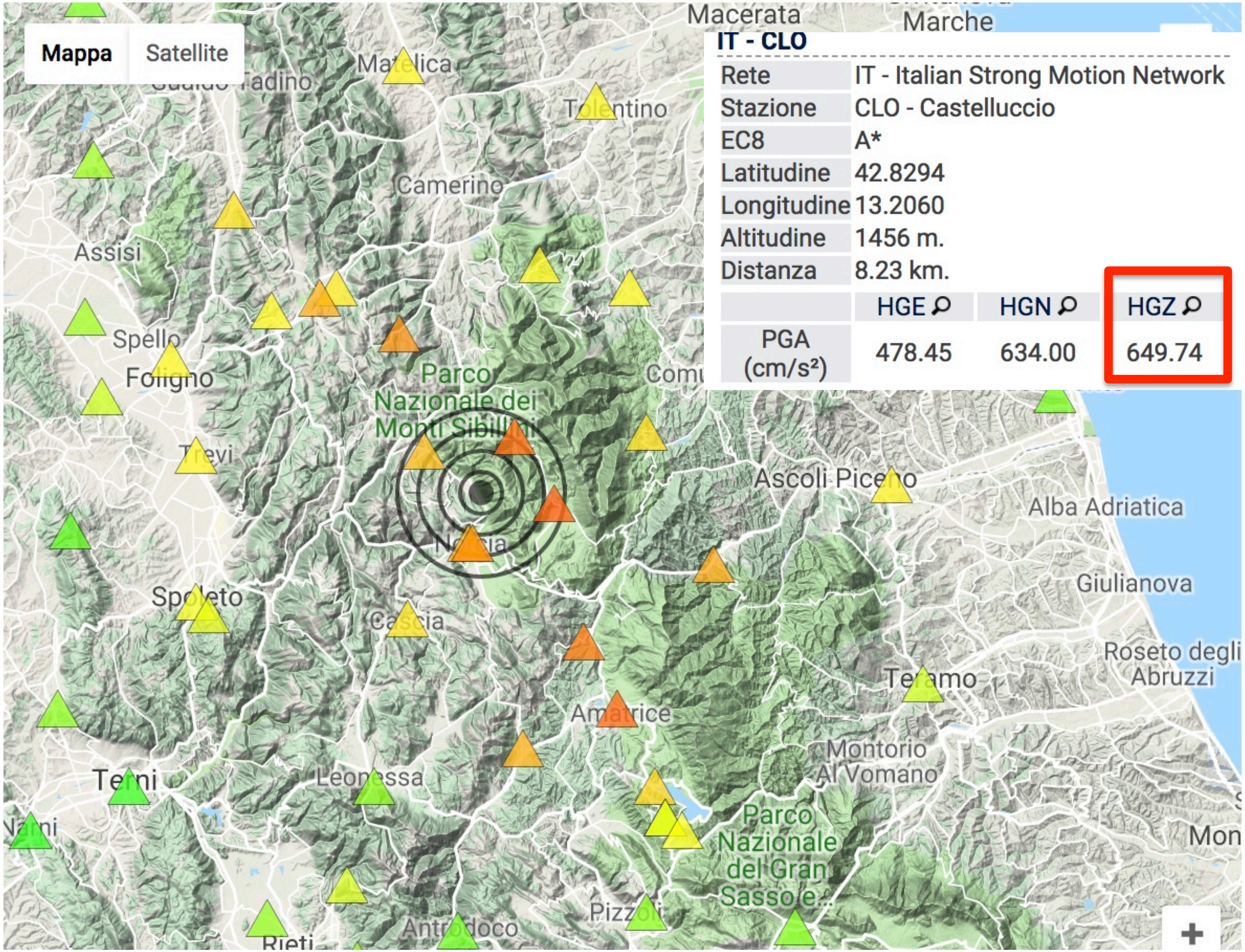

IT - CLO

Rete	IT - Italian Strong Motion Network		
Stazione	CLO - Castelluccio		
EC8	A*		
Latitudine	42.8294		
Longitudine	13.2060		
Altitudine	1456 m.		
Distanza	8.23 km.		
	HGE	HGN	HGZ
PGA (cm/s²)	478.45	634.00	649.74

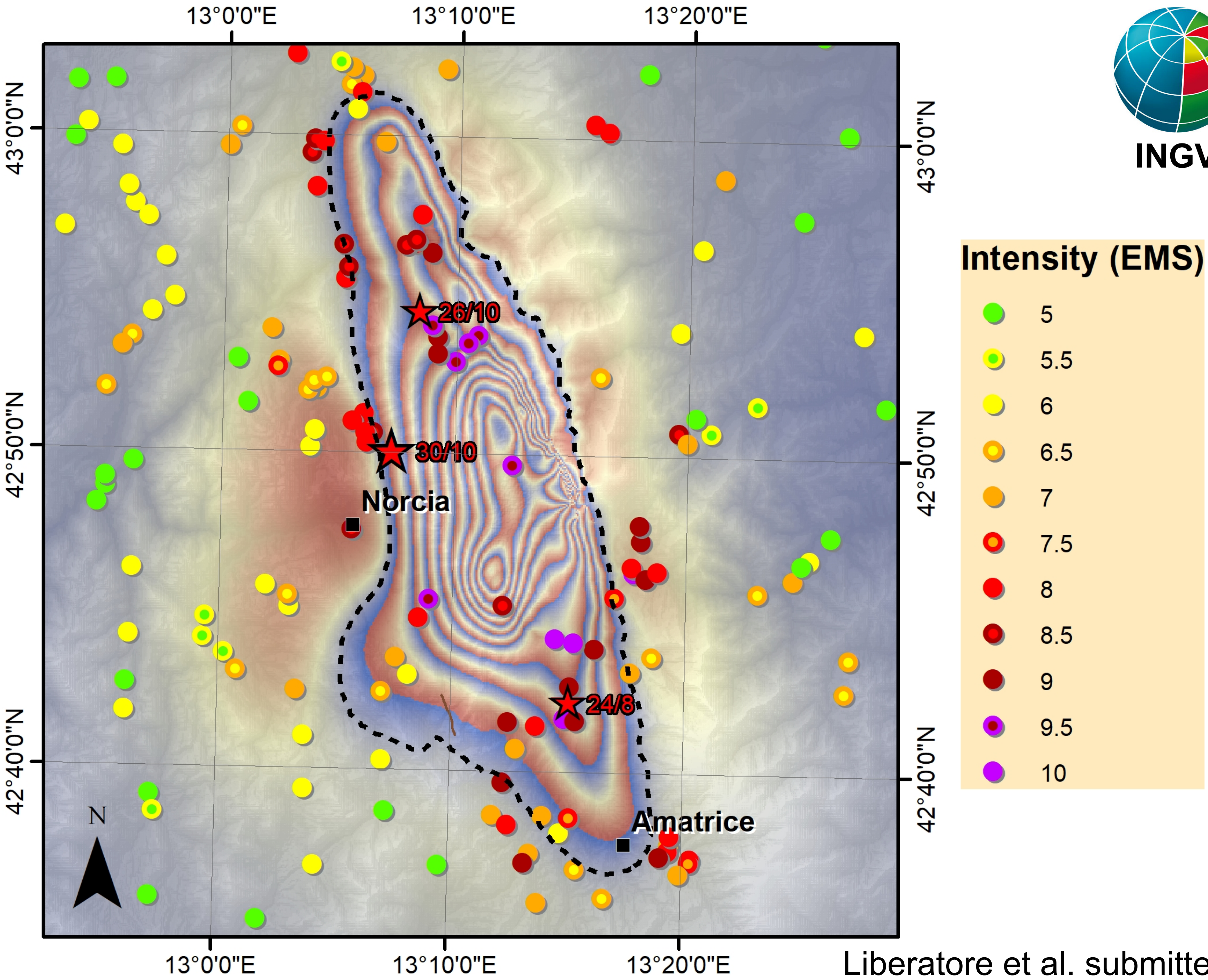

Liberatore et al. submitted

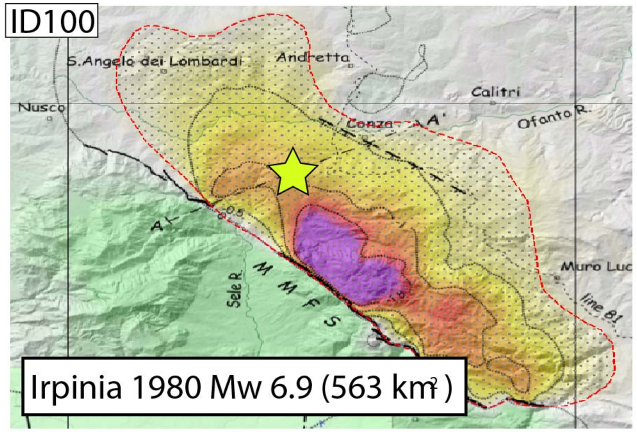

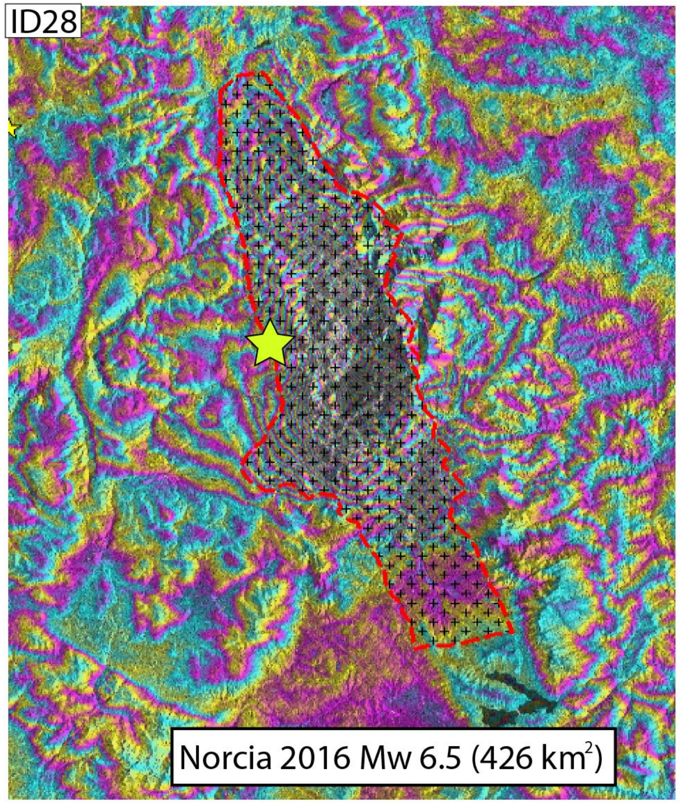

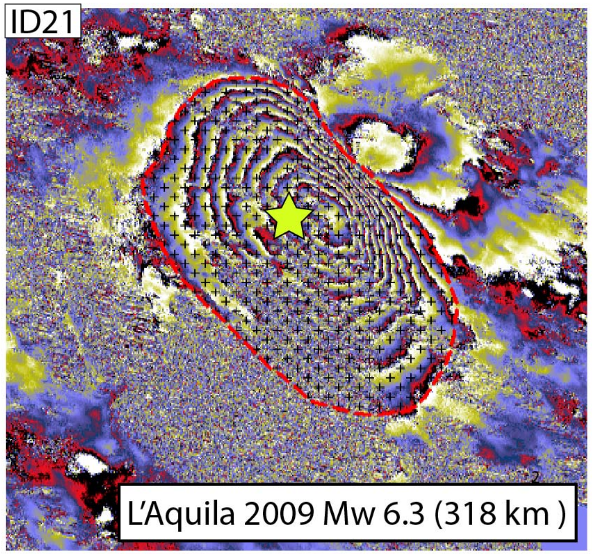

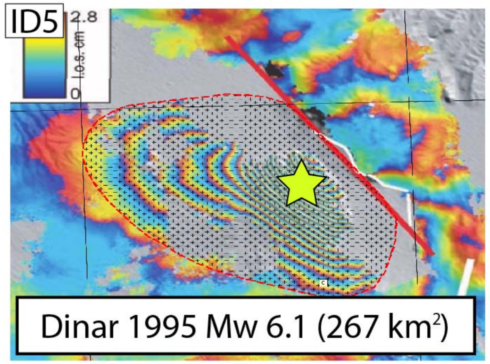

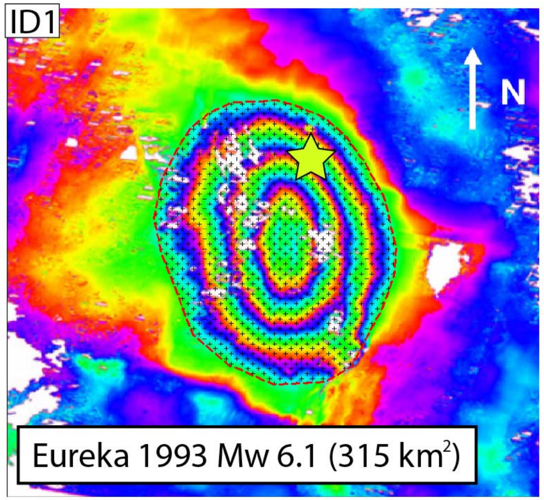

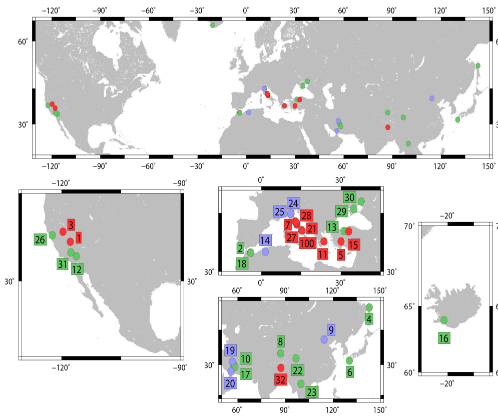

Petricca et al. 2021 ESR

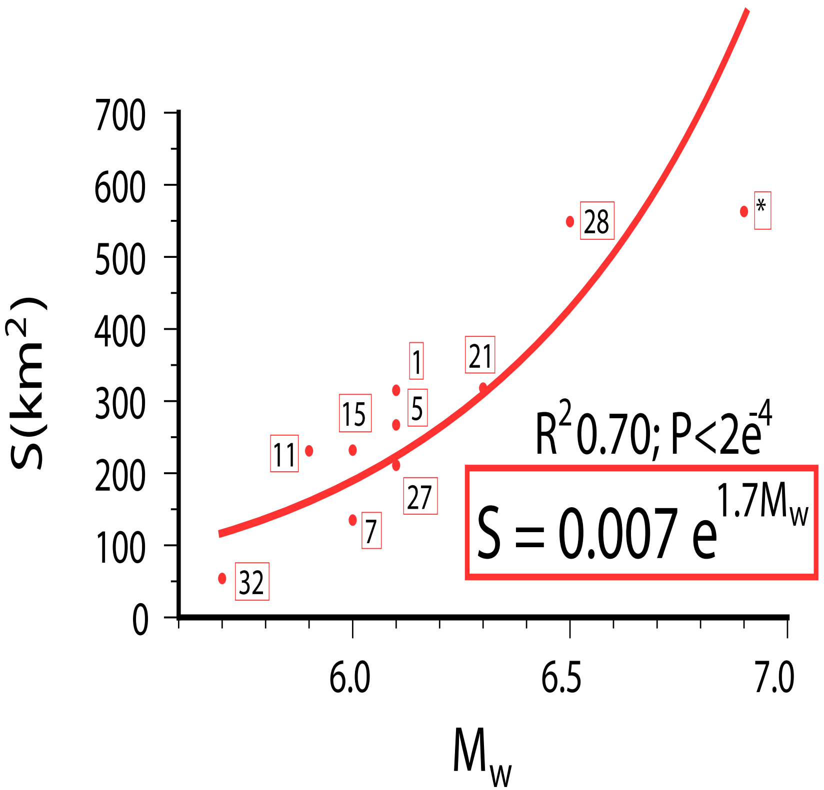

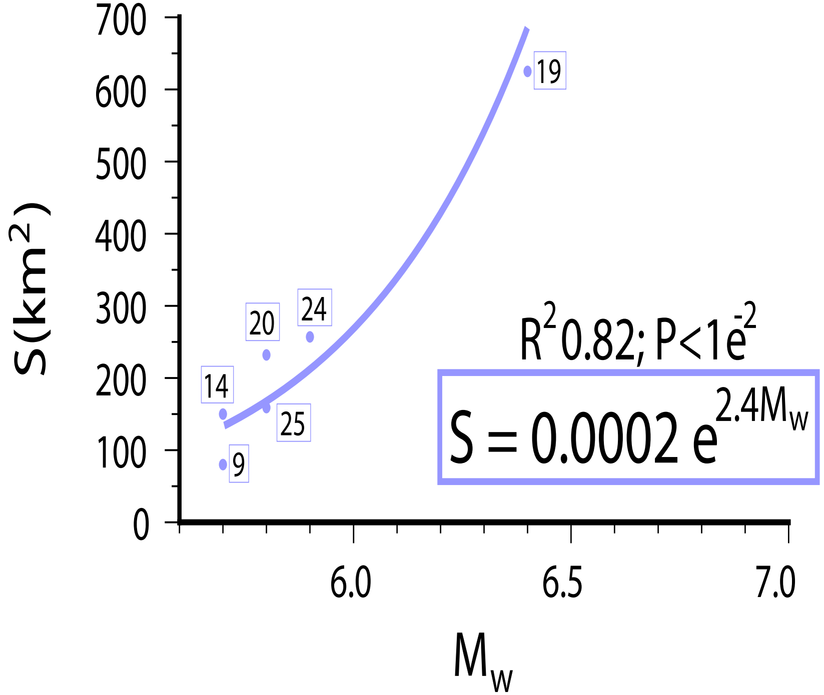

Petricca et al. 2021 ESR

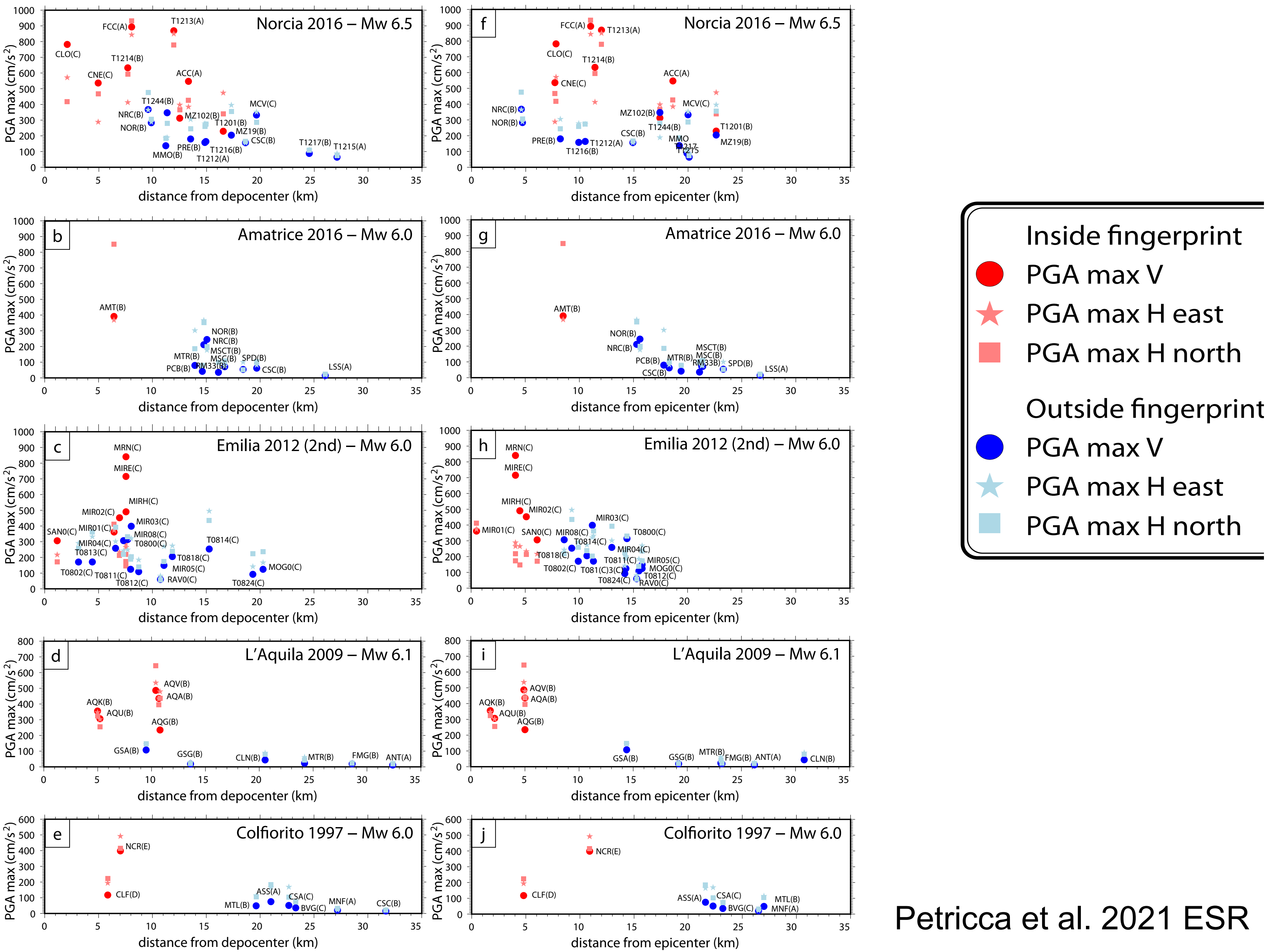

Petricca et al. 2021 ESR

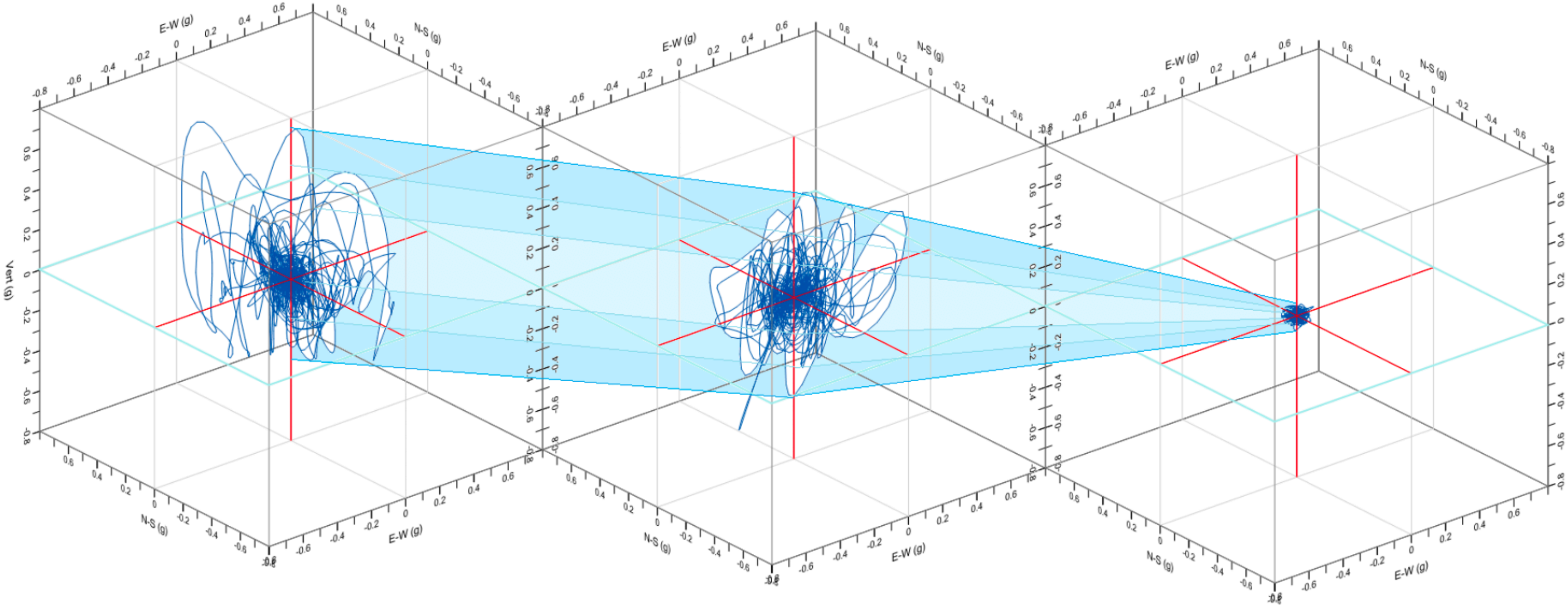

ITALIA CENTRALE, 30.10.2016
CASTELLUCCIO DI NORCIA CLO: 7.8 km → ACCUMULI ACC: 18.6 km → FABRIANO FBR: 59.1 km

Mariani & Pugi 2019 Ingenio

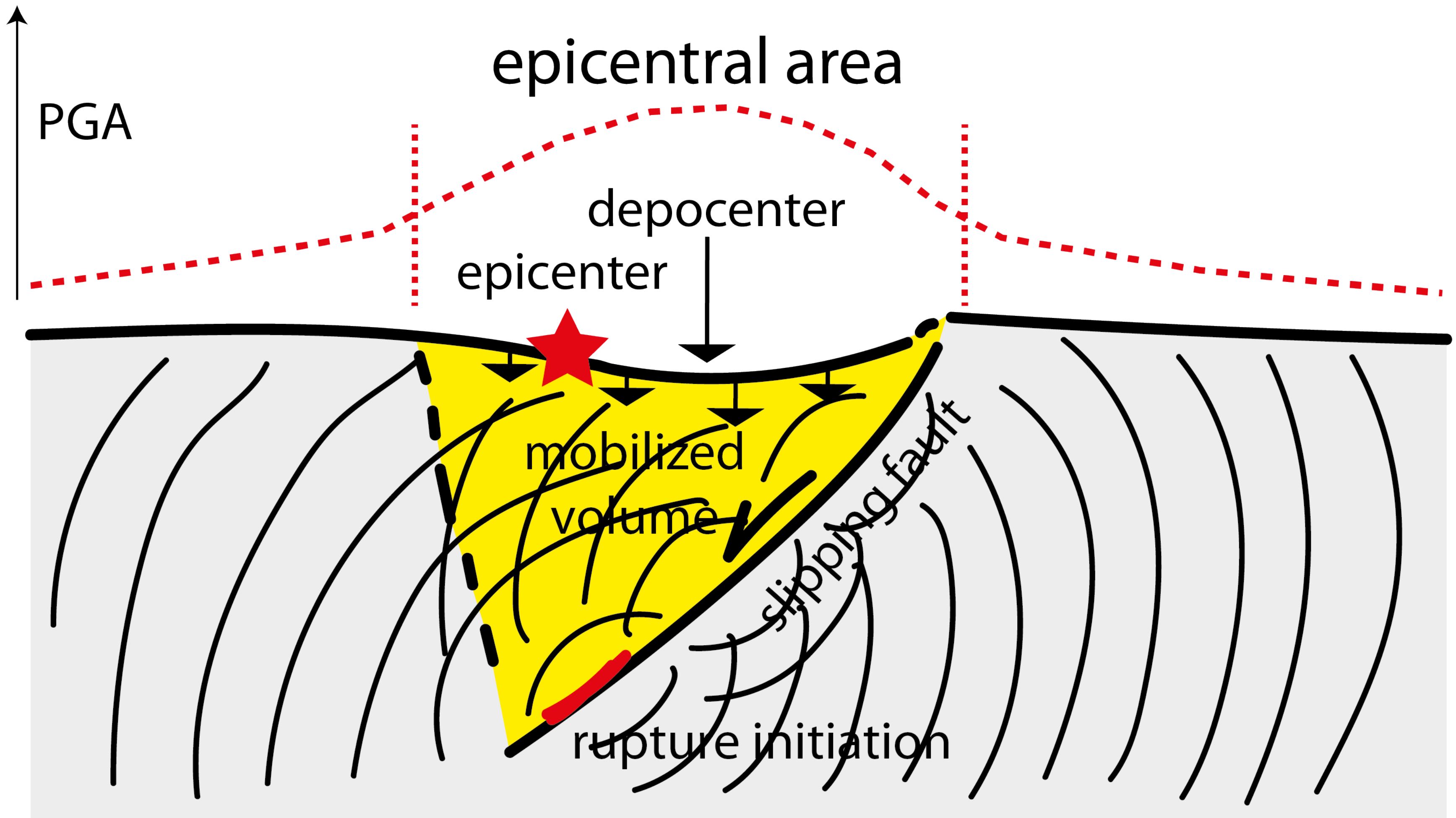

epicentral area
PGA
depocenter
epicenter
mobilized
volume
slipping fault
rupture initiation

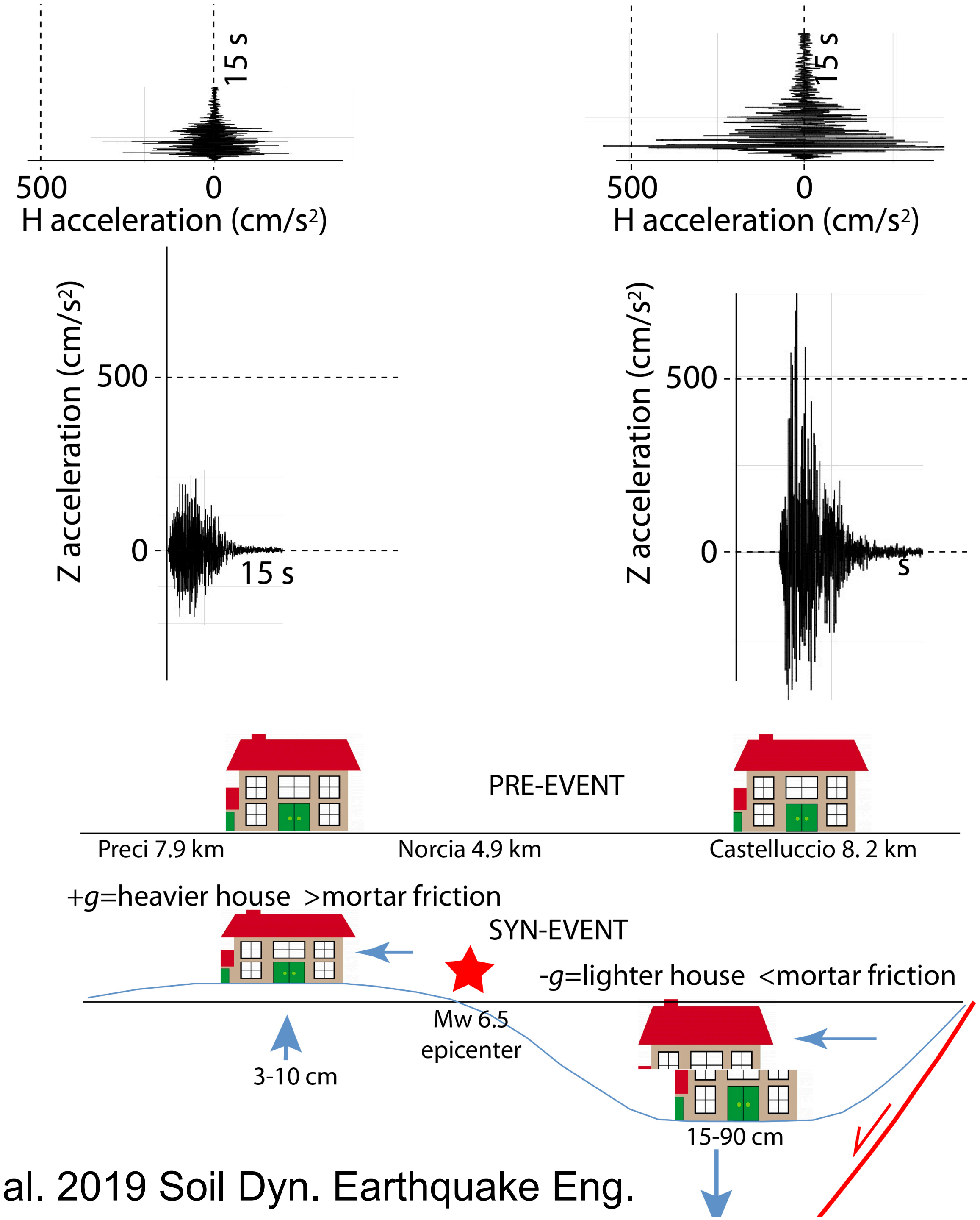

Liberatore et al. 2019 Soil Dyn. Earthquake Eng.

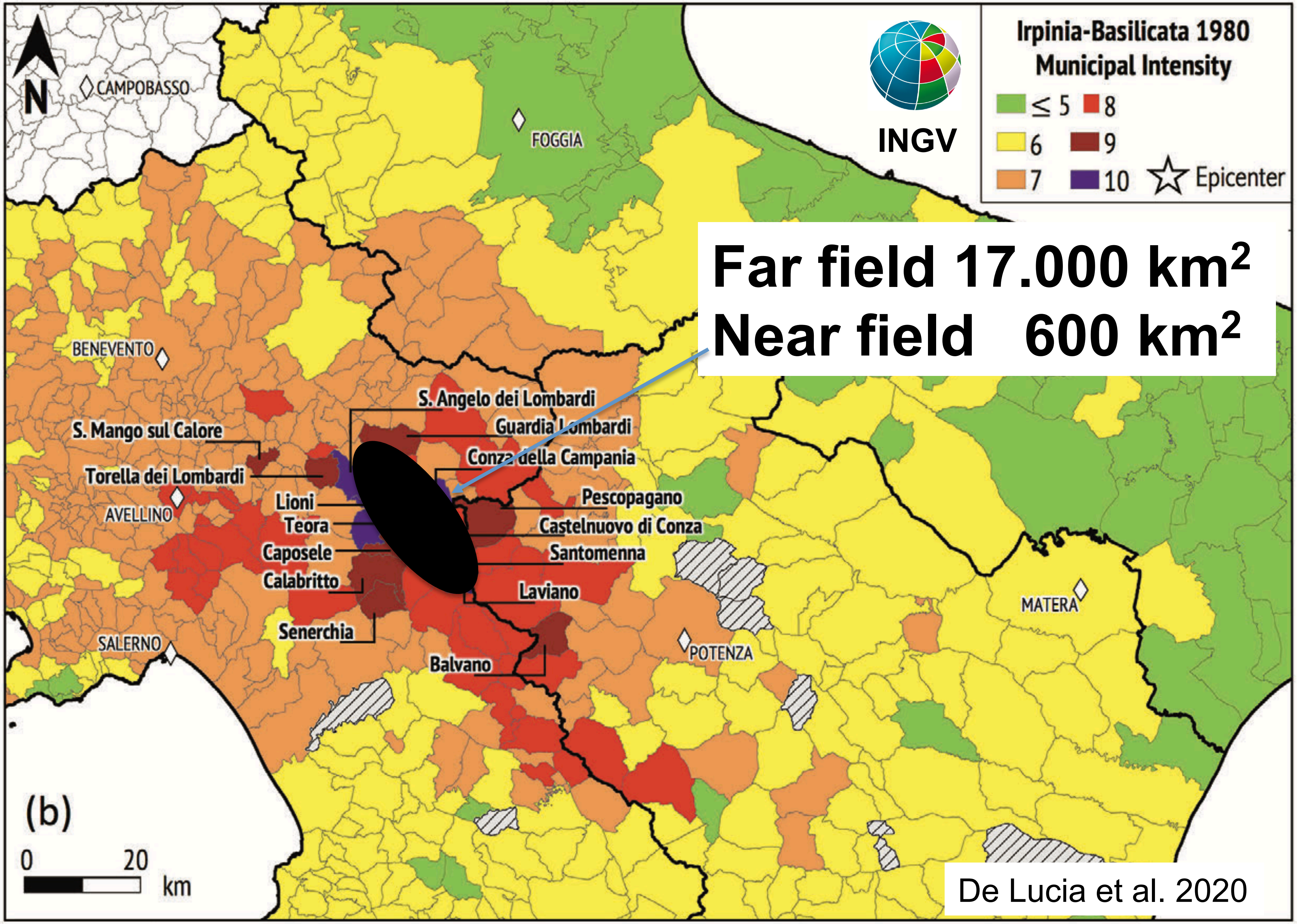

Far field 17.000 km²

Near field 600 km²

De Lucia et al. 2020

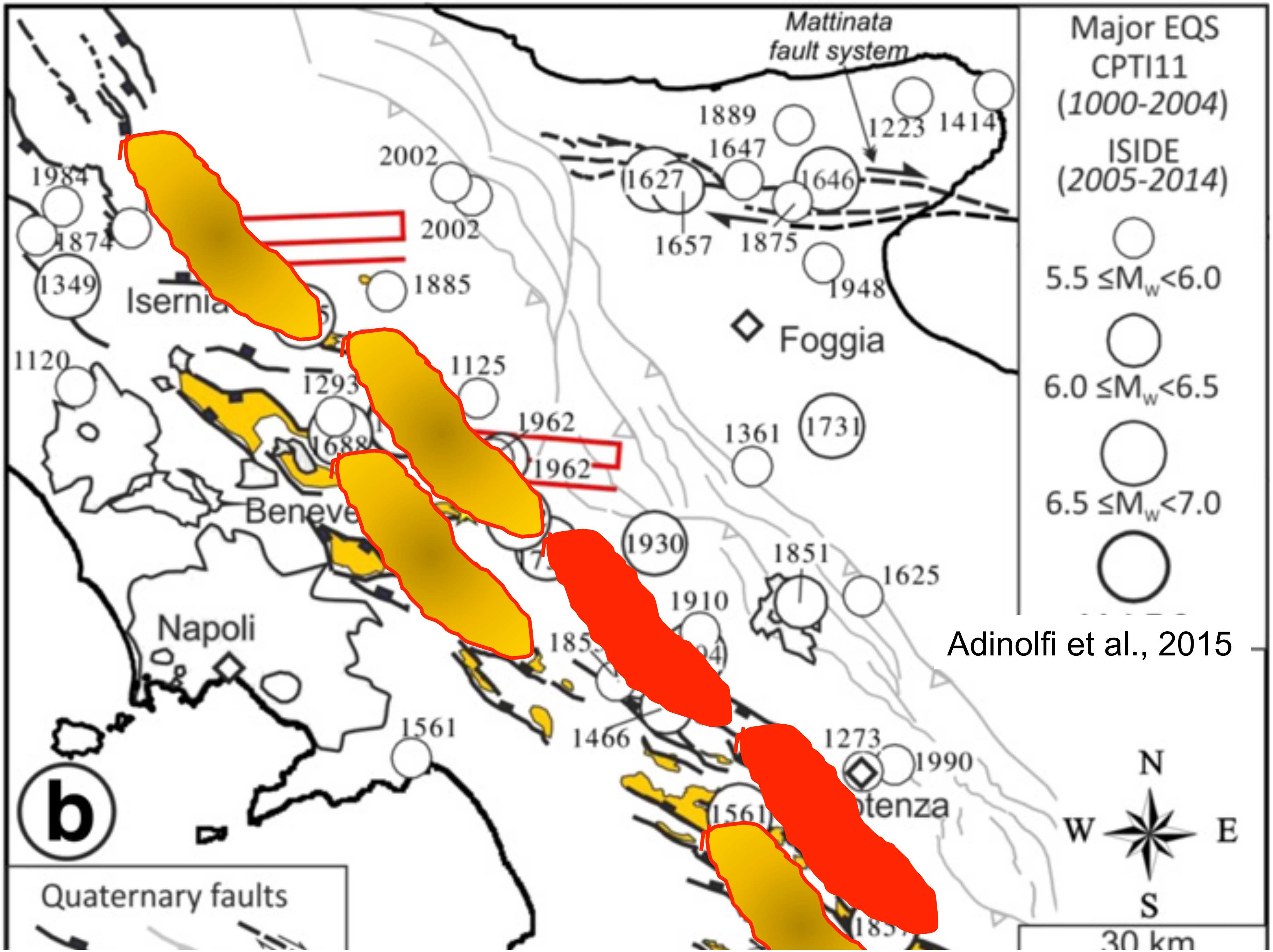

Adinolfi et al., 2015

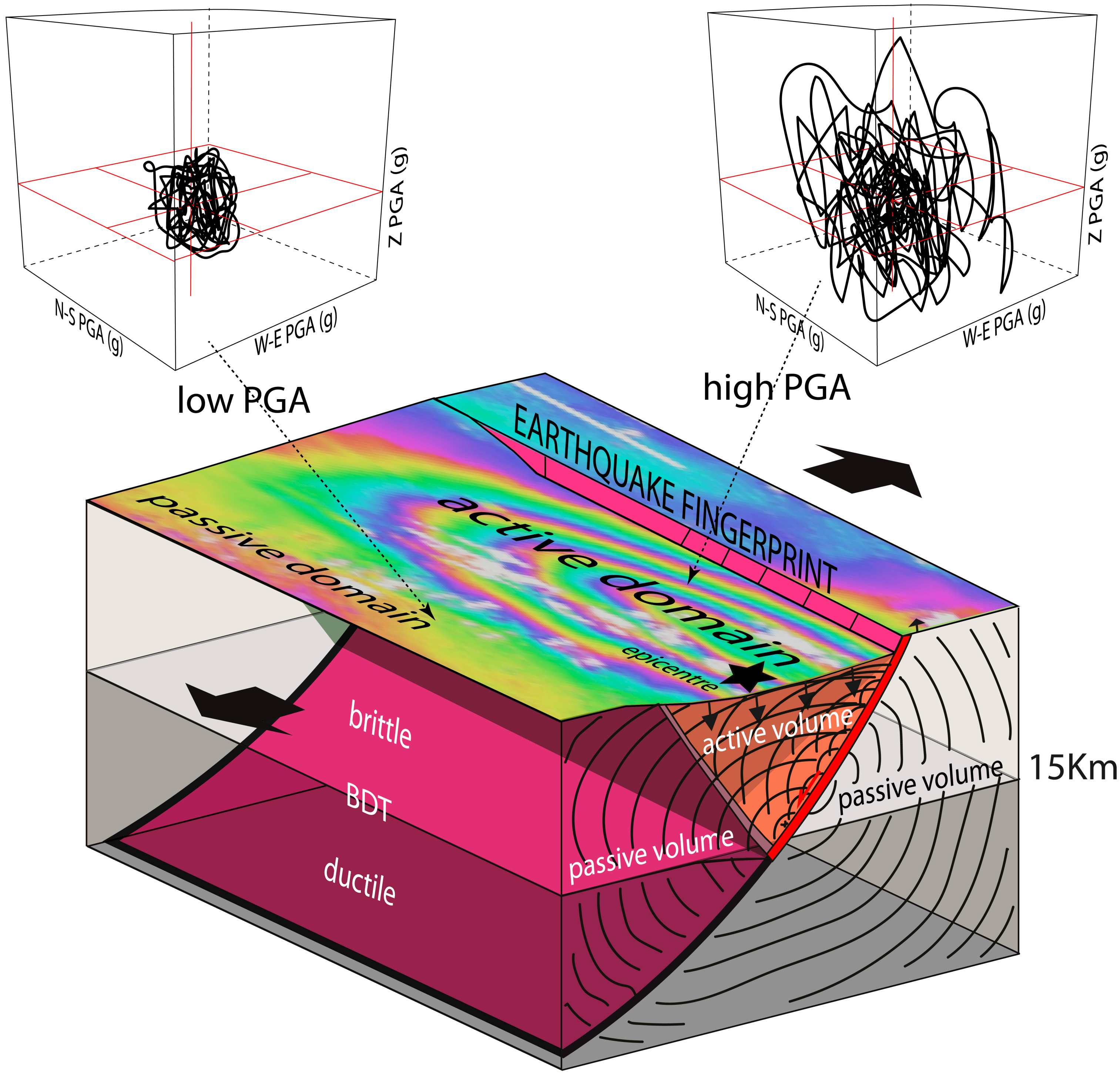

Z PGA (g)
N-S PGA (g)
W-E PGA (g)
low PGA
Z PGA (g)
N-S PGA (g)
W-E PGA (g)
high PGA
EARTHQUAKE FINGERPRINT
passive domain
active domain
epicentre
brittle
BDT
ductile
active volume
passive volume
passive volume
15Km

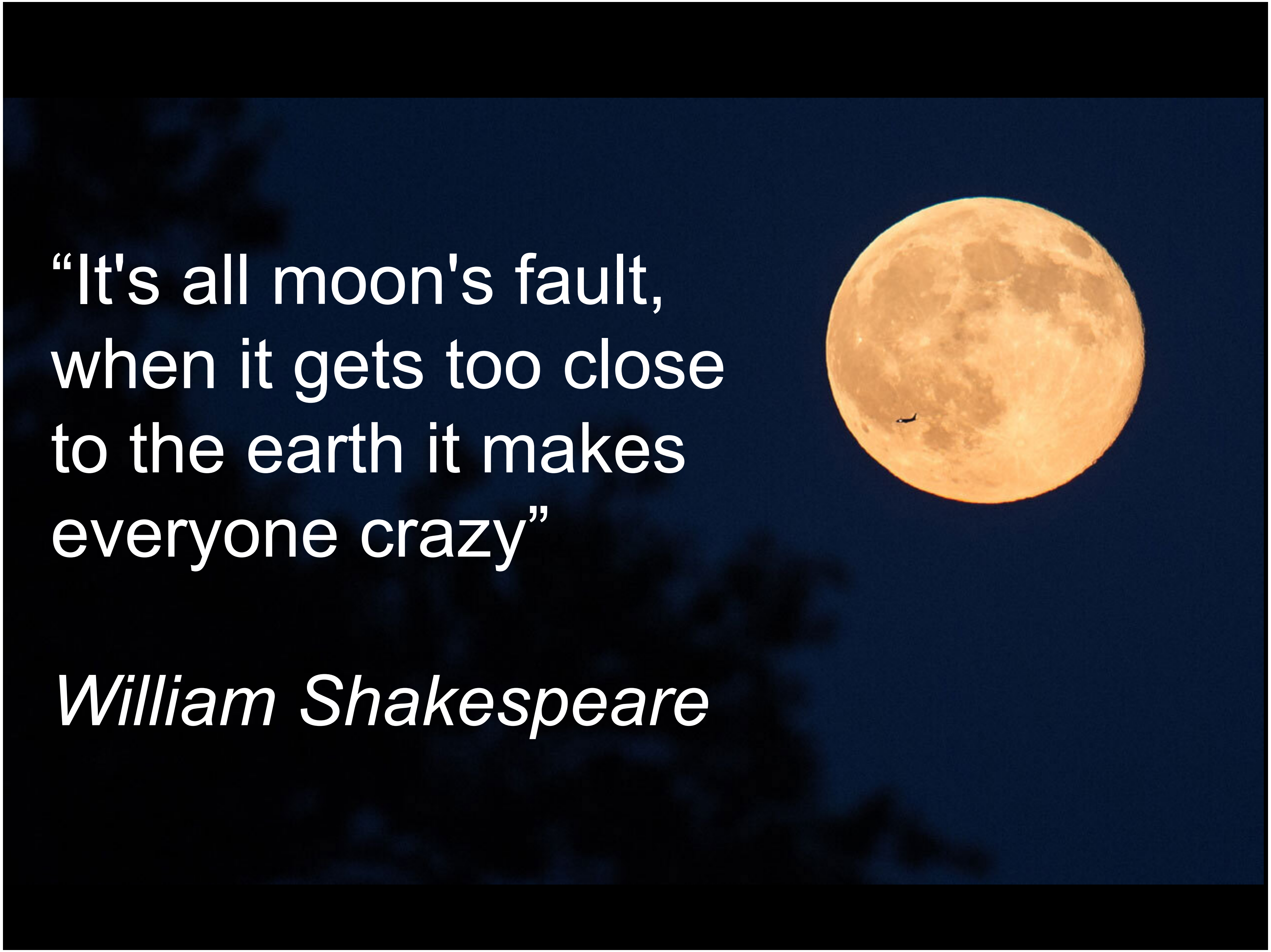
“It's all moon's fault, when it gets too close to the earth it makes everyone crazy”
William Shakespeare